Effective Field Theories for Inclusive B Decays

by

Keith S. M. Lee

Submitted to the Department of Physics
in partial fulfillment of the requirements for the degree of

Doctor of Philosophy

at the

MASSACHUSETTS INSTITUTE OF TECHNOLOGY
[June 2006]
May 2006

Author .....
Department of Physics
May 26, 2006

Certified by .....
Iain W. Stewart
Assistant Professor
Thesis Supervisor

Accepted by .....
Thomas J. Greytak
Chairman, Department Committee on Graduate Students

Effective Field Theories for Inclusive B Decays

by

Keith S. M. Lee

Submitted to the Department of Physics
on May 26, 2006, in partial fulfillment of the
requirements for the degree of
Doctor of Philosophy

Abstract

In this thesis, we study inclusive decays of the B meson. These allow one to determine CKM elements precisely and to search for physics beyond the Standard Model. We use the framework of effective field theories, in particular the Soft-Collinear Effective Theory, which is a suitable method when the decay products include a jet-like set of hadronic states.

We derive factorization theorems for $\Lambda_{\rm QCD}/m_b$ corrections (including all orders in α_s) to $B \to X_s\gamma$ and $B \to X_u\ell\bar{\nu}$ in the shape function region, where $m_X^2 \lesssim m_b\Lambda_{\rm QCD}$. A complete enumeration of $\Lambda_{\rm QCD}/m_b$ contributions is provided. We also point out the presence of new shape functions that arise from four-quark operators. These induce an additional uncertainty in certain inclusive determinations of $|V_{ub}|$.

Next, we derive the triply differential spectrum for $B \to X_s\ell^+\ell^-$ in the shape function region, consideration of which is necessitated by experimentally required cuts. It is shown that the same universal jet and shape functions appear as in the decays $B \to X_s\gamma$ and $B \to X_u\ell\bar{\nu}$. We also show that one can treat the perturbative power counting above and below the scale $\mu = m_b$ independently, using a procedure we call "split matching". This resolves the conflict between what is suitable in each of these regions.

Finally, we use these results to calculate the fraction of the total rate that is measured in the presence of a cut on the hadronic invariant mass, m_X. We find that the effect of this cut depends strongly on the value of $m_X^{\rm cut}$ and is approximately universal for all short-distance contributions. This feature can be exploited to minimize hadronic uncertainties and thereby maintain sensitivity to new physics.

Thesis Supervisor: Iain W. Stewart
Title: Assistant Professor

Acknowledgments

It is a pleasure to acknowledge Iain Stewart for his remarkable supervision. I am very grateful for all the time and guidance he has given to me. I have also benefited enormously from close collaboration with Zoltan Ligeti, and I thank him for this. I wish to thank my thesis-committee members, John Negele and Gabriella Sciolla, for their encouragement, and Omar Foda and Krishna Rajagopal for their advice. I also thank David Tong for his generous assistance.

Thanks to my collaborators, who include Frank Tackmann and Joydip Kundu. I have also enjoyed the friendly research environment created by Dan Pirjol, Vivek Mohta, Sonny Mantry, Ambar Jain, Bjorn Lange and Michael Forbes.

I am deeply indebted to Taehyun Kim, who has been an amazingly caring friend. I am also indebted to Chris Arnesen, whom I thank for many long and enlightening discussions, for research collaboration and for moral support. In addition, I appreciate his helpful comments on preliminary versions of this thesis. I am very fortunate to know Mark Hertzberg, and I thank him for all of his support. I also greatly appreciate his useful feedback on drafts of this thesis.

I thank my parents and sister for their constant love and practical help. Finally, I wish to acknowledge the inspiration provided by Ludwig van Beethoven and Johann Sebastian Bach.

Contents

List of Figures

List of Tables

Chapter 1

Introduction

1.1 B Physics

We are in the middle of a very fruitful era in B physics. The experiments at the B factories, *BABAR* and Belle, have been resoundingly successful. In addition, the Tevatron is running and LHCb is scheduled to begin taking data in 2007. On the theoretical side, much progress has been made within the context of effective field theories. One of these is the Soft Collinear Effective Theory (SCET), which describes processes involving energetic hadrons and is useful for studying QCD effects systematically and model-independently. This provides the framework for the original research in this thesis.

One of the main goals of heavy-quark physics is to test the flavour structure of the Standard Model. This is the least understood sector of the Standard Model, raising a host of so-far unanswered questions, including the following: Why are there three generations? Why do we have a hierarchy of fermion masses? What is the mechanism of electroweak symmetry breaking?

One would also like to learn about CP violation. Unlike typical extensions of the Standard Model, the Standard Model has only one source of CP violation[1], namely the single phase in the CKM matrix. Furthermore, it is well known that the observed

[1]Not including the QCD θ term, which bounds on the neutron's electric dipole moment imply must be tiny.

baryon asymmetry of the Universe cannot be accounted for by the Standard Model.

The B meson is particularly suitable for probing QCD and flavour physics, from both theoretical and experimental points of view. Consisting of a heavy b quark and a light anti-quark, it is the simplest hadron. (No meson involving the top quark exists, since it decays too rapidly for hadronization to occur.) The large mass of the b quark relative to $\Lambda_{\rm QCD}$ provides a useful expansion parameter, $\Lambda_{\rm QCD}/m_b \sim 0.1$. Consequently, theoretical expressions will typically involve both an α_s expansion and a power expansion in this parameter: the former gives perturbative corrections, whereas the latter gives non-perturbative corrections. On the phenomenological side, the large available phase space for possible decay states implies a rich decay spectrum. (It is useful to characterize B decays as either *exclusive* or *inclusive*. By *inclusive*, we mean that one sums over all hadronic final states in a given class, e.g. $B \to X_c \ell \bar{\nu}$ involves all hadronic decay states with one net c quark: $X_c = \{D, D^*, D\pi, D\pi\pi\pi, \ldots\}$.) Furthermore, B's have a long lifetime, e.g. $\tau = 1.6\,\text{ps}$ for $B^\pm$, and are abundantly produced in the B factories.

The payoff of the B physics program is, on the one hand, precision measurements of Standard Model parameters and, on the other hand, high sensitivity to new physics, i.e. physics beyond the Standard Model. We now consider each of these in turn in more detail.

1.1.1 Precision Measurements and the Unitarity Triangle

Precision measurements provide determinations of elements of the the Cabibbo-Kobayashi-Maskawa (CKM) matrix, which parameterizes the mixing between quark flavours in the Standard Model. A well-known example is the semileptonic decay $B \to X_c \ell \bar{\nu}$, which allows measurements of $|V_{cb}|$, m_b and m_c through moments of the decay spectra. Analyses of this type are performed at *BABAR* [13, 16], Belle [2], and CLEO [64], where simultaneously fitting a few fundamental hadronic parameters keeps the theoretical uncertainties under control [80]. From measurements of $B \to X_u \ell \bar{\nu}$ we can also determine $|V_{ub}|$ [15, 78, 94].

The CKM matrix appears in the part of the Lagrangian governing charged-current

weak interactions.

$$\mathcal{L} = \frac{g}{\sqrt{2}} \bar{u}_L^i \gamma^\mu V_{\rm CKM}^{ij} d_L^j W_\mu^+ + \text{h.c.}, \tag{1.1}$$

where $i, j = 1, 2, 3$ are family or generation indices. It can be conveniently parameterized in terms of the Wolfenstein variables λ, A, ρ and η as

$$\begin{aligned} V_{\rm CKM} &= \begin{pmatrix} V_{ud} & V_{us} & V_{ub} \\ V_{cd} & V_{cs} & V_{cb} \\ V_{td} & V_{ts} & V_{tb} \end{pmatrix} \\ &= \begin{pmatrix} 1 - \frac{\lambda^2}{2} & \lambda & A\lambda^3(\rho - i\eta) \\ -\lambda & 1 - \frac{\lambda^2}{2} & A\lambda^2 \\ A\lambda^3(1 - \rho - i\eta) & -A\lambda^2 & 1 \end{pmatrix} + \mathcal{O}(\lambda^4) \\ &\sim \begin{pmatrix} 1 & \lambda & \lambda^3 \\ -\lambda & 1 & \lambda^2 \\ \lambda^3 & -\lambda^2 & 1 \end{pmatrix}, \end{aligned} \tag{1.2}$$

where $\lambda = |V_{us}| \simeq 0.22$ is a small parameter. Note that the $\mathcal{O}(\lambda^4)$ terms are kept in current fits of these variables [57].

Now, unitarity of $V_{\rm CKM}$, namely $1 = V_{\rm CKM}^\dagger V_{\rm CKM}$, leads to unitarity relations involving the elements in pairs of rows or pairs of columns. For example, from the first and third columns, we have

$$V_{ud} V_{ub}^* + V_{cd} V_{cb}^* + V_{td} V_{tb}^* = 0. \tag{1.3}$$

This relation can be represented as a triangle in the complex plane, as shown in Fig. 1-1. This triangle is referred to as the *unitarity triangle*.[2]

Thus, obtaining the CKM matrix elements is equivalent to obtaining the angles

[2]There are actually six unitarity triangles. The one shown here is particularly interesting, because all of its sides are comparable in magnitude. The other triangle with this property is distinguishable from this one only when we include higher-order terms.

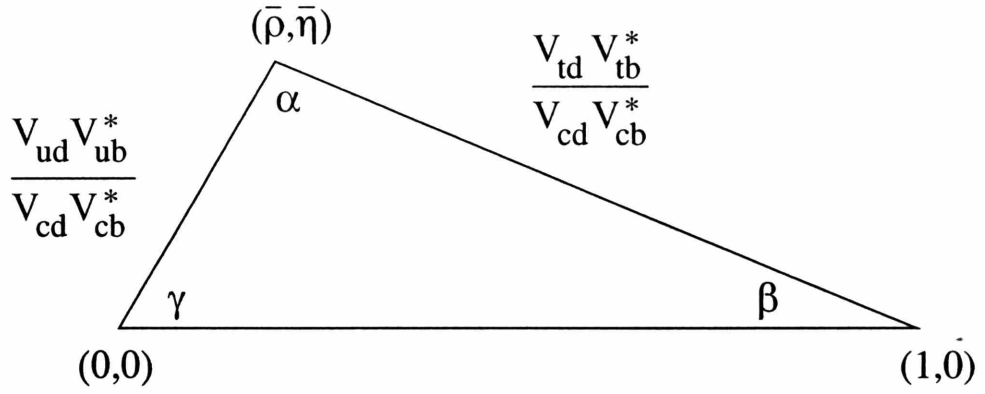

Figure 1-1: The unitarity triangle. $\bar{\rho} = \rho(1 - \lambda^2/2)$ and $\bar{\eta} = \eta(1 - \lambda^2/2)$.

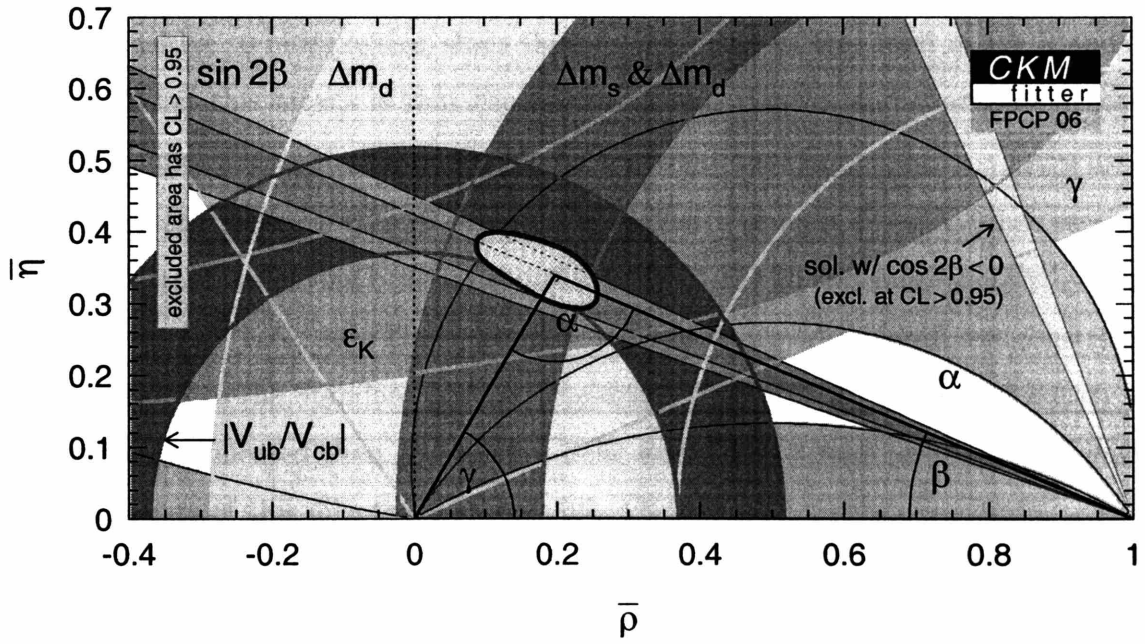

Figure 1-2: Global fit of the unitarity triangle [57].

and sides of the unitarity triangle. By overconstraining these, the flavour structure of the Standard Model is subjected to rigorous examination. The current global fit of the unitarity triangle is shown in Fig. 1-2. Here, ε_K is a CP-violation parameter related to the decays $K^0_{L,S} \to \pi^+\pi^-$ and $K^0_{L,S} \to \pi^0\pi^0$. Δm_d (Δm_s) is the mass difference between the two B^0 (B^0_s) mass eigenstates and is measured through the $B^0\bar{B}^0$ ($B^0_s\bar{B}^0_s$) oscillation rate. The work described in Chapter 3 is relevant for determining the V_{ub} side of the triangle.

1.1.2 Rare Decays and New Physics

In searching for physics beyond the Standard Model, an obvious approach is to try to create and observe new particles directly at particle accelerators. A complementary approach is the indirect search, in which one looks for discrepancies between measurements and theoretical predictions, signalling quantum corrections due to those new particles. This requires precise control of experimental and theoretical uncertainties.

Of great importance in the latter endeavour are the so-called *rare* decays, namely those channels involving flavour-changing neutral currents (FCNCs). These not only allow measurements of CKM matrix elements, in particular V_{ts} and V_{td}, but are also highly sensitive to new physics, since they do not occur at tree level in the Standard Model. What this means is that the effects of, say, Higgses and charginos in loops can be comparable to the Standard Model contributions.

Among the inclusive rare B decays, the radiative process $B \to X_s\gamma$ has received the most attention, having been measured first by CLEO [4] and subsequently by other experiments [18, 1, 62, 11]. These measurements have provided significant constraints on extensions to the Standard Model. The decay $B \to X_s\ell^+\ell^-$ is complementary to, and more complicated than, $B \to X_s\gamma$. Belle and *BABAR* have already made initial measurements of this dileptonic process [95, 12, 14].

1.2 Effective Field Theories

Heavy-quark physics involves disparate scales $m_W \gg m_b \gg \Lambda_{QCD}$ and the complex interplay between electroweak and strong interactions. A powerful, model-independent method for dealing with these complications is to use an effective field theory (EFT), which may be regarded as the low-energy limit of some more fundamental theory (either known or unknown). Many well-known theories are actually EFTs. For example, the Standard Model itself is an EFT.

The EFT is constructed from only the relevant infrared degrees of freedom and involves an expansion in some suitable small parameter. The resulting effective La-

grangian will take the form

$$\mathcal{L}_{\text{eff}} = \sum_{n\geq 0} \mathcal{L}^{(n)} = \mathcal{L}^{(0)} + \sum_{n\geq 1} \sum_{i_n} \frac{c_{i_n}}{\Lambda^n} \mathcal{O}_{i_n}^{(n)}, \tag{1.4}$$

where c_{i_n} are dimensionless coefficients, Λ represents the fundamental scale below which the EFT is valid, and the local operators $\mathcal{O}_{i_n}^{(n)}$ have the same symmetries as the underlying theory. This is an infinite series, but the higher the dimension of the operator the more powers of Λ it is suppressed by. In other words, the lowest-dimensional operators will be the most important ones.[3] Thus, in practice, one can truncate the series at some order dictated by the desired accuracy, so that one is left with a finite number of operators and hence a finite number of parameters c_{i_n} to determine. If the underlying theory is known and weakly coupled, one may be able to compute the parameters. Otherwise, one can take them to be experimental inputs.

EFTs have many advantages. They enable one to decouple long-distance and short-distance effects, a process known as *factorization*. This is a crucial step in studying QCD, for example, since the short-distance contributions are perturbatively calculable, whereas the long-distance contributions are non-perturbative. Furthermore, the power counting (in the small parameter) is transparent and power corrections can be systematically incorporated. Sometimes low-energy symmetries that are not manifest in the underlying theory become explicit. In this case the leading-order Lagrangian $\mathcal{L}^{(0)}$ exhibits the symmetries, which are broken by higher-order corrections. We shall see an example of this in the next chapter, when we consider the Heavy Quark Effective Theory (HQET).

Nevertheless, the influence of the EFT approach extends beyond just providing a tool for tackling otherwise intractable problems: in fact, it has profoundly changed our understanding of renormalizability. The traditional belief was that, in order to be predictive, a quantum field theory should be renormalizable, i.e. at any order in perturbation theory loop divergences can be absorbed into the same finite set of

[3]We have been describing a typical EFT. More generally, the expansion parameter need not be simply related to the mass dimension. For example, NRQCD and SCET use different kinds of power counting.

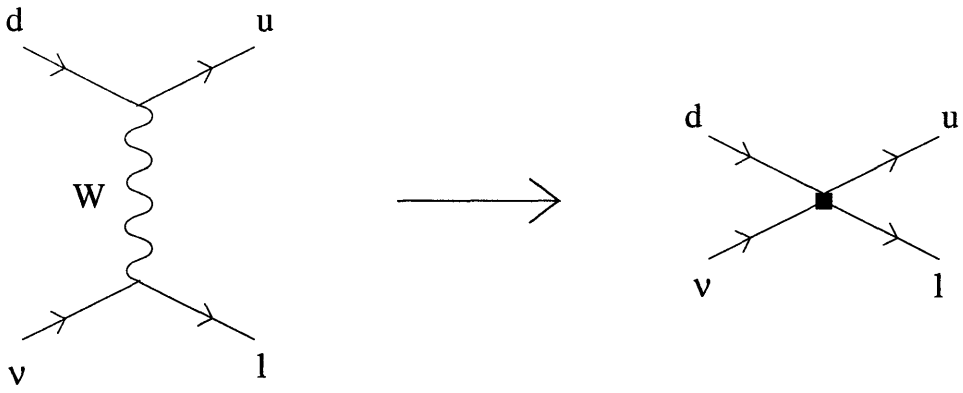

Figure 1-3: Integrating out the W boson.

parameters of the theory. A non-renormalizable theory, it seemed, would require an infinite number of experimental inputs. It is now clear that non-renormalizable theories still retain predictive power; there is simply a finite accuracy associated with these predictions, and renormalization is carried out order by order. Moreover, we do not claim that any quantum field theory is exact up to arbitrarily high energies. (One might be able to carry out exact calculations within some theory, but this is not the same as having that theory exactly describe the physical world at any scale.) On the contrary, a renormalizable theory such as the Standard Model itself can be viewed as an EFT, in which non-renormalizable terms have been neglected.

1.2.1 Effective Electroweak Hamiltonian

In Fermi theory, the four-fermion Hamiltonian is

$$\mathcal{H}_{\text{eff}} = \frac{4G_F}{\sqrt{2}} \left(\bar{l}_L \gamma^\mu \nu_L\right) \left(\bar{u}_L \gamma_\mu d_L\right) + \text{h.c.} \tag{1.5}$$

The modern interpretation is that this is an effective low-energy theory, in which the W boson has been removed as an explicit, dynamical degree of freedom. Pictorially, this corresponds to Fig. 1-3. In other words, terms of $\mathcal{O}\left(k^2/M_W^2\right)$ have been neglected in the propagator. This process is commonly referred to as "integrating out" the heavy particle, a term with origins in the path-integral formalism.

Generalizing this idea to incorporate the particles and interactions of the Standard

Model leads to the generic form

$$\mathcal{H}_{\text{eff}} = \frac{G_F}{\sqrt{2}} \sum_i V^i_{\text{CKM}} C_i(\mu) \mathcal{O}_i(\mu). \tag{1.6}$$

The $\mathcal{O}_i$ are the local operators relevant to the process being studied; the strengths of these operators are determined by the CKM factors V^i_{CKM} and the Wilson coefficients $C_i(\mu)$. We can regard the latter as the effective coupling constants of the effective vertices.

As an example, let's consider the effective Hamiltonian for $B \to X_s\gamma$. This is given by

$$\mathcal{H}_{\text{eff}} = -\frac{4G_F}{\sqrt{2}} V_{tb} V^*_{ts} \sum_{i=1}^{8} C_i(\mu) \mathcal{O}_i(\mu). \tag{1.7}$$

The operators $\mathcal{O}_i$ come from the Feynman diagrams shown in Fig. 1-4. The W boson and top quark are integrated out and the resulting operators are [85, 86]

$$\begin{aligned}
\text{Current-current:} \quad & \mathcal{O}_1 = (\bar{s}_{L\alpha}\gamma_\mu b_{L\beta})(\bar{c}_{L\beta}\gamma^\mu c_{L\alpha}), \\
& \mathcal{O}_2 = (\bar{s}_{L\alpha}\gamma_\mu b_{L\alpha})(\bar{c}_{L\beta}\gamma^\mu c_{L\beta}), \\
\text{QCD penguins:} \quad & \mathcal{O}_3 = (\bar{s}_{L\alpha}\gamma_\mu b_{L\alpha}) \sum_{q=u,d,s,c,b} (\bar{q}_{L\beta}\gamma^\mu q_{L\beta}), \\
& \mathcal{O}_4 = (\bar{s}_{L\alpha}\gamma_\mu b_{L\beta}) \sum_{q=u,d,s,c,b} (\bar{q}_{L\beta}\gamma^\mu q_{L\alpha}), \\
& \mathcal{O}_5 = (\bar{s}_{L\alpha}\gamma_\mu b_{L\alpha}) \sum_{q=u,d,s,c,b} (\bar{q}_{R\beta}\gamma^\mu q_{R\beta}), \\
& \mathcal{O}_6 = (\bar{s}_{L\alpha}\gamma_\mu b_{L\beta}) \sum_{q=u,d,s,c,b} (\bar{q}_{R\beta}\gamma^\mu q_{R\alpha}), \\
\text{Electromagnetic penguin:} \quad & \mathcal{O}_7 = \frac{e}{16\pi^2} \bar{s}\sigma_{\mu\nu} F^{\mu\nu} (\bar{m}_b P_R + \bar{m}_s P_L) b, \\
\text{Chromomagnetic penguin:} \quad & \mathcal{O}_8 = \frac{g}{16\pi^2} \bar{s}_\alpha T^a_{\alpha\beta} \sigma_{\mu\nu} (\bar{m}_b P_R + \bar{m}_s P_L) b_\beta G^{a\mu\nu},
\end{aligned} \tag{1.8}$$

where $P_{R,L} = (1 \pm \gamma_5)/2$, α, β are colour indices, and $F^{\mu\nu}$ and $G^{\mu\nu}$ are the photonic and gluonic field strength tensors. It is common to neglect the mass of the strange

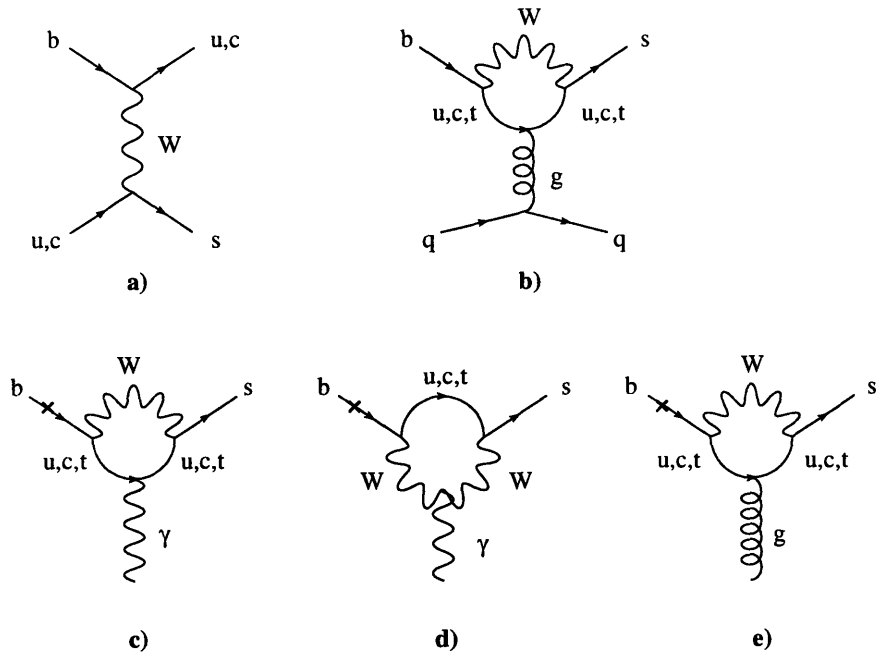

Figure 1-4: Feynman diagrams corresponding to $B \to X_s\gamma$: a) current-current, b) gluon penguin, c)-d) magnetic photon penguins, e) magnetic gluon penguin. The cross indicates a mass insertion. Diagrams with wave-function renormalization are not shown.

quark in $\mathcal{O}_{7,8}$, since m_s/m_b is of the order of a few percent.

Note the common CKM factor $V_{tb}V_{ts}^*$ in Eq. (1.7). We can see from the diagrams in Fig. (1-4) that we originally also had terms with $V_{ub}V_{us}^*$ or $V_{cb}V_{cs}^*$. However, $V_{ub}V_{us}^*$ is suppressed by λ^2 relative to $V_{tb}V_{ts}^*$ (see Eq. (1.2)) and so can be neglected. Similarly, we can use the unitarity relation from the second and third columns of the CKM matrix to eliminate $V_{cb}V_{cs}^*$:

$$\begin{aligned} V_{ub}V_{us}^* + V_{cb}V_{cs}^* + V_{tb}V_{ts}^* &= 0 \\ \Rightarrow V_{cb}V_{cs}^* &= -V_{tb}V_{ts}^*\left(1 + \frac{V_{ub}V_{us}^*}{V_{tb}V_{ts}^*}\right) \\ &= -V_{tb}V_{ts}^* + \mathcal{O}(\lambda^2)\,. \end{aligned} \tag{1.9}$$

At lowest order in α_s, only $\mathcal{O}_7$ contributes. The full operator basis listed consists

of dimension-6, gauge-invariant operators that have the right quantum numbers to contribute to $b \to s\gamma$ and are compatible with electroweak symmetries.[4] These dominate over higher-dimensional terms, because the latter are suppressed by powers of m_b^2/M_W^2. If we keep all of the terms (of all dimensions) in the series, then the result is equivalent to the original ("full") theory.

1.2.2 Matching and RG-Improved Perturbation Theory

The procedure for using the effective Hamiltonian (1.7) to obtain the amplitude for $B \to X_s\gamma$ is as follows. First, we *match* the full theory on to the effective theory at the scale $\mu = \mathcal{O}(M_W)$. What this means is that we calculate matrix elements in the full theory and in the effective theory. Comparing these gives the Wilson coefficients C_i. For this purpose, any external states - even unphysical ones - may be used, since the Wilson coefficients are independent of these, i.e. independent of the particular decay considered (just like gauge couplings, which are universal and process independent). It is important, however, that the same infrared regulator is used on both sides of the equation. The scale μ is large enough that this matching can be done in ordinary perturbation theory. The Wilson coefficients will, in general, depend upon the masses of the particles integrated out, namely the W boson and top quark.

Now, whereas the quark-level decay is governed by the electroweak scale $\mu_W \sim m_W$, the typical energy of the B meson is of order $m_b \ll m_W$. Thus one encounters the problem of large logarithms of the form $\log(m_W/\mu)$, $\mu \sim m_b$, with $\alpha_s(m_b)\log(m_W/m_b) \sim 1$. Terms of the form

$$\begin{aligned} &\alpha_s^n(m_b)\log^n(m_b/m_W) \qquad \text{(leading log [LL])}, \\ &\alpha_s^{n+1}(m_b)\log^n(m_b/m_W) \qquad \text{(next-to-leading log [NLL])}, \\ &\qquad\vdots \end{aligned}$$

are significant and should be resummed to all orders in α_s to get accurate values for

[4] There are actually ten two-quark operators, but by using the equations of motion and various gamma-matrix identities we can reduce these to linear combinations of four-quark operators and $\mathcal{O}_{7,8}$ [85].

the C_i.

The solution is to use the renormalization group equation (RGE) for $\vec{C}(\mu)$. Once again, this is completely analogous to the case of gauge coupling constants, which run and obey renormalization group equations. To illustrate that running down from the scale $\mu \sim m_W$ to $\mu \sim m_b$ takes care of large-log summation, consider the one-loop running of the strong coupling constant,

$$\begin{aligned} \alpha_s(\mu) &= \frac{\alpha_s(m_Z)}{1+\beta_0\frac{\alpha_s(m_Z)}{2\pi}\log\left(\frac{\mu}{m_Z}\right)} \\ &= \alpha_s(m_Z)\left[1+\sum_{n=1}^{\infty}\left(\beta_0\frac{\alpha_s(m_Z)}{2\pi}\log\left(\frac{m_Z}{\mu}\right)\right)^n\right], \end{aligned} \tag{1.10}$$

where we have expanded in $\alpha_s(m_Z)$. Thus, solving the RGE

$$\mu\frac{d}{d\mu}\alpha_s(\mu) = -\beta_0\frac{\alpha_s^2(\mu)}{2\pi} \tag{1.11}$$

automatically sums the large logarithms.

The renormalization group equation for $\vec{C}$ can be obtained as follows. The bare and renormalized operators are related by

$$\mathcal{O}_0^i = Z_{\mathcal{O}}^{ij}(\mu)\mathcal{O}_\mu^j, \tag{1.12}$$

i.e. in general, renormalization will involve *mixing* between operators. Then, because the bare operator is μ independent,

$$0 = \mu\frac{d}{d\mu}\mathcal{O}_0^i = \left(\mu\frac{d}{d\mu}Z_{\mathcal{O}}^{ij}\right)\mathcal{O}_\mu^j + Z_{\mathcal{O}}^{ij}\left(\mu\frac{d}{d\mu}\mathcal{O}_\mu^j\right), \tag{1.13}$$

so that

$$\mu\frac{d}{d\mu}\mathcal{O}_\mu^j = -\gamma_{\mathcal{O}}^{ij}\mathcal{O}_\mu^j, \tag{1.14}$$

where

$$\gamma_{\mathcal{O}}^{ij} = \left[Z_{\mathcal{O}}^{-1}(\mu)\right]^{ik} \mu \frac{d}{d\mu} \left[Z_{\mathcal{O}}(\mu)\right]^{kj} \tag{1.15}$$

is the *anomalous dimension matrix.*

Finally,

$$\begin{aligned} 0 &= \mu \frac{d}{d\mu} \mathcal{H}_{eff} \\ &= \mu \frac{d}{d\mu} \left(C^i \mathcal{O}_\mu^i\right) \\ &= \left(\mu \frac{d}{d\mu} C^i\right) \mathcal{O}_\mu^i - C^i \gamma_{\mathcal{O}}^{ij} \mathcal{O}_\mu^j \,, \end{aligned} \tag{1.16}$$

which (because the $\mathcal{O}_i$ are independent) implies that

$$\mu \frac{d}{d\mu} C_i = \gamma_{\mathcal{O}}^{ji} C_j \,. \tag{1.17}$$

The use of this equation to run the $C_i(\mu)$ down to the desired scale is known as *RG-Improved Perturbation Theory.*

The amplitude for the decay $B \to f$ is

$$\langle f|\mathcal{H}_{\text{eff}}|B\rangle = \frac{4G_F}{\sqrt{2}} \sum_i V_{\text{CKM}}^i C_i(\mu) \langle f|\mathcal{O}_i(\mu)|B\rangle \,. \tag{1.18}$$

The Wilson coefficients $C_i(\mu)$ summarize the physics from all scales greater than μ, whereas the matrix elements of the operators $\mathcal{O}_i$ summarize the contributions to the amplitude from scales less than μ. In other words, the problem has been separated into two parts: the short-distance calculation of the $C_i(\mu)$ and the long-distance calculation of the matrix elements $\langle \mathcal{O}_i(\mu) \rangle$. When we evolve the scale down from $\mu_W \sim m_W$ to μ, we transfer information about physics in the range between μ and m_W from the hadronic matrix elements to the C_i; equivalently, we split the logarithm

of the full amplitude:

$$\log\left(\frac{m_W^2}{-p^2}\right) = \log\left(\frac{m_W^2}{\mu^2}\right) + \log\left(\frac{\mu^2}{-p^2}\right), \tag{1.19}$$

where p^2 is an infrared regulator.

The third step (after matching and running) is to calculate the hadronic matrix elements, which are non-perturbative (in α_s). For exclusive decays, this is a difficult problem: one must determine a considerable number of form factors, which leads to the dominant theoretical uncertainties in the decay amplitudes. Semileptonic form factors have begun to be determined by lattice QCD, while form factors for other channels are related by symmetries. For inclusive decays (including the example we have been considering, $B \to X_s\gamma$) the theoretical situation is better: one can exploit quark-hadron duality and use the *heavy-quark expansion*, which gives an expansion in inverse powers of m_b. The leading term represents the decay of the b quark and can be calculated in RG-improved perturbation theory. The next term is suppressed by $1/m_b^2$.

From the optical theorem, the inclusive decay rate is

$$\Gamma(B \to X_s\gamma) \sim \frac{1}{2m_B}\mathrm{Im}\left[i\int d^4x\, e^{iq\cdot x}\langle B|T\mathcal{H}_{\mathrm{eff}}^{\dagger}(x)\mathcal{H}_{\mathrm{eff}}(0)|B\rangle\right]. \tag{1.20}$$

One can proceed by using a local operator product expansion (OPE), which writes the product of operators separated by some distance x as a series of local operators:

$$T\left[O_1(x)O_2(0)\right] = \sum_k C_{12}^k(x)\mathcal{O}_k(0). \tag{1.21}$$

Non-perturbative matrix elements are defined with the help of the Heavy Quark Effective Theory (HQET), which will be discussed in more detail in the next chapter.

At leading-log order, one must perform $\mathcal{O}(\alpha_s^0)$ matching, which corresponds to matching at tree level on to four-quark operators from Fig. 1-4a), and at one-loop level on to $\mathcal{O}_{7,8}$ from Fig. 1-4e)-f). The running requires the anomalous dimension matrix to order α_s^1; for the mixing of $\mathcal{O}_{1-6}$ into $\mathcal{O}_{7,8}$, this involves the calculation of

two-loop diagrams. Finally, one needs the matrix elements of the operators at order α_s^0. This step includes calculating $\langle s\gamma|\mathcal{O}_{1,2}|b\rangle$ at one-loop level and $\langle s\gamma|\mathcal{O}_7|b\rangle$ at tree level. The leading-log result with $1/m_b^2$ corrections is [70]

$$\Gamma(B \to X_s\gamma) = \frac{G_F^2 m_b^5}{32\pi^4}|V_{tb}V_{ts}^*|^2\alpha_{\rm em}|C_7(m_b)|^2\left[1+\frac{\lambda_1-9\lambda_2}{2m_b^2}+\cdots\right], \quad (1.22)$$

where λ_1, $\lambda_2 \sim \Lambda_{\rm QCD}^2$ are non-perturbative parameters that are matrix elements of local operators. Here, C_7 has been evolved down to the scale m_b. This takes care of the summation of leading logarithms. At next-to-leading order, the Standard Model predicts that the branching fraction, $\mathcal{B}(B \to X_s\gamma) = \Gamma(B \to X_s\gamma)/\Gamma_{tot}$, is [72, 52]

$$\mathcal{B}(B \to X_s\gamma)|_{\overline{MS}} = (3.73 \pm 0.30) \times 10^{-4}. \quad (1.23)$$

Averaging the experimental results of the various collaborations gives [19]

$$\mathcal{B}(B \to X_s\gamma) = (3.55 \pm 0.24^{+0.09}_{-0.10} \pm 0.03) \times 10^{-4}, \quad (1.24)$$

where the quoted errors are combined statistical and systematic, systematic due to the shape function, and the $b \to d\gamma$ fraction, respectively. This is in good agreement with Eq. (1.23).

1.2.3 The Endpoint Region

The study of inclusive B decays circumvents the need for hadronic form factors, thereby allowing model-independent tests. However, there is often a trade-off between theory and experiment, because cuts are necessary experimentally, but these less inclusive spectra make the theory more complicated. For $B \to X_s\gamma$, a lower cut on the photon energy is used to eliminate softer photons. In $B \to X_u\ell\bar{\nu}$, phase-space cuts are important to remove the dominant $b \to c$ background. In such cases, we are restricted to a region in which $m_X^2 \sim m_b\Lambda_{\rm QCD}$ and the local OPE breaks down.

Consider, for example, the photon energy spectrum for $B \to X_s\gamma$, for which the

OPE gives [124]

$$\begin{aligned}\frac{d\Gamma}{dx} &= \frac{G_F^2 m_b^5}{32\pi^4}|V_{tb}V_{ts}^*|^2\alpha_{\rm em}|C_7(m_b)|^2\left(1+\frac{\lambda_1-9\lambda_2}{2m_b^2}+\cdots\right) \\ &\quad\times\left[\delta(1-x)-\frac{\lambda_1+3\lambda_2}{2m_b^2}\delta'(1-x)-\frac{\lambda_1}{6m_b^2}\delta''(1-x)+\cdots\right],\end{aligned} \tag{1.25}$$

where $x = 2E_\gamma/m_b$ and the primes indicate derivatives of the delta function. This must be interpreted as a distribution, i.e. one must integrate it against some smooth weight function. In this way, one can obtain moments of the spectrum. The series of the most singular terms takes the generic form

$$\sum_{n=0}^{\infty}\frac{1}{n!}\frac{a_n}{m_b^n}\delta^{(n)}(1-x)\,. \tag{1.26}$$

The experimental cut puts us in the so-called endpoint region, where $1-x \sim \Lambda_{\rm QCD}/m_b$. A weight function of width $\sigma \sim \Lambda_{\rm QCD}/m_b$ results in all terms in (1.26) being of the same order of magnitude.

These most singular terms can be summed into a non-perturbative *shape function* [125, 124], which we shall denote by $f^{(0)}$. This is analogous to parton distribution functions in deep inelastic scattering. Similarly, series of subleading delta functions and their derivatives result in subleading shape functions. Since shape functions are non-perturbative, they are not calculable analytically. However, because they are properties of the B meson, they are universal, i.e. process-independent. At leading order, one can measure the relevant shape function from the photon energy spectrum of $B \to X_s\gamma$ and use the result in determining $|V_{ub}|$ from $B \to X_u\ell\bar{\nu}$, thereby avoiding model dependence. (In Chapter 4, it will be shown that the same function also occurs in $B \to X_s\ell^+\ell^-$.) As we shall see, at subleading order the situation is far more complicated, with several universal shape functions present, which occur in different combinations.

The study of the shape function region is greatly facilitated by using an appropriate theoretical method. When $m_X^2 \sim m_b\Lambda_{\rm QCD}$, the set of outgoing hadronic states becomes jet-like and the relevant degrees of freedom are collinear and (ultra)soft

modes. SCET is a powerful tool in this region. To summarize, we list the different regions of phase space, with the applicable theoretical methods shown in brackets:

$$\begin{aligned} &\Delta m_X^2 \sim m_b^2, && \text{totally inclusive} && \text{(local OPE, HQET)}, \\ &\Delta m_X^2 \sim m_b \Lambda_{\rm QCD}, && \text{endpoint region} && \text{(Factorization, SCET)}, \\ &\Delta m_X^2 \sim \Lambda_{\rm QCD}^2, && \text{resonance region} && \text{(exclusive methods)}, \end{aligned} \tag{1.27}$$

where Δm_X^2 denotes the region of m_X^2 extending out from $m_{X_{\rm min}}^2$.

1.3 Outline

The outline of the rest of this thesis is as follows. Chapter 2 is devoted to background theory: we provide a summary of HQET, followed by a review of the Soft-Collinear Effective Theory. Chapters 3 to 5 describe the original research of this thesis, which focuses on inclusive B decays.[5]

In Chapter 3 we derive a factorization theorem for $\Lambda_{\rm QCD}/m_b$ power corrections (to all orders in α_s) to the inclusive decays $B \to X_u \ell \bar{\nu}$ and $B \to X_s \gamma$ in the endpoint region. Our analysis separates perturbative corrections that appear at two different scales from the non-perturbative shape-function physics. We derive the complete set of subleading corrections for the triply differential spectrum and show how it factorizes into hard, jet and shape functions. This provides one of the only examples of an endpoint factorization theorem that has been worked out at subleading order. The triply differential decay rate thus obtained is important for phenomenological analyses of $|V_{ub}|$. We also point out the presence of four-quark-operator contributions that have previously been neglected in the literature; these induce an additional uncertainty in certain inclusive determinations of $|V_{ub}|$.

In Chapter 4, we investigate the decay $B \to X_s \ell^+ \ell^-$. Here, experimentally required cuts are made in the dileptonic mass spectrum to remove the largest $c\bar{c}$ resonances, namely the J/ψ and ψ'. This leaves two perturbative windows, the low-q^2

[5]This research is covered in somewhat less detail in Refs. [106, 107, 105].

and high-q^2 regions. The low-q^2 region has the higher rate, so experiments will obtain precise results for this region first. However, at low q^2 an additional cut is required: a hadronic invariant-mass cut is imposed in order to eliminate the background. *BABAR*'s current cut of $m_X \leq 1.8\,\text{GeV}$ means that, here also, we must deal with shape-function effects. We derive the spectra for $B \to X_s \ell^+ \ell^-$ in the shape function region for the first time. Without these results, no model-independent comparison between the Standard Model and experiment can be made: although the existing literature on this decay is vast, what has been calculated previously is different from what is actually being measured. We also show that the order of the perturbative expansion above $\mu \simeq m_b$ can be decoupled from that below $\mu \simeq m_b$, i.e. formulated so that the μ dependence cancels independently in the two regions. This is important because it turns out that the standard perturbative power counting for $\mu \geq m_b$ is no longer appropriate in the region $\mu \leq m_b$.

In Chapter 5, we apply the result of this analysis to calculate an experimentally important quantity in the low-q^2 region, namely the fraction ϵ of the total rate that is measured in the presence of a hadronic invariant-mass cut, m_X^{cut}. Experimentalists can use our ratio to relate their measurements to theoretical predictions for short-distance coefficients in the Standard Model. We find that ϵ has some noteworthy features:

1. it has strong m_X^{cut} dependence, and

2. the individual terms in the differential-decay-rate expression display a universality, yielding the same value of ϵ (to a good approximation), which demonstrates that hadronic uncertainties do not spoil the interpretation of short-distance measurements. In other words, we can still maintain sensitivity to new physics.

We conclude in Chapter 6.

Chapter 2

Soft-Collinear Effective Theory

2.1 Heavy Quark Effective Theory

Consider a physical system that consists of a heavy quark interacting with light degrees of freedom (quarks, antiquarks and gluons) that have four-momenta much less than the heavy-quark mass, m_Q. An example is a meson $\bar{Q}q$ containing one heavy quark, Q, and one light quark, q. The hadronic length scale is $r_{\rm QCD} \sim 1/\Lambda_{\rm QCD}$ and typical momenta exchanged are of the order of $\Lambda_{\rm QCD}$. The heavy quark's four-velocity, $v^\mu = p_Q^\mu/m_Q$, thus changes by an amount of order $\Lambda_{\rm QCD}/m_B$, which goes to zero as $m_Q \to \infty$. The appropriate effective theory is then the limit of QCD when $m_Q \to \infty$, with v^μ constant. This is known as the Heavy Quark Effective Theory (HQET) [82, 66, 74].

Since the heavy quark's Compton wavelength, $\lambda_Q \sim 1/m_Q$, is much less than the confinement scale, $r_{\rm QCD}$, the light degrees of freedom cannot resolve the heavy quark's quantum numbers beyond its static colour charge. Consequently, its mass (and hence flavour) and spin become irrelevant in the heavy-quark limit and the effective theory exhibits a spin-flavour symmetry, namely $SU(2N_h)$, where N_h is the number of heavy flavours. It is interesting to compare this approximate symmetry with chiral symmetry, $SU(3)_L \times SU(3)_R$, which manifests itself in the limit where the light-quark masses, m_u, m_d and m_s, are taken to zero. Approximate chiral symmetry is thus a result of the fact that m_u, m_d, $m_s \ll \Lambda_{\rm QCD}$: it exists even though the light-

quark masses are not even roughly equal. Similarly, heavy-quark symmetry results from the fact that m_b, $m_c \gg \Lambda_{\rm QCD}$, and exists even though m_b is not close to m_c.[1] Corrections to predictions in the chiral limit, $m_q \to 0$, are of order $m_q/\Lambda_{\rm QCD}$. We shall see that corrections in HQET can be systematically incorporated and are of order $\Lambda_{\rm QCD}/m_Q$.

2.1.1 The HQET Lagrangian

The terms in the QCD Lagrangian pertaining to the heavy quark are

$$\mathcal{L}_{QCD} = \bar{Q}(i\not{D} - m_Q)Q\,. \tag{2.1}$$

We wish to expand this in inverse powers of m_Q in order to be able to take the heavy-quark limit. This can be done by scaling out the factor $\exp(-im_Q v\cdot x)$ from the field Q. Thus, write

$$Q(x) = e^{-im_Q v\cdot x}\left[h_v(x) + \chi_v(x)\right], \tag{2.2}$$

where

$$h_v(x) = e^{+im_Q v\cdot x}\frac{1+\not{v}}{2}Q(x)\,, \qquad \chi_v(x) = e^{+im_Q v\cdot x}\frac{1-\not{v}}{2}Q(x)\,. \tag{2.3}$$

Note that $v^2 = 1$, so it follows from Eq. (2.3) that $\not{v}h_v = h_v$ and $\not{v}\chi_v = -\chi_v$. Substituting Eq. (2.2) into Eq. (2.1) and using these facts, we obtain

$$\begin{aligned}
\mathcal{L} &= \bar{h}_v i\not{D} h_v + \bar{\chi}_v i\not{D}\chi_v - 2m_Q\bar{\chi}_v\chi_v + \bar{h}_v i\not{D}\chi_v + \bar{\chi}_v i\not{D}h_v \\
&= \bar{h}_v\frac{1+\not{v}}{2}i\not{D}\frac{1+\not{v}}{2}h_v + \bar{\chi}_v\frac{1-\not{v}}{2}i\not{D}\frac{1-\not{v}}{2}\chi_v - 2m_Q\bar{\chi}_v\chi_v + \bar{h}_v i\not{D}\chi_v + \bar{\chi}_v i\not{D}h_v \\
&= \bar{h}_v iv\cdot D h_v - \bar{\chi}_v(iv\cdot D + 2m_Q)\chi_v + \bar{h}_v i\not{D}\chi_v + \bar{\chi}_v i\not{D}h_v\,.
\end{aligned} \tag{2.4}$$

[1] Recall that the top quark does not hadronize, and so is not relevant here.

Now, define the transverse component of a four-vector, V^μ, to be

$$V_T^\mu = V^\mu - v \cdot V v^\mu , \tag{2.5}$$

i.e. so that $v \cdot V_T = 0$. Then, since $\bar{h}_v \not{v} \chi_v = 0$, we can replace $\not{D}$ by $\not{D}_T$ in the last two terms in Eq. (2.4).

Since χ_v has mass $2m_Q$, we integrate it out. At tree level, we can eliminate χ_v using its equation of motion, which we obtain by varying the Lagrangian with respect to $\bar{h}_v$. This implies that

$$\chi_v = \frac{1}{iv \cdot D + 2m_Q} i \not{D}_T h_v . \tag{2.6}$$

Since we have factorized out the large component of the momentum in defining the heavy-quark field, the covariant derivative acting on h_v scales like $\Lambda_{\rm QCD}$. Hence Eq. (2.6) shows that χ_v is suppressed by $\Lambda_{\rm QCD}/m_Q$. This is as expected, since h_v is off-shell by only a small amount.

Substituting Eq. (2.6) into Eq. (2.4), we obtain

$$\begin{aligned} \mathcal{L} &= \bar{h}_v iv \cdot D h_v + \bar{h}_v \, i \not{D}_T \frac{1}{2m_Q + iv \cdot D} \, i \not{D}_T \, h_v \\ &= \bar{h}_v iv \cdot D h_v + \frac{1}{2m_Q} \bar{h}_v \, i \not{D}_T \, i \not{D}_T h_v + \mathcal{O}\left(\frac{1}{m_Q^2} \right) . \end{aligned} \tag{2.7}$$

The second term can be recast in a physically instructive form. First note that

$$\begin{aligned} \not{D}_T \not{D}_T &= \gamma^\mu \gamma^\nu D_\mu^T D_\nu^T = \frac{1}{2} \{ \gamma^\mu, \gamma^\nu \} D_\mu^T D_\nu^T + \frac{1}{2} [\gamma^\mu, \gamma^\nu] D_\mu^T D_\nu^T \\ &= D_T^2 + \frac{1}{4} [\gamma^\mu, \gamma^\nu] [D_\mu^T, D_\nu^T] . \end{aligned} \tag{2.8}$$

In terms of $\sigma^{\mu\nu} = \frac{i}{2}[\gamma^\mu, \gamma^\nu]$ and $igG_{\mu\nu} = [iD_\mu, iD_\nu]$, we then have

$$\bar{h}_v \not{D}_T \not{D}_T h_v = \bar{h}_v D_T^2 h_v - \frac{g}{2} \bar{h}_v \sigma^{\mu\nu} G_{\mu\nu} h_v . \tag{2.9}$$

where the fact that $\not{v} h_v = h_v$ allows us to drop T labels in the second term.

Our HQET Lagrangian is thus

$$\mathcal{L} = \mathcal{L}_0 + \mathcal{L}_1 + \cdots , \tag{2.10}$$

where

$$\mathcal{L}_0 = \bar{h}_v i v \cdot D h_v , \tag{2.11}$$

$$\mathcal{L}_1 = -\frac{1}{2m_Q} \bar{h}_v D_T^2 h_v + \frac{g}{4m_Q} \bar{h}_v \sigma^{\mu\nu} G_{\mu\nu} h_v . \tag{2.12}$$

We also have the relation between the QCD and HQET heavy-quark fields: Eqs. (2.2) and (2.6) give

$$Q = e^{-i m_Q v \cdot x} \left[1 + \frac{i \not{D}_T}{2m_Q} \right] h_v + \mathcal{O}\left(\frac{1}{m_Q^2} \right) . \tag{2.13}$$

We can see that the leading-order Lagrangian $\mathcal{L}_0$ has both spin symmetry and flavour symmetry. The first term in the subleading Lagrangian $\mathcal{L}_1$ corresponds to kinetic energy. It preserves the spin symmetry but breaks the flavour symmetry, since it explicitly involves m_Q. The second term in $\mathcal{L}_1$ corresponds to the (chromo)magnetic moment and breaks both flavour symmetry and spin symmetry, since it has a non-trivial Dirac structure.

When we take into account perturbative loop corrections, the chromomagnetic operator acquires a scale-dependent Wilson coefficient, $c_F(\mu)$. The above tree-level matching shows that $c_F(m_Q) = 1 + \mathcal{O}\big(\alpha_s(m_Q)\big)$. In contrast, the kinetic operator remains unrenormalized to all orders in perturbation theory. The reason for this will be discussed in the next subsection.

We can now read off the HQET Feynman rules from $\mathcal{L}_0$. Write the momentum of the heavy quark as

$$p_Q^\mu = m_Q v^\mu + k^\mu , \tag{2.14}$$

where the *residual* momentum k is of order $\Lambda_{\rm QCD}$. For the heavy-quark propagator, we then have

$$\left(\frac{1+\not{v}}{2}\right)\frac{i}{v\cdot k+i\varepsilon}\,. \tag{2.15}$$

The vertex for interactions between a heavy quark and a gluon is given by

$$igv^\mu T^A\,. \tag{2.16}$$

The same rules result when one takes the heavy-quark limit of the corresponding QCD Feynman rules. For the vertex, note that it is always sandwiched between quark propagators, so one can insert factors of the projector $(1+\not{v})/2$. Thus,

$$\begin{aligned} igT^A\gamma^\mu &\to igT^A\frac{1+\not{v}}{2}\gamma^\mu\frac{1+\not{v}}{2} \\ &= igT^Av^\mu\frac{1+\not{v}}{2} \to igT^Av^\mu\,. \end{aligned} \tag{2.17}$$

Finally, note that the non-perturbative parameters λ_1 and λ_2 encountered in Chapter 1 are essentially matrix elements of the terms in $\mathcal{L}_2$:

$$\begin{aligned} \lambda_1 &= \frac{1}{2}\langle B|\bar{h}_v(iD)^2h_v|B\rangle\,, \\ \lambda_2 &= \frac{1}{6}\langle B|\bar{h}_v\frac{1}{2}g\sigma^{\mu\nu}G_{\mu\nu}h_v|B\rangle\,. \end{aligned} \tag{2.18}$$

At this order, one can use D_T^2 instead of D^2 in the definition of λ_1, using the equation of motion $v\cdot Dh_v=0$, i.e. the difference is higher order.

2.1.2 Reparameterization Invariance

Introducing v^μ establishes a preferred frame and hence breaks Lorentz invariance. This is restored order by order in $1/m_Q$ by *reparameterization invariance* (RPI) in v^μ [114]. The decomposition of the heavy quark's momentum in Eq. (2.14) is not

unique, since p_Q^μ is unchanged under

$$\begin{aligned} v^\mu &\rightarrow v^\mu + \epsilon^\mu/m_Q\,, \\ k^\mu &\rightarrow k^\mu - \epsilon^\mu\,, \end{aligned} \tag{2.19}$$

where $\epsilon \sim \Lambda_{\rm QCD}$. Whatever the choice of the four-velocity, it must satisfy $v^2 = 1$, which at linear order in ϵ implies that

$$v \cdot \epsilon = 0\,. \tag{2.20}$$

Furthermore, maintaining the constraint $\not{v} h_v = h_v$ requires

$$h_v \rightarrow h_v + \delta h_v\,, \tag{2.21}$$

such that

$$\left(\not{v} + \frac{\not{\epsilon}}{m_Q}\right)(h_v + \delta h_v) \;=\; h_v + \delta h_v\,. \tag{2.22}$$

Hence, at linear order we obtain

$$(1 - \not{v})\delta h_v \;=\; \frac{\not{\epsilon}}{m_Q} h_v\,. \tag{2.23}$$

One solution is

$$\delta h_v = \frac{\not{\epsilon}}{2m_Q} h_v\,. \tag{2.24}$$

Other solutions are related to this choice by field redefinitions.

Thus, RPI amounts to invariance under

$$\begin{aligned} v^\mu &\rightarrow v^\mu + \epsilon^\mu/m_Q\,, \\ h_v &\rightarrow e^{i\epsilon\cdot x}\left(1 + \frac{\not{\epsilon}}{2m_Q}\right) h_v\,, \end{aligned} \tag{2.25}$$

where the factor $e^{i\epsilon\cdot x}$ corresponds to $k \to k - \epsilon$.

Transforming $\mathcal{L}_0$ according to Eq. (2.25) and simplifying using Eq. (2.20) (e.g. Eq. (2.20) and $\not{v} h_v = h_v$ imply that $\bar{h}_v \not{\epsilon} h_v = 0$), we obtain

$$\delta\mathcal{L}_0 = \frac{1}{m_Q}\bar{h}_v(i\epsilon\cdot D)h_v\,. \tag{2.26}$$

The change in $\mathcal{L}_1$ is due entirely to the kinetic-energy term and precisely cancels the change in $\mathcal{L}_0$:

$$\delta\mathcal{L}_1 = -\frac{1}{m_Q}\bar{h}_v(i\epsilon\cdot D)h_v\,. \tag{2.27}$$

Thus $\mathcal{L} = \mathcal{L}_0 + \mathcal{L}_1$ is reparameterization invariant, provided that the coefficient of the kinetic-energy operator is exactly unity. On the other hand, the magnetic-moment term is not protected from being renormalized by RPI.

We shall see that SCET also possesses a reparameterization invariance that connects operators at different orders in the power counting. Hence, one can obtain information about Wilson coefficients at higher orders from knowledge of coefficients at lower orders.

2.2 $\mathrm{SCET_I}$

For processes that involve energetic light hadrons, there is an additional (intermediate) scale. HQET alone is not sufficient for describing the jet-like and soft degrees of freedom: one also requires SCET [22, 23, 33, 30]. The large mass of the B meson means that many of its decay channels fall into this category, including exclusive decays such as $B \to D\pi$ and inclusive decays in the endpoint region. Since the light particles move close to the light cone, it is convenient to use light-cone coordinates, in which one introduces light-like vectors n and $\bar{n}$ such that $n^2 = \bar{n}^2 = 0$ and $n\cdot\bar{n} = 2$. For example, one possible choice is $n^\mu = (1.0, 0.-1)$ and $\bar{n}^\mu = (1.0, 0.1)$. Any

four-vector, p^μ, can then be written as

$$p^\mu = n\cdot p\frac{\bar{n}^\mu}{2} + \bar{n}\cdot p\frac{n^\mu}{2} + p_\perp^\mu, \tag{2.28}$$

and one can refer to the components as $(p^+, p^-, p_\perp) = (n\cdot p, \bar{n}\cdot p, p_\perp)$. Note that $p^2 = p^+p^- + p_\perp^2$.

2.2.1 Modes and Power Counting

The fast, light hadrons have energies much larger than their invariant masses and are described by collinear modes. Collinear hadronic states in the n direction have momenta scaling as $Q(\lambda^2, 1, \lambda)$, where Q is the large energy scale in the physical process and λ is a suitable small parameter. For exclusive decays $\lambda \sim \Lambda_{\rm QCD}/Q$, whereas for inclusive decays $\lambda \sim \sqrt{\Lambda_{\rm QCD}/Q}$. For example, consider $B \to D\pi$. In its rest frame, the pion has momenta of the order of the confinement scale: $p^\mu \sim (\Lambda_{\rm QCD}, \Lambda_{\rm QCD}, \Lambda_{\rm QCD})$. Boosting this in the n direction gives $p^\mu \sim (\Lambda_{\rm QCD}^2/Q, Q, \Lambda_{\rm QCD})$. On the other hand, inclusive decays in the endpoint region have $m_X^2 \sim m_b\Lambda_{\rm QCD}$, and hence jet momenta scale as $p^\mu \sim (\Lambda_{\rm QCD}, Q, \sqrt{\Lambda_{\rm QCD}Q})$, with $Q \sim m_b$.

We see that the effective theory has two cases, which we refer to as SCET_I (which describes inclusive decays) and SCET_II (which describes exclusive decays). The relevant degrees of freedom and power counting for the associated momenta are summarized in Table 2.1, in which we distinguish between the power-counting parameters for SCET_I and SCET_II by renaming the latter η. Note that the ultrasoft (usoft)

EFT	Power-counting parameter	Modes	Momenta p^μ	p^2
SCET_I	$\lambda = \sqrt{\frac{\Lambda_{\rm QCD}}{Q}}$	collinear	$Q(\lambda^2, 1, \lambda)$	$Q^2\lambda^2$
		ultrasoft	$Q(\lambda^2, \lambda^2, \lambda^2)$	$Q^2\lambda^4$
SCET_II	$\eta = \frac{\Lambda_{\rm QCD}}{Q}$	collinear	$Q(\eta^2, 1, \eta)$	$Q^2\eta^2$
		soft	$Q(\eta, \eta, \eta)$	$Q^2\eta^2$

Table 2.1: Infrared degrees of freedom and power counting for momenta in SCET_I and SCET_II.

modes of $\mathrm{SCET_I}$ are actually the same as the soft modes of $\mathrm{SCET_{II}}$. Since this thesis deals with inclusive B decays in the shape function region, we shall henceforth discuss only $\mathrm{SCET_I}$.

The collinear fermion propagator can be obtained by expanding the standard QCD propagator to leading order in λ. This gives

$$\begin{aligned}\frac{i\not{p}}{p^2+i\epsilon} &\to i\frac{\not{n}}{2}\frac{\bar{n}\cdot p}{n\cdot p\bar{n}\cdot p+p_\perp^2+i\epsilon}\\ &= i\frac{\not{n}}{2}\frac{1}{n\cdot p+p_\perp^2/\bar{n}\cdot p+i\epsilon\,\mathrm{sign}(\bar{n}\cdot p)}\,.\end{aligned}\tag{2.29}$$

In any gauge, the collinear gluon propagator remains the same as in QCD. We can now derive the power counting of the SCET fields. This is done by assigning a scaling that makes the kinetic terms in the action of order λ^0, or, equivalently, by counting powers of λ in expressions for the two-point functions. For the collinear quark field, denoted by ξ_n, we have

$$\langle 0|T\xi_n(x)\bar{\xi}_n(0)|0\rangle = \int\frac{d^4p}{(2\pi)^4}e^{-ip\cdot x}\,i\frac{\not{n}}{2}\frac{\bar{n}\cdot p}{n\cdot p\bar{n}\cdot p+p_\perp^2+i\epsilon}\,.\tag{2.30}$$

Since $d^4p=(1/2)dp^+dp^-d^2p_\perp\sim\lambda^4$, the right-hand side scales as λ^2 and we obtain $\xi_n\sim\lambda$. For the collinear gluon field, A_c^μ,

$$\langle 0|TA_c^\mu(x)A_c^\nu(0)|0\rangle = \int\frac{d^4p}{(2\pi)^4}e^{-ip\cdot x}\,\frac{-i}{p^2+i\epsilon}\left[g^{\mu\nu}-(1-\alpha)\frac{p^\mu p^\nu}{p^2}\right]\,.\tag{2.31}$$

Here, some care is required. In a general covariant gauge, the scaling will be that of $p^\mu p^\nu$ and so A^μ scales like a collinear momentum. The scaling of the remaining fields can be derived in a similar fashion. Note that for ultrasoft fields the measure will scale as λ^8. There are no heavy collinear fields, since they have hard off-shellness ($p^2-m_b^2\sim Q^2$) and hence are integrated out. Table 2.2 summarizes the fields and their scaling properties.

	Collinear		Ultrasoft		
	quark	gluon	light quark	heavy quark	gluon
Field	$\xi_{n,p}$	$(A_n^+, A_n^-, A_n^\perp)$	q_{us}	h_v	A_{us}^μ
Scaling	λ	$(\lambda^2, 1, \lambda)$	λ^3	λ^3	λ^2

Table 2.2: Fields and their scaling in $\mathrm{SCET_I}$. In $\mathrm{SCET_{II}}$, soft quarks and gluons have the scalings $q_s \sim \eta^{3/2}$ and $A_s^\mu \sim \eta$.

2.2.2 Leading-Order Lagrangian

The procedure for obtaining the leading-order SCET Lagrangian is analogous to, albeit more complicated than, that for HQET, which was described in the previous section. We start with the QCD Lagrangian for massless quarks, namely

$$\mathcal{L} = \bar{\psi} i \not{D} \psi \,, \tag{2.32}$$

where $D^\mu = \partial^\mu - igA^\mu$. Later, the gauge field will be split into collinear and ultrasoft fields. Recall that in HQET the momentum was decomposed into large and residual pieces ($p = m_b v + k$), and the velocity v became a label on the fields. In SCET, one does something similar, writing

$$p \;=\; \tilde{p} + k, \qquad \text{where} \qquad \tilde{p} \equiv \frac{1}{2}(\bar{n}\cdot p) n + p_\perp \,, \tag{2.33}$$

and labelling a collinear field with its large momentum components, $\tilde{p}$. A phase factor involving $\tilde{p}$ is scaled out and the four-component spinor is separated into two two-component spinors (c.f. Eqs. (2.2) and (2.3)):

$$\begin{aligned} \psi(x) &= \sum_{\tilde{p}\neq 0} e^{-i\tilde{p}\cdot x} \left(\psi_{n,p}^+ + \psi_{n,-p}^-\right) \\ &= \sum_{\tilde{p}\neq 0} e^{-i\tilde{p}\cdot x} \left(\xi_{n,p} + \xi_{\bar{n},p}\right) \,, \end{aligned} \tag{2.34}$$

where the superscript $+$ $(-)$ corresponds to particles (antiparticles) and

$$\xi_{n,p} \;=\; \frac{\not{n}\bar{\not{n}}}{4}\left(\psi_{n,p}^+ + \psi_{n,-p}^-\right) \,, \qquad \xi_{\bar{n},p} = \frac{\bar{\not{n}}\not{n}}{4}\left(\psi_{n,p}^+ + \psi_{n,-p}^-\right) \,. \tag{2.35}$$

Note that $\not{n}\not{\bar{n}}/4 + \not{\bar{n}}\not{n}/4 = 1$. We do not include $\tilde{p} = 0$ in the sum in Eq. (2.34), because that mode is covered by the field q_{us} (which one must include when deriving the subleading Lagrangians). Equation (2.35) implies that

$$\begin{aligned} \frac{\not{n}\not{\bar{n}}}{4}\xi_{n,p} &= \xi_{n,p}\,, \quad \not{n}\xi_{n,p} = 0\,, \\ \frac{\not{\bar{n}}\not{n}}{4}\xi_{\bar{n},p} &= \xi_{\bar{n},p}\,, \quad \not{\bar{n}}\xi_{\bar{n},p} = 0\,. \end{aligned} \tag{2.36}$$

Substituting Eq. (2.34) into Eq. (2.32) and using the relations above, we obtain

$$\begin{aligned} \mathcal{L} = \sum_{\tilde{p},\tilde{p}'} e^{-i(\tilde{p}-\tilde{p}')\cdot x} \Big[& \bar{\xi}_{n,p'}\frac{\not{\bar{n}}}{2}(in\cdot D)\xi_{n,p} + \bar{\xi}_{\bar{n},p'}\frac{\not{n}}{2}(\bar{n}\cdot p + i\not{\bar{n}}\cdot D)\xi_{\bar{n},p} \\ & + \bar{\xi}_{n,p'}(\not{p}_\perp + i\not{D}_\perp)\xi_{\bar{n},p} + \bar{\xi}_{\bar{n},p'}(\not{p}_\perp + i\not{D}_\perp)\xi_{n,p} \Big]\,. \end{aligned} \tag{2.37}$$

The small-component field $\xi_{\bar{n},p}$ is integrated out by using its equation of motion. By varying the Lagrangian with respect to $\bar{\xi}_{\bar{n},p'}$, this is found to be

$$\xi_{\bar{n},p} = \frac{1}{\bar{n}\cdot p + i\bar{n}\cdot D}(\not{p}_\perp + i\not{D}_\perp)\frac{\not{\bar{n}}}{2}\xi_{n,p}\,, \tag{2.38}$$

Substituting Eq. (2.38) into Eq. (2.37) gives

$$\mathcal{L} = \sum_{\tilde{p},\tilde{p}'} e^{-i(\tilde{p}-\tilde{p}')\cdot x}\bar{\xi}_{n,p'}\left[in\cdot D + (\not{p}_\perp + i\not{D}_\perp)\frac{1}{\bar{n}\cdot p + i\bar{n}\cdot D}(\not{p}_\perp + i\not{D}_\perp)\right]\frac{\not{\bar{n}}}{2}\xi_{n,p}\,. \tag{2.39}$$

The collinear gluon field has large momentum components, so it is useful to rescale it, as we did with the collinear quark field:

$$A_c^\mu(x) = \sum_{\tilde{q}} e^{-i\tilde{q}\cdot x}A_{n,q}^\mu(x)\,. \tag{2.40}$$

One can then factorize out the large phases from operators with arbitrary numbers of collinear quarks and gluons by introducing a *label operator*, $\mathcal{P}^\mu = \frac{n^\mu}{2}\bar{\mathcal{P}} + \mathcal{P}_\perp^\mu$ [33]. This acts on the large labels of a product of fields as follows: for an arbitrary function

f,

$$
\begin{aligned}
& f(\bar{\mathcal{P}})\,\phi^\dagger_{q_1}\cdots\phi^\dagger_{q_m}\phi_{p_1}\cdots\phi_{p_n} \qquad (2.41)\\
&= f(\bar{n}\cdot p_1+\cdots+\bar{n}\cdot p_n-\bar{n}\cdot q_1-\cdots-\bar{n}\cdot q_m)\,\phi^\dagger_{q_1}\cdots\phi^\dagger_{q_m}\phi_{p_1}\cdots\phi_{p_n}\,,
\end{aligned}
$$

with an analogous equation for $\mathcal{P}_\perp$. Here, ϕ_p can be a collinear quark, $\xi_{n,p}$, or a collinear gluon, $A^\mu_{n,p}$. The label operator thus satisfies

$$
i\partial^\mu e^{-ip\cdot x}\phi_{n,p}(x) \;=\; e^{-ip\cdot x}(\mathcal{P}^\mu+i\partial^\mu)\phi_{n,p}(x), \qquad (2.42)
$$

which facilitates the explicit separation of $\mathcal{O}(\lambda^{0,1})$ and $\mathcal{O}(\lambda^2)$ contributions, since $i\partial_\mu$ acting on $\xi_{n,p}$ or $A_{n,p}$ gives a momentum k of order λ^2.

Now it is straightforward to expand Eq. (2.39) in powers of λ. The resulting leading-order Lagrangian is

$$
\mathcal{L}^{(0)}_{\xi\xi} \;=\; e^{-ix\cdot\mathcal{P}}\sum_{\text{labels}}\bar{\xi}_{n,p'}\left[in\cdot D+\not{D}^\perp_c\frac{1}{i\bar{n}\cdot D^c}\not{D}^\perp_c\right]\frac{\not{\bar{n}}}{2}\xi_{n,p}\,, \qquad (2.43)
$$

where

$$
\begin{aligned}
in\cdot D &= in\cdot\partial+gn\cdot A_{n,q}+gn\cdot A_{us}\,, \qquad (2.44)\\
i\bar{n}\cdot D_c &= \bar{\mathcal{P}}+g\bar{n}\cdot A_{n,q}\,,\\
iD^{\perp\mu}_c &= \mathcal{P}^\mu_\perp+gA^{\perp\mu}_{n,q}\,.
\end{aligned}
$$

One can adopt the convention that field labels are summed over. Furthermore, the overall phase factor imposes conservation of large momenta (label conservation). The reason for this is that the exponential of a large phase will oscillate rapidly, and so the integral of this against a slowly-varying function will tend to a delta function as $\lambda\to 0$. One can therefore also suppress the phase factor if one remembers to maintain label conservation. Consequently, the Lagrangian can be written in the form [23, 33]

$$
\mathcal{L}^{(0)}_{\xi\xi} \;=\; \bar{\xi}_{n,p'}\left[in\cdot D+\not{D}^\perp_c\frac{1}{i\bar{n}\cdot D^c}\not{D}^\perp_c\right]\frac{\not{\bar{n}}}{2}\xi_{n,p}\,. \qquad (2.45)
$$

Both terms are of order λ^4 in the power counting. Since $p \cdot x = (1/2)p^+x^- + (1/2)p^-x^+ + p_\perp \cdot x_\perp$, x^μ scales as $(x^+, x^-, x_\perp^\mu) \sim (1, \lambda^{-2}, \lambda^{-1})$. Hence, $d^4x \sim \lambda^{-4}$ and the action scales as λ^0.

This was a tree-level derivation. One can, however, use gauge invariance and reparameterization invariance to show in full generality that Eq. (2.43) is the unique leading-order collinear-quark Lagrangian [30, 118]. From this, one can read off the Feynman rules for interactions involving a collinear quark. These are shown in Fig. 2-1.

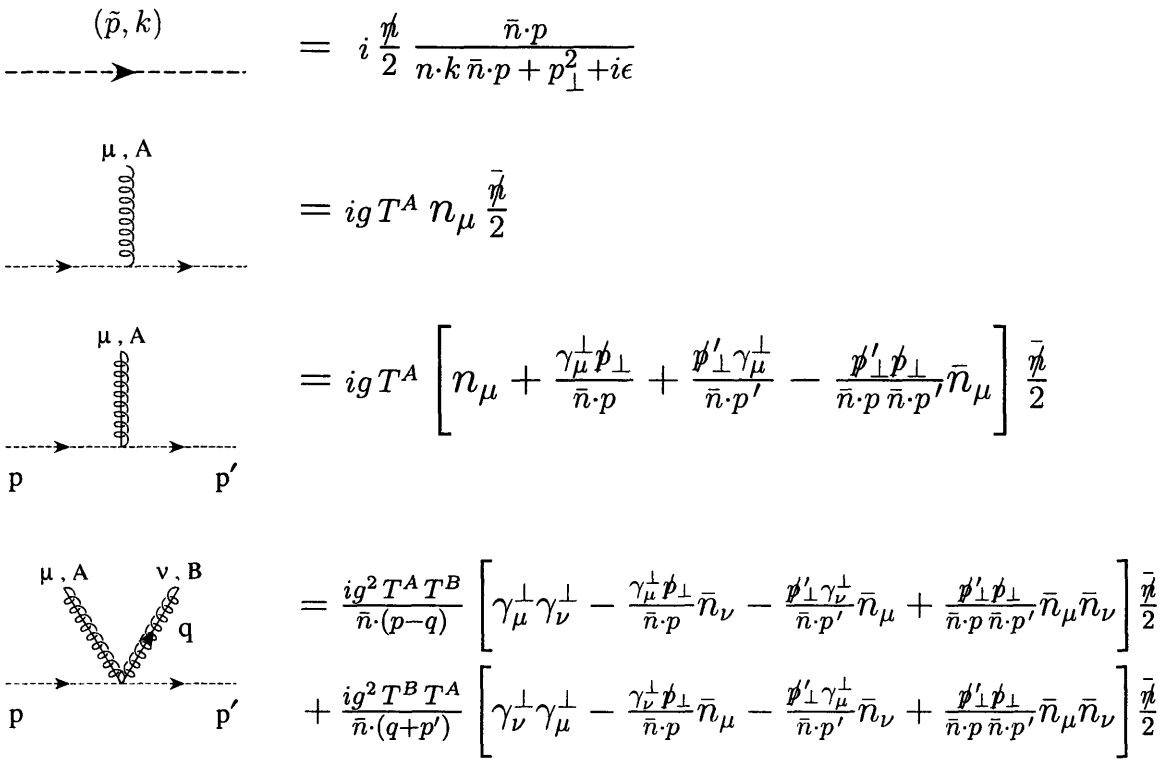

$$= i\,\frac{\bar{n}\!\!\!/}{2}\,\frac{\bar{n}\cdot p}{n\cdot k\,\bar{n}\cdot p + p_\perp^2 + i\epsilon}$$

$$= ig\,T^A\,n\!\!\!/_\mu\,\frac{\bar{n}\!\!\!/}{2}$$

$$= ig\,T^A\left[n\!\!\!/_\mu + \frac{\gamma_\mu^\perp p\!\!\!/_\perp}{\bar{n}\cdot p} + \frac{p\!\!\!/'_\perp \gamma_\mu^\perp}{\bar{n}\cdot p'} - \frac{p\!\!\!/'_\perp p\!\!\!/_\perp}{\bar{n}\cdot p\,\bar{n}\cdot p'}\bar{n}\!\!\!/_\mu\right]\frac{\bar{n}\!\!\!/}{2}$$

$$= \frac{ig^2 T^A T^B}{\bar{n}\cdot(p-q)}\left[\gamma_\mu^\perp\gamma_\nu^\perp - \frac{\gamma_\mu^\perp p\!\!\!/_\perp}{\bar{n}\cdot p}\bar{n}\!\!\!/_\nu - \frac{p\!\!\!/'_\perp\gamma_\nu^\perp}{\bar{n}\cdot p'}\bar{n}\!\!\!/_\mu + \frac{p\!\!\!/'_\perp p\!\!\!/_\perp}{\bar{n}\cdot p\,\bar{n}\cdot p'}\bar{n}\!\!\!/_\mu\bar{n}\!\!\!/_\nu\right]\frac{\bar{n}\!\!\!/}{2}$$

$$+ \frac{ig^2 T^B T^A}{\bar{n}\cdot(q+p')}\left[\gamma_\nu^\perp\gamma_\mu^\perp - \frac{\gamma_\nu^\perp p\!\!\!/_\perp}{\bar{n}\cdot p}\bar{n}\!\!\!/_\mu - \frac{p\!\!\!/'_\perp\gamma_\mu^\perp}{\bar{n}\cdot p'}\bar{n}\!\!\!/_\nu + \frac{p\!\!\!/'_\perp p\!\!\!/_\perp}{\bar{n}\cdot p\,\bar{n}\cdot p'}\bar{n}\!\!\!/_\mu\bar{n}\!\!\!/_\nu\right]\frac{\bar{n}\!\!\!/}{2}$$

Figure 2-1: Collinear-quark Feynman rules in SCET [23].

The Lagrangian for collinear gluons can be obtained in a similar manner. The result is [30]

$$\mathcal{L}_{cg}^{(0)} = \frac{1}{2g^2}\mathrm{tr}\left\{\left([i\mathcal{D}^\mu + gA_{n.q}^\mu, i\mathcal{D}^\nu + gA_{n.q'}^\nu]\right)^2\right\} + \text{g.f.}\,, \tag{2.46}$$

where $i\mathcal{D}^\mu = i\frac{\bar{n}^\mu}{2}n\cdot D_{us} + \mathcal{P}_\perp^\mu + \bar{\mathcal{P}}\frac{n^\mu}{2}$ (with $iD_{us}^\mu = i\partial^\mu + gA_{us}^\mu$) and g.f. stands for

gauge-fixing terms.

2.2.3 Decoupling Ultrasoft Fields

In the leading-order collinear Lagrangians for quarks and gluons, $\mathcal{L}^{(0)}_{\xi\xi} + \mathcal{L}^{(0)}_{cg}$, the usoft gluons can be decoupled from the collinear fields [30]. This is achieved by introducing the usoft Wilson line

$$Y = Y(x) = P \exp\left(ig \int_{-\infty}^{0} ds\, n\cdot A_{us}(x+ns)\right), \tag{2.47}$$

where P denotes path ordering, and making the field redefinitions

$$\xi_n \to Y \xi_n\,, \qquad A_n^\mu \to Y A_n^\mu Y^\dagger\,. \tag{2.48}$$

The Wilson line satisfies $[in\cdot D_{us} Y] = 0$, which implies that

$$Y^\dagger n\cdot D_{us} Y = n\cdot\partial\,. \tag{2.49}$$

Therefore, the result of making the substitutions (2.48) in Eq. (2.45) is

$$\mathcal{L}^{(0)}_{\xi\xi} \;=\; \bar\xi_{n,p'}\left[in\cdot\partial + gn\cdot A_{n,q} + \not{D}^\perp_c \frac{1}{i\bar n\cdot D^c} \not{D}^\perp_c\right]\frac{\not{\bar n}}{2}\xi_{n,p}\,, \tag{2.50}$$

since Y commutes with $\mathcal{P}$. Likewise, in the gluon Lagrangian (2.46),

$$i\mathcal{D}^\mu \to i\mathcal{D}^\mu_{(0)} = i\frac{\bar n^\mu}{2} n\cdot\partial + \mathcal{P}^\mu_\perp + \bar{\mathcal{P}}\frac{n^\mu}{2}\,. \tag{2.51}$$

We have found that the leading-order Lagrangians are independent of the usoft fields after the field redefinition. The usoft fields have not been removed entirely, since they appear in external operators or currents. They also appear in subleading collinear Lagrangians. Nevertheless, this result is an important ingredient in derivations of soft-collinear factorization theorems.

2.2.4 Reparameterizaton Invariance

We saw previously that, in HQET, Lorentz symmetry manifests itself as reparameterization invariance. Similarly, RPI appears in SCET, in which it comprises a larger set of transformations.The choice of the light-cone vectors n and $\bar{n}$ must satisfy

$$n^2 = \bar{n}^2 = 0, \quad n\cdot\bar{n} = 2\,, \tag{2.52}$$

but otherwise is arbitrary. Therefore one can make the following reparameterization (RPI) transformations [59, 118, 130]:

$$\text{(I)}\begin{cases} n_\mu \to n_\mu + \Delta^\perp_\mu \\ \bar{n}_\mu \to \bar{n}_\mu \end{cases} \quad \text{(II)}\begin{cases} n_\mu \to n_\mu \\ \bar{n}_\mu \to \bar{n}_\mu + \varepsilon^\perp_\mu \end{cases} \quad \text{(III)}\begin{cases} n_\mu \to (1+\alpha)\, n_\mu \\ \bar{n}_\mu \to (1-\alpha)\, \bar{n}_\mu \end{cases}, \tag{2.53}$$

where $\Delta^\perp \sim \lambda$, $\varepsilon^\perp \sim \lambda^0$ and $\alpha \sim \lambda^0$ are infinitesimal parameters. (In order to maintain Eq. (2.52) to linear order, $\Delta^\perp$ and $\varepsilon^\perp$ must satisfy $\bar{n}\cdot\varepsilon^\perp = n\cdot\varepsilon^\perp = \bar{n}\cdot\Delta^\perp = n\cdot\Delta^\perp = 0$.) Each parameter is assigned the largest scaling that leaves the power counting of collinear momenta intact. To derive the way in which the decomposition of a vector V^μ is changed by the transformations, we impose the condition that V^μ itself is invariant, i.e. $V^\mu \to V^\mu$. For example, under type-I transformations the components of $V^\mu = (n\cdot V, \bar{n}\cdot V, V^\mu_\perp)$ change to

$$\begin{aligned} n\cdot V &\to (n+\Delta^\perp)\cdot V = n\cdot V + \Delta^\perp\cdot V^\perp\,, \\ \bar{n}\cdot V &\to \bar{n}\cdot V\,, \\ V^\mu_\perp &= V^\mu - n\cdot V\frac{\bar{n}^\mu}{2} - \bar{n}\cdot V\frac{n^\mu}{2} \\ &\to V^\mu - (n+\Delta^\perp)\cdot V\frac{\bar{n}^\mu}{2} - \bar{n}\cdot V\frac{n^\mu+\Delta^\mu_\perp}{2} \\ &= V^\mu_\perp - \frac{\Delta^\mu_\perp}{2}\bar{n}\cdot V - \frac{\bar{n}^\mu}{2}\Delta^\perp\cdot V^\perp\,. \end{aligned} \tag{2.54}$$

Similarly, under type-II transformations,

$$(n\cdot V, \bar{n}\cdot V, V^\mu_\perp) \to \left(n\cdot V, \bar{n}\cdot V + \varepsilon^\perp\cdot V^\perp, V^\mu_\perp - \frac{\varepsilon^\mu_\perp}{2}n\cdot V - \frac{n^\mu}{2}\varepsilon^\perp\cdot V^\perp\right). \tag{2.55}$$

We can now see that if V^μ is collinear, scaling as $(\lambda^2, 1, \lambda)$, then it will stay collinear after a type-I (type-II) transformation if $\Delta^\perp \sim \lambda$ ($\varepsilon^\perp \sim \lambda^0$). Just as h_v transforms to maintain the condition $\not{v} h_v = h v$ in HQET, ξ_n transforms to maintain $\frac{\not{n}\bar{\not{n}}}{4}\xi_n = \xi_n$, $\not{n}\xi_n = 0$. One can derive the transformations as follows. From Eqs. (2.34) and (2.38), we find

$$\psi = \sum_{p,q} e^{-i\mathcal{P}\cdot x}\left[1 + \frac{1}{\bar{n}\cdot\mathfrak{D}}\not{\mathcal{D}}^\perp\frac{\bar{\not{n}}}{2}\right]\xi_{n,p}\,, \tag{2.56}$$

where the covariant derivative $\mathfrak{D}$ includes both ∂ and $\mathcal{P}$. This is invariant under the RPI transformations, i.e.

$$\begin{aligned}\sum_{p,q} e^{-i\mathcal{P}\cdot x}\left[1 + \frac{1}{\bar{n}\cdot\mathfrak{D}}\not{\mathcal{D}}_\perp\frac{\bar{\not{n}}}{2}\right]\xi_{n,p} \\ = \sum_{p',q'} e^{-i\mathcal{P}\cdot x}\left[1 + \frac{1}{\bar{n}\cdot\mathfrak{D}'}\not{\mathcal{D}}'_\perp\frac{\bar{\not{n}}'}{2}\right]\xi'_{n,p'}\,,\end{aligned} \tag{2.57}$$

where the prime indicates a transformed quantity. Multiplying both sides of this equation by $\frac{\not{n}'\bar{\not{n}}'}{4}$ leads to the following expressions for $\xi'_{n,p}$ under the three RPI transformations:

$$\begin{aligned}\xi_{n,p} &\xrightarrow{\text{I}} \left(1 + \frac{1}{4}\not{\mathbb{A}}^\perp\bar{\not{n}}\right)\xi_{n,p}\,, \\ \xi_{n,p} &\xrightarrow{\text{II}} \left(1 + \frac{1}{2}\not{\ell}^\perp\frac{1}{\bar{n}\cdot\mathfrak{D}}\mathfrak{D}^\perp\right)\xi_{n,p}\,, \\ \xi_{n,p} &\xrightarrow{\text{III}} \xi_{n,p}\,.\end{aligned} \tag{2.58}$$

We summarize all of these results in Table 2.3.

Type I	Type II	Type III
$n \to n + \Delta^\perp$	$n \to n$	$n \to (1+\alpha)n$
$\bar{n} \to \bar{n}$	$\bar{n} \to \bar{n} + \varepsilon^\perp$	$\bar{n} \to (1-\alpha)\bar{n}$
$n \cdot V \to n \cdot V + \Delta^\perp \cdot V^\perp$	$n \cdot V \to n \cdot V$	$n \cdot V \to (1+\alpha) n \cdot V$
$\bar{n} \cdot V \to \bar{n} \cdot V$	$\bar{n} \cdot V \to \bar{n} \cdot V + \varepsilon^\perp \cdot V^\perp$	$\bar{n} \cdot V \to (1-\alpha)\bar{n} \cdot V$
$V_\perp^\mu \to V_\perp^\mu - \frac{\Delta_\perp^\mu}{2} \bar{n} \cdot V$ $- \frac{\bar{n}^\mu}{2} \Delta^\perp \cdot V_\perp$	$V_\perp^\mu \to V_\perp^\mu - \frac{\varepsilon_\perp^\mu}{2} n \cdot V$ $- \frac{n^\mu}{2} \varepsilon^\perp \cdot V_\perp$	$V_\perp^\mu \to V_\perp^\mu$
$\xi_n \to \left(1 + \frac{1}{4} \not{\Delta}^\perp \not{\bar{n}}\right) \xi_n$	$\xi_n \to \left(1 + \frac{1}{2} \not{\varepsilon}^\perp \frac{1}{\bar{n} \cdot \mathcal{D}} \not{\mathcal{D}}^\perp\right) \xi_n$	$\xi_n \to \xi_n$
$W \to W$	$W \to \left[\left(1 - \frac{1}{\bar{n} \cdot D_c} \varepsilon^\perp \cdot D_c^\perp\right) W\right]$	$W \to W$

Table 2.3: Effect of type-I, II and III RPI transformations. V^μ is a vector, which may be the covariant derivative. For completeness, the table includes the transformation of W, which is the Wilson line constructed from $\bar{n} \cdot A_c$ gluons.

2.3 Heavy-to-light Currents

The weak-decay processes that we are studying have effective Hamiltonians of the form

$$\mathcal{H}_{\rm eff} \;=\; -\frac{4G_F}{\sqrt{2}} V_{\rm CKM} C(\mu) J_{\rm had}\, J\,, \tag{2.59}$$

which involves the QCD current $J_{\rm had} = \bar{q}\Gamma b$ (with the relevant Dirac structure, Γ) and the leptonic or photonic current J. For example, for the decays $B \to X_u \ell \bar{\nu}$ and $B \to X_s \gamma$ the hadronic currents are

$$J_\mu^u \;=\; \bar{u}\,\gamma^\mu P_L b \qquad \text{and} \qquad J_\mu^s = \bar{s}\, i\sigma_{\mu\nu} q^\nu P_R\, b\,, \tag{2.60}$$

respectively (the latter coming from the operator $\mathcal{O}_7$). In the endpoint region, in which the light quark is energetic, $\bar{q}\Gamma b$ is matched on to an SCET current. With no collinear gluon, we simply obtain $\bar{\xi}_n \Gamma h_v$. However, since $\bar{n} \cdot A_n \sim \lambda^0$, an arbitrary number of such gluons can be included without inducing any power suppression.

Consider then the case with one $A^-_{n,q}$ gluon attached to the heavy-quark line. The propagator in this diagram has momentum

$$\begin{aligned} p^\mu &= m_b v^\mu + \frac{n^\mu}{2}\bar{n}\cdot q + \mathcal{O}(\lambda) \\ \Rightarrow p^2 - m_b^2 &= n\cdot v m_b \bar{n}\cdot q + \cdots \sim m_b^2 \,. \end{aligned} \tag{2.61}$$

This large off-shellness means it must be integrated out. Expanding to lowest order in λ, we obtain

$$\begin{aligned} \bar{\xi}_n \Gamma \frac{i(\not{p}+m_b)}{p^2-m_b^2} igT^A \gamma^\mu h_v &\to -g\bar{\xi}_n\Gamma \frac{\left(m_b(1+\not{v}) + \frac{\not{n}}{2}\bar{n}\cdot q\right)}{n\cdot v m_b \bar{n}\cdot q}\frac{\not{n}}{2}\bar{n}^\mu T^A h_v \\ &= -\frac{g\bar{n}^\mu}{\bar{n}\cdot q}\bar{\xi}_n \Gamma T^A \frac{\left(\frac{\not{n}}{2}(1-\not{v}) + n\cdot v\right)}{n\cdot v} h_v \\ &= -\frac{g\bar{n}^\mu}{\bar{n}\cdot q}\bar{\xi}_n \Gamma T^A h_v \,. \end{aligned} \tag{2.62}$$

Thus, the Feynman rule for the SCET heavy-to-light current with no (one) gluon is $\Gamma^\mu \;\; (-g\bar{n}^\mu/\bar{n}\cdot q \Gamma^\mu T^A)$. When we add arbitrarily many A^-_n gluons, we obtain ΓW, where W is the Wilson line built out of A^-_n gluons:

$$\begin{aligned} W &= \sum_{m=0}^{\infty}\sum_{\text{perms}} \frac{(-g)^m}{m!} \frac{\bar{n}\cdot A_{n,q_m}\cdots \bar{n}\cdot A_{n,q_1}}{\bar{n}\cdot q_1 \bar{n}\cdot(q_1+q_2)\cdots \bar{n}\cdot(\sum_{i=1}^m q_i)} \\ &= \left[\sum_{\text{perms}} \exp\left(\frac{-g\bar{n}\cdot A_{n,q}}{\bar{\mathcal{P}}}\right)\right] , \end{aligned} \tag{2.63}$$

where "perms" means all permutations of the indices $1,\ldots,m$. W satisfies the equation $[i\bar{n}\cdot D_c W] = 0$, from which it follows that $f(i\bar{n}\cdot D_c) = W f(\bar{\mathcal{P}}) W^\dagger$.

The resulting heavy-to-light current is thus [23]

$$J = C_i(\mu, \bar{\mathcal{P}})\bar{\xi}_{n.p} W \Gamma h_v \,, \tag{2.64}$$

in which the Wilson coefficient may depend upon the large component of the total jet momentum.

The form of this current is actually determined by gauge symmetry [33, 30]. The allowed gauge transformations are those that leave us within $\mathrm{SCET_I}$. We are left with two classes, namely collinear and ultrasoft gauge transformations, denoted by $\mathcal{U}_c$ and V_{us}, respectively. These are defined by the scalings $\partial^\mu \mathcal{U}_c(x) \sim Q(\lambda^2, 1, \lambda)$ and $\partial^\mu V_{us}(x) \sim Q\lambda^2$. Under a collinear gauge transformation,

$$\begin{aligned} \xi_n &\to \mathcal{U}_c \xi_n \,, \\ A_n &\to \mathcal{U}_c A_n \mathcal{U}_c^\dagger + \frac{i}{g} \mathcal{U}_c [iD \,, \mathcal{U}_c^\dagger] \,, \\ W &\to \mathcal{U}_c W \,, \end{aligned} \tag{2.65}$$

where $\mathcal{U}_c \xi_n$ is shorthand notation for $\sum_q (\mathcal{U}_c)_{p-q} \xi_{n,q}$. Ultrasoft fields are not transformed by $\mathcal{U}_c$, since otherwise they would not maintain their momentum scaling.

We can now see that $\bar{\xi}_{n,p} W$ is a gauge-invariant block. The current $\bar{\xi}_{n,p} W \Gamma h_v$ is gauge invariant, whereas $\bar{\xi}_{n,p} \Gamma h_v$ is not.

We finish this section by noting that the Fourier transform of the momentum-space Wilson line is

$$W_n(y) \;=\; P \exp\left(ig \int_{-\infty}^{y} ds\, \bar{n} \cdot A_n(s\bar{n}) \right) . \tag{2.66}$$

Recall that we have already encountered an ultrasoft Wilson line in position space, Y(x), given by Eq. (2.47). This is the Fourier transform of

$$Y \;=\; \sum_{m=0}^{\infty} \sum_{\text{perms}} \frac{(-g)^m}{m!} \frac{n\cdot A_{us}^{a_1} \cdots n \cdot A_{us}^{a_m}}{n\cdot k_1 n \cdot (k_1 + k_2) \cdots n \cdot (\sum_{i=1}^{m} k_i])} T^{a_m} \cdots T^{a_1} . \tag{2.67}$$

The latter object arises when one sums all diagrams of attachments of ultrasoft gluons to a collinear-quark line.

2.4 Subleading Lagrangians

In order to include $\Lambda_{\rm QCD}/m_b$ power corrections, which we do for $B \to X_s\gamma$ and $B \to X_u\ell\bar{\nu}$ spectra in the next chapter, we need the subleading Lagrangians and heavy-to-light currents. As will be discussed, we require these to second order in $\lambda \sim \sqrt{\Lambda_{\rm QCD}/m_b}$, i.e.

$$\mathcal{L} = \mathcal{L}^{(0)} + \mathcal{L}^{(1)} + \mathcal{L}^{(2)}\,, \qquad J = J^{(0)} + J^{(1)} + J^{(2)}\,. \tag{2.68}$$

In this section, we summarize the results for the Lagrangians.

The LO Lagrangian for usoft light quarks and usoft gluons, $\mathcal{L}^{(0)}_{us}$, is identical to full QCD. For usoft heavy quarks we have the leading and subleading HQET Lagrangians, which were given in Eqs. (2.11) and (2.12). We repeat these here with slightly modified notation (showing that the gluon in HQET is ultrasoft, and that in SCET_I our power-counting parameter is λ):

$$\begin{aligned} \mathcal{L}^{(0)}_h &= \bar{h}_v iv\cdot D_{us} h_v\,, \\ \mathcal{L}^{(2)}_h &= \frac{1}{2m_b} O_h\,, \qquad O_h = \bar{h}_v (iD_T)^2 h_v + \frac{1}{2} c_F(\mu)\, \bar{h}_v \sigma_{\mu\nu}\, g G^{\mu\nu}_{us}\, h_v\,. \end{aligned} \tag{2.69}$$

For convenience, let's also define

$$\begin{aligned} \mathcal{H}_v &= Y^\dagger h_v\,, \qquad \psi_{us} = Y^\dagger q_{us}\,, \qquad \mathcal{D}_{us} = Y^\dagger D_{us} Y \\ \chi_n &= W^\dagger \xi_n\,, \qquad \mathcal{D}_c = W^\dagger D_c W\,, \qquad ig\mathcal{B}^\mu_c = \left[\frac{1}{\bar{\mathcal{P}}} W^\dagger [i\bar{n}\cdot D_c, iD^\mu_c] W\right]. \end{aligned} \tag{2.70}$$

The leading-order collinear Lagrangians (after one makes the field redefinitions (2.48)) are then

$$\mathcal{L}^{(0)}_{\xi\xi} = \bar{\chi}_n \left[in\cdot\mathcal{D}_c + i\not{\mathcal{D}}^\perp_c \frac{1}{\bar{\mathcal{P}}} i\not{\mathcal{D}}^\perp_c \right] \frac{\not{\bar{n}}}{2}\, \chi_n\,, \qquad \mathcal{L}^{(0)}_{cg} = -\frac{1}{2}\mathrm{tr}\left[G^{\mu\nu}_c G^c_{\mu\nu}\right] + \text{g.f.}\,, \tag{2.71}$$

where $igG^{\mu\nu}_c = [iD^\mu_c, iD^\nu_c]$. Here, $in\cdot D_c = in\cdot\partial + gn\cdot A_n$ and the other components of D_c are as given in Eq. (2.44).

The subleading Lagrangians that we require are all available in the literature [37, 130]. To obtain these Lagrangians, one must include q_{us} in the Lagrangian (2.32), by writing $\psi = \sum e^{-i\mathcal{P}\cdot x}(\xi_{n,p} + \xi_{\bar{n},p}) + q_{us}$, and expand to the desired power in λ. Here, one encounters a potential complication related to the choice of the full covariant derivative. One possible reparameterization-invariant choice is $i\bar{n}\cdot D = i\bar{n}\cdot D_c + i\bar{n}\cdot D_{us}$, $iD^\perp = iD_c^\perp + iD_{us}^\perp$. With this choice, one must redefine $\bar{n}\cdot A_c$ and $A_c^\perp$ if one wants the Lagrangian to be invariant order by order in λ under collinear gauge transformations [32]. This turns out to be equivalent to the choice

$$\begin{aligned} in\cdot D &= in\cdot\partial + gn\cdot A_c + gn\cdot A_{us}\,, \qquad iD^\perp = iD_c^\perp + WiD_{us}^\perp W^\dagger\,, \\ i\bar{n}\cdot D &= i\bar{n}\cdot D_c + Wi\bar{n}\cdot D_{us}W^\dagger\,, \end{aligned} \tag{2.72}$$

with the covariant derivatives defined in terms of the new gauge field. Furthermore, the Wilson line built out of the new gauge field has the same equation of motion as previously, and hence the same transformation law. Hence, using the redefined gauge field is simply a matter of using Eq. (2.72) above. The results that follow are written in terms of the redefined gauge field.

After one makes the field redefinitions (2.48), the subleading quark Lagrangians we require are [32]

$$\begin{aligned} \mathcal{L}_{\xi\xi}^{(1)} &= \bar{\chi}_n\, i\not{\mathcal{D}}_{us}^\perp \frac{1}{\bar{\mathcal{P}}}\, i\not{\mathcal{D}}_c^\perp \frac{\bar{\not{n}}}{2}\chi_n + \text{h.c.}\,, \\ \mathcal{L}_{\xi q}^{(1)} &= \bar{\chi}_n\, ig\not{\mathcal{B}}_c^\perp \psi_{us} + \text{h.c.}\,, \\ \mathcal{L}_{\xi\xi}^{(2a)} &= \bar{\chi}_n\, i\not{\mathcal{D}}_{us}^\perp i\not{\mathcal{D}}_{us}^\perp \frac{1}{\bar{\mathcal{P}}}\frac{\bar{\not{n}}}{2}\chi_n\,, \\ \mathcal{L}_{\xi\xi}^{(2b)} &= \bar{\chi}_n i\not{\mathcal{D}}_c^\perp i\bar{n}\cdot\mathcal{D}_{us}\frac{1}{\bar{\mathcal{P}}^2}\frac{\bar{\not{n}}}{2}\, i\not{\mathcal{D}}_c^\perp\,\chi_n\,. \end{aligned} \tag{2.73}$$

We also need the subleading terms in the mixed usoft-collinear gluon action,

$$\begin{aligned} \mathcal{L}_{cg}^{(1)} &= -2\,\mathrm{tr}\big[\mathcal{G}_c^{\mu\nu}\mathcal{H}_\mu{}^\tau\big] g_{\nu\tau}^\perp + \text{g.f.}\,, \\ \mathcal{L}_{cg}^{(2a)} &= \mathrm{tr}\big[\mathcal{H}^{\mu\nu}\mathcal{H}^{\sigma\tau}\big] g_{\mu\tau}^\perp\, g_{\nu\sigma}^\perp - \mathrm{tr}\big[\mathcal{H}^{\mu\nu}\mathcal{H}_\mu{}^\tau\big] g_{\nu\tau}^\perp - \mathrm{tr}\big[\mathcal{G}_c^{\mu\nu}\mathcal{G}_u^{\sigma\tau}\big] g_{\mu\sigma}^\perp\, g_{\nu\tau}^\perp + \text{g.f.}\,, \\ \mathcal{L}_{cg}^{(2b)} &= -\mathrm{tr}\big[\mathcal{G}_c^{\mu\nu}\mathcal{H}_\mu{}^\tau\big] n_\nu\bar{n}_\tau + \text{g.f.}\,, \end{aligned} \tag{2.74}$$

where

$$
\begin{aligned}
ig\,\mathcal{G}_c^{\mu\nu} &= W^\dagger[iD_c^\mu, iD_c^\nu]W\,, \qquad ig\,\mathcal{G}_u^{\mu\nu} = Y^\dagger[iD_{us}^\mu, iD_{us}^\nu]Y\,, \\
ig\,\mathcal{H}^{\mu\nu} &= [W^\dagger iD_c^\mu W, Y^\dagger iD_{us}^\nu Y]\,,
\end{aligned}
\tag{2.75}
$$

and g.f. denotes gauge-fixing terms that are required by reparameterization invariance.

Chapter 3

Factorization and Power Corrections to $B \to X_s\gamma$ and $B \to X_u\ell\bar{\nu}$

3.1 Introduction

In this chapter, we derive factorization theorems for $\Lambda_{\rm QCD}/m_b$ power corrections to $B \to X_s\gamma$ and $B \to X_u\ell\bar{\nu}$ in the shape function region, where $m_X^2 \sim m_b\Lambda_{\rm QCD}$. For $b \to u$ decays this region is important, because of cuts on E_ℓ or m_X^2, which are used to eliminate $b \to c$ events. In this region both the perturbative expansion and the power expansion become more complicated. In particular, there is the usual perturbative expansion at the scale $\mu^2 \simeq m_b^2$, as well as a second perturbative expansion at the smaller scale $\mu^2 \simeq m_X^2$. The rates also exhibit double Sudakov logarithms. In addition, instead of depending on non-perturbative parameters $(\lambda_1, \lambda_2, \ldots)$ that are matrix elements of local operators, the decay rates depend on non-perturbative shape functions. We shall refer to the expansion parameter for this region as $\lambda^2 \sim m_X^2/m_B^2 \sim \Lambda_{\rm QCD}/m_b$ to distinguish it from the $1/m_b$ expansion for the local OPE. In the endpoint region, the standard OPE no longer completely justifies the separation of short- and long-distance contributions. Instead, we must consider a more involved derivation of a QCD factorization theorem, as is the case in processes such as Drell-Yan and DIS as

$x \to 1$ [123, 134].

For $B \to X_s\gamma$ and $B \to X_u\ell\bar{\nu}$ at leading order (LO) in λ, the factorization theorem for the endpoint decay rates was determined in Ref. [99]. It separates QCD contributions that are hard (H), collinear ($\mathcal{J}^{(0)}$) and soft ($f^{(0)}$), so that, schematically, a differential decay rate takes the form

$$d\Gamma = H \times \mathcal{J}^{(0)} \otimes f^{(0)}\,, \tag{3.1}$$

where $\times$ is normal multiplication and $\otimes$ is a one-parameter convolution. Here the hard contributions are perturbative at the scale $\mu^2 \sim m_b^2$, the collinear contributions in $\mathcal{J}^{(0)}$ are associated with the inclusive X jet and are treated perturbatively at the scale $\mu^2 \sim m_b\Lambda_{\rm QCD}$, and the soft contributions are factored into a forward B-meson matrix element giving the non-perturbative shape function $f^{(0)}$ [124]. In Ref. [30] this factorization theorem was rederived using the Soft-Collinear Effective Theory (SCET) [22, 23, 33, 30]. The attraction of the effective-theory method is that it provides a formalism for extending the derivation of factorization theorems beyond LO in the power expansion. The main goal of this chapter is to derive a factorization theorem for $B \to X_s\gamma$ and $B \to X_u\ell\bar{\nu}$ at subleading order, i.e. $\mathcal{O}(\lambda^2)$, using SCET. This factorization theorem allows us to separate perturbative and non-perturbative corrections to all orders in α_s.

One method for studying the endpoint region is to start with the local OPE and sum up the infinite series of the operators that are most singular as we approach the $m_X^2 \sim m_b\Lambda_{\rm QCD}$ region. This technique was used in Refs. [124, 125, 41, 115, 69, 65], and provides a method of defining the non-perturbative functions. At LO the result is the shape function[1]

$$\begin{aligned}\frac{1}{2}\sum_{k=0}^{\infty}\frac{(-1)^k}{k!}\,\delta^{(k)}(\ell^+)\,\langle B_v|\bar{h}_v(in\cdot D)^k h_v|B_v\rangle &= \frac{1}{2}\langle B_v|\bar{h}_v\,\delta(\ell^+ - in\cdot D)\,h_v|B_v\rangle \\ &= f^{(0)}(\ell^+)\,. \end{aligned}\tag{3.2}$$

[1]We arbitrarily use the term "shape function" for $f(\ell^+)$ rather than "distribution function". Sometimes in the literature the term "shape function" is reserved for the distribution that enters $d\Gamma(B \to X_u\ell\bar{\nu})/dE_\ell$, which is an integral over f.

The result is simply the matrix element of a non-local HQET operator, where the states $|B_v\rangle$ and heavy b-quark fields h_v are defined in HQET, and n^μ is a light-like vector along the axis of the jet. This approach allows direct contact with the extensive calculations made with the local OPE, which give terms in the power series. There are several reasons for considering an approach where $f(\ell^+)$ is obtained without a summation. In particular, it is difficult to go beyond tree level with the summation approach. Also, owing to the presence of a kinked Wilson line [97], the renormalization of the local operators in the sum and final delta-function operator are not identical [27, 47] (see also [99]), essentially because the moment integrals introduce additional UV divergences.[2] For this reason the expansion in Eq. (3.2) should be considered to be formal, and care must be taken in drawing conclusions from operators in the expanded version, such as the fact that they have trivial dependence on n^μ. Care must also be taken in calculating the hard factor H, as pointed out recently [27, 47], since the one-loop matrix element for $f^{(0)}(\ell^+)$ has finite pieces in pure dimensional regularization. This implies that the quark-level QCD computation does not directly give the hard contribution, unlike factorization theorems involving massless quarks such as in DIS. The matching calculation in SCET handles this in a simple manner because matrix elements of the effective-theory graphs are necessarily subtracted from the full-theory graphs in order to compute H.

For any precision calculation, perturbative corrections play an important role, and both the resummation of large logarithms and fixed-order calculations need to be considered. The position-space version of Eq. (3.2) has a kinked Wilson line along v-n-v, which leads to double Sudakov logarithms [97, 99]. These occur between both the $m_b^2 \to m_b\Lambda_{\rm QCD}$ and the $m_b\Lambda_{\rm QCD} \to \Lambda_{\rm QCD}^2$ scales and can be summed using renormalization-group techniques. In moment space the leading and next-to-leading anomalous dimensions can be found in Ref. [99]. For phenomenological purposes, formulae for the differential rates with resummed logarithms are

[2] From the point of view of effective field theory this makes sense, since the summation in Eq. (3.2) attempts to connect one effective theory (HQET) to a region with a different expansion parameter that is described by a different effective theory (SCET). Generically the renormalization in two EFTs is not interconnected.

of practical importance and were obtained using inverse Mellin transformations in Refs. [113, 112, 110, 3]. These resummations have also been considered in SCET, both in moment space [22, 27] and for the differential rates [47]. Finite-order perturbative corrections are currently known to order α_s for the H and $\mathcal{J}$ functions [23, 27, 47].

Since in the endpoint region $\Lambda_{\rm QCD}/Q \sim 1/5$ to $1/10$, it is important to consider the effect of power corrections for precision phenomenology. By matching from QCD at tree level, contributions of subleading NLO shape functions have been derived for $B \to X_s\gamma$ [26] and for $B \to X_u\ell\bar\nu$ [108, 25], followed by further analysis in Refs. [100, 55, 127]. A single NNLO contribution has also been considered, corresponding to the "annihilation" contribution, which is phase space enhanced by $16\pi^2$ [136, 108]. These power corrections provide the dominant source of theoretical uncertainty in current measurements of $|V_{ub}|$ and are the focus of this chapter, so we discuss them in more detail.

To build some intuition, it is useful to contrast the power expansion in the endpoint region with the expansion for the local OPE. For the local OPE, all contributions can be assigned a power of $(\Lambda_{\rm QCD}/m_b)^{k-3}$. The power of $\Lambda_{\rm QCD}$ and thus k is simply determined by the dimension of the operator, and the -3 accounts for the dimension of the HQET states, $\langle B_v|\cdots|B_v\rangle$. For example, the set of local operators up to dimension 6 is

$$
\begin{aligned}
&O^3 = \bar h_v\, h_v\,, \qquad O^{5a} = \bar h_v (iD_T)^2 h_v\,, \qquad O^{5b} = g\,\bar h_v \sigma_{\alpha\beta} G^{\alpha\beta} h_v\,, \\
&O^{6a} = \bar h_v (iD_\alpha^T)(iv\cdot D)(iD_T^\alpha) h_v\,, \qquad O^{6b} = i\epsilon^{\alpha\beta\gamma\delta} v_\delta\, \bar h_v (iD_\alpha)(iv\cdot D)(iD_\beta)\gamma_\gamma\gamma_5\, h_v\,, \\
&O^{6c} = (\bar h_v \gamma^\alpha q_L)\,(\bar q_L \gamma_\alpha h_v)\,, \qquad O^{6d} = (\bar h_v\, q_L)\,(\bar q_L\ h_v)\,, \\
&O^{6e} = (\bar h_v T^a \gamma^\alpha q_L)\,(\bar q_L T^a \gamma_\alpha h_v)\,, \qquad O^{6f} = (\bar h_v T^a q_L)\,(\bar q_L\, T^a\, h_v)\,,
\end{aligned}
\tag{3.3}
$$

where dimensions are shown as superscripts, a superscript/subscript T means transverse to the HQET velocity parameter v^μ, and an L means left-handed.[3] Dimension-4 operators are absent so there are no $1/m_b$ corrections, except the trivial ones that

[3]We write O^3 in terms of HQET fields, although strictly speaking at lowest order this is not necessary.

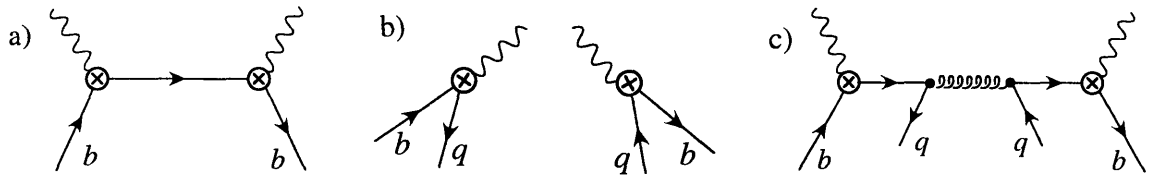

Figure 3-1: Comparison of the ratio of annihilation contributions to the lowest-order result. In the total decay rate, b) is $\sim 16\pi^2(\Lambda^3/m_b^3)\Delta B \simeq 0.02$, while c) is $\sim 4\pi\alpha_s(m_b)(\Lambda^3/m_b^3) \simeq 0.003$ when compared to a). In the endpoint region, b) is $\sim 16\pi^2(\Lambda^2/m_b^2)\Delta B \simeq 0.16$, a large correction, while c) becomes $\sim 4\pi\alpha_s(\mu_J)(\Lambda/m_b)\epsilon' \simeq 0.6\epsilon'$, a potentially large correction.

may be induced by switching to hadronic variables. For dimension-5 and 6 operators there are two naming conventions in common use. For $\langle \bar{B}_v|\{O^{5a}, O^{5b}, O^{6a}, O^{6b}\}|\bar{B}_v\rangle$, the parameters are $\{\lambda_1, \lambda_2, \rho_1, \rho_2\}$ or $\{\mu_\pi, \mu_G, \rho_D^3, \rho_{LS}^3\}$. These operators are generated by connected graphs from the time-ordered product of two currents, as in Fig. 3-1a. On the other hand, the four-quark operators $O^{6c,6d}$ give parameters $f_B^2 B_{1,2}$ and are disconnected (or rather connected by leptons or photons only), as shown in Fig. 3-1b, and thus exhibit a phase-space enhancement relative to Fig. 3-1a. The simplest way to see this is to note that for the total rate to $B \to X_u \ell\bar{\nu}$, we would cut a two-loop graph for Fig. 3-1a, while Fig. 3-1b would be at one-loop level (the ℓ–$\bar{\nu}$ loop). For later convenience, we also consider the perturbative correction to the four-quark operators shown in Fig. 3-1c, which is suppressed by $\alpha_s/(4\pi)$ relative to Fig. 3-1b, and gives the operators $O^{6e,6f}$. In the total decay rate, if we normalize so that Fig. 3-1a ~ 1 then

$$\text{Fig. 3-1b} \sim 16\pi^2 \frac{\Lambda^3}{m_b^3}\Delta B \sim 0.02\,, \qquad \text{Fig. 3-1c} \sim 4\pi\alpha_s(m_b)\frac{\Lambda^3}{m_b^3}\epsilon \sim 0.003\epsilon\,. \quad (3.4)$$

Here $\Delta B = B_2 - B_1 \sim 0.1$ accounts for the fact that the matrix elements of the operators generated by Fig. 3-1b vanish in the factorization approximation. The factor of ϵ accounts for any dynamical suppression of Fig. 3-1c. The definitions of $B_{1,2}$ are

$$\langle B_v|\left[\bar{h}_v\gamma_\sigma q_L\right]\left[\bar{q}_L\gamma_\tau h_v\right]|B_v\rangle = \frac{f_B^2 m_B}{12}\left[(B_1 - B_2)g_{\sigma\tau} + (4B_2 - B_1)v_\sigma v_\tau\right]. \quad (3.5)$$

Without the ΔB suppression factor, Fig. 3-1b would dominate over other $1/m_b^2$ operators rather than just competing with them. The $\mathcal{O}(\alpha_s)$ corrections to annihilation are still a small contribution in the local OPE, for any $\epsilon \leq 1$. In particular, possible enhancements of these contributions have been shown to cancel for the total $b \to u$ decay rate [42].

In the endpoint region there are extra enhancement factors and the dimensions of the operators no longer determine the size of their contributions. The fact that annihilation effects are larger in the endpoint was first pointed out in Ref. [42]. The power counting in SCET organizes these contributions in a systematic fashion and allows us to be more quantitative about how large these contributions are. Since some background material is required, we postpone this power counting until Sec. 3.3. The derivation given here is more heuristic, but leads to the same results. For Fig. 3-1a the intermediate quark propagator becomes collinear, giving an m_b/Λ enhancement. This explains why a larger portion of the decay rate is concentrated in the endpoint region. For Fig. 3-1b there is no quark-propagator enhancement but also no reduction from the phase space. A numerical estimate for this contribution was made in Ref. [136]. Finally, for Fig. 3-1c in the endpoint region there can be *three* collinear propagators, giving a large m_b^3/Λ^3 enhancement to this diagram. In Sec. 3.6 we show that this graph contains the maximum possible enhancement. In summary, if we consider the rate integrated only over the endpoint region then Fig. 3-1a ~ 1 and

$$\text{Fig. 3-1b} \sim 16\pi^2 \frac{\Lambda^2}{m_b^2} \Delta B \sim 0.2\,, \qquad \text{Fig. 3-1c} \sim 4\pi\alpha_s(1.4\,\text{GeV}) \frac{\Lambda}{m_b} \epsilon' \sim 0.6\,\epsilon'\,. \quad (3.6)$$

The non-perturbative function that gives ϵ' differs from the local operators that give ϵ in Eq. (3.4). Since $\epsilon' \sim 0.3$ is possible[4], we conclude that it is possible that the contribution from Fig. 3-1c gives a significant uncertainty in extracting V_{ub} with methods such as E_ℓ or m_X^2 cuts that depend on the endpoint region. It has not been considered in recent error estimates in the literature. The main phenomenological

[4]The only rigorous scaling argument for a dynamical suppression that we are aware of is the large-N_c limit, where $\Delta B \sim 1/N_c$. For Fig.3-1c the $q\bar{q}$ contraction gives a matrix element that is leading order in N_c. If these contributions are small, then a rough estimate is $\epsilon' \sim 1/N_c \sim 0.3$.

outcome of our analysis is a proper consideration of this term for endpoint spectra.

Theoretically, the main result of our analysis is a complete theoretical description for the NLO term, $\Gamma^{(2)}$, in the power expansion of decay spectra in the endpoint region,

$$\left.\frac{d\Gamma}{dZ_i}\right|_{\text{endpoint}} = \frac{d\Gamma^{(0)}}{dZ_i} + \frac{d\Gamma^{(2)}}{dZ_i} + \dots . \tag{3.7}$$

Here Z_i denotes a generic choice of the possible spectrum variables, $\{P^+, P^-, E_\gamma, q^2, s_H, m_b, \dots\}$. At NLO we use SCET to determine the contributions to the spectra. These contributions are tabulated in the body of the chapter, but the generic structure of a term in $(1/\Gamma_0)d\Gamma^{(2)}/dZ_i$ is

$$\int [dz_{n'}] H^{(j_1)}(z_{n'}, m_b, Z_i) \int [dk_n^+]\, \mathcal{J}^{(j_2)}(z_{n'}, k_n^+, P^\pm)\, f^{(j_3)}(k_n^+)\,, \tag{3.8}$$

where the number of convolution parameters varies from $n = 1$ to $n = 3$ and $n' = 1$ or 2, and for $n = 2$ $[dk_n^+] = dk_1^+ dk_2^+$ etc. The dependence on the $z_{n'}$ parameters appears only in jet functions that vanish at tree level. In Eq. (3.8) the (j_1), (j_2), (j_3) powers indicate whether the power suppression occurs in the hard, jet or soft regions respectively. The power corrections start at $\mathcal{O}(\lambda^2)$, which is $\sim 1/m_b$, and so $j_1 + j_2 + j_3 = 2$. Here $j_{1,3} \geq 0$ while j_2 can be negative. Phase-space and kinematic corrections give an $H^{(2)}$ with the same jet and shape functions as at leading order. Other more dynamic power corrections involve new hard $H^{(0)}$ functions, and obtain their power suppression from the product of jet and soft factors. We show that the operators at NLO allow $-4 \leq j_2 \leq 2$ and $0 \leq j_3 \leq 6$. The largest jet function ($j_2 = -4$) occurs for exactly the endpoint contribution generated by the four-quark operators ($j_3 = 6$) from Fig. 1c.

Our analysis can be compared with the closely related physical problem of deep inelastic scattering with $Q^2 \gg \Lambda^2$, in the limit where Bjorken $x \sim 1 - \Lambda/Q$. With no parametric scaling for x, the power corrections in DIS at twist 4 were computed in Refs. [92, 93, 68, 67, 133, 132]. As $x \to 1$ the relative importance of the power-

suppressed operators changes and the importance of contributions from four-quark operators has been discussed in Ref. [73].

The outline of the remainder of this chapter is as follows. In Sec. 3.2 we give the basic ingredients needed for our computations, including the weak Hamiltonian (Sec. 3.2.1) and expressions for the hadronic tensors and decay rates (Sec. 3.2.2). In Sec. 3.2.3 we give a detailed discussion of the endpoint kinematics and light-cone variables, and in Sec. 3.2.4 we briefly summarize a few results obtained using the optical theorem for the forward scattering amplitude, and the procedure for switching between partonic and hadronic variables that is relevant in the endpoint region. In Sec. 3.3 we turn to the discussion of the SCET heavy-to-light currents. Many of the ingredients necessary for our computation are readily available in the literature. Of particular note are expressions for the heavy-to-light currents at $\mathcal{O}(\lambda^2)$ [38], which we have verified. In Sec. 3.4 we review the derivation of the factorization theorem at LO, but do so in a way that makes the extension beyond LO more accessible. We consider power corrections of $\mathcal{O}(\lambda)$ in Sec. 3.5, and show that they vanish. In Sec. 3.6 we discuss the true NLO factorization theorem, which is $\mathcal{O}(\lambda^2)$. In particular, in Sec. 3.6.1 we switch to hadronic variables and re-expand the LO result, in Sec. 3.6.2 we enumerate all the time-ordered products that occur at this order, and in Sec. 3.6.3 we show that the tree-level matching is simplified by using the SCET formalism. In Sec. 3.6.4 we give definitions for the non-perturbative shape functions that appear, and then in Sec. 3.6.5 we derive the factorization theorems for the most important contributions in some detail. Finally, in Sec. 3.6.6 we summarize the hard coefficient functions for the subleading time-ordered products. Next, in Sec. 3.7 we present a useful summary of the NLO decay-rate results, including the phase-space corrections. We also compare with results in the literature where they are available. Our conclusions and discussion are given in Sec. 3.8. Further details are relegated to appendices, including the expansion of the heavy quark field and calculation of the power-suppressed heavy-to-light currents at tree level in Appendix A, and a review of constraints on the currents from reparameterization invariance in Appendix B. For the reader interested in getting an overview of our results while skipping the details, we suggest reading

Secs. 3.2, 3.3 and 3.4, the introduction to Sec. 3.6, and Secs. 3.6.1, 3.6.2 and 3.7. A reader interested only in final results may skip directly to the summary in Sec. 3.7.

3.2 Basic Ingredients

In this section we give the ingredients necessary for studying the decays $B \to X_s\gamma$ and $B \to X_u\ell\bar{\nu}$ in the endpoint region to NLO. A proper treatment requires a separation of the scales $m_W^2 \gg m_b^2 \gg m_b\Lambda_{\rm QCD} \gg \Lambda_{\rm QCD}^2$ in the form of a factorization theorem. This is accomplished by the following steps:

1) Match on to the weak Hamiltonian, H_W, at $\mu^2 = m_W^2$ and run down to $\mu^2 = m_b^2$, just as in the standard local OPE.

2) Match H_W at $\mu^2 \simeq m_b^2$ on to SCET, with collinear and usoft degrees of freedom and an expansion in $\lambda \sim \sqrt{\Lambda_{\rm QCD}/m_b}$. Run from $\mu^2 = m_b^2$ to $\mu^2 = \mu_0^2 \simeq m_b\Lambda_{\rm QCD}$.

3) At $\mu^2 = \mu_0^2$ integrate out the collinear modes, which, given a complete factorization in step 2), is trivial. Then run from $\mu^2 = \mu_0^2$ to $\mu^2 \sim 1\,{\rm GeV}^2 \gtrsim \Lambda_{\rm QCD}^2$.

In Sec. 3.2.1 we discuss the weak Hamiltonian. The kinematics and differential decay rates for the endpoint region are given in Sec. 3.2.3. Then in Sec. 3.3 we give the necessary effective-theory currents to $\mathcal{O}(\lambda^2)$.

3.2.1 Weak Effective Hamiltonians

For $B \to X_u\ell\bar{\nu}$ the effective Hamiltonian is simply

$$\mathcal{H}_{\rm eff}^u = -\frac{4G_F}{\sqrt{2}} V_{ub} (\bar{u}\gamma_\mu P_L b)(\bar{\ell}\gamma^\mu P_L \nu_\ell)\,, \tag{3.9}$$

and the current $\bar{u}\gamma_\mu P_L b$ is the basis for our analysis of the QCD part of the problem. The Hamiltonian for the weak radiative decay $B \to X_s\gamma$ was given in Chapter 1, Eq. (1.7).

For the total $B \to X_s\gamma$ rate the perturbative corrections are known at NLO [53, 90]. Effective scheme-independent coefficients $C_{7,8}^{\rm eff}$ are defined in a way that includes

contributions from the penguin operators (C_{3-6}). A totally inclusive analysis is considerably simplified by the fact that at leading order in $1/m_b$ the matrix elements can be evaluated directly in full QCD rather than first having to match on to HQET. For an endpoint analysis, the matching at m_W and running to $\mu \sim m_b$ is the same. However, at the scale $\mu \simeq m_b$ the operators in H_W need to be matched on to operators in SCET before the OPE is performed. In performing the matching, the only subtle complication is the treatment of the charm mass. For simplicity, the approach we take here is formally to let $m_c \sim m_b$, so that charm-mass effects are all hard and are integrated out in matching on to SCET. This agrees with the treatment of the $O_{i\neq 7}$ advocated in Ref. [126] for the endpoint region. Since numerically $m_c^2 \sim m_b\Lambda$, perhaps a better alternative would be to keep charm-mass effects in the operators of SCET until below the jet scale $m_b\Lambda$. This second approach is more involved, and in particular it is clear from Ref. [51] that it would necessitate introducing two types of collinear charm quark, as well as soft and ultrasoft charm quarks. For this reason, we stick to the former approach and leave the latter for future investigation.

At lowest order in the λ power expansion, there is only the SCET analog of the $\bar{s}\sigma_{\mu\nu}P_R b$ current called $J^{(0)}$ (cf. Eq. (3.51)), and $\mathcal{O}_{1-8}$ can make contributions to its Wilson coefficient. At NLL order in α_s the effect of the other operators can be taken into account by using [81, 63]

$$C_\gamma(\mu, z) = C_7^{\text{eff}(0)}(\mu) + \frac{\alpha_s}{4\pi} C_7^{\text{eff}(1)}(\mu) + \sum_k C_k^{\text{eff}(0)}(\mu)\Big[r_k(\rho) + \gamma_{k7}^{\text{eff}(0)} \ln\Big(\frac{m_b}{\mu}\Big)\Big]\,, \quad (3.10)$$

in place of C_7 when matching on to SCET. Here the dependence on $\rho = m_c^2/m_b^2$ enters from the four-quark operators with charm quarks. In the endpoint region the $\mathcal{O}(\alpha_s)$ effects from the process $b \to s\gamma g$ all appear in the jet and shape functions. For later convenience, we define

$$\Delta_\gamma(\mu, \rho) = \frac{C_\gamma(\mu, \rho)}{C_7^{\text{eff}(0)}(\mu)} - 1\,. \quad (3.11)$$

The photon in $B \to X_s\gamma$ is collinear in the opposite direction to the jet X_s, so

propagators connecting the two are hard. Thus, beyond LO in the power expansion, the photon will typically be emitted by effective-theory currents $J^{(i)}$ (which could be four-quark operators). We shall discuss the matching on to these subleading currents for $\mathcal{O}_7$ only. Some of the contributions from the other $\mathcal{O}_i$ will just change the Wilson coefficients of the subleading currents and thus not modify the structure of the power-suppressed factorization theorems (indeed some of them are already known since they are fixed by reparameterization invariance). These other operators may also induce time-ordered products that would involve operators with quarks collinear to the photon direction, but these are not considered here.

3.2.2 Hadronic Tensors and Decay Rates

In this subsection, we summarize general results for the hadronic tensors and decay rates, without restricting ourselves to the endpoint region. For both decays $B \to X_s\gamma$ and $B \to X_u\ell\bar{\nu}$, momentum conservation for the hadrons gives

$$p_B^\mu = m_B v^\mu = p_X^\mu + q^\mu \,, \tag{3.12}$$

where p_X^μ is the sum of the four-momenta of all the hadrons in X, q^μ is the momentum of the γ or the pair of leptons $(\ell\bar{\nu})$, and the velocity v^μ satisfies $v^2 = 1$. For $B \to X_s\gamma$, $q^\mu = n{\cdot}q\,\bar{n}^\mu/2 = E_\gamma \bar{n}^\mu$, where $v \cdot q = E_\gamma$ is the photon energy in the rest frame of the B meson. In this case $q^2 = 0$ and

$$m_{X_s}^2 = m_B(2E_{X_s} - m_B) = m_B(m_B - 2E_\gamma) \,, \tag{3.13}$$

so the differential rate involves only one variable, m_X or E_γ. For $B \to X_u\ell\bar{\nu}$, Eq. (3.12) implies

$$E_X = v{\cdot}p_X = \frac{m_B^2 + m_X^2 - q^2}{2m_B} \,, \qquad v \cdot q = m_B - E_X = E_\ell + E_\nu \,. \tag{3.14}$$

where $p_X^2 = m_X^2$. The differential decay rate involves three variables, several common choices of which are $\{E_\ell, E_\nu, q^2\}$, $\{E_\ell, v{\cdot}q, q^2\}$, or $\{E_\ell, m_X^2, q^2\}$.

To derive the inclusive decay rates for $\bar{B} \to X_s\gamma$ and $\bar{B} \to X_u\ell\bar{\nu}$, the matrix elements are separated into a leptonic/photonic part $L_{\mu\nu}$ and a hadronic part $W_{\mu\nu}$. Here

$$\begin{aligned} W_{\mu\nu} &= \frac{1}{2m_B}\sum_X (2\pi)^3\delta^4(p_B - q - p_X)\langle\bar{B}|J_\mu^\dagger|X\rangle\langle X|J_\nu|\bar{B}\rangle \\ &= -g_{\mu\nu}W_1 + v_\mu v_\nu W_2 + i\epsilon_{\mu\nu\alpha\beta}v^\alpha q^\beta W_3 + q_\mu q_\nu W_4 + (v_\mu q_\nu + v_\nu q_\mu)W_5\,, \end{aligned} \tag{3.15}$$

in which we use the hadronic current J and relativistic normalization for the $|\bar{B}\rangle$ states. For convenience we define projection tensors $P_i^{\mu\nu}$ so that

$$W_i = P_i^{\mu\nu}\, W_{\mu\nu}\,. \tag{3.16}$$

They are

$$\begin{aligned} P_1^{\mu\nu} &= -\frac{1}{2}g^{\mu\nu} + \frac{q^2\, v^\mu v^\nu + q^\mu q^\nu - v\cdot q(v^\mu q^\nu + v^\nu q^\mu)}{2[q^2 - (v\cdot q)^2]}\,, \\ P_2^{\mu\nu} &= \frac{3q^2\, P_1^{\mu\nu} + q^2 g^{\mu\nu} - q^\mu q^\nu}{[q^2 - (v\cdot q)^2]}\,, \qquad P_3^{\mu\nu} = \frac{-i\epsilon^{\mu\nu\alpha\beta}q_\alpha v_\beta}{2[q^2 - (v\cdot q)^2]}\,, \\ P_4^{\mu\nu} &= \frac{g^{\mu\nu} - v^\mu v^\nu + 3P_1^{\mu\nu}}{[q^2 - (v\cdot q)^2]}\,, \qquad P_5^{\mu\nu} = \frac{g^{\mu\nu} + 4P_1^{\mu\nu} - P_2^{\mu\nu} - q^2 P_4^{\mu\nu}}{2v\cdot q}\,. \end{aligned} \tag{3.17}$$

Contracting the lepton/photon tensor $L^{\mu\nu}$ with $W^{\mu\nu}$ and neglecting the mass of the leptons gives the differential decay rates

$$\begin{aligned} \frac{d\Gamma^s}{dE_\gamma} &= \Gamma_0^s\,\frac{8E_\gamma}{m_B^3}(4W_1^s - W_2^s - 2E_\gamma W_5^s)\,, \\ \frac{d^3\Gamma^u}{dE_\ell dq^2 dE_\nu} &= \Gamma_0^u\,\frac{96}{m_B^5}\Big[q^2 W_1^u + (2E_c E_\nu - q^2/2)W_2^u + q^2(E_e - E_\nu)W_3^u\Big]\theta(4E_e E_\nu - q^2)\,. \end{aligned} \tag{3.18}$$

where $W_i = W_i(q^2, v\cdot q)$ and the normalization factors are

$$\Gamma_0^s = \frac{G_F^2\, m_B^3}{32\pi^4}\,|V_{tb}V_{ts}^*|^2\,\alpha_{\rm em}\,[\overline{m}_b(m_b)]^2|C_7^{\rm eff(0)}(m_b)|^2\,, \qquad \Gamma_0^u = \frac{G_F^2\, m_B^5}{192\pi^3}\,|V_{ub}|^2 \tag{3.19}$$

Here $\overline{m}_b(\mu)$ is the $\overline{\rm MS}$ mass. For convenience, we have pulled out a Wilson coefficient $C_7^{\rm eff(0)}$ so that contributions from other coefficients appear in ratios $C_i/C_7^{\rm eff(0)}$ in the SCET Wilson coefficients (for example the quantity Δ_γ in Eq. (3.11)). Note that we have chosen to stick with hadronic variables here (using m_B rather than m_b). When we eventually compute the W_i, we shall have to deal with switching between partonic and hadronic variables. However, we shall see that the situation is quite different from that in the local OPE (as we discuss further in Sec. 3.2.4 below). In particular, it is the hadronic phase space that turns out to be required.

In Eq. (3.18), $0 \le E_\ell, E_\nu \le (m_B^2 - m_\pi^2)/(2m_B)$. A set of useful dimensionless hadronic variables is

$$x_H^\gamma = \frac{2E_\gamma}{m_B}\,, \qquad x_H = \frac{2E_\ell}{m_B}\,, \qquad y_H = \frac{q^2}{m_B^2}\,, \qquad s_H = \frac{m_X^2}{m_B^2}\,. \tag{3.20}$$

In terms of these variables,

$$\frac{2E_\nu}{m_B} = 1 - s_H + y_H - x_H\,, \qquad \frac{2E_X}{m_B} = 1 + s_H - y_H\,, \tag{3.21}$$

and $W_i = W_i(y_H, s_H)$. For $B \to X_s\gamma$,

$$\frac{d\Gamma^s}{dx_H^\gamma} \;=\; \Gamma_0^s \,\frac{2x_\gamma^H}{m_B}\Big\{4W_1^s - W_2^s - m_B\, x_H^\gamma W_5^s\Big\}\,, \tag{3.22}$$

with $0 \le x_H^\gamma \le 1 - m_{K^*}^2/m_B^2$. For $B \to X_u\ell\bar\nu$,

$$\begin{aligned}\frac{d^3\Gamma^u}{dx_H\,dy_H\,ds_H} \;=\; & \Gamma_0^u\, 24m_B\Big\{y_H W_1^u + \frac{1}{2}\big[(1-x_H)(x_H-y_H) - x_H s_H\big]W_2^u \\ & + \frac{1}{2}\,m_B y_H\big(2x_H + s_H - y_H - 1\big)W_3^u\Big\}\theta\big[(1-x_H)(x_H-y_H) - x_H s_H\big]\,,\end{aligned} \tag{3.23}$$

and, depending on the order of integration, there are several useful combinations of the limits, which are shown in Table 3.1. If we integrate over all values of x_H (cases

i)	$0 \le x_H \le 1 - r_\pi^2$	$r_\pi^2 \le s_H \le 1 - x_H$	$0 \le y_H \le x_H - \frac{s_H x_H}{1-x_H}$
ii)	$0 \le x_H \le 1 - r_\pi^2$	$0 \le y_H \le x_H - \frac{r_\pi^2 x_H}{1-x_H}$	$r_\pi^2 \le s_H \le \frac{1-x_H}{x_H}(x_H - y_H)$
iii)	$r_\pi^2 \le s_H \le 1$	$0 \le x_H \le 1 - s_H$	$0 \le y_H \le x_H - \frac{s_H x_H}{1-x_H}$
iv)	$r_\pi^2 \le s_H \le 1$	$0 \le y_H \le \left(1 - \sqrt{s_H}\right)^2$	$x_H^{\rm min} \le x_H \le x_H^{\rm max}$
v)	$0 \le y_H \le \left(1 - r_\pi\right)^2$	$r_\pi^2 \le s_H \le \left(1 - \sqrt{y_H}\right)^2$	$x_H^{\rm min} \le x_H \le x_H^{\rm max}$
vi)	$0 \le y_H \le \left(1 - r_\pi\right)^2$	$x_H^{\rm min\,*} \le x_H \le x_H^{\rm max\,*}$	$r_\pi^2 \le s_H \le 1 + y_H - \frac{y_H}{x_H} - x_H$

Table 3.1: Limits for different orders of integration in $B \to X_u \ell \bar{\nu}$ with variables $\{x_H, s_H, y_H\}$. Here $r_\pi = m_\pi/m_B$, while $\{x_H^{\rm max}, x_H^{\rm min}\} = \left[(1 + y_H - s_H) \pm \sqrt{(1 + y_H - s_H)^2 - 4y_H}\right]/2$ and $\{x_H^{\rm max\,*}, x_H^{\rm min\,*}\} = \{x_H^{\rm max}, x_H^{\rm min}\}|_{s_H = r_\pi^2}$. Results for the phase-space limits of partonic variables are obtained by dropping the H-subscripts and setting $r_\pi = 0$.

iv) & v)), the rate becomes

$$\frac{d^2\Gamma^u}{dy_H\, ds_H} = \Gamma_0^u\, 2m_B \sqrt{(1-y_H+s_H)^2 - 4\,s_H}\, \Big\{ 12 y_H W_1^u + \left[(1-y_H+s_H)^2 - 4s_H\right] W_2^u \Big\}. \tag{3.24}$$

3.2.3 Light-cone Hadronic Variables and Endpoint Kinematics

We are interested in the jet-like region corresponding to $\Lambda_{\rm QCD} \ll m_X \ll E_X$ for both $B \to X_s\gamma$ and $B \to X_u \ell \bar{\nu}$. In this region, the hadrons in the X occur in a jet in the B rest frame with $E_X \sim m_B$ and $m_X^2 \lesssim m_B \Lambda_{\rm QCD}$.[5] The momentum of the states X is therefore restricted, but they still form a complete set for Eq. (3.15). The width of the jet is determined by noting that the typical perpendicular momentum between any two final-state hadrons is $\Delta p_\perp \lesssim \sqrt{m_B \Lambda} \sim 1.6\,{\rm GeV}$, where we use $\Lambda \sim 0.5\,{\rm GeV}$ to denote a typical hadronic scale for B-mesons (examples being $\Lambda_{\rm QCD}$ and $\overline{\Lambda}$). We also assume that there are enough states with $m_X^2 \lesssim m_B \Lambda$ that the endpoint region is still inclusive and Eq. (3.46) is valid. As we shall see below, the factorization in

[5] In Refs. [27, 47] an intermediate situation, $m_X^2 \lesssim \Delta^2$ with $\sqrt{m_B \Lambda_{\rm QCD}} \ll \Delta \ll m_B$, was also considered, but we do not consider it here.

this region gives non-perturbative shape functions rather than just local operators.

As previously discussed, it is natural to introduce light-cone coordinates, in which some useful decompositions are

$$g_\perp^{\mu\nu} = g^{\mu\nu} - \frac{1}{2}(n^\mu\bar{n}^\nu + n^\nu\bar{n}^\mu), \qquad g_T^{\mu\nu} = g^{\mu\nu} - v^\mu v^\nu, \qquad \epsilon_\perp^{\mu\nu} = \frac{1}{2}\epsilon^{\mu\nu\alpha\beta}\bar{n}_\alpha n_\beta\,,$$
$$p_\perp^\mu = p^\mu - \frac{\bar{n}\cdot p}{2}\,n^\mu - \frac{n\cdot p}{2}\,\bar{n}^\mu\,, \qquad p_T^\mu = p^\mu - v^\mu v\cdot p\,, \tag{3.25}$$

where we take $\epsilon^{0123} = 1$. Note that the subscript T means transverse to v^μ, so $p_T^\mu \neq p_\perp^\mu$. For the final factorization theorem for the differential decay rates we shall use a frame where $q_\perp^\mu = v_\perp^\mu = 0$, and $v^\mu = (n^\mu + \bar{n}^\mu)/2$.[6] Thus $q^\mu = \bar{n}\cdot q\, n^\mu/2 + n\cdot q\,\bar{n}^\mu/2$ and

$$n\cdot q = m_B - n\cdot p_X\,, \qquad \bar{n}\cdot q = m_B - \bar{n}\cdot p_X\,. \tag{3.26}$$

For $B \to X_s\gamma$ the photon momentum is taken along the $\bar{n}$ light-like direction, i.e. $q_\mu = E_\gamma\bar{n}_\mu$, and

$$\bar{n}\cdot p_X = m_B\,, \qquad n\cdot p_X = m_B - 2E_\gamma = m_B(1 - x_H^\gamma)\,. \tag{3.27}$$

For $B \to X_u\ell\bar{\nu}$ the phase space is more complicated and for convenience we define the dimensionless variables

$$\overline{y}_H = \frac{\bar{n}\cdot p_X}{m_B}\,, \qquad u_H = \frac{n\cdot p_X}{m_B}\,. \tag{3.28}$$

Now $m_X^2 = n\cdot p_X\,\bar{n}\cdot p_X$ and $n\cdot p_X + \bar{n}\cdot p_X = (m_B^2 - q^2 + m_X^2)/m_B$, so

$$s_H = u_H\overline{y}_H\,, \qquad y_H = (1 - u_H)(1 - \overline{y}_H)\,, \tag{3.29}$$

[6] If one desires, he or she can take $v = (1,0,0,0)$, $n = (1,0,0,-1)$, and $\bar{n} = (1,0,0,1)$. A more general frame is required only for working out the constraints from reparameterization invariance.

i)	$0 \le x_H \le 1 - r_\pi^2$	$r_\pi^2 \le u_H \le 1 - x_H$	$\max\{1-x_H\,,\,\frac{r_\pi^2}{u_H}\} \le \overline{y}_H \le 1$
ii)	$0 \le x_H \le 1 - r_\pi^2$	$\max\{1-x_H,\frac{r_\pi^2}{1-x_H}\} \le \overline{y}_H \le 1$	$\frac{r_\pi^2}{\overline{y}_H} \le u_H \le 1 - x_H$
iii)	$r_\pi^2 \le u_H \le 1$	$0 \le x_H \le 1 - u_H$	$\max\{1-x_H,\frac{r_\pi^2}{u_H}\} \le \overline{y}_H \le 1$
iv)	$r_\pi^2 \le u_H \le 1$	$\max\{\frac{r_\pi^2}{u_H}, u_H\} \le \overline{y}_H \le 1$	$1 - \overline{y}_H \le x_H \le 1 - u_H$
v)	$r_\pi \le \overline{y}_H \le 1$	$\frac{r_\pi^2}{\overline{y}_H} \le u_H \le \overline{y}_H$	$1 - \overline{y}_H \le x_H \le 1 - u_H$
vi)	$r_\pi \le \overline{y}_H \le 1$	$1 - \overline{y}_H \le x_H \le 1 - \frac{r_\pi^2}{\overline{y}_H}$	$\frac{r_\pi^2}{\overline{y}_H} \le u_H \le 1 - x_H$

Table 3.2: Full phase-space limits for $B \to X_u \ell \bar{\nu}$ with variables x_H, $\overline{y}_H$, and u_H. The parameter $r_\pi = m_\pi / m_B$. Results for the phase-space limits of partonic variables are obtained by dropping the H-subscripts and setting $r_\pi = 0$.

and, making the choice $\overline{y}_H \ge u_H$, we have

$$\{\overline{y}_H, u_H\} \;=\; \frac{1}{2}\Big[1 - y_H + s_H \pm \sqrt{(1 - y_H + s_H)^2 - 4 s_H}\Big]\,. \tag{3.30}$$

So far we have not made any restriction to the endpoint. The variables $\overline{y}_H$ and u_H provide an equally good description of the full $B \to X_u \ell \bar{\nu}$ phase space as y_H and s_H, namely

$$\begin{aligned}\frac{1}{\Gamma_0^u}\frac{d^3\Gamma^u}{dx_H\, d\overline{y}_H\, du_H} \;=\; 24 m_B(\overline{y}_H - u_H)\Big\{&(1-u_H)(1-\overline{y}_H)W_1^u \\ &+ \frac{1}{2}(1-x_H-u_H)(x_H+\overline{y}_H-1)W_2^u \\ &+ \frac{m_B}{2}(1-u_H)(1-\overline{y}_H)\big(2x_H+u_H+\overline{y}_H-2\big)W_3^u\Big\}\,,\end{aligned} \tag{3.31}$$

where $W_i = W_i(u_H, \overline{y}_H)$ and we have suppressed the theta function from Eq. (3.23). Integrating over x_H from Table 3.2 (cases iv) & v)) gives

$$\frac{1}{\Gamma_0^u}\frac{d^2\Gamma^u}{d\overline{y}_H\, du_H} 24 m_B(\overline{y}_H - u_H)^2\Big\{(1-u_H)(1-\overline{y}_H)W_1^u + \frac{1}{12}(\overline{y}_H - u_H)^2 W_2^u\Big\}\,. \tag{3.32}$$

The full limits for $\overline{y}_H$ and u_H are given in Table 3.2.

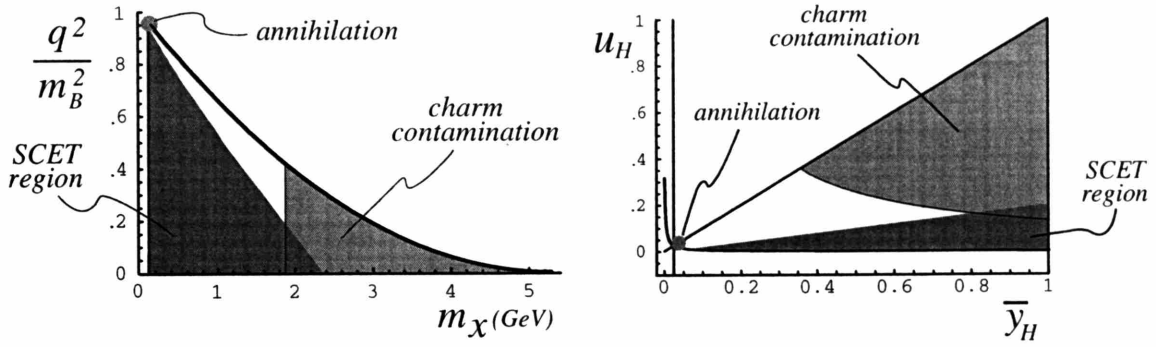

Figure 3-2: Allowed phase space for $B \to X_u \ell \bar{\nu}$, where $m_\pi < m_X < m_B$. The second figure shows the same regions using the variables defined in Eq. (3.28). We indicate the region where charm contamination enters, $m_X > m_D$, and the region of phase space where annihilation contributions enter. Also shown is the region where the SCET expansion converges, which is taken to be $u_H/\overline{y}_H \leq 0.2$ and corresponds to $m_X^2/(4E_X^2) \lesssim 0.14$.

In Ref. [48], it was pointed out that a natural set of variables in the endpoint region consists of the hadronic variable $n \cdot p_X$ and partonic variable $\bar{n} \cdot p$, where

$$\begin{aligned} \bar{n}\cdot p &= \bar{n}\cdot p_X + m_b - m_B = \bar{n}\cdot p_X - \overline{\Lambda} + \dots , \\ p_\omega^\mu &= \frac{n^\mu}{2}\bar{n}\cdot p + \frac{\bar{n}^\mu}{2} n\cdot p_X \,. \end{aligned} \tag{3.33}$$

They are natural because the LO factorization theorem dictates that the kinematic variables appear in the jet functions and soft functions only as

$$\mathcal{J}(\bar{n}\cdot p\, k^+)\,, \qquad f(n\cdot p_X - k^+)\,, \tag{3.34}$$

where k^+ is the convolution parameter (cf. Sec. 3.4). We shall see that this remains true of the shape functions and jet functions at subleading order in the power expansion. For a dimensionless version of $\bar{n}\cdot p$ we use $\overline{y} = \bar{n}\cdot p/m_b$. A comparison of the phase space with the variables $\{y_H = q^2/m_B^2, \sqrt{s_H} = m_X/m_B\}$ and $\{u_H, \overline{y}_H\}$ is shown in Fig. 3-2 and corresponds to the limits shown in columns iv) and v) of Tables 3.1 and 3.2. The figure on the right is the analog of Fig. 1 in Ref. [48] with dimensionless variables.

For a strict SCET expansion we want

$$\frac{n\cdot p_X}{\bar{n}\cdot p_X} \leq \lambda_H^2 \ll 1\,, \tag{3.35}$$

where the expansion is in the parameter λ_H. Eq. (3.35) is equivalent to $u_H/\overline{y}_H \leq \lambda_H^2$. For $B \to X_s\gamma$, Eqs. (3.13) and (3.35) imply that the endpoint region is

$$E_\gamma \gtrsim (m_B/2 - \Lambda) \sim 2.1\,\mathrm{GeV}\,. \tag{3.36}$$

For $B \to X_u\ell\bar{\nu}$, satisfying the criterion in Eq. (3.35) with values $\lambda_H^2 \simeq 0.2$ is equivalent to

$$\frac{m_X}{2E_X} \lesssim \frac{\lambda_H}{1+\lambda_H^2} = 0.37\,, \tag{3.37}$$

or $y_H \lesssim 1 - 2.68\sqrt{s_H} + s_H$. Not exceeding a given expansion parameter in Eq. (3.35) corresponds to specifying a triangular region of phase space (shown for $u_H/\overline{y}_H \leq 0.2$ in Fig. 3-2). We refer to this as the SCET region of phase space.[7] As can be seen from Fig. 3-2, the simpler restriction $y_H \leq 1 - 2.44\sqrt{s_H}$ gives a very good approximation to the SCET region since the boundary is roughly linear in the q^2 and m_X variables.

In calculating decay rates at subleading order, it is important to define carefully how the phase-space integrals are treated once we compute doubly differential or singly differential decay rates. The philosophy we adopt for $B \to X_u\ell\bar{\nu}$ is that we use SCET to compute the W_i, and hence the triply differential decay rate, for the SCET region in Eq. (3.35). In general, one may wish to integrate this rate over a larger region of phase space, and thus need to construct the full W_i's. This could be done using

$$W_i^{\rm full} \;=\; W_i^{\rm SCET}\theta(\lambda_H^2\overline{y}_H - u_H) + W_i^{\rm OPE}\theta(u_H - \lambda_H^2\overline{y}_H)\,, \tag{3.38}$$

[7]Note that the SCET expansion here is actually in powers of λ^2 since odd terms in SCET$_{\rm I}$ tend to be absent [39]. In Sec. 3.5 we show that the $\mathcal{O}(\lambda)$ contributions for inclusive decays indeed vanish. Thus $\lambda^2 = 0.2$ is not a large expansion parameter. A smaller value $\lambda_H^2 = 0.1$ could be chosen if desired.

where the SCET expansion in λ is used for the first term and the standard local OPE in Λ/m_b is used for the second term. Thus, λ_H does not play the role of a strict expansion parameter, but rather provides us with a means of interpolating any differential spectrum between the full OPE and full SCET results by varying λ_H between 0 and 1. We only consider the first term in Eq. (3.38) here. Depending on the final spectrum that one looks at and the other cuts imposed, the error in including a larger region of phase space than the SCET region may be power suppressed. The parameter λ_H provides us with a way of testing this by considering the difference between taking $\lambda_H = 0.2$ and $\lambda_H = 1$. We present our final results in a manner that makes it easy to take the $\lambda_H \to 1$ limit for situations where a large enough region has been smeared over that this is the case.

One can also refer to a shape-function region, corresponding to the region $0 \leq u_H \lesssim 0.1$ where the non-perturbative function f is important. The expansion for $B \to X_s\gamma$ to second order in λ, where $1 - x_H^\gamma \sim \lambda^2$, is

$$\frac{d\Gamma^s}{dx_H^\gamma} = \Gamma_0^s \frac{2}{m_B}\left[\left\{4W_1^s - W_2^s - m_B\, W_5^s\right\} - (1-x_H^\gamma)\left\{4W_1^s - W_2^s - 2m_B\, W_5^s\right\}\right]. \quad (3.39)$$

For $B \to X_u \ell\bar{\nu}$, if we integrate over all x_H and expand in $u_H \sim \lambda^2$, then from Eq. (3.32) the first two orders in the expansion are

$$\begin{aligned}\frac{1}{\Gamma_0^u}\frac{d^2\Gamma^u}{d\overline{y}_H\, du_H} &= 24 m_B\left[\left\{\overline{y}_H^2(1-\overline{y}_H)W_1^u + \frac{\overline{y}_H^4}{12}W_2^u\right\}\right. \\ &\qquad \left. + u_H\left\{\overline{y}_H(\overline{y}_H^2+\overline{y}_H-2)W_1^u - \frac{\overline{y}_H^3}{3}W_2^u\right\}\right]. \end{aligned} \quad (3.40)$$

By the endpoint region in x_H we mean $x_H^c \leq x_H \leq 1 - r_\pi^2$, where $1 - x_H^c \sim 0.1$ corresponds to making a cut on the lepton's energy spectrum. The limit on u_H forces it to be small, $u_H \leq 1 - x_H^c$, so shape-function effects are important here. This cut still allows a large range for $\overline{y}_H$. Expanding the triply differential rate in Eq. (3.31)

and keeping the first two orders in the expansion for $1-x_H \sim u_H \sim \lambda^2$ give

$$\begin{aligned}\frac{1}{\Gamma_0^u}\frac{d^3\Gamma^u}{dx_H^{cut}\,d\overline{y}_H\,du_H} &= 24m_B\Big[\Big\{\overline{y}_H(1-\overline{y}_H)\big(W_1^u+\frac{m_B\overline{y}_H}{2}W_3^u\big)\Big\} \\ &\quad -u_H\Big\{(1-\overline{y}_H^2)W_1^u+\frac{m_B}{2}\overline{y}_H(2-\overline{y}_H-\overline{y}_H^2)W_3^u\Big\} \\ &\quad +(1-x_H-u_H)\Big\{\frac{\overline{y}_H^2}{2}W_2^u-m_B\overline{y}_H(1-\overline{y}_H)W_3^u\Big\}\Big]\,.\end{aligned} \tag{3.41}$$

Finally, to consider the $d\Gamma/(dq^2dm_X^2)$ spectrum in the endpoint region we let $\zeta = 1-y_H+s_H$ and expand in s_H/ζ^2, which to linear order gives

$$\frac{1}{\Gamma_0^u}\frac{d^2\Gamma^u}{dy_H\,ds_H} = 2m_B\Big[\Big\{12\zeta(1-\zeta)W_1^u+\zeta^3W_2^u\Big\}+\frac{6s_H}{\zeta}\Big\{2(\zeta^2+2\zeta-2)W_1^u-\zeta^2W_2^u\Big\}\Big]\,. \tag{3.42}$$

In each of Eqs. (3.39)–(3.42) there will also be an expansion of the W_i themselves, which we discuss later on.

The results in this section can easily be extended to any desired order in Λ/m_B by expanding to higher order in the phase space.

3.2.4 OPE and Partonic Variables

We have not yet made use of quark-hadron duality or formulated the method for computing the W_i. The usual procedure to compute the W_i is to use an operator product expansion and calculate the forward scattering amplitude

$$\begin{aligned}T_{\mu\nu} &= \frac{1}{2m_B}\langle\bar{B}|\hat{T}_{\mu\nu}|\bar{B}\rangle \\ &= -g_{\mu\nu}T_1+v_\mu v_\nu T_2+i\epsilon_{\mu\nu\alpha\beta}v^\alpha q^\beta T_3+q_\mu q_\nu T_4+(v_\mu q_\nu+v_\nu q_\mu)T_5\,,\end{aligned} \tag{3.43}$$

where

$$\hat{T}_{\mu\nu} = -i\int d^4x\,e^{-iq\cdot x}\,T\,J_\mu^\dagger(x)J_\nu(0)\,, \tag{3.44}$$

and for the $T_i^{(s,u)}(q^2, v\cdot q)$ we use the corresponding hadronic currents, which are

$$J_\mu^s = \bar{s}\, i\sigma_{\mu\nu} q^\nu P_R\, b\,, \qquad J_\mu^u = \bar{u}\,\gamma^\mu P_L b\,. \tag{3.45}$$

Here J_μ^s comes from the operator $\mathcal{O}_7$. The operator product expansion relates the $W_i^{(u,s)}$ to the forward scattering amplitudes through

$$W_i = -\frac{1}{\pi}\,\mathrm{Im}\, T_i\,. \tag{3.46}$$

When we compute the W_i with an OPE, the partonic variables depending on m_b and the hadronic variables involving m_B will need to be related order by order in the $1/m_b$ expansion. In particular, the heavy meson mass to second order is

$$m_B = m_b + \overline{\Lambda} - \frac{\lambda_1}{2m_b} - \frac{3c_F(\mu)\lambda_2(\mu)}{2m_b} + \ldots\,, \tag{3.47}$$

where we shall also use $\lambda_2 = c_F(\mu)\lambda_2(\mu)$ as a definition of the non-perturbative matrix element that has the perturbative coefficient $c_F(\mu)$ absorbed.

In applying the local OPE, part of the expansion involved in switching to hadronic variables occurs because the phase-space limits are partonic. In fact, if we calculate the triply differential rate for $B \to X_u \ell\bar{\nu}$ with the local OPE, and then consider integrating it over the hadronic phase space, then the integrand has support over the partonic phase space only, so the limits are reduced to this more restricted case. In the local OPE the signal for this is the occurrence of factors like

$$\delta^{(n)}[(m_b v - q)^2]\,, \tag{3.48}$$

which must be smeared sufficiently so that quark-hadron duality can be used. For the $\delta[(m_b v - q)^2]$ that occurs at LO, integrating once to get the doubly differential rate gives a theta function that imposes partonic limits.

On the other hand, with the SCET expansion in the endpoint region the support of the triply differential rate is larger. We never encounter singular distributions like

the one in Eq. (3.48), but instead obtain a non-trivial forward B-hadronic matrix element that gives $f^{(0)}(\ell^+)$. This function knows about the difference between the hadronic and partonic phase space already at leading order in the power counting, and more generally the LO factorization result with $\mathcal{O}(\alpha_s)$ corrections (cf. Eq. (3.82) below) does not cause a restriction of the hadronic phase space. Therefore, we shall use the full hadronic phase-space limits in our computation.[8]

3.3 Heavy-to-light currents

To derive the expansion of the T_i in the endpoint region, we determine the SCET currents and Lagrangians in a power expansion in λ, and use this expansion to separate the collinear jet-like effects from the non-perturbative ultrasoft shape functions. This will allow us to determine results for the T_i order by order in the expansion. We write

$$T_i = T_i^{(0)} + T_i^{(1)} + T_i^{(2)} + \dots . \tag{3.49}$$

The ingredients required for this include expansions of the Lagrangians and currents to second order in λ. The Lagrangian expansions were given in Chapter 2, while the heavy-to-light currents are presented here.

For simplicity, we work in a frame where $v_\perp = 0$. Expanding the J^u current to $\mathcal{O}(\lambda^2)$ gives

$$\begin{aligned} J^u = e^{-i(\bar{\mathcal{P}}\frac{n}{2}+\mathcal{P}_\perp+m_b v)\cdot x} \Big\{ & \sum_j \int d\omega C_j^{(v)}(\omega) J_j^{u(0)}(\omega) + \sum_j \int d\omega B_j^{(v)}(\omega) J_j^{u(1)}(\omega) \\ & + \sum_j \int d\omega A_j^{(v)}(\omega) J_j^{u(2)}(\omega) \Big\} , \end{aligned} \tag{3.50}$$

where the superscript (0), (1), (2) indicates the order in λ. We have an analogous

[8]Note that this might imply that direct calculations of less differential subleading spectra must be treated with care. For example, if one directly computes a singly differential rate by tying up lepton lines then the partonic phase-space restrictions might appear to creep back in if one is not sufficiently careful about the structure of the factorization theorem.

result for J^s with $(v) \to (t)$ and $u \to s$. After one makes the field redefinition in Eq. (2.48), the leading-order SCET heavy-to-light current is [23]

$$J_j^{(0)}(\omega) \;=\; (\bar\xi_n W)_\omega \Gamma_j^{(0)} (Y^\dagger h_v) = \bar\chi_{n,\omega} \Gamma_j^{(0)} \mathcal{H}_v \,, \tag{3.51}$$

where j = 1-3 for u and j = 1-4 for s. Despite the fact that the operator in $J^{(0)}$ is $\mathcal{O}(\lambda^4)$, we use the superscript (0), to indicate that it is the lowest-order current. At the first subleading order, we have the $\mathcal{O}(\lambda^5)$ currents [59, 37, 31, 130]

$$\begin{aligned} J_j^{(1a)}(\omega) &= \frac{1}{\omega} \big(\bar\chi_n \, i\overleftarrow{\mathcal{D}}_{c\perp}^\alpha\big)_\omega \Upsilon_j^{(1a)} \, \mathcal{H}_v \,, \\ J_j^{(1b)}(\omega_1,\omega_2) &= \frac{1}{m_b \, n\!\cdot\! v} \, \bar\chi_{n,\omega_1} \, (ig\mathcal{B}_{c\perp}^\alpha)_{\omega_2} \, \Upsilon_j^{(1b)} \, \mathcal{H}_v \,. \end{aligned} \tag{3.52}$$

The subscript ω notation in Eqs. (3.51) and (3.52) indicates that the field carries momentum ω, for example

$$\bar\chi_{n,\omega} = \bar\chi_n \, \delta(\omega - \bar{\mathcal{P}}^\dagger) \,, \qquad (ig\mathcal{B}_{c\perp}^\alpha)_{\omega_2} = (ig\mathcal{B}_{c\perp}^\alpha) \, \delta(\omega_2 - \bar{\mathcal{P}}^\dagger) \,. \tag{3.53}$$

Finally, at second order we find that the basis of $\mathcal{O}(\lambda^6)$ currents consists of

$$\begin{aligned} J_j^{(2a)}(\omega) &= \frac{1}{2m_b} \, \bar\chi_{n,\omega} \, \Upsilon_{j\,\alpha}^{(2a)} \, i\overrightarrow{\mathcal{D}}_{us}^{T\,\alpha} \, \mathcal{H}_v \,, \\ J_j^{(2b)}(\omega) &= \frac{1}{\omega} \, \bar\chi_{n,\omega} \, \Upsilon_{j\,\alpha}^{(2b)} \, i\overleftarrow{\mathcal{D}}_{us}^{\perp\,\alpha} \, \mathcal{H}_v \,, \\ J_j^{(2c)}(\omega) &= -\Big(\bar\chi_n \frac{\bar n\!\cdot\! v}{\bar{\mathcal{P}}} \frac{ign\!\cdot\!\mathcal{B}_c}{n\!\cdot\! v}\Big)_\omega \Upsilon_j^{(2c)} \, \mathcal{H}_v \,, \\ J_j^{(2d)}(\omega_1,\omega_2) &= \frac{-1}{m_b} \bar\chi_{n,\omega_1} \Big(\frac{ign\!\cdot\!\mathcal{B}_c}{n\!\cdot\! v}\Big)_{\omega_2} \Upsilon_j^{(2d)} \, \mathcal{H}_v \,, \\ J_j^{(2e)}(\omega_1,\omega_2) &= \frac{-1}{m_b \, n\!\cdot\! v \, \omega_1} \big(\bar\chi_n i\overleftarrow{\mathcal{D}}_{c\perp}^\alpha\big)_{\omega_1} (ig\mathcal{B}_{c\perp}^\beta)_{\omega_2} \Upsilon_{j\alpha\beta}^{(2e)} \, \mathcal{H}_v \,, \\ J_j^{(2f)}(\omega_1,\omega_2) &= \frac{-1}{m_b} \bar\chi_{n,\omega_1} \Big(\frac{1}{n\!\cdot\! v \, \bar{\mathcal{P}}} i\mathcal{D}_{c\perp}^\alpha \, ig\mathcal{B}_{c\perp}^\beta\Big)_{\omega_2} \Upsilon_{j\,\alpha\beta}^{(2f)} \, \mathcal{H}_v \,. \end{aligned} \tag{3.54}$$

These currents were first derived in Ref. [38] (see also [37]) and we agree with their results. Two differences are that in Eq. (3.54) we have determined the functional dependence and the number of parameters ω_i, and that terms from the separation

of label and residual momenta (or equivalently the multipole expansion of the fields) are treated differently here from Ref. [38]. In Appendix A we give a more detailed comparison, along with the details of our calculation.

For the LO Dirac structures we use the basis from Refs. [59, 130], which is the most convenient for considering reparameterization invariance, i.e.

$$\Gamma_{1-3}^{u(0)} = P_R\Big\{\gamma^\mu\,, v^\mu\,, \frac{n^\mu}{n\cdot v}\Big\}\,, \quad \Gamma_{1-4}^{s(0)} = P_R\; q_\tau\,\Big\{i\sigma^{\mu\tau}\,, \gamma^{[\mu,}v^{\tau]}\,, \frac{\gamma^{[\mu,}n^{\tau]}}{n\cdot v}\,, \frac{n^{[\mu,}v^{\tau]}}{n\cdot v}\Big\}\,. \tag{3.55}$$

Here we slightly reorganize the basis in Ref. [130] to reflect the constraints from RPI and to use subscripts $j > 11$ for the currents that vanish when $v_\perp = 0$. This gives

$$\begin{aligned}
\Upsilon_{1-3}^{u(1a)} &= P_R\Big\{\gamma_\perp^\alpha\frac{\bar{n}\!\!\!/}{2}\gamma^\mu, \gamma_\perp^\alpha\frac{\bar{n}\!\!\!/}{2}v^\mu, \gamma_\perp^\alpha\frac{\bar{n}\!\!\!/}{2}n^\mu - 2g_\perp^{\alpha\mu}\Big\}\,, \quad \Upsilon_{4-7}^{u(1b)} = P_R\Big\{\gamma^\mu\gamma_\perp^\alpha, v^\mu\gamma_\perp^\alpha\,, n^\mu\gamma_\perp^\alpha, g_\perp^{\mu\alpha}\Big\}\,,\\
\Upsilon_{1-4}^{s(1a)} &= P_R\, q_\nu\,\Big\{i\gamma_\perp^\alpha\frac{\bar{n}\!\!\!/}{2}\sigma^{\mu\nu}\,,\; \gamma_\perp^\alpha\frac{\bar{n}\!\!\!/}{2}\gamma^{[\mu,}v^{\nu]}\,,\; \gamma_\perp^\alpha\frac{\bar{n}\!\!\!/}{2}\gamma^{[\mu,}n^{\nu]} + 2g_\perp^{\alpha[\mu,}\gamma^{\nu]}\,,\; \gamma_\perp^\alpha\frac{\bar{n}\!\!\!/}{2}n^{[\mu,}v^{\nu]} - 2g_\perp^{\alpha[\mu,}v^{\nu]}\Big\}\,,\\
\Upsilon_{5-11}^{s(1b)} &= P_R\, q_\nu\,\Big\{i\sigma^{\mu\nu}\gamma_\perp^\alpha\,,\; \gamma^{[\mu,}v^{\nu]}\gamma_\perp^\alpha\,,\; \gamma^{[\mu,}n^{\nu]}\gamma_\perp^\alpha\,,\; n^{[\mu,}v^{\nu]}\gamma_\perp^\alpha\,,\; g_\perp^{\alpha[\mu,}\gamma^{\nu]}\,,\; g_\perp^{\alpha[\mu,}v^{\nu]}\,,\; g_\perp^{\alpha[\mu,}n^{\nu]}\Big\}\,.
\end{aligned} \tag{3.56}$$

Note that we do not list evanescent Dirac structures that can become necessary when computing perturbative corrections in dimensional regularization (see for example Refs. [40, 34]). For our purposes, the Dirac structures for the $J^{(2)}$ currents that appear at lowest order in $\alpha_s(m_b)$ will suffice; these are

$$\begin{aligned}
\Upsilon_1^{u(2a)} &= P_R\,\gamma^\mu\gamma_T^\alpha\,, \quad \Upsilon_1^{u(2b)} = P_R\,\gamma_\perp^\alpha\frac{\bar{n}\!\!\!/}{2}\gamma^\mu\,, \quad \Upsilon_1^{u(2c)} = P_R\,\gamma^\mu\,, \quad \Upsilon_1^{u(2d)} = P_R\,\gamma^\mu\frac{\bar{n}\!\!\!/ n\!\!\!/}{4}\,,\\
\Upsilon_1^{u(2e)} &= P_R\,\gamma_\alpha^\perp\frac{\bar{n}\!\!\!/}{2}\gamma^\mu\frac{n\!\!\!/}{2}\gamma_\beta^\perp\,, \qquad \Upsilon_1^{u(2f)} = P_R\,\gamma^\mu\gamma_\alpha^\perp\gamma_\beta^\perp\,,\\
\Upsilon_1^{s(2a)} &= P_R\,i\sigma^{\mu\tau}\gamma_T^\alpha q_\tau\,, \qquad \Upsilon_1^{s(2b)} = P_R\,\gamma_\perp^\alpha\frac{\bar{n}\!\!\!/}{2}\,i\sigma^{\mu\tau}q_\tau\,, \qquad \Upsilon_1^{s(2c)} = P_R\,i\sigma^{\mu\tau}q_\tau\,,\\
\Upsilon_1^{s(2d)} &= P_R\,i\sigma^{\mu\tau}q_\tau\frac{\bar{n}\!\!\!/ n\!\!\!/}{4}\,, \quad \Upsilon_1^{s(2c)} = P_R\,\gamma_\alpha^\perp\frac{\bar{n}\!\!\!/}{2}i\sigma^{\mu\tau}q_\tau\frac{n\!\!\!/}{2}\gamma_\beta^\perp\,, \quad \Upsilon_1^{s(2f)} = P_R\,i\sigma^{\mu\tau}q_\tau\gamma_\alpha^\perp\gamma_\beta^\perp\,.
\end{aligned} \tag{3.57}$$

The complete tree-level currents for arbitrary $v_\perp$ are given in Appendix A, and in Appendix B we show how the $v_\perp$ dependence is necessary to satisfy the full constraints

from RPI at this order. When the $\mathcal{O}(\lambda^2)$ currents that show up at order $\alpha_s(m_b)$ are determined, the number of possible $\Upsilon_j^{(2)}$ structures will increase, as occurred in Eq. (3.56). However, this will not affect the form of the factorization theorems we derive, since they are expressed in terms of traces of the $\Upsilon_j^{(2)}$ factors; this makes it trivial to incorporate new Dirac structures that arise beyond tree level.

At lowest order in $\alpha_s(m_b)$, the non-zero coefficients in Eq. (3.50) are

$$C_1^{(v)} = C_1^{(t)} = B_1^{(v)} = B_{1,7}^{(t)} = -B_6^{(v)} = 1\,. \tag{3.58}$$

The one-loop results and RGE-improved coefficients C_i can be found in Ref. [23]. Our coefficients are linear combinations of these:

$$\begin{aligned}
C_1^{(v)}(\hat{\omega},1) &= 1 - \frac{\alpha_s(m_b)C_F}{4\pi}\left\{2\ln^2(\hat{\omega}) + 2\mathrm{Li}_2(1-\hat{\omega}) + \ln(\hat{\omega})\left(\frac{3\hat{\omega}-2}{1-\hat{\omega}}\right) + \frac{\pi^2}{12} + 6\right\},\\
C_2^{(v)}(\hat{\omega},1) &= \frac{\alpha_s(m_b)C_F}{4\pi}\left\{\frac{2}{(1-\hat{\omega})} + \frac{2\hat{\omega}\ln(\hat{\omega})}{(1-\hat{\omega})^2}\right\},\\
C_3^{(v)}(\hat{\omega},1) &= \frac{\alpha_s(m_b)C_F}{4\pi}\left\{\frac{(1-2\hat{\omega})\hat{\omega}\ln(\hat{\omega})}{(1-\hat{\omega})^2} - \frac{\hat{\omega}}{1-\hat{\omega}}\right\},\\
C_1^{(t)}(\hat{\omega},1) &= 1 + \Delta_\gamma(m_b,\rho)\\
&\quad - \frac{\alpha_s(m_b)C_F}{4\pi}\left\{2\ln^2(\hat{\omega}) + 2\mathrm{Li}_2(1-\hat{\omega}) + \ln(\hat{\omega})\left(\frac{4\hat{\omega}-2}{1-\hat{\omega}}\right) + \frac{\pi^2}{12} + 6\right\},\\
C_2^{(t)}(\hat{\omega},1) &= 0\,,\\
C_3^{(t)}(\hat{\omega},1) &= \frac{\alpha_s(m_b)C_F}{4\pi}\left\{\frac{-2\hat{\omega}\ln(\hat{\omega})}{1-\hat{\omega}}\right\},\\
C_4^{(t)}(\hat{\omega},1) &= 0\,,
\end{aligned} \tag{3.59}$$

where $\hat{\omega} = \omega/m_b$ and $\Delta_\gamma(m_b,\rho)$ was given in Eq. (3.11). Thus, non-zero values for $C_{2,3}^{(v)}$ and $C_3^{(t)}$ are generated at one-loop order, while $C_{2,4}^{(t)}$ are still zero at this order. For the $J^{(1b)}$ currents, the one-loop matching coefficients were derived in Ref. [40], and the anomalous dimensions and RGE-improved coefficients were computed in Ref. [87].

By reparameterization invariance $B_{1-3}^{(v)}(\omega) = C_{1-3}^{(v)}(\omega)$ and $B_{1-4}^{(t)}(\omega) = C_{1-4}^{(t)}(\omega)$, so their one-loop matching coefficients are in Eq. (3.59). For the $\mathcal{O}(\lambda^2)$ current

T-product	Example Diagram	Hard, Jet, and Shape Functions	Usoft Operator
$T^{(0)}$	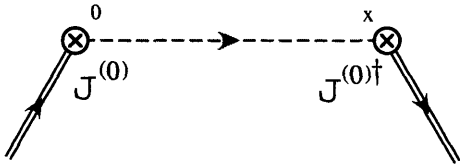	$h^{[0]}\,\mathcal{J}^{(0)}\,f^{(0)}$	$\bar{h}_v(x)h_v(0)$

Table 3.3: Lowest-order insertion of SCET currents. The double lines are heavy quarks and the dashed line is a collinear light quark.

coefficients the RPI constraints are

$$\begin{aligned} A_1^{(v)} = A_2^{(v)} = -\frac{1}{2}A_3^{(v)} = C_1^{(v)}(\omega)\,, \qquad A_4^{(v)} = A_5^{(v)} = A_6^{(v)} = B_7^{(v)}(\omega_1,\omega_2)\,, \\ A_1^{(t)} = A_2^{(t)} = -\frac{1}{2}A_3^{(t)} = C_1^{(t)}(\omega)\,, \qquad A_4^{(t)} = A_5^{(t)} = A_6^{(t)} = B_7^{(t)}(\omega_1,\omega_2)\,. \end{aligned} \tag{3.60}$$

Note that we have not included effects associated with a non-zero strange-quark mass in our basis of subleading SCET operators, and it would be interesting from a formal view-point to consider the possibility of such power-suppressed terms in the future (cf. [109]).

3.4 Leading-Order Factorization

In this section we review the leading-order factorization theorem [99] as derived using SCET [30]. The result is discussed in detail, which will allow us to refer back to this section when some of the steps are repeated at NLO. Throughout this section we shall suppress the u and s superscripts, since all the manipulations are identical in both cases, $B \to X_u \ell\bar{\nu}$ and $B \to X_s\gamma$.

To derive the leading order $T_i^{(0)}$ we need only consider $\hat{T}_{\mu\nu}^{(0)}$, given by taking two LO currents $J^{(0)}$, as shown in Table 3.3. The phase factor in Eq. (3.50) gives

$$e^{-i(q+\frac{n}{2}\bar{\mathcal{P}}-m_b v)\cdot x} \equiv e^{-ir\cdot x} \tag{3.61}$$

and $\exp(-i\mathcal{P}_\perp \cdot x)$. The current has $q_\perp = 0$, so this $\mathcal{P}_\perp$ term will contribute only to fixing the perpendicular momentum of the jet function to be zero. The large label momentum in the phase in Eq. (3.50) also gets fixed by momentum conservation:

$$\bar{\mathcal{P}} = m_b - \bar{n}\cdot q = m_b - m_B + \bar{n}\cdot p_X \equiv \bar{n}\cdot p\,, \tag{3.62}$$

where $\bar{n}\cdot p_X$ is the large momentum in the jet X. Then the remaining momentum $r^\mu \sim \Lambda$ since $\bar{n}\cdot r = \bar{n}\cdot q + \bar{\mathcal{P}} - m_b = 0$ and

$$n\cdot r \;=\; n\cdot q - m_b = m_B - m_b - n\cdot p_X\,. \tag{3.63}$$

At lowest order

$$\bar{n}\cdot p = \bar{n}\cdot p_X\,, \qquad\qquad n\cdot r = \overline{\Lambda} - n\cdot p_X\,, \tag{3.64}$$

where both $\overline{\Lambda}, n\cdot p_X \sim \Lambda$ (and higher-order terms in $m_B - m_b$ will be needed only when we go beyond LO). For the time being we stick to the partonic variables $\bar{n}\cdot p$ and $n\cdot r$; later, we shall perform the expansion involved in switching to hadronic variables. Using the states defined with HQET, we get

$$\begin{aligned} W^{(0)}_{\mu\nu} &= \frac{(-1)}{\pi}\mathrm{Im}\,\frac{1}{2}\langle \bar{B}_v|\hat{T}^{(0)}_{\mu\nu}|\bar{B}_v\rangle\,, \\ \hat{T}^{(0)}_{\mu\nu} &= -i\int d^4x\, e^{-ir\cdot x}\; T\; J^{(0)\dagger}_{j'\,\mu}(x)\; J^{(0)}_{j\,\nu}(0)\,. \end{aligned} \tag{3.65}$$

Separating out the hard Wilson coefficients, we have

$$\hat{T}^{(0)}_{\mu\nu} = \sum_{j,j'}\int d\omega d\omega'\, C_{j'}(\omega')C_j(\omega)\delta(\omega' - \bar{n}\cdot p)(-i)\int d^4x\, e^{-ir\cdot x}\; T\; J^{(0)\dagger}_{j'\,\mu}(\omega', x)\; J^{(0)}_{j\,\nu}(\omega, 0). \tag{3.66}$$

The effective-theory currents in the remaining time-ordered product depend only on

collinear and usoft fields describing momenta $p^2 \ll m_b^2$, i.e.

$$T\, J^{(0)\dagger}_{j'\mu}(\omega',x)\, J^{(0)}_{j\nu}(\omega,0) \;=\; \big[\bar{\mathcal{H}}_v \overline{\Gamma}^{(0)}_{j'\mu} \chi_{n,\omega'}\big](x)\, \big[\bar{\chi}_{n,\omega} \Gamma^{(0)}_{j\nu} \mathcal{H}_v\big](0)\,, \tag{3.67}$$

where $\bar{\Gamma} \equiv \gamma^0 \Gamma^\dagger \gamma^0$. It is useful to group the collinear and usoft fields into common brackets by using a Fierz rearrangement. For spin and colour we can use

$$\begin{aligned} 1 \otimes 1 \;&=\; \frac{1}{2} \sum_{k=1}^{6} F_k^{\bar{n}} \otimes F_k^n \qquad\qquad (3.68)\\ &=\; \frac{1}{2}\Big[\big(\frac{\bar{n}\!\!\!/}{2N_c}\big)\otimes\big(\frac{n\!\!\!/}{2}\big) + \big(\frac{-\bar{n}\!\!\!/\gamma_5}{2N_c}\big)\otimes\big(\frac{n\!\!\!/\gamma_5}{2}\big) + \big(\frac{-\bar{n}\!\!\!/\gamma_\perp^\alpha}{2N_c}\big)\otimes\big(\frac{n\!\!\!/\gamma_\alpha^\perp}{2}\big) \\ &\qquad + \big(\bar{n}\!\!\!/ T^a\big)\otimes\big(\frac{n\!\!\!/ T^a}{2}\big) + \big(-\bar{n}\!\!\!/\gamma_5 T^a\big)\otimes\big(\frac{n\!\!\!/\gamma_5 T^a}{2}\big) + \big(-\bar{n}\!\!\!/\gamma_\perp^\alpha T^a\big)\otimes\big(\frac{n\!\!\!/\gamma_\alpha^\perp T^a}{2}\big)\Big]\,. \end{aligned}$$

Equation (3.68) is valid as long as the identity matrices on the LHS are inserted such that on the RHS the $F_k^{\bar{n}}$ appear as $\bar{\xi}_n A F_k^{\bar{n}} B \xi_n$, where A and B do not contain $\bar{n}\!\!\!/$ factors. In Eq. (3.67) we insert identity matrices to the right of the $\overline{\Gamma}^{(0)}_{j'\mu}$ and to the left of the $\Gamma^{(0)}_{j\nu}$, which gives

$$\begin{aligned} \langle \bar{B}_v | T\, J^{(0)\dagger}_{j'\mu}(\omega',x)\, J^{(0)}_{j\nu}(\omega,0) | \bar{B}_v\rangle \;&=\; \frac{(-1)}{2}\, \langle \bar{B}_v | T\big[\bar{\mathcal{H}}_v(x) \overline{\Gamma}^{(0)}_{j'\mu} F_k^n\, \Gamma^{(0)}_{j\nu}\, \mathcal{H}_v(0)\big] | \bar{B}_v\rangle \\ &\quad \times \langle 0 | T\big[\bar{\chi}_{n,\omega}(0)\, F_k^{\bar{n}}\, \chi_{n,\omega'}(x)\big] | 0\rangle\,. \end{aligned} \tag{3.69}$$

Here the states $|\bar{B}_v\rangle$ have HQET normalization, $\langle B_v(k')|B_v(k)\rangle = 2v^0(2\pi)^3\delta^3(\mathbf{k}'-\mathbf{k})$, and are defined as energy eigenstates of the LO usoft Hamiltonian generated from $\mathcal{L}^{(0)}_{us}$.

Only the vacuum matrix element with $k = 1$ is non-zero:[9]

$$\begin{aligned} \langle 0 | T\big[\bar{\chi}_{n,\omega}(0) \frac{\bar{n}\!\!\!/}{2N_c} \chi_{n,\omega'}(x)\big] | 0\rangle &= \langle 0 | T\big[(\bar{\xi}_n W)_\omega(0) \frac{\bar{n}\!\!\!/}{2N_c} (W^\dagger \xi_n)_{\omega'}(x)\big] | 0\rangle \\ &=\; (-2i)\,\delta(\omega-\omega')\delta^2(x_\perp)\delta(x^+) \int \frac{dk^+}{2\pi}\, e^{-ik^+x^-/2}\, \mathcal{J}^{(0)}_\omega(k^+)\,. \end{aligned} \tag{3.70}$$

[9]Note that in Eq. (3.70) $\delta^2(x_\perp) \sim \lambda^2$, since from the momentum-space view-point it is obtained by combining integrals over both the label momentum $p_\perp \sim \lambda$ and residual momenta $k_\perp \sim \lambda^2$, rather than just the latter.

This definition of $\mathcal{J}_\omega^{(0)}$ agrees with Ref. [30].[10] Owing to the forward matrix element, the momentum-conserving delta function gives the $\delta(\omega' - \omega)$, which can be used to eliminate the ω' integral in Eq. (3.65), and the delta function in Eq. (3.66) then sets

$$\omega = \bar{n}\cdot p\,. \tag{3.71}$$

The appearance of the $\delta(x^+)$ ensures that in the remaining usoft matrix element in Eq. (3.69) time ordering is the same as path ordering along x^-. Up to order α_s, the one-loop diagrams plus counterterms give

$$\mathcal{J}_\omega^{(0)}(k^+) = \frac{\omega}{\omega k^+ + i\epsilon}\left\{1 + \frac{\alpha_s(\mu)C_F}{4\pi}\left[2\ln^2\left(\frac{-\omega k^+ - i\epsilon}{\mu^2}\right) - 3\ln\left(\frac{-\omega k^+ - i\epsilon}{\mu^2}\right) + 7 - \frac{\pi^2}{3}\right]\right\}, \tag{3.72}$$

which agrees with Refs. [27, 47].

Next, we simplify the spin structure of the B matrix element in Eq. (3.69) using the formula

$$P_v\Gamma P_v = P_v \mathrm{Tr}\Big[\frac{1}{2}P_v\Gamma\Big] + s_\mu \mathrm{Tr}\Big[-\frac{1}{2}s^\mu\Gamma\Big] \equiv \sum_{m=1}^{2} P_m^h\,\mathrm{Tr}[P_m^H\Gamma]\,, \tag{3.73}$$

which is valid between heavy quark fields. Here, $P_1^h = P_v$, $P_1^H = P_v/2$, $P_2^h = s_\mu$, $P_2^H = -s^\mu/2$ for $P_v = (1+\not{v})/2$ and $s_\mu \equiv P_v\gamma_\mu^T\gamma_5 P_v$. For our LO matrix element the s^μ term vanishes and, taking into account the delta functions in Eq. (3.70), we have only a function of

$$\tilde{x}^\mu = \bar{n}\cdot x\, n^\mu/2\,, \tag{3.74}$$

[10] To check this, one must note that here we contract colour indices on the LHS and have an extra minus sign, since the χ_n fields are in the opposite order to Ref. [30].

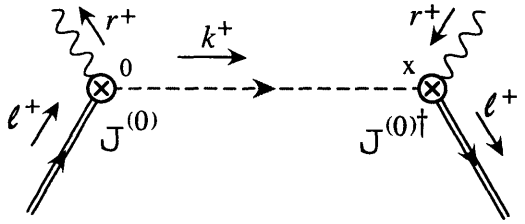

Figure 3-3: Momentum routing for leading-order insertion of currents.

namely

$$\langle \bar{B}_v | T\Big[\bar{\mathcal{H}}_v(\tilde{x})\,\overline{\Gamma}^{(0)}_{j'\mu}\,\frac{\not{n}}{2}\,\Gamma^{(0)}_{j\nu}\,\mathcal{H}_v(0)\Big] | \bar{B}_v\rangle = \mathrm{Tr}\Big[\frac{P_v}{2}\,\overline{\Gamma}^{(0)}_{j'\mu}\,\frac{\not{n}}{2}\,\Gamma^{(0)}_{j\nu}\Big]\langle \bar{B}_v|\bar{h}_v(\tilde{x})Y(\tilde{x},0)h_v(0)|\bar{B}_v\rangle\,. \tag{3.75}$$

where $Y(\tilde{x},\tilde{y}) \equiv Y(\tilde{x})Y^\dagger(\tilde{y}) = \mathrm{P}\,\exp\Big(ig\int_{y^-}^{x^-} \mathrm{d}s\; n\cdot A_{us}(sn/2)\Big)$. Combining the phases from Eqs. (3.65) and (3.70) and noting that $d^4x = (dx^+dx^-d^2x_\perp)/2$, we see that the matrix element in Eq. (3.69) is now

$$i\,\mathrm{Tr}\Big[\frac{P_v}{2}\,\overline{\Gamma}^{(0)}_{j'\mu}\,\frac{\not{n}}{2}\,\Gamma^{(0)}_{j\nu}\Big]\int dk^+\int\frac{dx^-}{4\pi}e^{-ix^-(r^++k^+)/2}\,\mathcal{J}^{(0)}_\omega(k^+)\langle \bar{B}_v|\bar{h}_v(\tilde{x})Y(\tilde{x},0)h_v(0)|\bar{B}_v\rangle\,. \tag{3.76}$$

After we pull out the large phases, the residual momenta are as shown in Fig. 3-3, where $\ell^+ = r^+ + k^+$. Equation (3.76) involves just the leading-order shape function

$$\begin{aligned} f^{(0)}(\ell^+) &= \frac{1}{2}\int\frac{dx^-}{4\pi}e^{-ix^-\ell^+/2}\,\langle \bar{B}_v|\bar{h}_v(\tilde{x})Y(\tilde{x},0)h_v(0)|\bar{B}_v\rangle \\ &= \frac{1}{2}\,\langle \bar{B}_v|\bar{h}_v\delta(\ell^+ - in\cdot D)h_v|\bar{B}_v\rangle\,. \end{aligned} \tag{3.77}$$

Note that we have taken $m_b \gg \Lambda$, and that Eq. (3.77) depends only on the residual momentum and masses that are of order Λ. Since we are free to integrate by parts in the forward matrix element, it is evident that $f^{(0)}(\ell^+)$ is real. Momentum conservation implies that the residual momentum of the b-quark should not be larger than the residual mass $\bar{\Lambda}$ of the B-meson, so $f(\ell^+)$ is non-zero only for $\ell^+ \le m_B - m_b = \bar{\Lambda}$. Inserting r^+ from Eq. (3.63), this implies that $k^+ \le p_X^+$. In $\overline{\mathrm{MS}}$ the renormalized shape function depends only on ratios of the dimensional regularization scale μ and

momentum scales $\sim \Lambda$.

To derive the leading-order jet function we need the imaginary part of $(-i)$ times the result in Eq. (3.76), which is the imaginary part of $\mathcal{J}_\omega^{(0)}(k^+)\, f^{(0)}(\ell^+)$. Although the B matrix element integrated over x^- is real, it does provide a theta function that restricts $k^+ < p_X^+$ and therefore cannot be ignored in taking the imaginary part. The function $\mathcal{J}_\omega^{(0)}(k^+)$ has an imaginary part for $k^+ > 0$ only, so we have support for the imaginary part over a finite interval only. The crucial point is that these theta functions are generated by dynamics within the effective theory and occur even though we have taken the $m_b \to \infty$ limit. For the leading-order jet function for $B \to X_{u,s}$ we therefore have $[\omega = \bar{n}\cdot p]$

$$\mathcal{J}^{(0)}(\omega\, k^+) = -\frac{1}{\pi}\,\mathrm{Im}\Big[\,\mathcal{J}_\omega^{(0)}(k^+)\;\theta(p_X^+ - k^+)\theta(k^+)\,\Big]\,. \tag{3.78}$$

By RPI-III invariance [118], this $\mathcal{J}^{(0)}$ is a non-trivial function of only the invariant product (ωk^+), times an overall factor of ω and the theta functions. For notational convenience, we suppress these extra dependences when writing the arguments of $\mathcal{J}^{(0)}$ as ωk^+.

Since $r^+ = n\cdot q - m_b \le \ell^+ \le \overline{\Lambda}$, or equivalently $0 \le k^+ \le p_X^+$, it is convenient to use the variables $p_\omega^2 = \bar{n}\cdot p\, n\cdot p_X$ and z, where

$$k^+ = z\; p_X^+\,, \tag{3.79}$$

so that $\omega k^+ = z\,\bar{n}\cdot p\, n\cdot p_X = z\, p_\omega^2$, and $J_\omega^{(0)}(k^+)$ is non-zero only for $0 \le z \le 1$. At order α_s, taking the imaginary part of Eq. (3.72) gives

$$\begin{aligned}\mathcal{J}^{(0)}(z, p_\omega^2, \mu) \;=\; & \frac{\omega}{p_\omega^2}\Bigg\{\delta(z)\bigg[1 + \frac{\alpha_s(\mu)C_F}{4\pi}\Big(2\ln^2\frac{p_\omega^2}{\mu^2} - 3\ln\frac{p_\omega^2}{\mu^2} + 7 - \pi^2\Big)\bigg] \\ & + \frac{\alpha_s(\mu)C_F}{4\pi}\bigg[\Big(\frac{4\ln z}{z}\Big)_+ + \Big(4\ln\frac{p_\omega^2}{\mu^2} - 3\Big)\frac{1}{(z)_+}\bigg]\Bigg\}\theta(1-z)\,\theta(z)\,,\end{aligned} \tag{3.80}$$

with the standard definitions for the plus functions. Our definition for the jet function agrees with Refs. [27, 47] once we compensate for the extra $\theta(p_X^+ - k^+)$ that we included

in Eq. (3.78). The jet function depends only on the dimensionless parameter z and ratios of μ^2 and the momentum at the jet scale, $p_\omega^2 \sim Q\Lambda$.

At this point we have separated momentum scales in $\mathrm{SCET_I}$, and, combining Eqs. (3.65), (3.69), (3.70), (3.78), (3.75), and (3.77), we arrive at the LO factorization theorem in terms of partonic variables,

$$\begin{aligned} W_i^{(0)} &= h_i(\bar{n}\cdot p, m_b, \mu) \int_{r^+}^{\bar{\Lambda}} d\ell^+ \, \mathcal{J}^{(0)}(\bar{n}\cdot p(\ell^+ - r^+), \mu) \, f^{(0)}(\ell^+, \mu) \\ &= h_i(\bar{n}\cdot p, m_b, \mu) \int_0^{\bar{\Lambda}-r^+} dk^+ \, \mathcal{J}^{(0)}(\bar{n}\cdot p \, k^+, \mu) \, f^{(0)}(k^+ + r^+, \mu) \,. \end{aligned} \tag{3.81}$$

Using Eq. (3.64), the final LO result in terms of hadronic variables can be written as

$$\begin{aligned} W_i^{(0)} &= h_i(p_X^-, m_b, \mu) \int_{\bar{\Lambda}-p_X^+}^{\bar{\Lambda}} d\ell^+ \, \mathcal{J}^{(0)}(p_X^-(\ell^+ - \bar{\Lambda} + p_X^+), \mu) \, f^{(0)}(\ell^+, \mu) \\ &= h_i(p_X^-, m_b, \mu) \int_0^{p_X^+} dk^+ \, \mathcal{J}^{(0)}(p_X^- \, k^+, \mu) \, f^{(0)}(k^+ + \bar{\Lambda} - p_X^+, \mu) \\ &= h_i(p_X^-, m_b, \mu) \, p_X^+ \int_0^1 dz \; \mathcal{J}^{(0)}(z \, m_X^2, \mu) \, f^{(0)}\big(\bar{\Lambda} - p_X^+(1-z), \mu\big) \,. \end{aligned} \tag{3.82}$$

For practical applications we would also make use of a short-distance mass definition for m_b (the cancellation of infrared renormalon ambiguities for the shape function was demonstrated recently in Ref. [73]). Here, the dependence on whether it is X_s or X_u occurs only in $h_i^{(0)}$ and the values of the kinematic variables $\bar{n}\cdot p$ and $n\cdot p_X$. The functional forms of $\mathcal{J}^{(0)}$ and $f^{(0)}$ are independent of which process we consider. The hard coefficients are given by

$$h_i(\omega, m_b, \mu) = \sum_{j,j'} C_{j'}(\omega, m_b, \mu) C_j(\omega, m_b, \mu) \; \mathrm{Tr}\Big[\frac{P_v}{2} \, \bar{\Gamma}_{j'\mu}^{(0)} \, \frac{\not{n}}{2} \, \Gamma_{j\nu}^{(0)}\Big] P_i^{\mu\nu} \,, \tag{3.83}$$

with the projectors $P_i^{\mu\nu}$ defined in Eq. (3.17).

Taking the traces in Eq. (3.83) for $B \to X_u \ell \bar{\nu}$, we find that

$$
\begin{aligned}
h_1^u &= \frac{1}{4}\big[C_1^{(v)}\big]^2 , \qquad (3.84)\\
h_2^u &= \frac{n\cdot q\,\big[(C_1^{(v)})^2 + C_1^{(v)}C_2^{(v)} + C_2^{(v)}C_3^{(v)}\big]}{(n\cdot q - \bar{n}\cdot q)} + \frac{(C_2^{(v)})^2}{4} + \frac{(n\cdot q)^2\,\big[(C_3^{(v)})^2 + 2C_1^{(v)}C_3^{(v)}\big]}{(n\cdot q - \bar{n}\cdot q)^2} ,\\
h_3^u &= \frac{(C_1^{(v)})^2}{2(n\cdot q - \bar{n}\cdot q)} , \qquad h_4^u = \frac{C_3^{(v)}\,(2C_1^{(v)} + C_3^{(v)})}{(n\cdot q - \bar{n}\cdot q)^2} ,\\
h_5^u &= -\frac{\big[(C_1^{(v)})^2 + C_1^{(v)}C_2^{(v)} + C_2^{(v)}C_3^{(v)}\big]}{2(n\cdot q - \bar{n}\cdot q)} - \frac{\big[(C_3^{(v)})^2 + 2C_1^{(v)}C_3^{(v)}\big] n\cdot q}{(n\cdot q - \bar{n}\cdot q)^2} .
\end{aligned}
$$

For $B \to X_s \gamma$, where $\bar{n}\cdot q = 0$, the traces give

$$
\begin{aligned}
h_1^s &= \frac{(n\cdot q)^2}{4}\big(C_1^{(t)} - \frac{1}{2}C_2^{(t)} - C_3^{(t)}\big)^2 , \quad h_2^s = 0 , \quad h_3^s = \frac{n\cdot q}{2}\big(C_1^{(t)} - \frac{1}{2}C_2^{(t)} - C_3^{(t)}\big)^2 ,\\
h_4^s &= -\frac{1}{4}\big(3C_1^{(t)} - 2C_2^{(t)} - 2C_3^{(t)} - C_4^{(t)}\big)\big(C_1^{(t)} - 2C_3^{(t)} + C_4^{(t)}\big) ,\\
h_5^s &= \frac{n\cdot q}{2}\big(C_1^{(t)} - \frac{1}{2}C_2^{(t)} - C_3^{(t)}\big)^2 . \qquad (3.85)
\end{aligned}
$$

Here the h_i^{0u}'s depend on $\ln(\mu/m_b)$ and in addition $\bar{y} = \bar{n}\cdot p/m_b$ through the $\mathcal{O}(\alpha_s)$ corrections to the C_i's (see Eqs. (3.59) for results at $\mu = m_b$).

The factors of $nq = m_B x_H^\gamma$ (for $B \to X_s\gamma$) and $\bar{n}q = m_B(1-\bar{y}_H)$, $nq = m_B(1-u_H)$ (for $B \to X_u \ell\bar{\nu}$) are purely kinematic and so can be directly replaced by these hadronic variables. Expanding to leading order about $x_H^\gamma = 1$ and $u_H = 0$ gives the results that should be used at LO in the SCET expansion. For notational convenience, we write

$$
h_i^u = h_i^{0u} + h_i^{0'u} + \ldots , \qquad h_i^s = h_i^{0s} + h_i^{0's} + \ldots . \qquad (3.86)
$$

For $B \to X_u \ell \bar{\nu}$ we have

$$
\begin{aligned}
h_1^{0u} &= \frac{1}{4}\big[C_1^{(v)}\big]^2 , \\
h_2^{0u} &= \frac{1}{\overline{y}_H}\big[(C_1^{(v)})^2 + C_1^{(v)}\, C_2^{(v)} + C_2^{(v)}\, C_3^{(v)}\big] + \frac{1}{4}(C_2^{(v)})^2 + \frac{1}{\overline{y}_H^2}\big[(C_3^{(v)})^2 + 2C_1^{(v)}\, C_3^{(v)}\big] , \\
h_3^{0u} &= \frac{1}{2m_B \overline{y}_H}(C_1^{(v)})^2 , \qquad h_4^{0u} = \frac{1}{m_B^2\, \overline{y}_H^2}\, C_3^{(v)}\, (2C_1^{(v)} + C_3^{(v)}) , \\
h_5^{0u} &= -\frac{1}{2m_B \overline{y}_H}\big[(C_1^{(v)})^2 + C_1^{(v)}\, C_2^{(v)} + C_2^{(v)}\, C_3^{(v)}\big] - \frac{1}{m_B \overline{y}_H^2}\, C_3^{(v)}\big[2C_1^{(v)} + C_3^{(v)}\big] ,
\end{aligned}
\tag{3.87}
$$

while for $B \to X_s \gamma$ we have

$$
\begin{aligned}
h_1^{0s} &= \frac{m_B^2}{4}\big(C_1^{(t)} - \frac{1}{2}\, C_2^{(t)} - C_3^{(t)}\big)^2 , \qquad h_2^{0s} = 0 , \qquad h_3^{0s} = \frac{m_B}{2}\big(C_1^{(t)} - \frac{1}{2} C_2^{(t)} - C_3^{(t)}\big)^2 , \\
h_4^{0s} &= -\frac{1}{4}\big(3C_1^{(t)} - 2C_2^{(t)} - 2C_3^{(t)} - C_4^{(t)}\big)\big(C_1^{(t)} - 2C_3^{(t)} + C_4^{(t)}\big) , \\
h_5^{0s} &= \frac{m_B}{2}\big(C_1^{(t)} - \frac{1}{2} C_2^{(t)} - C_3^{(t)}\big)^2 .
\end{aligned}
\tag{3.88}
$$

The results in Eqs. (3.87) and (3.88) agree with Refs. [27, 47]. At NLO in the power expansion, it will be necessary to keep the next term $h_i^{0'f}$ from the expansion of the kinematic prefactors in Eqs. (3.84) and (3.85). For $B \to X_u \ell \bar{\nu}$ we find

$$
\begin{aligned}
h_1^{0'u} &= 0 , \\
h_2^{0'u} &= u_H \left\{ \frac{(1-\overline{y}_H)}{\overline{y}_H^2}\big[(C_1^{(v)})^2 + C_1^{(v)}\, C_2^{(v)} + C_2^{(v)}\, C_3^{(v)}\big] + \frac{2(1-\overline{y}_H)}{\overline{y}_H^3}\big[(C_3^{(v)})^2 + 2C_1^{(v)}\, C_3^{(v)}\big] \right\} , \\
h_3^{0'u} &= \frac{u_H}{2m_B \overline{y}_H^2}(C_1^{(v)})^2 , \\
h_4^{0'u} &= \frac{2u_H}{m_B^2\, \overline{y}_H^3}\, C_3^{(v)}\, (2C_1^{(v)} + C_3^{(v)}) , \\
h_5^{0'u} &= -u_H \left\{ \frac{1}{2m_B \overline{y}_H^2}\big[(C_1^{(v)})^2 + C_1^{(v)}\, C_2^{(v)} + C_2^{(v)}\, C_3^{(v)}\big] + \frac{(2-\overline{y}_H)}{m_B \overline{y}_H^3}\, C_3^{(v)}\big[2C_1^{(v)} + C_3^{(v)}\big] \right\} ,
\end{aligned}
\tag{3.89}
$$

while for $B \to X_s\gamma$ we have

$$\begin{aligned} h_1^{0's} &= \frac{m_B^2(x_H^\gamma-1)}{2}\big(C_1^{(t)}-\frac{1}{2}C_2^{(t)}-C_3^{(t)}\big)^2, \qquad h_2^{0's}=0, \\ h_3^{0's} &= \frac{m_B(x_H^\gamma-1)}{2}\big(C_1^{(t)}-\frac{1}{2}C_2^{(t)}-C_3^{(t)}\big)^2, \qquad h_4^{0's}=0, \\ h_5^{0's} &= \frac{m_B(x_H^\gamma-1)}{2}\big(C_1^{(t)}-\frac{1}{2}C_2^{(t)}-C_3^{(t)}\big)^2. \end{aligned} \tag{3.90}$$

In Ref. [99], the LO triply differential rate for $B \to X_u\ell\bar{\nu}$ was found to satisfy $d^3\Gamma^u/dxdydy_0 \propto (x-y)(y_0-x)$. In terms of the h_i^{0u}, this corresponds to the relations $h_2^{0u} = 4h_1^{0u}/\bar{y}_H$ and $m_B h_3^{0u} = 2h_1^{0u}/\bar{y}_H$ (where at LO we can set $y = (1-u_H)(1-\bar{y}_H)$, $y_0 = 2-u_H-\bar{y}_H$). Eqs. (3.87) agree with this result at tree level in the hard functions, but give non-zero corrections to the first (h_2^{0u}) relation of order $\alpha_s(m_b)$ from the Wilson coefficients $C_2^{(v)}$ and $C_3^{(v)}$.

3.5 Vanishing Time-Ordered Products at $\mathcal{O}(\lambda)$

To work out the factorization beyond LO is now simply a matter of going to higher order in λ in SCET. At order λ the time-ordered products are

$$\begin{aligned} \hat{T}^{1a} &= -i\int d^4x\, e^{-ir\cdot x}\, \mathrm{T}\big[J^{(0)\dagger}(x)\, J^{(1a)}(0) + J^{(1a)\dagger}(x)\, J^{(0)}(0)\big], \\ \hat{T}^{1b} &= -i\int d^4x\, e^{-ir\cdot x}\, \mathrm{T}\big[J^{(0)\dagger}(x)\, J^{(1b)}(0) + J^{(1b)\dagger}(x)\, J^{(0)}(0)\big], \\ \hat{T}^{1L} &= -i\int d^4x\, d^4y\, e^{-ir\cdot x}\, \mathrm{T}\big[J^{(0)\dagger}(x)\, i\mathcal{L}^{(1)}_{\xi\xi}(y) J^{(0)}(0)\big]. \end{aligned} \tag{3.91}$$

We shall see that these time-ordered products give vanishing matrix elements for $B \to X_s\gamma$ and $B \to X_u\ell\bar{\nu}$. The result follows almost directly from chirality and the fact that the currents in Eqs. (3.51), (3.52) and (3.54) all involve left-handed collinear quark fields. However, we must be careful to check that terms proportional to the chiral condensate do not contribute. We follow an approach similar to the previous section: by using the Fierz transformation in Eq. (3.68), we can collect the usoft and collinear fields into separate parts $\mathcal{J} \otimes \mathcal{S}$, and the matrix element then factorizes to

give $\langle 0|\mathcal{J}|0\rangle \otimes \langle B_v|\mathcal{S}|B_v\rangle$. These parts are still connected by indices and spacetime integrals, which are represented here by the $\otimes$.

For T^{1a} and T^{1b}, we take the expressions for the currents from Eqs. (3.51) and (3.52). The same usoft fields appear as in the leading-order $T^{(0)}$, and so the T-products involve soft matrix elements that are similar to the one in Eq. (3.69), namely

$$\begin{aligned}
&\left\langle \bar{B}_v \middle| T\left[\bar{\mathcal{H}}_v(x)\,\overline{\Gamma}^{(0)}_{j\mu}\,F^n_k\,\Upsilon^{(1a)}_{j'\nu\alpha}\,\mathcal{H}_v(0)\right]\middle|\bar{B}_v\right\rangle,\\
&\left\langle \bar{B}_v \middle| T\left[\bar{\mathcal{H}}_v(x)\overline{\Upsilon}^{(1a)}_{j'\mu\alpha}\,F^n_k\,\Gamma^{(0)}_{j\nu}\,\mathcal{H}_v(0)\right]\middle|\bar{B}_v\right\rangle,
\end{aligned} \tag{3.92}$$

with similar matrix elements for T^{1b} but with $\Upsilon^{(1a)}_{j'\mu} \to \Upsilon^{(1b)}_{j'\mu}$. The first term in Eq. (3.92) is multiplied by the collinear matrix element

$$\mathcal{J}^{(1a)}(0,x) \;=\; \frac{1}{\omega'}\left\langle 0\middle| T\left[(\bar{\chi}^L_n\, i\overleftarrow{\mathcal{D}}^{\alpha}_{c\perp})_{\omega'}(0)\,F^{\bar{n}}_k\,\chi^L_{n,\omega}(x)\right]\middle|0\right\rangle, \tag{3.93}$$

while the second term is multiplied by $[\mathcal{J}^{(1a)}(x,0)]^\dagger$. For T^{1b} the analogous result is

$$\mathcal{J}^{(1b)}(0,x) \;=\; \frac{-1}{m_b n\cdot v}\left\langle 0\middle| T\left[\bar{\chi}^L_{n,\omega'}(0)\,(ig\,\mathcal{B}^{\alpha}_{c\perp})_{\omega_2}(0)\,F^{\bar{n}}_k\,\chi^L_{n,\omega}(x)\right]\middle|0\right\rangle. \tag{3.94}$$

In both $\mathcal{J}^{(1a)}$ and $\mathcal{J}^{(1b)}$, the fact that we need an overall colour singlet eliminates the possibilities $k = 4,5,6$. Owing to the presence of the α $\perp$-index, rotational invariance also eliminates $k = 1,2$, leaving only $F^{\bar{n}}_3 = -\bar{n}\!\!\!/\gamma^\beta_\perp/(2N_c)$. However, this term has the wrong chiral structure and also vanishes, i.e.

$$\bar{\chi}^L_n F^{\bar{n}}_3 \chi^L_n \propto \bar{\chi}_n P_R \bar{n}\!\!\!/\gamma^\beta_\perp P_L \chi_n = 0\,, \tag{3.95}$$

so both T^{1a} and T^{1b} give vanishing corrections.

For T^{1L} we need to use the Fierz identity in Eq. (3.68) twice to group together all usoft and collinear factors. This gives the usoft matrix element

$$\left\langle B_v\middle|\bar{\mathcal{H}}_v(x)\overline{\Gamma}^{(0)}_{j'}\,F^n_{k'}\left(i\mathcal{D}^{\perp}_{us}\gamma^\beta_\perp\frac{\bar{n}\!\!\!/}{2}\right)(y)F^n_k\Gamma^{(0)}_j\mathcal{H}_v(0)\middle|B_v\right\rangle \tag{3.96}$$

multiplied by the collinear matrix element of a four-quark operator, which we claim satisfies

$$\left\langle 0\left|\left[\bar{\chi}_n^L(y)F_{k'}^{\bar{n}}\chi_n^L(x)\right]\left[\bar{\chi}_n^L(0)F_k^{\bar{n}}(i\mathcal{D}_{c\perp}^{\beta}\chi_n^L)(y)\right]\right|0\right\rangle = 0\,. \tag{3.97}$$

To prove Eq. (3.97) we begin by noting that colour now allows T^a terms as long as they occur in both F's, so either $k,k' \in \{1,2,3\}$ or $k,k' \in \{4,5,6\}$. For either possibility the argument is the same, so for convenience we take the former case. Rotational invariance now demands that one of k,k' is equal to 3 and the other is 1 or 2. If $k' = 3$, then the first pair of collinear quark fields vanishes, just as in Eq. (3.95), while if $k = 3$, then the second pair of collinear quark fields vanishes.

The results in Eqs. (3.95) and (3.97) rely on the underlying assumption that there is no structure in the vacuum that can flip the chirality. In QCD we know that this is not the case, since the chiral condensate (and instantons) take $L \leftrightarrow R$. The above argument is valid because we have used chirality only at the $\mu^2 \sim Q\Lambda$ scale where we are matching perturbatively, and not for $\mu^2 \sim \Lambda^2 \ll Q\Lambda$, where it is badly broken. The same argument applies when perturbatively matching on to the weak Hamiltonian at $\mu \simeq m_W \gg \Lambda$.

3.6 Factorization at Next-to-Leading Order

Since the order λ contributions vanish, the first power corrections occur at order $\lambda^2 = \Lambda/Q$ and will be referred to as NLO corrections. The NLO contributions to the decay rates have several sources, including the following:

i) expansion of kinematic factors occurring in front of the W_i in the decay rates given by Eqs. (3.31) and (3.32),

ii) expansion of the kinematic factors appearing in the h_i at LO, i.e. in Eqs. (3.84) and (3.85),

iii) expansion associated with the conversion from partonic to hadronic variables,

given in Eq. (3.100),

iv) higher-order operators contributing to the time-ordered products, given in Eq. (3.105).

Once the region of phase space where the SCET expansion is valid is properly defined, as in Sec. 3.2.3, the corrections in i) and ii) are straightforward to compute. The corrections from i) do depend on the choice of how the x_H charged-lepton variable is treated, for example whether we integrate over all of x_H or instead look at an x_H spectrum with a cut. Results for i) are given in Eqs. (3.40), (3.41) and (3.39). For ii) the required terms are derived by keeping one more term in the Taylor series in passing from Eqs. (3.84) and (3.85) to Eqs. (3.87) and (3.88). We give the results for i) and ii) in Sec. 3.7.2. Note that these terms are already in terms of hadronic variables and are therefore unaffected by the conversion in iii).

The NLO terms from category iii) are discussed in Sec. 3.6.1 below. The contributions from category iv) require several sections. In Sec. 3.6.2 we give a complete list of the time-ordered products arising at second order in SCET (category iv)), along with a summary of the jet and shape functions they generate. In Sec. 3.6.3 we carry out the tree-level matching calculations for these time-ordered products and define the jet functions at leading order in α_s. In Sec. 3.6.4 we give operator definitions for the shape functions. Detailed derivations of the NLO factorization theorems for these time-ordered products are presented in Sec. 3.6.5. Finally, results for the computation of the traces that give the NLO hard coefficients are given in Sec. 3.6.6.

Note that the final results for contributions from i), ii), iii) and iv) are summarized in Sec. 3.7.

3.6.1 Switching to hadronic variables at order λ^2

At LO the factorization theorem in terms of partonic variables was given in Eq. (3.81):

$$W_i^{(0)} = h_i^0(\bar{n}\cdot p, m_b, \mu) \int_0^{\bar{\Lambda}-r^+} dk^+ \, \mathcal{J}^{(0)}(\bar{n}\cdot p\, k^+, \mu)\, f^{(0)}(k^+ + r^+, \mu)\,. \quad (3.98)$$

In this expression, the variables $\bar{n}\cdot p$ and $n\cdot r$ have a series expansion once we switch to hadronic variables. For the accuracy needed at NLO we have

$$\bar{n}\cdot p = \bar{n}\cdot p_X - \overline{\Lambda}\,, \qquad\qquad n\cdot r = (\overline{\Lambda} - n\cdot p_X) - \frac{(\lambda_1+3\lambda_2)}{2m_b}\,. \tag{3.99}$$

Expanding Eq. (3.98) gives the LO term in Eq. (3.82) plus the NLO terms

$$\begin{aligned}
\big[W_i^{(0)}\big]^{\rm NLO} &= -\frac{(\lambda_1+3\lambda_2)}{2m_b}\, h_i^0(p_X^-,m_b)\int_0^{p_X^+} dk^+\, \mathcal{J}^{(0)}(p_X^-\,k^+) \\
&\quad\times\Big\{\frac{df^{(0)}(k^+ + \overline{\Lambda} - p_X^+)}{dk^+} - \delta(k^+ - p_X^+) f^{(0)}(k^+ + \overline{\Lambda} - p_X^+)\Big\} \\
&\quad -\overline{\Lambda}\int_0^{p_X^+} dk^+\,\frac{d}{d\bar{n}\cdot p}\Big\{h_i^0(\bar{n}\cdot p,m_b)\,\mathcal{J}^{(0)}(\bar{n}\cdot p\,k^+)\Big\}\Big|_{\bar{n}\cdot p=p_X^-} f^{(0)}(k^+ + \overline{\Lambda} - p_X^+) \\
&= -\frac{(\lambda_1+3\lambda_2)}{2m_B} h_i^0(p_X^-,m_b)\big[\mathcal{J}^{(0)}\otimes\widetilde{f^{(0)}}\big](p_X^+,p_X^-) \\
&\quad -\overline{\Lambda}\,\big[(h_i^{0f}\mathcal{J}^{(0)})'\otimes f^{(0)}\big](p_X^+,p_X^-)\,.
\end{aligned} \tag{3.100}$$

Note that in taking the derivative with respect to $\bar{n}p$ we differentiate only the $C_j(\bar{n}p)$'s in h_i^0 and not the prefactors depending on $\bar{n}\cdot q$. For later convenience, we switched to hadronic variables in the final line of Eq. (3.100) and defined

$$\begin{aligned}
\big[\mathcal{J}^{(0)}\otimes\widetilde{f^{(0)}}\big](p_X^+,p_X^-) &= \int_0^{p_X^+} dk^+\,\mathcal{J}^{(0)}(p_X^-\,k^+)\,\Big\{\frac{df^{(0)}(k^+ + \overline{\Lambda} - p_X^+)}{dk^+} \\
&\qquad -\delta(k^+ - p_X^+) f^{(0)}(k^+ + \overline{\Lambda} - p_X^+)\Big\}, \\
\big[(h^{0f}\mathcal{J}^{(0)})'\otimes f^{(0)}\big](p_X^+,p_X^-) &= \int_0^{p_X^+} dk^+\,\frac{d}{d\bar{n}\cdot p}\Big\{h^{0f}(\bar{n}\cdot p,m_b)\,\mathcal{J}^{(0)}(\bar{n}\cdot p\,k^+)\Big\}\Big|_{\bar{n}\cdot p=p_X^-} \\
&\qquad \times f^{(0)}(k^+ + \overline{\Lambda} - p_X^+).
\end{aligned} \tag{3.101}$$

T-product	Example Diagram	Hard, Jet, and Shape Functions	Usoft Operator
$\hat{T}^{(2H)}$	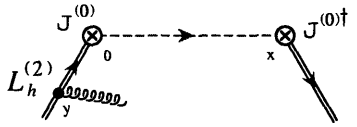	$h^0 \mathcal{J}^{(0)} f_0^{(2)}$	$\bar{h}_v(x) h_v(0) i\mathcal{L}_{\rm h}^{(2)}(y)$
$\hat{T}^{(2a)}$	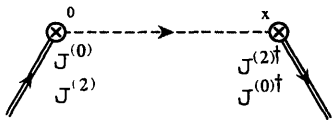	$h^{1,2} \mathcal{J}^{(0)} f_{1,2}^{(2)}$	$\bar{h}_v(x)(D_{T,\perp} h_v)(0)$ $(\bar{h}_v D_{T,\perp})(x) h_v(0)$
$\hat{T}^{(2L)}$	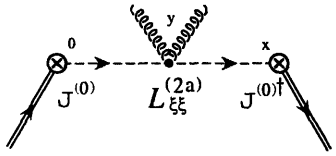	$h^{3,4} \mathcal{J}_{1,2}^{(-2)} f_{3,4}^{(4)}$ $h^{3,4} \mathcal{J}_{3,4}^{(-2)} g_{3,4}^{(4)}$	$\bar{h}_v(x)(D_\perp D_\perp)(y) h_v(0)$
$\hat{T}^{(2q)}$	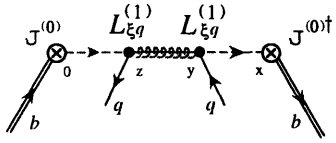	$h^{5,6} \mathcal{J}_1^{(-4)} f_{5,6}^{(6)}$ $h^{5-8} \mathcal{J}_{2-4}^{(-4)} g_{5-10}^{(6)}$	$\bar{h}_v(x) q(y) \bar{q}(z) h_v(0)$

Table 3.4: Time-ordered products that are of order $\lambda^2 = \Lambda/m_b$ overall, and that are non-zero at tree level. The power of λ^2 is obtained by adding the powers from the jet functions $\mathcal{J}$ to those from the shape functions f or g. We suppress colour and Dirac structure in the usoft operators listed, which can be found in the text. The time-ordered product in the last row has not been considered in the literature and is enhanced relative to the other entries by a prefactor of $4\pi\alpha_s(E_X\Lambda) \sim 5$.

T-product	Example Diagram	Hard, Jet, and Shape Functions	Usoft Operator
$\hat{T}^{(2b)}$	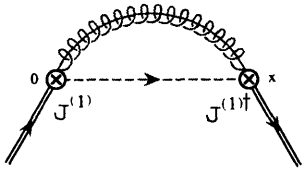	$h^{[2b]}\,\mathcal{J}^{(2)}_{1,2}\,f^{(0)}$	$\bar{h}_v(x)h_v(0)$
$\hat{T}^{(2c)}$	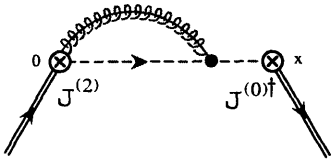	$h^{[2c]}\,\mathcal{J}^{(2)}_{3-10}\,f^{(0)}$	$\bar{h}_v(x)h_v(0)$
$\hat{T}^{(2La)}$	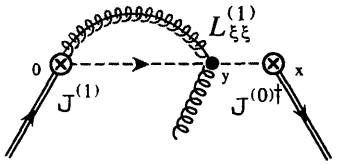	$h^{[2La]}\,\mathcal{J}^{(0)}_{j'}\,g^{(2)}_{11,12}$	$\bar{h}_v(x)D_\perp(y)h_v(0)$
$\hat{T}^{(2Lb)}$	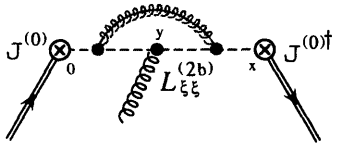	$h^{[2Lb]}\,\mathcal{J}^{(0)}_{j'}\,g^{(2)}_{13,14}$	$\bar{h}_v(x)\bar{n}\cdot D(y)h_v(0)$
$\hat{T}^{(2LL)}$	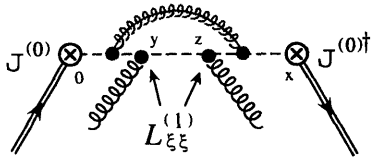	$h^{[2LL]}\,\mathcal{J}^{(-2)}_{j'}\,g^{(4)}_{15-26}$	$\bar{h}_v(x)D_\perp(y)D_\perp(z)h_v(0)$

Table 3.5: Time-ordered products that are of order Λ/m_b, but have jet functions that start at one-loop order. The last three rows introduce new shape functions that were not present at tree level. Vertices that are not labeled are from $\mathcal{L}^{(0)}_{\xi\xi}$.

T-product	Example Diagram	Hard, Jet, and Shape Functions	Usoft Operator
$\hat{T}^{(2Ga)}$	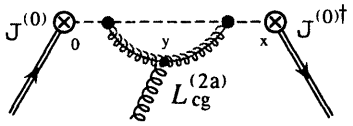	$h^{[2Ga]}\,\mathcal{J}^{(-2)}_{j'}\,f^{(4)}_{3,4}$	$\bar{h}_v(x)(D_\perp D_\perp)(y)h_v(0)$
$\hat{T}^{(2Lb)}$	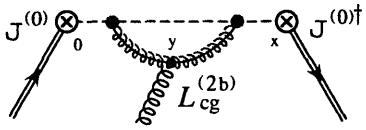	$h^{[2Lb]}\,\mathcal{J}^{(0)}_{j'}\,g^{(2)}_{13,14}$	$\bar{h}_v(x)\bar{n}\cdot D(y)h_v(0)$
$\hat{T}^{(2La)}$	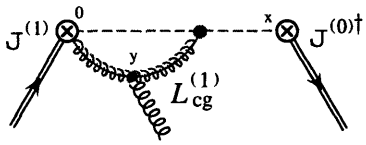	$h^{[2La]}\,\mathcal{J}^{(0)}_{j'}\,g^{(2)}_{11,12}$	$\bar{h}_v(x)D_\perp(y)h_v(0)$

Table 3.6: Examples of non-abelian terms in time-ordered products that are of order Λ/m_b and have jet functions that start at one-loop order.

3.6.2 Time-Ordered Products at order λ^2

To enumerate all the possible time-ordered product contributions at this order we consider all possible combinations of SCET currents and Lagrangians from Sec. 3.3,

$$J^{(n_1)\dagger}\mathcal{L}^{(n_2)}\ldots\mathcal{L}^{(n_{j-1})}J^{(n_j)}\,, \tag{3.102}$$

where $n_1+\ldots+n_j=2$ for NLO, i.e. $\mathcal{O}(\lambda^2)$. It is useful to divide these time-ordered products into two categories, those that have a jet function that starts at tree level and those whose jet function starts at one-loop order only. To determine into which category a time-ordered product falls, we first note that the jet functions are vacuum-to-vacuum matrix elements, so all collinear fields are contracted. Since there are no external $\perp$-momenta, at tree level all collinear lines have no $\perp$-momentum and factors of $\mathcal{P}_\perp$ all vanish. (This is also true beyond tree level for factors of $\mathcal{P}_\perp$ that act on all collinear fields in a J or $J^\dagger$.) Thus, for example, the product $J^{(1b)\dagger}J^{(1b)}$ has a jet function that starts at one-loop order since we must contract both the collinear quark and gluon lines. A second example consists of time-ordered products that involve a

$\mathcal{L}^{(1)}_{\xi\xi}$ insertion, in which neither the $\mathcal{P}_\perp$ nor the $A^\perp_n$ in the $D^c_\perp$ can contribute at tree level.

The time-ordered products that appear already at tree level will be most important phenomenologically, and include

$$\begin{aligned}
\hat{T}^{(2H)} &= -i\int d^4x\, d^4y\, e^{-ir\cdot x}\, \mathrm{T}\big[J^{(0)\dagger}(x)\, i\mathcal{L}^{(2)}_h(y)\, J^{(0)}(0)\big]\,, \qquad (3.103)\\
\hat{T}^{(2a)} &= -i\int d^4x\, e^{-ir\cdot x} \sum_{\kappa=a,b} \mathrm{T}\big[J^{(2\kappa)\dagger}(x)\, J^{(0)}(0) + J^{(0)\dagger}(x)\, J^{(2\kappa)}(0)\big]\,,\\
\hat{T}^{(2L)} &= -i\int d^4x\, d^4y\, e^{-ir\cdot x}\, \mathrm{T}\big[J^{(0)\dagger}(x)\, i\mathcal{L}^{(2a)}_{\xi\xi}(y) J^{(0)}(0)\big]\,,\\
\hat{T}^{(2q)} &= -\frac{i}{2}\int d^4x\, d^4y\, d^4z\, e^{-ir\cdot x}\, \mathrm{T}\big[J^{(0)\dagger}(x)\, i\mathcal{L}^{(1)}_{\xi q}(y)\, i\mathcal{L}^{(1)}_{\xi q}(z) J^{(0)}(0)\big]\,.
\end{aligned}$$

These time-ordered products give jet functions that are either the same as at lowest order, namely $J^{(0)}$, or enhanced by two or four powers of λ, namely $J^{(-2,-4)}$. The corresponding shape functions are power suppressed relative to $f^{(0)}$ by two, four and six powers respectively.

The most pertinent information is summarized in Table 3.4, along with examples of Feynman diagrams and the forms of the non-perturbative usoft operators. The overall power of λ^2 is obtained by simply adding the superscripts in the operator insertions. Dividing this overall power into that of the jet and usoft terms is slightly more involved since it depends on the individual operators. At tree level it is simply that every additional collinear propagator enhances the corresponding jet function by λ^{-2}. Generating additional propagators requires inserting subleading operators with additional usoft fields that produce power-suppressed shape functions. The power counting in $\mathrm{SCET_I}$ restricts us to consider at most two $\mathcal{O}(\lambda)$ operator insertions, so this guarantees that the greatest enhancement from the jet function is $\mathcal{O}(\lambda^{-4})$ and the set of possible terms is finite.

From Table 3.4, we see that for $T^{(2a)}$ and $T^{(2H)}$ the collinear fields give a jet function that is identical to $\mathcal{J}^{(0)}$ defined in Eq. (3.78), but have Λ/Q-suppressed shape functions $f^{(2)}_{1,2}$ and $f^{(2)}_0$. For $T^{(2L)}$ we find an enhancement of Q/Λ in the jet function $\mathcal{J}^{(-2)}$, but shape functions that are further suppressed, namely $f^{(4)}_{3,4}$, which

are down by Λ^2/Q^2.[11] Finally for $T^{(2q)}$ we have the biggest enhancement, Q^2/Λ^2, through the jet function $\mathcal{J}^{(-4)}$, and a shape function $f_{5,6}^{(6)}$ involving a four-quark operator, which is down by Λ^3/Q^3.

In Table 3.4 we also notice that it's only the $J^{(0)}$ currents that appear, plus the subleading currents $J^{(2a)}$ and $J^{(2b)}$ whose Wilson coefficients are related to the coefficients in $J^{(0)}$ by reparameterization invariance (see Appendix B). This implies that the logarithms encoded in the running of the subleading hard functions h^{1-8} are the same as the logarithms that can be resummed in h^0. (Here the term "logarithms" includes Sudakov double logarithms as well as the usual single logarithms.) This result depends on the fact that the Lagrangians that are inserted do not run. This implies that the logarithms resummed between the scales m_b^2 and $m_b\Lambda$ are universal for these terms (besides the simple HQET running from $c_F(\mu)$ in $\mathcal{L}_h^{(2)}$, which is easily taken into account). Additional logarithms occur below the $m_b\Lambda$ scale and there is no reason to expect that they are universal. A computation of the anomalous dimensions of the corresponding soft operators would allow these additional logarithms to be resummed. Finally, for the time-ordered products that appear at one-loop order in the jet functions, even the logarithms between m_b^2 and $m_b\Lambda$ are not the same as at LO. They are, however, entirely determined by the running of the $J^{(1)}$ currents that were calculated in Ref. [87].

At one-loop order in the jet function, the remaining time-ordered products start

[11] Note that in the subleading Lagrangian $\mathcal{L}_{\xi\xi}^{(2)}$ the two $\perp$ derivatives appear at the same spacetime point, providing a simple explanation for why this occurred to all orders in the twist expansion in Ref. [26].

contributing. They are

$$\hat{T}^{(2b)} = -i \int d^4x\, e^{-ir\cdot x} \sum_{\kappa=a,b,\,\ell=a,b} \mathrm{T}\big[J^{(1\kappa)\dagger}(x)\, J^{(1\ell)}(0)\big]\,, \tag{3.104}$$

$$\hat{T}^{(2c)} = -i \int d^4x\, e^{-ir\cdot x} \sum_{\ell=c,d,e,f} \mathrm{T}\big[J^{(2\ell)\dagger}(x)\, J^{(0)}(0) + J^{(0)\dagger}(x)\, J^{(2\ell)}(0)\big]\,,$$

$$\begin{aligned}\hat{T}^{(2La)} = {}& -i \int d^4x\, d^4y\, e^{-ir\cdot x} \sum_{\kappa=a,b} \mathrm{T}\big[J^{(1\kappa)\dagger}(x)\, i\mathcal{L}^{(1)}_{\xi\xi}(y) J^{(0)}(0) + J^{(0)\dagger}(x)\, i\mathcal{L}^{(1)}_{\xi\xi}(y) J^{(1\kappa)}(0)\big] \\ & - i \int d^4x\, d^4y\, e^{-ir\cdot x} \sum_{\kappa=a,b} \mathrm{T}\big[J^{(1\kappa)\dagger}(x)\, i\mathcal{L}^{(1)}_{cg}(y) J^{(0)}(0) + J^{(0)\dagger}(x)\, i\mathcal{L}^{(1)}_{cg}(y) J^{(1\kappa)}(0)\big]\,,\end{aligned}$$

$$\begin{aligned}\hat{T}^{(2Lb)} = {}& -i \int d^4x\, d^4y\, e^{-ir\cdot x}\, \mathrm{T}\big[J^{(0)\dagger}(x)\, i\mathcal{L}^{(2b)}_{\xi\xi}(y) J^{(0)}(0)\big] \\ & - i \int d^4x\, d^4y\, e^{-ir\cdot x}\, \mathrm{T}\big[J^{(0)\dagger}(x)\, i\mathcal{L}^{(2b)}_{cg}(y) J^{(0)}(0)\big]\,,\end{aligned}$$

$$\begin{aligned}\hat{T}^{(2LL)} = {}& -\frac{i}{2} \int d^4x\, d^4y\, d^4z\, e^{-ir\cdot x}\, \mathrm{T}\big[J^{(0)\dagger}(x)\, i\mathcal{L}^{(1)}_{\xi\xi}(y)\, i\mathcal{L}^{(1)}_{\xi\xi}(z) J^{(0)}(0)\big] \\ & - i \int d^4x\, d^4y\, d^4z\, e^{-ir\cdot x}\, \mathrm{T}\big[J^{(0)\dagger}(x)\, i\mathcal{L}^{(1)}_{\xi\xi}(y)\, i\mathcal{L}^{(1)}_{cg}(z) J^{(0)}(0)\big] \\ & - \frac{i}{2} \int d^4x\, d^4y\, d^4z\, e^{-ir\cdot x}\, \mathrm{T}\big[J^{(0)\dagger}(x)\, i\mathcal{L}^{(1)}_{cg}(y)\, i\mathcal{L}^{(1)}_{cg}(z) J^{(0)}(0)\big]\,,\end{aligned}$$

$$\hat{T}^{(2Ga)} = -i \int d^4x\, d^4y\, e^{-ir\cdot x}\, \mathrm{T}\big[J^{(0)\dagger}(x)\, i\mathcal{L}^{(2a)}_{cg}(y) J^{(0)}(0)\big]\,.$$

Information about how these time-ordered products contribute to the factorization theorems at $\mathcal{O}(\lambda^2)$ is summarized in Tables 3.5 and 3.6. Note that $T^{(2b)}$ and $T^{(2c)}$ match on to subleading jet functions and the leading-order shape function, and so these $\mathcal{O}(\alpha_s)$ corrections can be calculated without introducing new non-perturbative information. The remaining T-products give new subleading shape functions that were not present at tree level. Together the terms in Eqs. (3.103) and (3.104) provide the complete set of time-ordered products that contribute at this order in λ and at any order in α_s.

Adding up the contributions from the various subleading time-ordered products,

we find that

$$
\begin{aligned}
W_i^{(2)f} = & \frac{h_i^{0f}(\bar{n}\cdot p)}{2m_b} \int_0^{p_X^+} dk^+ \; \mathcal{J}^{(0)}(\bar{n}\cdot p\, k^+,\mu)\, f_0^{(2)}\big(k^+ + r^+,\mu\big) \\
& + \sum_{r=1}^{2} \frac{h_i^{rf}(\bar{n}\cdot p)}{m_b} \int_0^{p_X^+} dk^+ \; \mathcal{J}^{(0)}(\bar{n}\cdot p\, k^+,\mu)\, f_r^{(2)}\big(k^+ + r^+,\mu\big) \\
& + \sum_{r=3}^{4} \frac{h_i^{rf}(\bar{n}\cdot p)}{m_b} \int dk_1^+\, dk_2^+ \; \mathcal{J}_{1\pm2}^{(-2)}(\bar{n}\cdot p\, k_j^+,\mu)\, f_r^{(4)}\big(k_j^+ + r^+,\mu\big) \\
& + \sum_{r=5}^{6} \frac{h_i^{rf}(\bar{n}\cdot p)}{\bar{n}\cdot p} \int dk_1^+ dk_2^+ dk_3^+ \; \mathcal{J}_1^{(-4)}(\bar{n}\cdot p\, k_{j'}^+,\mu)\, f_r^{(6)}\big(k_{j'}^+ + r^+,\mu\big) \\
& + \frac{h_i^{00f}(\bar{n}\cdot p)}{m_b} \int_0^{p_X^+} dk^+ \; \mathcal{J}^{(0)}(\bar{n}\cdot p\, k^+,\mu)\, g_0^{(2)}\big(k^+ + r^+,\mu\big) \\
& + \sum_{r=3}^{4} \frac{h_i^{rf}(\bar{n}\cdot p)}{m_b} \int dk_1^+\, dk_2^+ \; \mathcal{J}_{3\pm4}^{(-2)}(\bar{n}\cdot p\, k_j^+,\mu)\, g_r^{(4)}\big(k_j^+ + r^+,\mu\big) \\
& + \sum_{r=5}^{6} \frac{h_i^{rf}(\bar{n}\cdot p)}{\bar{n}\cdot p} \int dk_1^+ dk_2^+ dk_3^+ \; \mathcal{J}_2^{(-4)}(\bar{n}\cdot p\, k_{j'}^+,\mu)\, g_r^{(6)}\big(k_{j'}^+ + r^+,\mu\big) \\
& + \sum_{r=7}^{8} \frac{h_i^{rf}(\bar{n}\cdot p)}{\bar{n}\cdot p} \int dk_1^+ dk_2^+ dk_3^+ \; \Big[\mathcal{J}_3^{(-4)}(\bar{n}\cdot p\, k_{j'}^+,\mu)\, g_r^{(6)}\big(k_{j'}^+ + r^+,\mu\big) \\
& \qquad\qquad + \mathcal{J}_4^{(-4)}(\bar{n}\cdot p\, k_{j'}^+,\mu)\, g_{r+2}^{(6)}\big(k_{j'}^+ + r^+,\mu\big)\Big] \\
& + \sum_{m=1,2} \int dz_1 dz_2 \; \frac{h_i^{[2b]m+8}(z_1,z_2,\bar{n}\cdot p)}{m_b} \int_0^{p_X^+} dk^+ \; \mathcal{J}_m^{(2)}(z_1,z_2,p_X^-\, k^+)\, f^{(0)}(k^+ + \overline{\Lambda} - p_X^+) \\
& + \sum_{m=3,4} \frac{h_i^{[2c]m+8}(\bar{n}\cdot p)}{m_b} \int_0^{p_X^+} dk^+ \; \mathcal{J}_m^{(2)}(p_X^-\, k^+)\, f^{(0)}(k^+ + \overline{\Lambda} - p_X^+) \\
& + \sum_{m=5}^{10} \int dz_1 \; \frac{h_i^{[2c]m+8}(z_1,\bar{n}\cdot p)}{m_b} \int_0^{p_X^+} dk^+ \; \mathcal{J}_m^{(2)}(z_1,p_X^-\, k^+)\, f^{(0)}(k^+ + \overline{\Lambda} - p_X^+) \\
& + W_i^{[2La]f}\big[\, g_{11,12}^{(2)}\,\big] \\
& + W_i^{[2Lb]f}\big[\, g_{13,14}^{(2)}\,\big] \\
& + W_i^{[2LL]f}\big[\, g_{15-26}^{(4)}\,\big] \\
& + W_i^{[2Ga]f}\big[\, f_{3,4}^{(4)}\,\big]\,,
\end{aligned}
\tag{3.105}
$$

where $j = 1,2$ and $j' = 1,2,3$ and $\mathcal{J}_{1\pm2}^{(-2)} = \mathcal{J}_1^{(-2)} \pm \mathcal{J}_2^{(-2)}$ for $r = 3,4$ respectively. Recall that $f = s$ for $B \to X_s\gamma$ and $f = u$ for $B \to X_u\ell\bar{\nu}$. If we work at tree level

in the jet functions, then only the first four lines of Eq. (3.105) are required (with shape functions f_{0-6}). In our notation, the f_i denote shape functions that appear from tree-level matching, while the g_i denote shape functions that show up only when one-loop corrections are considered for the jet functions.

3.6.3 Tree-Level Matching Calculations

In this section, we show how computing the four tree-level diagrams in Table 3.4 immediately allows us to obtain the tree-level jet functions, properly convoluted with the non-perturbative shape functions that show up at NLO order. Note that no summation of operators is necessary. An operator-based derivation of the factorization theorems at all orders in the jet functions is given later, in Sec. 3.6.5.

First consider the computation of Fig. 3-3 using the LO jet function from the time-ordered product in Eq. (3.65), with currents as in Eq. (3.67). Working entirely in momentum space and contracting the collinear quark fields in the diagram gives

$$(-i)\overline{\mathcal{H}}_v(\ell^+)\overline{\Gamma}^{(0)}_\mu i\frac{\not{\bar{n}}}{2}\frac{\bar{n}\cdot p}{(\bar{n}\cdot p k^+ + i\epsilon)}\Gamma^{(0)}_\nu\mathcal{H}_v(\ell^+)\,, \tag{3.106}$$

where $\bar{n}\cdot p$ is the large momentum flowing through the collinear quark propagator. Taking $(-1/\pi)$ times the imaginary part gives

$$\mathcal{J}^{(0)}(k^+) \;=\; \delta(k^+) + \mathcal{O}(\alpha_s)\,, \tag{3.107}$$

for the tree-level jet function. which is equal to $\delta(\ell^+ - r^+)$ by momentum conservation since

$$\ell^+ = k^+ + r^+\,. \tag{3.108}$$

Thus, from Eq. (3.106) we can directly write the convolution of jet and soft factors

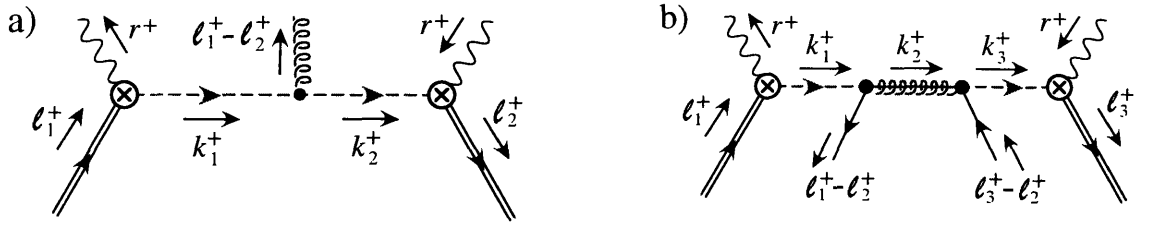

Figure 3-4: Momentum routing for a) $T^{(2L)}$ and b) $T^{(2q)}$. In a), the operator with one gluon comes from $[i\not{\mathcal{D}}_{us}^{\perp} i\not{\mathcal{D}}_{us}^{\perp}]$.

as

$$\frac{1}{2}\mathrm{Tr}\big[P_v\overline{\Gamma}_\mu^{(0)}\frac{\not{n}}{2}\Gamma_\nu^{(0)}\big]\int d\ell^+\Big\{\mathcal{J}^{(0)}(\ell^+-r^+)\Big\}\Big\{\bar{h}_v Y\delta(\ell^+-in\cdot\partial)Y^\dagger h_v\Big\}\,, \tag{3.109}$$

where we have used $\mathcal{H}_v = Y^\dagger h_v$. Performing the integral at tree level gives the well-known fact that the decay spectrum is determined by the shape function evaluated at r^+. Note that in SCET we needed to compute only one diagram rather than resumming an infinite sum of operators.

At NLO the tree-level diagrams are shown in Table 3.4. The graphs for $T^{(2H)}$ and $T^{(2a)}$ involve the same calculation as in Eq. (3.106) but just leave different soft operators.

For $T^{(2L)}$ the momentum routing is shown in Fig. 3-4a. Contracting the collinear quark propagators in the graph gives

$$\begin{aligned}
&(-i)(i)^3\overline{\mathcal{H}}_v(\ell_2^+)\overline{\Gamma}_\mu^{(0)}\frac{\not{n}}{2}\frac{\bar{n}\cdot p}{(\bar{n}\cdot p\,k_2^+ + i\epsilon)}[i\not{\mathcal{D}}_{us}^{\perp} i\not{\mathcal{D}}_{us}^{\perp}](\ell_2^+-\ell_1^+)\,\frac{1}{\bar{n}\cdot p}\frac{\not{\bar{n}}}{2}\frac{\not{n}}{2}\frac{\bar{n}\cdot p}{(\bar{n}\cdot p\,k_1^+ + i\epsilon)}\Gamma_\nu^{(0)}\mathcal{H}_v(\ell_1^+)\\
&= -\frac{1}{2\bar{n}\cdot p}\mathrm{Tr}\Big[P_v\overline{\Gamma}_\mu^{(0)}\frac{\not{n}}{2}\gamma_\alpha^\perp\gamma_\beta^\perp\Gamma_\nu^{(0)}\Big]\frac{1}{(k_1^+ + i\epsilon)(k_2^+ + i\epsilon)}\overline{\mathcal{H}}_v(\ell_2^+)[i\mathcal{D}_{us}^{\perp\alpha}\, i\mathcal{D}_{us}^{\perp\beta}](\ell_2^+-\ell_1^+)\mathcal{H}_v(\ell_1^+)\\
&+\frac{1}{2\bar{n}\cdot p}\mathrm{Tr}\Big[s_\tau\overline{\Gamma}_\mu^{(0)}\frac{\not{n}}{2}\gamma_\alpha^\perp\gamma_\beta^\perp\Gamma_\nu^{(0)}\Big]\frac{1}{(k_1^+ + i\epsilon)(k_2^+ + i\epsilon)}\overline{\mathcal{H}}_v(\ell_2^+)[i\mathcal{D}_{us}^{\perp\alpha}\, i\mathcal{D}_{us}^{\perp\beta}](\ell_2^+-\ell_1^+)\gamma_T^\tau\gamma_5\mathcal{H}_v(\ell_1^+)\,,
\end{aligned} \tag{3.110}$$

where momentum conservation sets $k_1^+ = \ell_1^+ - r^+$ and $k_2^+ = \ell_2^+ - r^+$. Taking $(-1/\pi)$ times the imaginary part gives the tree-level jet function

$$\mathcal{J}_1^{(-2)}(k_j^+) \;=\; \frac{\delta(k_1^+)-\delta(k_2^+)}{k_2^+-k_1^+} + \mathcal{O}(\alpha_s)\,, \tag{3.111}$$

and the convolutions

$$
\begin{aligned}
&-\frac{1}{2\bar{n}\cdot p}\mathrm{Tr}\Big[P_v\overline{\Gamma}_\mu^{(0)}\frac{\bar{n}\!\!\!/}{2}\gamma_\alpha^\perp\gamma_\beta^\perp\Gamma_\nu^{(0)}\Big]\int d\ell_1^+ d\ell_2^+\Big\{\mathcal{J}^{(-2)}(\ell_j^+-r^+)\Big\}\\
&\quad\times\Big\{\bar{h}_v Y\delta(\ell_2^+-in\cdot\partial)Y^\dagger iD_{us}^{\perp\alpha}iD_{us}^{\perp\beta}Y\delta(\ell_1^+-in\cdot\partial)Y^\dagger h_v\Big\}\\
&+\frac{1}{2\bar{n}\cdot p}\mathrm{Tr}\Big[s_\tau\overline{\Gamma}_\mu^{(0)}\frac{\bar{n}\!\!\!/}{2}\gamma_\alpha^\perp\gamma_\beta^\perp\Gamma_\nu^{(0)}\Big]\int d\ell_1^+ d\ell_2^+\Big\{\mathcal{J}^{(-2)}(\ell_j^+-r^+)\Big\}\\
&\quad\times\Big\{\bar{h}_v Y\delta(\ell_2^+-in\cdot\partial)Y^\dagger iD_{us}^{\perp\alpha}iD_{us}^{\perp\beta}\gamma_T^\tau\gamma_5 Y\delta(\ell_1^+-in\cdot\partial)Y^\dagger h_v\Big\}\,. \qquad (3.112)
\end{aligned}
$$

Finally, we consider the NLO time-ordered product $T^{(2q)}$ with the momentum routing in Fig. 3-4b. This graph gives

$$
\begin{aligned}
&(-i)^2(i)^4g^2\Big[\overline{\mathcal{H}}_v(\ell_3^+)\overline{\Gamma}_\mu^{(0)}\frac{\bar{n}\!\!\!/}{2}\frac{\bar{n}\cdot p}{(\bar{n}\cdot p\,k_3^+ + i\epsilon)}\gamma_\perp^\tau T^A\psi_{us}(\ell_3^+-\ell_2^+)\Big]\frac{1}{\bar{n}\cdot p\,k_2^+ + i\epsilon} \qquad (3.113)\\
&\times\Big[\bar{\psi}_{us}(\ell_1^+-\ell_2^+)\gamma_\tau^\perp T^A\frac{\bar{n}\!\!\!/}{2}\frac{\bar{n}\cdot p}{(\bar{n}\cdot p\,k_1^+ + i\epsilon)}\Gamma_\nu^{(0)}\mathcal{H}_v(\ell_1^+)\Big]\\
&=-\frac{1}{\bar{n}\cdot p}\frac{g^2}{(k_1^+ + i\epsilon)(k_2^+ + i\epsilon)(k_3^+ + i\epsilon)}\Big[\overline{\mathcal{H}}_v\overline{\Gamma}_\mu^{(0)}\frac{\bar{n}\!\!\!/}{2}\gamma_\perp^\tau T^A\psi_{us}\Big]\Big[\bar{\psi}_{us}T^A\gamma_\tau^\perp\frac{\bar{n}\!\!\!/}{2}\Gamma_\nu^{(0)}\mathcal{H}_v\Big]\,,
\end{aligned}
$$

where $k_1^+ = \ell_1^+ - r^+$, $k_2^+ = \ell_2^+ - r^+$, and $k_3^+ = \ell_3^+ - r^+$. Taking $(-1/\pi)$ times the imaginary part gives the tree-level jet function

$$
\mathcal{J}_1^{(-4)}(k_j^+) = g^2\left[\frac{\delta(k_1^+)}{(k_2^+)(k_3^+)} + \frac{\delta(k_2^+)}{(k_1^+)(k_3^+)} + \frac{\delta(k_3^+)}{(k_1^+)(k_2^+)} - \pi^2\delta(k_1^+)\delta(k_2^+)\delta(k_3^+)\right]\,. \qquad (3.114)
$$

Writing out the convolutions for these four-quark operators, we find

$$
\begin{aligned}
&-\frac{1}{\bar{n}\cdot p}\int d\ell_1^+ d\ell_2^+ d\ell_3^+\Big\{\mathcal{J}^{(-4)}(\ell_j^+-r^+)\Big\}\Big[\bar{h}_v Y\delta(\ell_3^+-in\cdot\partial)\overline{\Gamma}_\mu^{(0)}\frac{\bar{n}\!\!\!/}{2}\gamma_\perp^\tau T^A Y^\dagger q_{us}\Big]\\
&\quad\times\delta(\ell_2^+-in\cdot\partial)\Big[\bar{q}_{us}YT^A\gamma_\tau^\perp\frac{\bar{n}\!\!\!/}{2}\Gamma_\nu^{(0)}\delta(\ell_1^+-in\cdot\partial)Y^\dagger h_v\Big]\,. \qquad (3.115)
\end{aligned}
$$

3.6.4 NLO Soft Operators and Shape Functions

In this section, we define the shape functions that can appear in the NLO factorization theorem. At tree level, many of these functions have already been defined in Ref. [26] (we use a sequential enumeration of these functions. and translate to the notation in

Ref. [26] in Table 3.7). We also define the additional shape functions with four-quark operators that are not given in Ref. [26], and later in section 3.6.5 the shape functions that appear only beyond tree level in the subleading jet functions.

We begin by enumerating the usoft operators. For the time-ordered product of the LO shape-function operator and the subleading HQET Lagrangian we define

$$O_0^{(2)}(\ell^+) \;=\; \int\frac{dx^-}{8\pi}\,e^{-\frac{i}{2}x^-\ell^+}\int d^4y\,T\left[\bar h_v(\tilde x)Y(\tilde x,0)h_v(0)\;iO_h(y)\right]. \qquad (3.116)$$

With $igG^{\mu\nu}_{us\perp}=[iD^{\perp\mu}_{us},iD^{\perp\nu}_{us}]$, the remaining ultrasoft operators that play an important role include

$$\begin{aligned}
O_1^\beta(\ell^+) &= \int\frac{dx^-}{8\pi}\,e^{-\frac{i}{2}\ell^+x^-}\Big[\overline{\mathcal{H}}_v(\tilde x)(i\overrightarrow{\mathcal{D}}^\beta_{us}\mathcal{H}_v)(0)+(\text{h.c.},\,\tilde x\leftrightarrow 0)\Big]\\
&= \frac{1}{2}\bar h_v\big\{iD^\beta_{\rm us},\delta(\ell^+-in\cdot D_{\rm us})\big\}h_v\,, \qquad (3.117)\\
P_{1\lambda}^\beta(\ell^+) &= \int\frac{dx^-}{8\pi}\,e^{-\frac{i}{2}\ell^+x^-}\Big[\overline{\mathcal{H}}_v(\tilde x)\gamma_\lambda^T\gamma_5(i\overrightarrow{\mathcal{D}}^\beta_{us}\mathcal{H}_v)(0)+(\text{h.c.},\,\tilde x\leftrightarrow 0)\Big]\\
&= \frac{1}{2}\,\bar h_v\big\{iD^\beta_{\rm us},\delta(\ell^+-in\cdot D_{\rm us})\big\}\gamma_T^\lambda\gamma_5 h_v\,,\\
O_2^\beta(\ell^+) &= \int\frac{dx^-}{8\pi}\,e^{-\frac{i}{2}\ell^+x^-}\Big[-i\mathrm{T}\,\overline{\mathcal{H}}_v(\tilde x)(i\overrightarrow{\mathcal{D}}^\beta_{us}\mathcal{H}_v)(0)+(\text{h.c.},\,\tilde x\leftrightarrow 0)\Big]\\
&= \frac{i}{2}\,\bar h_v\big[iD^\beta_{\rm us},\delta(\ell^+-in\cdot D_{\rm us})\big]h_v\,,\\
P_{2\lambda}^\beta(\ell^+) &= \int\frac{dx^-}{8\pi}\,e^{-\frac{i}{2}\ell^+x^-}\Big[-i\mathrm{T}\,\overline{\mathcal{H}}_v(\tilde x)\gamma_\lambda^T\gamma_5(i\overrightarrow{\mathcal{D}}^\beta_{us}\mathcal{H}_v)(0)+(\text{h.c.},\,\tilde x\leftrightarrow 0)\Big]\\
&= \frac{i}{2}\,\bar h_v\big[iD^\beta_{\rm us},\delta(\ell^+-in\cdot D_{\rm us})\big]\gamma_T^\lambda\gamma_5 h_v\,,\\
O_3^{\alpha\beta}(\ell_1^+,\ell_2^+) &= \int\frac{dx^-\,dy^-}{32\pi^2}e^{-\frac{i}{2}\ell_2x^-}e^{-\frac{i}{2}(\ell_1^+-\ell_2^+)y^-}\big[\overline{\mathcal{H}}_v(\tilde x)\{iD^{\perp\alpha}_{us},iD^{\perp\beta}_{us}\}(\tilde y)\mathcal{H}_v(0)\big]\\
&= \frac{1}{2}\,\bar h_v\delta(\ell_2^+-in\cdot D_{us})\left\{iD^{\perp\alpha}_{us},iD^{\perp\beta}_{us}\right\}\delta(\ell_1^+-in\cdot D_{us})h_v\,,\\
P_{4\lambda}^{\alpha\beta}(\ell_1^+,\ell_2^+) &= i\int\frac{dx^-\,dy^-}{32\pi^2}e^{-\frac{i}{2}\ell_2x^-}e^{-\frac{i}{2}(\ell_1^+-\ell_2^+)y^-}\big[\overline{\mathcal{H}}_v(\tilde x)[iD^{\perp\alpha}_{us},iD^{\perp\beta}_{us}](\tilde y)\gamma_\lambda^T\gamma_5\,\mathcal{H}_v(0)\big]\\
&= -\frac{1}{2}\,\bar h_v\delta(\ell_2^+-in\cdot D_{us})gG^{\alpha\beta}_{us\perp}\delta(\ell_1^+-in\cdot D_{us})\gamma_\lambda^T\gamma_5 h_v\,.
\end{aligned}$$

and the four-quark operators

$$
\begin{aligned}
O_5^{\alpha\beta}(\ell^+_{1,2,3}) =& \int \frac{dx^- dy^- dz^-}{128\pi^3} e^{-\frac{i}{2}\{\ell_3^+ x^- + (\ell_2^+ - \ell_3^+) y^- + (\ell_1^+ - \ell_2^+) z^-\}} \big[\overline{\mathcal{H}}_v(\tilde{x}) \gamma^\beta P_L T^A \psi^{\bar{n}}_{us}(\tilde{y}) \\
& \times \bar{\psi}^{\bar{n}}_{us}(\tilde{z}) \gamma^\alpha P_L T^A \mathcal{H}_v(0)\big] \qquad (3.118) \\
=& \frac{1}{2}\big\{\bar{h}_v \delta(\ell_3^+ - in\cdot D_{us}) \gamma^\beta P_L T^A q^{\bar{n}}\big\}\, \delta(\ell_2^+ - in\cdot\partial)\, \big\{\bar{q}^{\bar{n}} \gamma^\alpha P_L \delta(\ell_1^+ - in\cdot D_{us}) T^A h_v\big\}, \\
O_6^{\alpha\beta}(\ell^+_{1,2,3}) =& \int \frac{dx^- dy^- dz^-}{128\pi^3} e^{-\frac{i}{2}\{\ell_3^+ x^- + (\ell_2^+ - \ell_3^+) y^- + (\ell_1^+ - \ell_2^+) z^-\}} \big[\overline{\mathcal{H}}_v(\tilde{x}) \gamma^\beta P_L \psi^{\bar{n}}_{us}(\tilde{y}) \\
& \times \bar{\psi}^{\bar{n}}_{us}(\tilde{z}) \gamma^\alpha P_L \mathcal{H}_v(0)\big] \\
=& \frac{1}{2}\left[\bar{h}_v \delta(\ell_3^+ - in\cdot D_{us}) \gamma^\beta P_L q^{\bar{n}}\right] \delta(\ell_2^+ - in\cdot\partial)\, \left[\bar{q}^{\bar{n}} \gamma^\alpha P_L \delta(\ell_1^+ - in\cdot D_{us}) h_v\right].
\end{aligned}
$$

Here $\psi^{\bar{n}}_{us} = (\bar{n}\!\!\!/ n\!\!\!/)/4\, \psi_{us}$ and the flavour of the quarks in these operators is s for $B \to X_s\gamma$ and u for $B \to X_u \ell\bar{\nu}$. Note that a minimal basis of Dirac structures for the bilinears is $\bar{h}_v\{1, \gamma_T^\mu \gamma_5\} h_v$. In the second line for each operator we have used our freedom to integrate by parts since only the forward part of these usoft operators is required. The operators in Eq. (3.117) were obtained by matching with tree-level quark propagators in Ref. [26] and we agree with these.[12] The four-quark operator $O_5^{\alpha\beta}$ appears when gluon propagators are included at tree level, as we discuss further below. The operator $\int d\ell_1^+ d\ell_3^+ O_6^{\alpha\beta}$ occurs from the disconnected annihilation contribution, as shown in Ref. [108]. However, since this contribution is of order $(\Lambda/m_b)^2$ in the endpoint region, we do not include it in our analysis here.

When $\mathcal{O}(\alpha_s)$ corrections are included in the subleading factorization theorems, then in general we require additional usoft operators. For example, at $\mathcal{O}(\alpha_s)$ there are two additional soft operators generated by $T^{(2L)}$, and six additional operators from $T^{(2q)}$. Definitions for these operators can be found in Sec. 3.6.5.

The subleading shape functions of the operators in Eq. (3.117) are defined by the

[12] It seems that Ref. [26] has a typographical error in the phase factor of $O_3^{\mu\nu}$ and $P_{4\alpha}^{\mu\nu}$ and that it should read $e^{i(\omega_1-\omega_2)t_1} e^{-i\omega_1 t_2}$, in which case the variables in that paper are related to ours by $\omega_i = -\ell_i/m_b$.

matrix elements

$$
\begin{aligned}
\langle \bar{B}_v | O_0(\ell^+) | \bar{B}_v \rangle &= f_0^{(2)}(\ell^+)\,, \\
\langle \bar{B}_v | O_1^\beta(\ell^+) | \bar{B}_v \rangle &= \left(v^\beta - \frac{n^\beta}{n\cdot v}\right) f_1^{(2)}(\ell^+)\,, \\
\langle \bar{B}_v | P_1^{\beta\lambda}(\ell^+) | \bar{B}_v \rangle &= \epsilon_\perp^{\beta\lambda}\, g_0^{(2)}(\ell^+)\,, \\
\langle \bar{B}_v | P_2^{\beta\lambda}(\ell^+) | \bar{B}_v \rangle &= \epsilon_\perp^{\beta\lambda}\, f_2^{(2)}(\ell^+)\,, \\
\langle \bar{B}_v | O_3^{\alpha\beta}(\ell^+) | \bar{B}_v \rangle &= g_\perp^{\alpha\beta}\, f_3^{(4)}(\ell_1^+, \ell_2^+)\,, \\
\langle \bar{B}_v | P_{4\lambda}^{\alpha\beta}(\ell^+) | \bar{B}_v \rangle &= -\epsilon_\perp^{\alpha\beta}\left(v_\lambda - \frac{n_\lambda}{n\cdot v}\right) f_4^{(4)}(\ell_1^+, \ell_2^+)\,,
\end{aligned}
\tag{3.119}
$$

where we take $v_\perp = 0$ and $\epsilon_\perp^{\beta\lambda} = \epsilon^{\beta\lambda\sigma\tau} v_\sigma n_\tau/(n\cdot v)$. For the four-quark operators we need

$$
\begin{aligned}
n_\alpha n_\beta \langle \bar{B}_v | O_5^{\alpha\beta}(\ell_{1,2,3}^+) | \bar{B}_v \rangle &= f_5^{(6)}(\ell_1^+, \ell_2^+, \ell_3^+)\,, \\
(g_{\alpha\beta}^\perp - i\epsilon_{\alpha\beta}^\perp) \langle \bar{B}_v | O_5^{\alpha\beta}(\ell_{1,2,3}^+) | \bar{B}_v \rangle &= f_6^{(6)}(\ell_1^+, \ell_2^+, \ell_3^+)\,.
\end{aligned}
\tag{3.120}
$$

Recall that we use the notation f_i to indicate shape functions that appear from tree-level matching and g_i to indicate shape functions that show up only when higher-order perturbative corrections for the jet functions are considered. Definitions for all the g_i functions are given with the derivation of the factorization theorems in Sec. 3.6.5. For the f_i, we give the translation to the notation in Ref. [26] in Table 3.7.

In Ref. [26], it was shown that the equations of motion for h_v imply that

$$
f_1^{(2)}(\omega) = 2\omega f^{(0)}(\omega)\,, \tag{3.121}
$$

which reduces the number of NLO unknowns, and that the B matrix element of the operator $O_{2,3}$ vanishes, so we shall not need it for our results. The same is true of two additional operators, $O_4^{\alpha\beta}$ and $P_{3\lambda}^{\alpha\beta}$, which are the analogs of $P_4^{\alpha\beta}$ but with anticommutators. Ref. [26] also removes $P_{1\lambda}^\beta$ from the basis by noting that all the moments of the corresponding shape function vanish. However, we keep this operator

Our Notation	Notation in Ref. [26]
$f^{(0)}(\ell^+)$	$f(-\hat{\ell}^+)$
$f_0^{(2)}(\ell^+)$	$t(-\hat{\ell}^+)$
$f_1^{(2)}(\ell^+)$	$g_1(-\hat{\ell}^+)$
$f_2^{(2)}(\ell^+)$	$h_1(-\hat{\ell}^+)$
$f_3^{(4)}(\ell_1^+,\ell_2^+)$	$g_2(-\hat{\ell}_1^+,-\hat{\ell}_2^+)$
$f_4^{(4)}(\ell_1^+,\ell_2^+)$	$h_2(-\hat{\ell}_1^+,-\hat{\ell}_2^+)$
$f_5^{(6)}(\ell_1^+,\ell_2^+,\ell_3^+)$	—
$f_6^{(6)}(\ell_1^+,\ell_2^+,\ell_3^+)$	—

Table 3.7: Relation of our f_i functions to the notation in Ref. [26], up to an overall normalization. Here, $\hat{\ell}^+ = \ell^+/m_b$.

since it is unclear whether the moments are sufficient to define the function completely beyond tree level in the jet function. (We do show, however, that this operator is not matched on to at tree level in the hard function.)

3.6.5 Factorization Calculations at $\mathcal{O}(\lambda^2)$

We now derive the factorization theorems for the subleading $\mathcal{O}(\lambda^2)$ terms. We show that it is exactly the soft functions defined in the previous section that appear in the decay rates, and give operator definitions for the jet functions that can be used beyond tree level.

Calculation of $\hat{T}^{(2H)}$

For $T^{(2H)}$ the factorization is identical to that at LO in Sec. 3.4, except that the final usoft matrix element is the time-ordered product

$$\int\frac{dx^-}{8\pi}e^{-\frac{i}{2}x^-\ell^+}\int d^4y\,\left\langle\bar{B}_v\middle|T\left[\bar{h}_v(\tilde{x})Y(\tilde{x},0)h_v(0)\,\frac{i\,O_h(y)}{2m_b}\right]\middle|\bar{B}_v\right\rangle=\frac{f_0^{(2)}(\ell^+)}{2m_b}\,. \quad (3.122)$$

The factorization theorem for $\hat{T}^{(2H)}$ is therefore

$$W_i^{(2H)}=h_i^0(\bar{n}\cdot p,m_b,\mu)\int_{n\cdot q-m_b}^{\bar{\Lambda}}d\ell^+\,\mathcal{J}^{(0)}(\bar{n}\cdot p(\ell^++m_b-n\cdot q),\mu)\,\frac{f_0^{(2)}(\ell^+,\mu)}{2m_b}\,. \quad (3.123)$$

As noted in Ref. [26], the function $f_0^{(2)}$ can simply be absorbed into the LO $f^{(0)}$, since at this order they always appear together in the combination

$$f^{(0)}(\ell^+) + \frac{1}{2m_b} f_0^{(2)}(\ell^+) \,. \tag{3.124}$$

Calculation of $\hat{T}^{(2a)}$

For the remaining time-ordered products, the factorization is more complicated. However, some aspects of the LO analysis in Sec. 3.4 remain the same at subleading order. In particular, we still have the $\exp(-ir\cdot x)$ phase factor in Eq. (3.61), a $\delta(\omega' - \bar{n}\cdot p)$ appears in the separation of hard Wilson coefficients, as it does in Eq. (3.66), and the vacuum matrix element of collinear fields still gives a $\delta(\omega - \omega')$. For convenience, we integrate over ω and ω' and remove these delta functions right from the start when considering $T^{(2a)}$, $T^{(2L)}$, and $T^{(2q)}$.

For $\hat{T}^{(2a)}$ the analog of Eq. (3.66) is

$$\begin{aligned} \hat{T}^{(2a)}_{\mu\nu} \;=\; & -i \sum_{j,j'} \sum_{\kappa=a,b} C_{j'}(\bar{n}\cdot p) A_j^{(2\kappa)}(\bar{n}\cdot p) \int d^4x\, e^{-ir\cdot x} \\ & \times \mathrm{T}\left[J^{(0)\dagger}_{j'\,\mu}(\bar{n}\cdot p, x)\, J^{(2\kappa)}_{j\,\nu}(\bar{n}\cdot p, 0) + J^{(2\kappa)\dagger}_{j\,\mu}(\bar{n}\cdot p, x)\, J^{(0)}_{j'\,\nu}(\bar{n}\cdot p, 0) \right], \end{aligned} \tag{3.125}$$

where $A_j^{(2\kappa)}(\omega,\mu)$ are the Wilson coefficients for the $J^{(2k)}$ currents, as in Eq. (3.50). The products of currents in square brackets are

$$\begin{aligned} J^{(0)\dagger}_{j'} J^{(2a)}_j + J^{(2a)\dagger}_j J^{(0)}_{j'} &= \frac{1}{2m_b} \big[\bar{\mathcal{H}}_v \overline{\Gamma}^{(0)}_{j'} \chi_{n\omega'}\big](x) \big[\bar{\chi}_{n,\omega} \Upsilon^{(2a)}_{j\alpha}\, i\overrightarrow{\mathcal{D}}^{T\alpha}_{us}\, \mathcal{H}_v\big](0) \\ &\quad + \frac{1}{2m_b} \big[\bar{\mathcal{H}}_v (-i) \overleftarrow{\mathcal{D}}^{T\alpha}_{us} \overline{\Upsilon}^{(2a)}_{j\alpha} \chi_{n,\omega}\big](x)\, \big[\bar{\chi}_{n,\omega'} \Gamma^{(0)}_{j'} \mathcal{H}_v\big](0)\,, \\ J^{(0)\dagger}_{j'} J^{(2b)}_j + J^{(2b)\dagger}_j J^{(0)}_{j'} &= \frac{1}{\omega} \big[\bar{\mathcal{H}}_v \overline{\Gamma}^{(0)}_{j'} \chi_{n\omega'}\big](x) \big[\bar{\chi}_{n,\omega} \Upsilon^{(2b)}_{j\alpha}\, i\overleftarrow{\mathcal{D}}^{\perp\alpha}_{us} \mathcal{H}_v\big](0) \\ &\quad + \frac{1}{\omega} \big[(\bar{\mathcal{H}}_v (-i) \overrightarrow{\mathcal{D}}^{\perp\alpha}_{us}) \overline{\Upsilon}^{(2b)}_{j\alpha} \chi_{n,\omega}\big](x)\, \big[\bar{\chi}_{n,\omega'} \Gamma^{(0)}_{j'} \mathcal{H}_v\big](0)\,. \end{aligned} \tag{3.126}$$

Next we insert identity matrices to Fierz transform using Eq. (3.68) and take the

$\langle B_v|\cdots|B_v\rangle/2$ matrix element. These two terms then become

$$\begin{aligned}
\big\langle J_{j'}^{(0)\dagger} J_j^{(2a)} + J_j^{(2a)\dagger} J_{j'}^{(0)} \big\rangle &= \frac{(-1)}{8m_b} \Big\{ \big\langle \bar B_v \big| \bar{\mathcal{H}}_v(x) \overline{\Gamma}_{j'}^{(0)} F_k^n \Upsilon_{j\alpha}^{(2a)} (i\overrightarrow{\mathcal{D}}_{us}^{T\alpha} \mathcal{H}_v)(0) \big| \bar B_v \big\rangle \\
&\quad - \big\langle \bar B_v \big| (\bar{\mathcal{H}}_v i\overleftarrow{\mathcal{D}}_{us}^{T\alpha})(x) \overline{\Upsilon}_{j\alpha}^{(2a)} F_k^n \Gamma_{j'}^{(0)} \mathcal{H}_v(0) \big| \bar B_v \big\rangle \Big\} \big\langle 0 \big| \bar\chi_{n,\omega}(0) F_k^{\bar n} \chi_{n,\omega'}(x) \big| 0 \big\rangle \,, \\
\big\langle J_{j'}^{(0)\dagger} J_j^{(2b)} + J_j^{(2b)\dagger} J_{j'}^{(0)} \big\rangle &= \frac{1}{4\bar n\cdot p} \Big\{ \big\langle \bar B_v \big| \bar{\mathcal{H}}_v(x) \overline{\Gamma}_{j'}^{(0)} F_k^n \Upsilon_{j\alpha}^{(2b)} (i\overrightarrow{\mathcal{D}}_{us}^{\perp\alpha} \mathcal{H}_v)(0) \big| \bar B_v \big\rangle \\
&\quad - \big\langle \bar B_v \big| (\bar{\mathcal{H}}_v i\overleftarrow{\mathcal{D}}_{us}^{\perp\alpha})(x) \overline{\Upsilon}_{j\alpha}^{(2b)} F_k^n \Gamma_{j'}^{(0)} \mathcal{H}_v(0) \big| \bar B_v \big\rangle \Big\} \big\langle 0 \big| \bar\chi_{n,\omega}(0) F_k^{\bar n} \chi_{n,\omega'}(x) \big| 0 \big\rangle \,,
\end{aligned} \tag{3.127}$$

where it is understood that we have $\omega = \omega' = \bar n\cdot p$, and we have used $q_\perp = 0$ in order to integrate the $iD^\perp$ derivatives by parts in the $J^{(2b)}$ terms. From Eq. (3.127) we see that the collinear vacuum matrix elements are the same as in the LO case. Hence they are non-zero only for $k = 1$ and are given by the LO jet function $\mathcal{J}_\omega^{(0)}(k^+)$ from Eq. (3.70).

Using the trace formula in Eq. (3.73), we can simplify the spin structures in the usoft matrix elements in Eq. (3.127), where we can now set $F_1^n = \bar n\!\!\!//2$. Here both the P_v and s^μ terms in the $F_{k'}^H$ matrices will give non-zero contributions, so $k' = 1, 2$ and we have

$$\begin{aligned}
&- \mathrm{Tr}\Big\{ P_{k'}^H \overline{\Gamma}_{j'}^{(0)} \frac{\bar n\!\!\!/}{2} \Big[\frac{g_{\alpha\beta}^T}{8m_b} \Upsilon_{j\alpha}^{(2a)} A_j^{(2a)} - \frac{g_{\alpha\beta}^\perp}{4\bar n\cdot p} \Upsilon_{j\alpha}^{(2b)} A_j^{(2b)} \Big] \Big\} \big\langle \bar B_v \big| \mathrm{T}\, \bar{\mathcal{H}}_v(x) P_{k'}^h (i\overrightarrow{\mathcal{D}}_{us}^\beta \mathcal{H}_v)(0) \big| \bar B_v \big\rangle \\
&+ \mathrm{Tr}\Big\{ P_{k'}^H \Big[\frac{g_{\alpha\beta}^T}{8m_b} \overline{\Upsilon}_{j\alpha}^{(2a)} A_j^{(2a)} - \frac{g_{\alpha\beta}^\perp}{4\bar n\cdot p} \overline{\Upsilon}_{j\alpha}^{(2b)} A_j^{(2b)} \Big] \frac{\bar n\!\!\!/}{2} \Gamma_{j'}^{(0)} \Big\} \big\langle \bar B_v \big| \mathrm{T}\, (\bar{\mathcal{H}}_v i\overleftarrow{\mathcal{D}}_{us}^\beta)(x) P_{k'}^h \mathcal{H}_v(0) \big| \bar B_v \big\rangle \\
&= -\frac{1}{4} \mathrm{Tr}\big\{ X_\beta^{k'=1} \big\} \langle \bar B_v | (O_1^\beta + iO_2^\beta) | \bar B_v \rangle + \frac{1}{4} \mathrm{Tr}\big\{ \overline{X}_\beta^{k'=1} \big\} \langle \bar B_v | (-O_1^\beta + iO_2^\beta) | \bar B_v \rangle \\
&- \frac{1}{4} \mathrm{Tr}\big\{ X_{\beta\lambda}^{k'=2} \big\} \langle \bar B_v | (P_1^{\beta\lambda} + iP_2^{\beta\lambda}) | \bar B_v \rangle + \frac{1}{4} \mathrm{Tr}\big\{ \overline{X}_{\beta\lambda}^{k'=2} \big\} \langle \bar B_v | (-P_1^{\beta\lambda} + iP_2^{\beta\lambda}) | \bar B_v \rangle \,,
\end{aligned} \tag{3.128}$$

where

$$\begin{aligned}
X^{k'} &= P_{k'}^H \overline{\Gamma}_{j'\mu}^{(0)} \frac{\bar n\!\!\!/}{2} \Big[\frac{g_{\alpha\beta}^T}{4m_b} \Upsilon_{j\alpha\nu}^{(2a)} A_j^{(2a)} - \frac{g_{\alpha\beta}^\perp}{2\bar n\cdot p} \Upsilon_{j\alpha\nu}^{(2b)} A_j^{(2b)} \Big] \,, \\
\overline{X}^{k'} &= P_{k'}^H \Big[\frac{g_{\alpha\beta}^T}{4m_b} \overline{\Upsilon}_{j\alpha\mu}^{(2a)} A_j^{(2a)} - \frac{g_{\alpha\beta}^\perp}{2\bar n\cdot p} \overline{\Upsilon}_{j\alpha\mu}^{(2b)} A_j^{(2b)} \Big] \frac{\bar n\!\!\!/}{2} \Gamma_{j'\nu}^{(0)} \,.
\end{aligned} \tag{3.129}$$

Note that the second trace is the complex conjugate of the first with $(\mu \leftrightarrow \nu)$, since $\gamma_0 (F^H_{k'})^\dagger \gamma_0 = F^H_{k'}$ and $\mathrm{Tr}[\overline{X}] = \mathrm{Tr}[X^\dagger] = \mathrm{Tr}[X^*] = (\mathrm{Tr}X)^*$. These usoft matrix elements give the shape functions f_1, g_0, and f_2 in Eq. (3.119) at any matching order in α_s. The index β is transverse to v, as follows from Eq. (3.128) with $v_\perp = 0$. Combining Eq. (3.128) with the delta functions and prefactors from the jet function and the $(-i)$ from $\hat{T}^{(2a)}$ gives

$$\begin{aligned} &\int dk^+ \mathcal{J}^{(0)}_\omega(k^+) \Big[\mathrm{Tr}\big\{ X^{k'=1}_\beta + \overline{X}^{k'=1}_\beta \big\} \Big(-\frac{n^\beta}{n\cdot v} \Big) f_1^{(2)}(k^+ + r^+) \\ &+ \mathrm{Tr}\big\{ X^{k'=2}_{\beta\lambda} + \overline{X}^{k'=2}_{\beta\lambda} \big\} \epsilon_\perp^{\beta\lambda} \, g_0^{(2)}(k^+ + r^+) + \mathrm{Tr}\big\{ X^{k'=2}_{\beta\lambda} - \overline{X}^{k'=2}_{\beta\lambda} \big\} i\epsilon_\perp^{\beta\lambda} \, f_2^{(2)}(k^+ + r^+) \Big] . \end{aligned} \tag{3.130}$$

We include these traces in the definition of the hard coefficients at subleading order, as was done in Eq. (3.83), defining

$$\begin{aligned} h_i^{[2a]1} &= \frac{1}{8} \sum_{j,j'} C_{j'} \, A_j^{(2a)} \, \mathrm{Tr}\Big\{ P_v \overline{\Gamma}^{(0)}_{j'\mu} \frac{\bar{n}\!\!\!/}{2} \Big(-\frac{n^\alpha}{n\cdot v} \Big) \Upsilon^{(2a)}_{j\alpha\nu} + (\text{h.c. } \mu \leftrightarrow \nu) \Big\} \, P_i^{\mu\nu} , \\ h_i^{[2a]2} &= \frac{1}{2} \sum_{j,j'} C_{j'} \, \mathrm{Tr}\Big\{ P_v \gamma_5 \gamma_\lambda^T P_v \overline{\Gamma}^{(0)}_{j'\mu} \frac{\bar{n}\!\!\!/}{2} \Big[\frac{i\epsilon_\perp^{\alpha\lambda}}{4} \Upsilon^{(2a)}_{j\alpha\nu} A_j^{(2a)} - \frac{i\epsilon_\perp^{\alpha\lambda} \, m_b}{2\bar{n}\cdot p} \Upsilon^{(2b)}_{j\alpha\nu} A_j^{(2b)} \Big] \\ &\quad + (\text{h.c. } \mu \leftrightarrow \nu) \Big\} \, P_i^{\mu\nu} , \\ h_i^{[2a]00} &= \frac{1}{2} \sum_{j,j'} C_{j'} \, \mathrm{Tr}\Big\{ P_v \gamma_5 \gamma_\lambda^T P_v \overline{\Gamma}^{(0)}_{j'\mu} \frac{\bar{n}\!\!\!/}{2} \Big[\frac{\epsilon_\perp^{\alpha\lambda}}{4} \Upsilon^{(2a)}_{j\alpha\nu} A_j^{(2a)} - \frac{\epsilon_\perp^{\alpha\lambda} \, m_b}{2\bar{n}\cdot p} \Upsilon^{(2b)}_{j\alpha\nu} A_j^{(2b)} \Big] \\ &\quad + (\text{h.c. } \mu \leftrightarrow \nu) \Big\} \, P_i^{\mu\nu} . \end{aligned} \tag{3.131}$$

For the Dirac structures $\Upsilon^{(2a)}$ and $\Upsilon^{(2b)}$ that are present at tree level $h_i^{[2a]00}$ is zero, so $g_0^{(2)}$ comes in with $\alpha_s(m_b)$ suppression. We were unable to prove our suspicion that $g_0^{(2)}$ would not appear beyond this level.

Using Eq. (3.131) with Eq. (3.130) and taking $(-1/\pi)$ times the imaginary part

gives the NLO factorization theorem for $W_i^{(2a)}$:

$$\begin{aligned} W_i^{(2a)} &= \frac{h_i^{[2a]1}(\bar{n}\cdot p, m_b, \mu)}{m_b} \int_0^{p_X^+} dk^+ \; \mathcal{J}^{(0)}(\bar{n}\cdot p\, k^+, \mu)\, f_1^{(2)}(k^+ + r^+, \mu) \\ &+ \frac{h_i^{[2a]2}(\bar{n}\cdot p, m_b, \mu)}{m_b} \int_0^{p_X^+} dk^+ \; \mathcal{J}^{(0)}(\bar{n}\cdot p\, k^+, \mu)\, f_2^{(2)}(k^+ + r^+, \mu) \\ &+ \frac{h_i^{[2a]00}(\bar{n}\cdot p, m_b, \mu)}{m_b} \int_0^{p_X^+} dk^+ \; \mathcal{J}^{(0)}(\bar{n}\cdot p\, k^+, \mu)\, g_0^{(2)}(k^+ + r^+, \mu)\,. \end{aligned} \tag{3.132}$$

Explicit results for the coefficients $h_i^{[2a]}$ are summarized in Sec. 3.6.6.

Calculation of $T^{(2L)}$

For $T^{(2L)}$ the heavy-to-light currents are identical to those in $T^{(0)}$, and so the same Wilson coefficients appear as in Eq. (3.66), i.e.

$$\hat{T}_{\mu\nu}^{(2L)} = -i \sum_{j,j'} C_{j'}(\bar{n}\cdot p) C_j(\bar{n}\cdot p) \int d^4x \int d^4y\, e^{-ir\cdot x}\, \mathrm{T}\left[J_{j'\mu}^{(0)\dagger}(\bar{n}\cdot p, x)\, \mathcal{L}_{\xi\xi}^{(2a)}(y) J_{j\nu}^{(0)}(\bar{n}\cdot p, 0) \right]. \tag{3.133}$$

The difference is the extra Lagrangian insertion with mixed collinear and usoft fields, namely

$$\begin{aligned} & J_{j'}^{(0)\dagger}(x) \mathcal{L}_{\xi\xi}^{(2a)}(y) J_j^{(0)}(0) \\ &= \left[\bar{\mathcal{H}}_v \overline{\Gamma}_{j'}^{(0)} \chi_{n,\omega'}^L\right](x) \left[\bar{\chi}_n i\not{\mathcal{D}}_{us}^\perp i\not{\mathcal{D}}_{us}^\perp \frac{\bar{\not{n}}}{2} \frac{1}{\bar{\mathcal{P}}} \chi_n\right](y) \left[\bar{\chi}_{n,\omega}^L \Gamma_j^{(0)} \mathcal{H}_v\right](0) \\ &= \frac{1}{4} \sum_{k,k'=1}^{4} \left[\bar{\mathcal{H}}_v(x) \overline{\Gamma}_{j'}^{(0)} F_{k'}^{Ln} \left(i\not{\mathcal{D}}_{us}^\perp i\not{\mathcal{D}}_{us}^\perp \frac{\bar{\not{n}}}{2}\right)(y) F_k^{nR} \Gamma_j^{(0)} \mathcal{H}_v(0)\right] \\ &\qquad \times \left[\bar{\chi}_n(y) F_{k'}^{\bar{n}L} \chi_{n,\omega'}^L(x)\right] \left[\bar{\chi}_{n,\omega}^L(0) F_k^{R\bar{n}} \frac{1}{\bar{\mathcal{P}}} \chi_n(y)\right]. \end{aligned} \tag{3.134}$$

where in the second line we have used analogs of the Fierz formula in Eq. (3.68) that are appropriate with left- and right-handed projectors,

$$
\begin{aligned}
P_L \otimes 1 &= \frac{1}{2}\sum_{k=1}^{4} F_k^{\bar{n}L} \otimes F_k^{Ln} = \frac{1}{2}\Big[\big(\frac{\bar{n}\!\!\!/}{N_c} P_L\big)\otimes\big(P_L \frac{n\!\!\!/}{2}\big) + \big(\frac{-\bar{n}\!\!\!/\gamma_\perp^\alpha P_L}{2N_c}\big)\otimes\big(P_L \frac{n\!\!\!/\gamma_\alpha^\perp}{2}\big) \\
&\quad + \big(2\bar{n}\!\!\!/ P_L T^a\big)\otimes\big(P_L \frac{n\!\!\!/}{2} T^a\big) + \big(-\bar{n}\!\!\!/\gamma_\perp^\alpha P_L T^a\big)\otimes\big(P_L \frac{n\!\!\!/\gamma_\alpha^\perp}{2} T^a\big)\Big], \\
P_R \otimes 1 &= \frac{1}{2}\sum_{k'=1}^{4} F_{k'}^{R\bar{n}} \otimes F_{k'}^{nR} = \frac{1}{2}\Big[\big(P_R \frac{\bar{n}\!\!\!/}{N_c}\big)\otimes\big(\frac{n\!\!\!/}{2} P_R\big) + \big(P_R \frac{-\bar{n}\!\!\!/\gamma_\perp^\beta}{2N_c}\big)\otimes\big(\frac{n\!\!\!/\gamma_\beta^\perp}{2} P_R\big) \\
&\quad + \big(2P_R \bar{n}\!\!\!/ T^b\big)\otimes\big(\frac{n\!\!\!/}{2} P_R T^b\big) + \big(-P_R \bar{n}\!\!\!/\gamma_\perp^\beta T^b\big)\otimes\big(\frac{n\!\!\!/\gamma_\beta^\perp}{2} P_R T^b\big)\Big]. \qquad (3.135)
\end{aligned}
$$

The vacuum matrix element of the collinear four-quark operator in Eq. (3.134) must be a colour singlet, implying that either $k, k' \in \{1,2\}$, so that both $F^{\bar{n}}$'s have no T^a's, or $k, k' \in \{3,4\}$ and the colour structure gets reduced when we take the matrix element, using $T^a \otimes T^b = T^A \otimes T^A\, \delta^{ab}/(N_c^2-1)$. Rotational invariance then implies that the matrix element gives $\delta_{k,k'}$ so we do the sum over k' and set $k = k'$. This leaves four terms in $[\bar{\chi}_n F_{k'}^{\bar{n}L} \chi_n^L][\bar{\chi}_n^L F_k^{R\bar{n}} \chi_n]$:

$$
\begin{aligned}
&\big[F_k^{\bar{n}L}\big] \otimes \big[F_k^{R\bar{n}}\big] = \delta_{k1}\big[\frac{\bar{n}\!\!\!/}{N_c} P_L\big] \otimes \big[\frac{\bar{n}\!\!\!/}{N_c} P_L\big] + \delta_{k2} \frac{(g_{\alpha\beta}^\perp + i\epsilon_{\alpha\beta}^\perp)}{2} \big[\frac{\bar{n}\!\!\!/\gamma_\perp^\lambda}{2N_c} P_L\big] \otimes \big[\frac{\bar{n}\!\!\!/\gamma_\lambda^\perp}{2N_c} P_R\big] \\
&+ \delta_{k3} \frac{4\delta^{ab}}{(N_c^2-1)} \big[\bar{n}\!\!\!/ P_L T^A\big] \otimes \big[\bar{n}\!\!\!/ P_L T^A\big] + \delta_{k4} \frac{(g_{\alpha\beta}^\perp + i\epsilon_{\alpha\beta}^\perp)}{2} \frac{4\delta^{ab}}{N_c^2-1} \big[\frac{\bar{n}\!\!\!/\gamma_\perp^\lambda}{2} P_L T^A\big] \otimes \big[\frac{\bar{n}\!\!\!/\gamma_\lambda^\perp}{2} P_R T^A\big].
\end{aligned} \qquad (3.136)
$$

When we use Eq. (3.73) to reduce the Dirac structure between the heavy quark fields in Eq. (3.134), and take into account the δ^{ab}'s from Eq. (3.136), the usoft operators become

$$
\begin{aligned}
&\frac{1}{4}\sum_{k''=1}^{2} \mathrm{Tr}\Big[P_{k''}^H \bar{\Gamma}_{j'}^{(0)} F_k^{Ln} \gamma_\perp^\sigma \gamma_\perp^\tau \frac{\bar{n}\!\!\!/}{2} F_k^{nR} \Gamma_j^{(0)}\Big]\Big[\bar{\mathcal{H}}_v(x) F_{k''}^h \big(i\mathcal{D}_{us}^{\perp\sigma} i\mathcal{D}_{us}^{\perp\tau}\big)(y) \mathcal{H}_v(0)\Big], \qquad (3.137) \\
&\frac{1}{4}\sum_{k''=1}^{2} \mathrm{Tr}\Big[P_{k''}^H \bar{\Gamma}_{j'}^{(0)} F_k^{Ln} \gamma_\perp^\sigma \gamma_\perp^\tau \frac{\bar{n}\!\!\!/}{2} F_k^{nR} \Gamma_j^{(0)}\Big]\Big[\bar{\mathcal{H}}_v(x) F_{k''}^h T^A \big(i\mathcal{D}_{us}^{\perp\sigma} i\mathcal{D}_{us}^{\perp\tau}\big)(y) T^A \mathcal{H}_v(0)\Big],
\end{aligned}
$$

for $k \in \{1,2\}$ and $k \in \{3,4\}$, respectively. The spin-trace that occurs in both terms

can be simplified with $\gamma_\perp^\sigma \gamma_\perp^\tau \not{\bar{n}} = (g_\perp^{\sigma\tau} - i\epsilon_\perp^{\sigma\tau}\gamma_5)\not{\bar{n}}$ and $\not{n}\gamma_\perp^\alpha \gamma_\perp^\beta = \not{n}(g_\perp^{\alpha\beta} - i\epsilon_\perp^{\alpha\beta}\gamma_5)$:

$$\begin{aligned}\mathrm{Tr}\Big[P_{k''}^H \overline{\Gamma}_{j'}^{(0)} F_k^{Ln} \gamma_\perp^\sigma \gamma_\perp^\tau \frac{\not{\bar{n}}}{2} F_k^{nR} \Gamma_j^{(0)}\Big] &= \Big[(\delta_{k1}+\delta_{k3})(g_\perp^{\sigma\tau} - i\epsilon_\perp^{\sigma\tau}) \\ &+(\delta_{k2}+\delta_{k4})(g_\perp^{\sigma\tau} + i\epsilon_\perp^{\sigma\tau})(g_\perp^{\alpha\beta} - i\epsilon_\perp^{\alpha\beta})\Big] \mathrm{Tr}\Big[P_{k''}^H \overline{\Gamma}_{j'}^{(0)} \frac{\not{n}}{2} P_R \Gamma_j^{(0)}\Big]. \quad (3.138)\end{aligned}$$

The $(g_\perp^{\alpha\beta} - i\epsilon_\perp^{\alpha\beta})$ terms contract with the $(g_{\alpha\beta}^\perp + i\epsilon_{\alpha\beta}^\perp)/2$'s in Eq. (3.136) to give a 2.

From Eq. (3.136) there are four jet functions:

$$\begin{aligned}&\Big\langle 0\Big|\Big[\bar{\chi}_n(y)\frac{\not{\bar{n}}P_L}{N_c}\chi_{n,\omega'}^L(x)\Big]\Big[\bar{\chi}_{n,\omega}^L(0)\frac{\not{\bar{n}}P_L}{N_c}\frac{1}{\overline{\mathcal{P}}}\chi_n(y)\Big]\Big|0\Big\rangle \quad (3.139)\\ &\quad = \frac{-4\delta(\omega-\omega')}{\omega}\,\delta^2(x_\perp)\delta(x^+)\delta^2(y_\perp)\delta(y^+)\int\frac{dk_1^+\,dk_2^+}{(2\pi)^2}\,e^{-\frac{i}{2}[k_2^+x^- + (k_1^+-k_2^+)y^-]}\mathcal{J}_{1\omega}^{(-2)}(k_j^+),\\ &2\Big\langle 0\Big|\Big[\bar{\chi}_n(y)\frac{\not{\bar{n}}\gamma_\perp^\lambda}{2N_c}\chi_{n,\omega'}^L(x)\Big]\Big[\bar{\chi}_{n,\omega}^L(0)\frac{\not{\bar{n}}\gamma_\lambda^\perp}{2N_c}\frac{1}{\overline{\mathcal{P}}}\chi_n(y)\Big]\Big|0\Big\rangle\\ &\quad = \frac{-4\delta(\omega-\omega')}{\omega}\,\delta^2(x_\perp)\delta(x^+)\delta^2(y_\perp)\delta(y^+)\int\frac{dk_1^+\,dk_2^+}{(2\pi)^2}\,e^{-\frac{i}{2}[k_2^+x^- + (k_1^+-k_2^+)y^-]}\mathcal{J}_{2\omega}^{(-2)}(k_j^+),\\ &\frac{4}{(N_c^2-1)}\Big\langle 0\Big|\Big[\bar{\chi}_n(y)\not{\bar{n}}P_L T^A\chi_{n,\omega'}^L(x)\Big]\Big[\bar{\chi}_{n,\omega}^L(0)\not{\bar{n}}P_L T^A\frac{1}{\overline{\mathcal{P}}}\chi_n(y)\Big]\Big|0\Big\rangle\\ &\quad = \frac{-4\delta(\omega-\omega')}{\omega}\,\delta^2(x_\perp)\delta(x^+)\delta^2(y_\perp)\delta(y^+)\int\frac{dk_1^+\,dk_2^+}{(2\pi)^2}\,e^{-\frac{i}{2}[k_2^+x^- + (k_1^+-k_2^+)y^-]}\mathcal{J}_{3\omega}^{(-2)}(k_j^+),\\ &\frac{2}{(N_c^2-1)}\Big\langle 0\Big|\Big[\bar{\chi}_n(y)\not{\bar{n}}\gamma_\perp^\lambda P_L T^A\chi_{n,\omega'}^L(x)\Big]\Big[\bar{\chi}_{n,\omega}^L(0)\not{\bar{n}}\gamma_\lambda^\perp P_R T^A\frac{1}{\overline{\mathcal{P}}}\chi_n(y)\Big]\Big|0\Big\rangle\\ &\quad = \frac{-4\delta(\omega-\omega')}{\omega}\,\delta^2(x_\perp)\delta(x^+)\delta^2(y_\perp)\delta(y^+)\int\frac{dk_1^+\,dk_2^+}{(2\pi)^2}\,e^{-\frac{i}{2}[k_2^+x^- + (k_1^+-k_2^+)y^-]}\mathcal{J}_{4\omega}^{(-2)}(k_j^+).\end{aligned}$$

At tree level, only $\mathcal{J}_{1\omega}^{(-2)}$ is non-zero. It has the value

$$\mathcal{J}_{1\omega}^{(-2)}(n\cdot k_1, n\cdot k_2) = \frac{1}{[n\cdot k_1 + i\epsilon]}\frac{1}{[n\cdot k_2 + i\epsilon]}. \quad (3.140)$$

At one-loop order, $\mathcal{J}_{3\omega}^{(-2)}$ will become non-zero, while $\mathcal{J}_{2\omega}^{(-2)}$ and $\mathcal{J}_{4\omega}^{(-2)}$ are non-zero only at two-loop order. The expansion here is in α_s at the jet scale, $\mu^2 \sim m_\chi^2$. We denote the imaginary parts by

$$\mathcal{J}_j^{(-2)} = \Big(\frac{-1}{\pi}\Big)\,\mathrm{Im}\,\mathcal{J}_{j\omega}^{(-2)}. \quad (3.141)$$

Eqs. (3.136) and (3.138) also show that if we work at any order in α_s there are four shape functions generated by $T^{(2L)}$, i.e.

$$
\begin{aligned}
&(g_{\sigma\tau}^{\perp} - i\epsilon_{\sigma\tau}^{\perp}) \int \frac{dx^- dy^-}{32\pi^2} e^{-\frac{i}{2}[x^-\ell_2^+ + y^-\ell_1^+]} \, \langle \bar{B}_v | \bar{\mathcal{H}}_v(\tilde{x}) F_{k''}^h \big(iD_{us}^{\perp\sigma} iD_{us}^{\perp\tau}\big)(\tilde{y}) \mathcal{H}_v(0) | \bar{B}_v \rangle \\
&\quad = \delta_{k''1} \, f_3(\ell_1^+, \ell_2^+) + \delta_{k''2} \left(v_\eta - \frac{n_\eta}{n\cdot v}\right) f_4(\ell_1^+, \ell_2^+) \,, \\
&(g_{\sigma\tau}^{\perp} - i\epsilon_{\sigma\tau}^{\perp}) \int \frac{dx^- dy^-}{32\pi^2} e^{-\frac{i}{2}[x^-\ell_2^+ + y^-\ell_1^+]} \, \langle \bar{B}_v | \bar{\mathcal{H}}_v(\tilde{x}) F_{k''}^h T^A \big(iD_{us}^{\perp\sigma} iD_{us}^{\perp\tau}\big)(\tilde{y}) T^A \mathcal{H}_v(0) | \bar{B}_v \rangle \\
&\quad = \delta_{k''1} \, g_3(\ell_1^+, \ell_2^+) + \delta_{k''2} \left(v_\eta - \frac{n_\eta}{n\cdot v}\right) g_4(\ell_1^+, \ell_2^+) \,, \\
&(g_{\sigma\tau}^{\perp} + i\epsilon_{\sigma\tau}^{\perp}) \int \frac{dx^- dy^-}{32\pi^2} e^{-\frac{i}{2}[x^-\ell_2^+ + y^-\ell_1^+]} \, \langle \bar{B}_v | \bar{\mathcal{H}}_v(\tilde{x}) F_{k''}^h \big(iD_{us}^{\perp\sigma} iD_{us}^{\perp\tau}\big)(\tilde{y}) \mathcal{H}_v(0) | \bar{B}_v \rangle \\
&\quad = \delta_{k''1} \, f_3(\ell_1^+, \ell_2^+) - \delta_{k''2} \left(v_\eta - \frac{n_\eta}{n\cdot v}\right) f_4(\ell_1^+, \ell_2^+) \,, \\
&(g_{\sigma\tau}^{\perp} + i\epsilon_{\sigma\tau}^{\perp}) \int \frac{dx^- dy^-}{32\pi^2} e^{-\frac{i}{2}[x^-\ell_2^+ + y^-\ell_1^+]} \, \langle \bar{B}_v | \bar{\mathcal{H}}_v(\tilde{x}) F_{k''}^h T^A \big(iD_{us}^{\perp\sigma} iD_{us}^{\perp\tau}\big)(\tilde{y}) T^A \mathcal{H}_v(0) | \bar{B}_v \rangle \\
&\quad = \delta_{k''1} \, g_3(\ell_1^+, \ell_2^+) - \delta_{k''2} \left(v_\eta - \frac{n_\eta}{n\cdot v}\right) g_4(\ell_1^+, \ell_2^+) \,. \qquad (3.142)
\end{aligned}
$$

Here the index η is from $F_2^h = P_v \gamma_\eta^T \gamma_5 P_v$. At tree level in the jet function, only the first of these four combinations occurs. The functions $f_{3,4}$ were defined in Eq. (3.119). The definitions of $g_{3,4}$ are

$$
\begin{aligned}
\langle \bar{B}_v | O_7^{\alpha\beta}(\ell^+) | \bar{B}_v \rangle &= g_\perp^{\alpha\beta} \, g_3^{(4)}(\ell_1^+, \ell_2^+) \,, \\
\langle \bar{B}_v | P_{7\lambda}^{\alpha\beta}(\ell^+) | \bar{B}_v \rangle &= -\epsilon_\perp^{\alpha\beta} \left(v_\lambda - \frac{n_\lambda}{n\cdot v}\right) g_4^{(4)}(\ell_1^+, \ell_2^+) \,, \qquad (3.143)
\end{aligned}
$$

where

$$
\begin{aligned}
O_7^{\alpha\beta}(\ell_1^+, \ell_2^+) &= \int \frac{dx^- \, dy^-}{32\pi^2} e^{-\frac{i}{2}\ell_2 x^-} e^{-\frac{i}{2}(\ell_1^+ - \ell_2^+) y^-} \left[\overline{\mathcal{H}}_v(\tilde{x}) T^A \{iD_{us}^{\perp\alpha}, iD_{us}^{\perp\beta}\}(\tilde{y}) T^A \mathcal{H}_v(0)\right] , \\
P_{7\lambda}^{\alpha\beta}(\ell_1^+, \ell_2^+) &= i \int \frac{dx^- \, dy^-}{32\pi^2} e^{-\frac{i}{2}\ell_2 x^-} e^{-\frac{i}{2}(\ell_1^+ - \ell_2^+) y^-} \left[\overline{\mathcal{H}}_v(\tilde{x}) T^A [iD_{us}^{\perp\alpha}, iD_{us}^{\perp\beta}](\tilde{y}) T^A \gamma_\lambda^T \gamma_5 \, \mathcal{H}_v(0)\right] .
\end{aligned}
\qquad (3.144)
$$

The hard coefficients can now be defined to be

$$h_i^{[2L]3} = -\frac{m_b}{\bar{n}\cdot p}\sum_{j,j'} C_{j'}\,C_j\,\mathrm{Tr}\Big\{\frac{P_v}{2}\overline{\Gamma}_{j'}^{(0)}\,\frac{\not{\bar{n}}}{2}P_R\Gamma_j^{(0)}\Big\}\,P_i^{\mu\nu} = -\frac{m_b}{\bar{n}\cdot p}\,h_i^0\,, \qquad (3.145)$$

$$h_i^{[2L]4} = \frac{m_b}{\bar{n}\cdot p}\sum_{j,j'} C_{j'}\,C_j\,\frac{n_\eta}{n\cdot v}\mathrm{Tr}\Big\{\frac{P_v}{2}\gamma_T^\eta\gamma_5 P_v\overline{\Gamma}_{j'}^{(0)}\,\frac{\not{\bar{n}}}{2}P_R\Gamma_j^{(0)}\Big\}\,P_i^{\mu\nu}\,.$$

Combining equations, we get the final result for the $T^{(2L)}$ contributions:

$$\begin{aligned} W_i^{(2L)} &= \frac{h_i^{[2L]3}(\bar{n}\cdot p, m_b)}{m_b}\int dk_1^+ dk_2^+\Big\{\big[\mathcal{J}_1^{(-2)}(\bar{n}\cdot p\,k_j^+) + \mathcal{J}_2^{(-2)}(\bar{n}\cdot p\,k_j^+)\big]\,f_3(k_j^+ + r^+) \\ &\qquad + \big[\mathcal{J}_3^{(-2)}(\bar{n}\cdot p\,k_j^+) + \mathcal{J}_4^{(-2)}(\bar{n}\cdot p\,k_j^+)\big]\,g_3(k_j^+ + r^+)\Big\} \\ &+ \frac{h_i^{[2L]4}(\bar{n}\cdot p, m_b)}{m_b}\int dk_1^+ dk_2^+\Big\{\big[\mathcal{J}_1^{(-2)}(\bar{n}\cdot p\,k_j^+) - \mathcal{J}_2^{(-2)}(\bar{n}\cdot p\,k_j^+)\big]\,f_4(k_j^+ + r^+) \\ &\qquad + \big[\mathcal{J}_3^{(-2)}(\bar{n}\cdot p\,k_j^+) - \mathcal{J}_4^{(-2)}(\bar{n}\cdot p\,k_j^+)\big]\,g_4(k_j^+ + r^+)\Big\}\,. \qquad (3.146) \end{aligned}$$

Explicit results for the hard coefficients $h_i^{[2L]}$ are summarized in Sec. 3.6.6.

Calculation of $T^{(2q)}$

For $T^{(2q)}$ the heavy-to-light currents are also identical to those in Eq. (3.65), but now we have two insertions of the Lagrangian $\mathcal{L}_{\xi q}^{(1)}$, i.e.

$$\hat{T}_{\mu\nu}^{(2q)} = -\frac{i}{2}\sum_{j,j'} C_{j'}(\bar{n}\cdot p)C_j(\bar{n}\cdot p)\int d^4x\int d^4y\,e^{-ir\cdot x}\,\mathrm{T}\big[J_{j'\mu}^{(0)\dagger}(\bar{n}\cdot p, x)\,\mathcal{L}_{\xi q}^{(1)}(y)\,\mathcal{L}_{\xi q}^{(1)}(z)\,J_{j\nu}^{(0)}(\bar{n}\cdot p, 0)\big]\,. \qquad (3.147)$$

Owing to the hermitian-conjugate terms in each $\mathcal{L}_{\xi q}^{(1)}$, there are two ways to generate the four-quark operator shown in Table 3.4, where the positions in the figure are labeled either $0-z-y-x$ or $0-y-z-x$. This average over $z \leftrightarrow y$ cancels the $1/2$ in the definition of $T^{(2q)}$. Fierz transforming the product of operators with

Eq. (3.135) in order to group the collinear and usoft fields, we have

$$
\begin{aligned}
&J_{j'}^{(0)\dagger}(x)\mathcal{L}_{\xi q}^{(1)}(y)\mathcal{L}_{\xi q}^{(1)}(z)J_j^{(0)}(0) \qquad (3.148)\\
&= \big[\bar{\mathcal{H}}_v\overline{\Gamma}_{j'}^{(0)}\chi_{n,\omega'}^L\big](x)\Big[\bar{\chi}_n ig\not{\mathcal{B}}_c^\perp\psi_{us}\Big](y)\Big[\bar{\psi}_{us}\big(-ig\not{\mathcal{B}}_c^\perp\big)\chi_n\Big](z)\big[\bar{\chi}_{n,\omega}^L\Gamma_j^{(0)}\mathcal{H}_v\big](0)\\
&= \frac{1}{4}\sum_{k,k'=1}^{4}\Big[\Big(\bar{\chi}_n ig\not{\mathcal{B}}_\perp^c\Big)(y)F_{k'}^{\bar{n}L}\chi_{n,\omega'}^L(x)\Big]\bar{\chi}_{n,\omega}^L(0)F_k^{R\bar{n}}\Big(-ig\not{\mathcal{B}}_\perp^c\chi_n\Big)(z)\\
&\quad\times\big[\bar{\mathcal{H}}_v(x)\overline{\Gamma}_{j'}^{(0)}F_{k'}^{Ln}\psi_{us}(y)\big]\big[\bar{\psi}_{us}(z)F_k^{nR}\Gamma_j^{(0)}\mathcal{H}_v(0)\big] + (y\leftrightarrow z)\,.
\end{aligned}
$$

The vacuum matrix element of the collinear operator must be a colour singlet, so either $k,k'\in\{1,2\}$ or $k,k'\in\{3,4\}$, and then rotational invariance implies that $k=k'$. This leaves four non-trivial collinear operators, which are given by

$$
\Big[\Big(\bar{\chi}_n ig\not{\mathcal{B}}_\perp^c\Big)(y)F_k^{\bar{n}L}\chi_{n,\omega'}^L(x)\Big]\bar{\chi}_{n,\omega}^L(0)F_k^{R\bar{n}}\Big(-ig\not{\mathcal{B}}_\perp^c\chi_n\Big)(z)\,, \qquad (3.149)
$$

with the decomposition of $F_k^{\bar{n}L}\otimes F_k^{R\bar{n}}$ given by exactly Eq. (3.136). For the usoft operators we always have $\not{n}\psi_{us}=\not{n}\psi_{us}^{\bar{n}}$, so this projects on to two components of the light quark fields given by $\psi_{us}^{\bar{n}}$ with $\not{\bar{n}}\psi_{us}^{\bar{n}}=0$. The Dirac structure can therefore be simplified by noting that

$$
\begin{aligned}
\bar{\psi}_{us}^{\bar{n}}P_{L,R}\Gamma\mathcal{H}_v &= \mathrm{Tr}\big[\not{\bar{n}}P_{L,R}\Gamma P_v\big]\bar{\psi}_{us}^{\bar{n}}P_{L,R}\frac{\not{n}}{2}\mathcal{H}_v + \mathrm{Tr}\big[\gamma_\sigma^\perp\frac{\not{n}\not{\bar{n}}}{4}\Gamma P_v\big]\bar{\psi}_{us}^{\bar{n}}P_{L,R}\gamma_\perp^\sigma\mathcal{H}_v\,,\\
\bar{\mathcal{H}}_v\Gamma P_{R,L}\psi_{us}^{\bar{n}} &= \mathrm{Tr}\big[\Gamma P_{R,L}\not{\bar{n}}P_v\big]\bar{\mathcal{H}}_v\frac{\not{n}}{2}P_{R,L}\psi_{us}^{\bar{n}} + \mathrm{Tr}\big[\Gamma\frac{\not{\bar{n}}\not{n}}{4}\gamma_\tau^\perp P_v\big]\bar{\mathcal{H}}_v\gamma_\perp^\tau P_{R,L}\psi_{us}^{\bar{n}}\,, \qquad (3.150)
\end{aligned}
$$

and using rotational invariance of the usoft matrix element to determine that $\gamma_\perp^\sigma$ and $\gamma_\perp^\tau$ terms are restricted to appearing together. Thus $\big[\bar{\mathcal{H}}_v\overline{\Gamma}_{j'}^{(0)}F_k^{Ln}\psi_{us}\big]\big[\bar{\psi}_{us}F_k^{nR}\Gamma_j^{(0)}\mathcal{H}_v\big]$

together with the $(g_{\alpha\beta}^{\perp}+i\epsilon_{\alpha\beta}^{\perp})/2$ factor from Eq. (3.136) gives

$$
\begin{aligned}
&\delta_{k1}\Big\{ \mathrm{Tr}\Big[\overline{\Gamma}_{j'}^{(0)}\frac{\bar{n}\!\!\!/}{2}P_R n\!\!\!/ P_v\Big]\mathrm{Tr}\Big[n\!\!\!/ P_L\frac{\bar{n}\!\!\!/}{2}\Gamma_j^{(0)}P_v\Big]\big[\bar{\mathcal{H}}_v\frac{\bar{n}\!\!\!/}{2}P_R\psi_{us}^{\bar{n}}\big]\big[\bar{\psi}_{us}\frac{n\!\!\!/}{2}P_R\mathcal{H}_v\big] \\
&\quad +\mathrm{Tr}\Big[\overline{\Gamma}_{j'}^{(0)}P_L\frac{\bar{n}\!\!\!/}{2}\gamma_\perp^\tau P_v\Big]\mathrm{Tr}\Big[\gamma_\perp^\sigma\frac{n\!\!\!/}{2}P_R\Gamma_j^{(0)}P_v\Big]\big[\bar{\mathcal{H}}_v\gamma_\tau^\perp P_R\psi_{us}^{\bar{n}}\big]\big[\bar{\psi}_{us}^{\bar{n}}\gamma_\sigma^\perp P_R\mathcal{H}_v\big]\Big\} \\
&-\delta_{k2}\frac{(g_{\alpha\beta}^{\perp}+i\epsilon_{\alpha\beta}^{\perp})}{2}\Big\{ \mathrm{Tr}\Big[\overline{\Gamma}_{j'}^{(0)}\frac{\bar{n}\!\!\!/ n\!\!\!/}{2}\gamma_\perp^\alpha P_R P_v\Big]\mathrm{Tr}\Big[\frac{\bar{n}\!\!\!/ n\!\!\!/}{2}\gamma_\perp^\beta P_R\Gamma_j^{(0)}P_v\Big]\big[\bar{\mathcal{H}}_v\frac{\bar{n}\!\!\!/}{2}P_L\psi_{us}^{\bar{n}}\big]\big[\bar{\psi}_{us}^{\bar{n}}\frac{n\!\!\!/}{2}P_L\mathcal{H}_v\big] \\
&\quad +\mathrm{Tr}\Big[\overline{\Gamma}_{j'}^{(0)}P_L\frac{\bar{n}\!\!\!/}{2}\gamma_\perp^\alpha\gamma_\perp^\tau P_v\Big]\mathrm{Tr}\Big[\frac{n\!\!\!/}{2}\gamma_\perp^\sigma\gamma_\perp^\beta P_R\Gamma_j^{(0)}P_v\Big]\big[\bar{\mathcal{H}}_v\gamma_\tau^\perp P_L\psi_{us}^{\bar{n}}\big]\big[\bar{\psi}_{us}^{\bar{n}}\gamma_\sigma^\perp P_L\mathcal{H}_v\big]\Big\} \\
&+\delta_{k3}\Big\{\cdots\Big\}+\delta_{k4}\Big\{\cdots\Big\}\,,
\end{aligned}
\tag{3.151}
$$

where the structures for the δ_{k3} (δ_{k4}) term are identical to those of δ_{k1} (δ_{k2}) except with extra $T^A\otimes T^A$ factors in the operators. Simplifying the Dirac structures and using rotational invariance of the $\langle\bar{B}_v|\cdots|\bar{B}_v\rangle$ matrix element gives

$$
\begin{aligned}
&\delta_{k1}\Big\{ \mathrm{Tr}\Big[\overline{\Gamma}_{j'}^{(0)}\frac{\bar{n}\!\!\!/ n\!\!\!/}{2}P_L P_v\Big]\mathrm{Tr}\Big[\frac{\bar{n}\!\!\!/ n\!\!\!/}{2}P_R\Gamma_j^{(0)}P_v\Big]\big[\bar{\mathcal{H}}_v\frac{\bar{n}\!\!\!/}{2}P_R\psi_{us}^{\bar{n}}\big]\big[\bar{\psi}_{us}^{\bar{n}}\frac{n\!\!\!/}{2}P_R\mathcal{H}_v\big] \\
&\quad +\mathrm{Tr}\Big[\overline{\Gamma}_{j'}^{(0)}\frac{\bar{n}\!\!\!/}{2}\gamma_\perp^\tau P_L P_v\Big]\mathrm{Tr}\Big[\gamma_\perp^\tau\frac{n\!\!\!/}{2}P_R\Gamma_j^{(0)}P_v\Big]\big[\bar{\mathcal{H}}_v\gamma_\sigma^\perp P_R\psi_{us}^{\bar{n}}\big]\big[\bar{\psi}_{us}^{\bar{n}}\gamma_\perp^\sigma P_R\mathcal{H}_v\big]\Big\} \\
&-\delta_{k2}\Big\{ \mathrm{Tr}\Big[\overline{\Gamma}_{j'}^{(0)}\frac{\bar{n}\!\!\!/ n\!\!\!/}{2}\gamma_\perp^\tau P_R P_v\Big]\mathrm{Tr}\Big[\frac{\bar{n}\!\!\!/ n\!\!\!/}{2}\gamma_\tau^\perp P_R\Gamma_j^{(0)}P_v\Big]\big[\bar{\mathcal{H}}_v\frac{\bar{n}\!\!\!/}{2}P_L\psi_{us}^{\bar{n}}\big]\big[\bar{\psi}_{us}^{\bar{n}}\frac{n\!\!\!/}{2}P_L\mathcal{H}_v\big] \\
&\quad +\mathrm{Tr}\Big[\overline{\Gamma}_{j'}^{(0)}n\!\!\!/ P_R P_v\Big]\mathrm{Tr}\Big[n\!\!\!/ P_R\Gamma_j^{(0)}P_v\Big]\big[\bar{\mathcal{H}}_v\gamma_\sigma^\perp P_L\psi_{us}^{\bar{n}}\big]\big[\bar{\psi}_{us}^{\bar{n}}\gamma_\perp^\sigma P_L\mathcal{H}_v\big]\Big\} \\
&+\delta_{k3}\Big\{\cdots\Big\}+\delta_{k4}\Big\{\cdots\Big\}\,.
\end{aligned}
\tag{3.152}
$$

From Eq. (3.149) the jet functions are

$$
\begin{aligned}
&\frac{4}{N_c^2-1}\Big\langle 0\Big|\big[\bar{\chi}_n g\mathcal{B}_\perp^c\big](y)\frac{\bar{n}\!\!\!/\gamma_\alpha^\perp P_L T^A}{2}\chi_{n,\omega'}^L(x)\bar{\chi}_{n,\omega}^L(0)\frac{\bar{n}\!\!\!/\gamma_\perp^\alpha P_L T^A}{2}\big[g\mathcal{B}_\perp^c\chi_n\big](z)\Big|0\Big\rangle \\
&\quad=\frac{4iN_\delta}{\omega}\int\frac{dk_1^+\,dk_2^+\,dk_3^+}{(2\pi)^3}\,e^{-\frac{i}{2}[k_3^+x^-+(k_2^+-k_3^+)y^-+(k_1^+-k_2^+)z^-]}\,\mathcal{J}_{1\omega}^{(-4)}(k_j^+)\,, \\
&\Big\langle 0\Big|\big[\bar{\chi}_n g\mathcal{B}_\perp^c\big](y)\frac{\bar{n}\!\!\!/\gamma_\alpha^\perp P_L}{2N_c}\chi_{n,\omega'}^L(x)\bar{\chi}_{n,\omega}^L(0)\frac{\bar{n}\!\!\!/\gamma_\perp^\alpha P_L}{2N_c}\big[g\mathcal{B}_\perp^c\chi_n\big](z)\Big|0\Big\rangle \\
&\quad=\frac{4iN_\delta}{\omega}\int\frac{dk_1^+\,dk_2^+\,dk_3^+}{(2\pi)^3}\,e^{-\frac{i}{2}[k_3^+x^-+(k_2^+-k_3^+)y^-+(k_1^+-k_2^+)z^-]}\,\mathcal{J}_{2\omega}^{(-4)}(k_j^+)\,,
\end{aligned}
$$

$$\frac{4}{N_c^2-1}\Big\langle 0\Big|\big[\bar{\chi}_n g\not{\mathcal{B}}^c_\perp\big](y)\bar{\not{n}}P_L T^A\chi^L_{n,\omega'}(x)\bar{\chi}^L_{n,\omega}(0)\bar{\not{n}}P_L T^A\big[g\not{\mathcal{B}}^c_\perp\chi_n\big](z)\Big|0\Big\rangle$$
$$= \frac{4iN_\delta}{\omega}\int\frac{dk_1^+\,dk_2^+\,dk_3^+}{(2\pi)^3}\,e^{-\frac{i}{2}[k_3^+x^-+(k_2^+-k_3^+)y^-+(k_1^+-k_2^+)z^-]}\;\mathcal{J}^{(-4)}_{3\omega}(k_j^+)\,,$$
$$\Big\langle 0\Big|\big[\bar{\chi}_n g\not{\mathcal{B}}^c_\perp\big](y)\frac{\bar{\not{n}}P_L}{N_c}\chi^L_{n,\omega'}(x)\bar{\chi}^L_{n,\omega}(0)\frac{\bar{\not{n}}P_L}{N_c}\big[g\not{\mathcal{B}}^c_\perp\chi_n\big](z)\Big|0\Big\rangle$$
$$= \frac{4iN_\delta}{\omega}\int\frac{dk_1^+\,dk_2^+\,dk_3^+}{(2\pi)^3}\,e^{-\frac{i}{2}[k_3^+x^-+(k_2^+-k_3^+)y^-+(k_1^+-k_2^+)z^-]}\;\mathcal{J}^{(-4)}_{4\omega}(k_j^+)\,, \quad (3.153)$$

where the common prefactor is $N_\delta = \delta(\omega\text{–}\omega')\delta^2(x_\perp)\delta(x^+)\delta^2(y_\perp)\delta(y^+)\delta^2(z_\perp)\delta(z^+)$ and the $1/\bar{\mathcal{P}}$ factors in the operators do not act outside the square brackets. At tree level, only $\mathcal{J}^{(-4)}_{1\omega}(k_j^+)$ is non-zero. It has the value

$$\mathcal{J}^{(-4)}_{1\omega}(n\cdot k_1, n\cdot k_2, n\cdot k_3) = \frac{1}{[n\cdot k_1+i\epsilon][n\cdot k_2+i\epsilon][n\cdot k_3+i\epsilon]}\,. \quad (3.154)$$

As before, we denote the imaginary parts by

$$\mathcal{J}^{(-4)}_j = \left(\frac{-1}{\pi}\right)\text{Im}\;\mathcal{J}^{(-4)}_{j\omega}\,. \quad (3.155)$$

From Eq. (3.152) there are eight shape functions with different Dirac and colour

structures, namely

$$\int\frac{dx^-dy^-dz^-}{128\pi^3}e^{-\frac{i}{2}\{\ell_3^+x^-+(\ell_2^+-\ell_3^+)y^-+(\ell_1^+-\ell_2^+)z^-\}}\langle\bar{B}_v|\bar{\mathcal{H}}_v(\tilde{x})\,\bar{n}\!\!\!/P_R\psi_{us}^{\bar{n}}(\tilde{y})\bar{\psi}_{us}^{\bar{n}}(\tilde{z})\,\bar{n}\!\!\!/P_R\mathcal{H}_v(0)|\bar{B}_v\rangle$$
$$=g_9(\ell_1^+,\ell_2^+,\ell_2^+)\,,$$
$$2\int\frac{dx^-dy^-dz^-}{128\pi^3}e^{-\frac{i}{2}\{\ell_3^+x^-+(\ell_2^+-\ell_3^+)y^-+(\ell_1^+-\ell_2^+)z^-\}}\langle\bar{B}_v|\bar{\mathcal{H}}_v(\tilde{x})\gamma_\perp^\eta P_R\psi_{us}^{\bar{n}}(\tilde{y})\bar{\psi}_{us}^{\bar{n}}(\tilde{z})\gamma_\eta^\perp P_R\mathcal{H}_v(0)|\bar{B}_v\rangle$$
$$=g_{10}(\ell_1^+,\ell_2^+,\ell_2^+)\,,$$
$$\int\frac{dx^-dy^-dz^-}{128\pi^3}e^{-\frac{i}{2}\{\ell_3^+x^-+(\ell_2^+-\ell_3^+)y^-+(\ell_1^+-\ell_2^+)z^-\}}\langle\bar{B}_v|\bar{\mathcal{H}}_v(\tilde{x})\,\bar{n}\!\!\!/P_L\psi_{us}^{\bar{n}}(\tilde{y})\bar{\psi}_{us}^{\bar{n}}(\tilde{z})\,\bar{n}\!\!\!/P_L\mathcal{H}_v(0)|\bar{B}_v\rangle$$
$$=g_5(\ell_1^+,\ell_2^+,\ell_2^+)\,,$$
$$2\int\frac{dx^-dy^-dz^-}{128\pi^3}e^{-\frac{i}{2}\{\ell_3^+x^-+(\ell_2^+-\ell_3^+)y^-+(\ell_1^+-\ell_2^+)z^-\}}\langle\bar{B}_v|\bar{\mathcal{H}}_v(\tilde{x})\gamma_\perp^\eta P_L\psi_{us}^{\bar{n}}(\tilde{y})\bar{\psi}_{us}^{\bar{n}}(\tilde{z})\gamma_\eta^\perp P_L\mathcal{H}_v(0)|\bar{B}_v\rangle$$
$$=g_6(\ell_1^+,\ell_2^+,\ell_2^+)\,,$$
$$\int\frac{dx^-dy^-dz^-}{128\pi^3}e^{-\frac{i}{2}[\,\cdots\,]}\langle\bar{B}_v|\bar{\mathcal{H}}_v(\tilde{x})\,\bar{n}\!\!\!/P_RT^A\psi_{us}^{\bar{n}}(\tilde{y})\bar{\psi}_{us}^{\bar{n}}(\tilde{z})\,\bar{n}\!\!\!/P_RT^A\mathcal{H}_v(0)|\bar{B}_v\rangle$$
$$=g_7(\ell_1^+,\ell_2^+,\ell_2^+)\,,$$
$$2\int\frac{dx^-dy^-dz^-}{128\pi^3}e^{-\frac{i}{2}[\,\cdots\,]}\langle\bar{B}_v|\bar{\mathcal{H}}_v(\tilde{x})\gamma_\perp^\eta P_RT^A\psi_{us}^{\bar{n}}(\tilde{y})\bar{\psi}_{us}^{\bar{n}}(\tilde{z})\gamma_\eta^\perp P_RT^A\mathcal{H}_v(0)|\bar{B}_v\rangle$$
$$=g_8(\ell_1^+,\ell_2^+,\ell_2^+)\,,$$
$$\int\frac{dx^-dy^-dz^-}{128\pi^3}e^{-\frac{i}{2}[\,\cdots\,]}\langle\bar{B}_v|\bar{\mathcal{H}}_v(\tilde{x})\,\bar{n}\!\!\!/P_LT^A\psi_{us}^{\bar{n}}(\tilde{y})\bar{\psi}_{us}^{\bar{n}}(\tilde{z})\,\bar{n}\!\!\!/P_LT^A\mathcal{H}_v(0)|\bar{B}_v\rangle$$
$$=f_5(\ell_1^+,\ell_2^+,\ell_2^+)\,,$$
$$2\int\frac{dx^-dy^-dz^-}{128\pi^3}e^{-\frac{i}{2}[\,\cdots\,]}\langle\bar{B}_v|\bar{\mathcal{H}}_v(\tilde{x})\gamma_\perp^\eta P_LT^A\psi_{us}^{\bar{n}}(\tilde{y})\bar{\psi}_{us}^{\bar{n}}(\tilde{z})\gamma_\eta^\perp P_LT^A\mathcal{H}_v(0)|\bar{B}_v\rangle$$
$$=f_6(\ell_1^+,\ell_2^+,\ell_2^+)\,, \tag{3.156}$$

where $\psi_{us}^{\bar{n}}=(\bar{n}\!\!\!/n\!\!\!/)/4\,\psi_{us}$ and the ellipses denote exactly the same exponent as in the preceding expressions. Only the last two of these shape functions show up when we work at tree level in the jet functions.

We define the hard coefficients to be

$$
\begin{aligned}
h_i^{[2q]5} &= \frac{1}{4}\frac{m_b}{\bar{n}\cdot p}\sum_{j,j'} C_{j'}\, C_j\, \mathrm{Tr}\Big\{ P_v \overline{\Gamma}_{j'}^{(0)}\, \frac{\not{\bar{n}}\not{n}}{2}\gamma_\perp^\tau P_R \Big\}\, \mathrm{Tr}\Big\{ P_v \frac{\not{\bar{n}}\not{n}}{2}\gamma_\tau^\perp P_R \Gamma_j^{(0)} \Big\} P_i^{\mu\nu}\,, \\
h_i^{[2q]6} &= \frac{1}{2}\frac{m_b}{\bar{n}\cdot p}\sum_{j,j'} C_{j'}\, C_j\, \mathrm{Tr}\Big\{ P_v \overline{\Gamma}_{j'}^{(0)}\, \not{n} P_R \Big\}\, \mathrm{Tr}\Big\{ P_v \not{n} P_R \Gamma_j^{(0)} \Big\} P_i^{\mu\nu}\,, \\
h_i^{[2q]7} &= \frac{1}{4}\frac{m_b}{\bar{n}\cdot p}\sum_{j,j'} C_{j'}\, C_j\, \mathrm{Tr}\Big\{ P_v \overline{\Gamma}_{j'}^{(0)}\, \frac{\not{\bar{n}}\not{n}}{2} P_L \Big\}\, \mathrm{Tr}\Big\{ P_v \frac{\not{\bar{n}}\not{n}}{2} P_R \Gamma_j^{(0)} \Big\} P_i^{\mu\nu}\,, \\
h_i^{[2q]8} &= \frac{1}{2}\frac{m_b}{\bar{n}\cdot p}\sum_{j,j'} C_{j'}\, C_j\, \mathrm{Tr}\Big\{ P_v \overline{\Gamma}_{j'}^{(0)}\, \frac{\not{n}}{2}\gamma_\tau^\perp P_L \Big\}\, \mathrm{Tr}\Big\{ P_v \gamma_\perp^\tau \frac{\not{n}}{2} P_R \Gamma_j^{(0)} \Big\} P_i^{\mu\nu}\,, \qquad (3.157)
\end{aligned}
$$

and the final result from the $T^{(2q)}$ contributions is then

$$
\begin{aligned}
W_i^{(2q)} = {} & \frac{h_i^{[2q]7}}{m_b}\int dk_1^+ dk_2^+ dk_3^+ \Big\{ \mathcal{J}_4^{(-4)}(\bar{n}\cdot p\, k_j^+) g_9(k_j^+ + r^+) + \mathcal{J}_3^{(-4)}(\bar{n}\cdot p\, k_j^+)\, g_7(k_j^+ + r^+) \Big\} \\
& + \frac{h_i^{[2q]8}}{m_b}\int dk_1^+ dk_2^+ dk_3^+ \Big\{ \mathcal{J}_4^{(-4)}(\bar{n}\cdot p\, k_j^+) g_{10}(k_j^+ + r^+) + \mathcal{J}_3^{(-4)}(\bar{n}\cdot p\, k_j^+)\, g_8(k_j^+ + r^+) \Big\} \\
& + \frac{h_i^{[2q]5}}{m_b}\int dk_1^+ dk_2^+ dk_3^+ \Big\{ \mathcal{J}_2^{(-4)}(\bar{n}\cdot p\, k_j^+) g_5(k_j^+ + r^+) + \mathcal{J}_1^{(-4)}(\bar{n}\cdot p\, k_j^+)\, f_5(k_j^+ + r^+) \Big\} \\
& + \frac{h_i^{[2q]6}}{m_b}\int dk_1^+ dk_2^+ dk_3^+ \Big\{ \mathcal{J}_2^{(-4)}(\bar{n}\cdot p\, k_j^+) g_6(k_j^+ + r^+) + \mathcal{J}_1^{(-4)}(\bar{n}\cdot p\, k_j^+)\, f_6(k_j^+ + r^+) \Big\}\,. \qquad (3.158)
\end{aligned}
$$

Explicit results for the hard coefficients $h_i^{[2q]5,6}$ are summarized in Sec. 3.6.6.

Calculation of $\hat{T}^{(2b)}$ and $\hat{T}^{(2c)}$

For later convenience we set

$$
B_j^{(1a)} J_j^{(1a)} + B_j^{(1b)} J_j^{(1b)} = \int d\omega_1 d\omega_2\, B_j^{(1)}(\omega_1,\omega_2)\; J_j^{(1)}(\omega_1,\omega_2)\,, \qquad (3.159)
$$

where

$$
J_j^{(1)}(\omega_1,\omega_2) = \frac{1}{m_b}\overline{\chi}_{n,\omega_1}(ig\mathcal{B}_{c\perp}^a)_{\omega_2}\, \Upsilon_{j\alpha}^{(1)}\, \mathcal{H}_v\,, \qquad (3.160)
$$

and $B_j^{(1)f}(\omega_1,\omega_2) = -B_j^{(1a)f}(\omega_1+\omega_2)\, m_b/(\omega_1+\omega_2)$ for j = 1–3 when $f = u$, and for j = 1–4 when $f = s$, and $B_j^{(1)f}(\omega_1,\omega_2) = B_j^{(1b)f}(\omega_1,\omega_2)/(n\cdot v)$ for the remaining j's.

Both $\hat{T}^{(2b)}$ and $\hat{T}^{(2c)}$ have jet functions that vanish at tree level but are non-zero at one-loop order. The steps are the same as in previous sections. Here we have

$$\begin{aligned}\hat{T}^{(2b)} \;=\; -i\sum_{j,j'}\int d\omega_1 d\omega_2 d\omega_3 d\omega_4\, B_j^{(1)}(\omega_{1,2}) B_{j'}^{(1)}(\omega_{3,4})\delta(\omega_3+\omega_4-\bar{n}\cdot p) \\ \times\int d^4x\, e^{-ir\cdot x}\;\mathrm{T}\big[J_{j'}^{(1)\dagger}(\omega_{3,4},x)\; J_j^{(1)}(\omega_{1,2},0)\big]\,. \qquad (3.161)\end{aligned}$$

To Fierz transform we can use

$$P_L\otimes P_R = \big(\frac{\not n}{2}P_R\big)\otimes\big(\frac{\bar{\not n}}{2N_c}P_L\big) + \big(\frac{\not n}{2}P_R T^a\big)\otimes\big(\bar{\not n}P_L T^a\big)\,, \qquad (3.162)$$

and we can drop the second term, since colour implies that it does not contribute in the matrix elements. Thus,

$$\begin{aligned}J_{j'}^{(1)\dagger}J_j^{(1)} \;&=\; \frac{-1}{2m_b^2}\mathrm{Tr}\Big[\frac{P_v}{2}\,\overline{\Upsilon}_{j'\alpha'}^{(1)}\frac{\not n}{2}P_R\Upsilon_{j\alpha}^{(1)}\Big]\Big[\bar{\mathcal{H}}_v(x)\mathcal{H}_v(0)\Big] \qquad (3.163)\\ &\quad\times\Big[\big(\bar{\chi}_{n,\omega_1}ig\mathcal{B}_{c,\omega_2}^{\perp\alpha}\big)(0)\frac{\bar{\not n}}{N_c}P_L\big(-ig\mathcal{B}_{c,\omega_4}^{\perp\alpha'}\chi_{n,\omega_3}\big)(x)\Big]\,,\end{aligned}$$

where we have used the fact that the second term in the reduction in Eq. (3.73) gives a vanishing matrix element. Between $\bar{B}$ mesons, the soft operator in Eq. (3.163) gives the leading-order shape function $f^{(0)}$. The matrix element of the collinear operator gives the jet functions

$$\begin{aligned}&\big\langle 0\big|\Big[\big(\bar{\chi}_{n,\omega_1}ig\mathcal{B}_{c,\omega_2}^{\perp\alpha}\big)(0)\frac{\bar{\not n}}{N_c}P_L\big(-ig\mathcal{B}_{c,\omega_4}^{\perp\alpha'}\chi_{n,\omega_3}\big)(x)\Big]\big|0\big\rangle \qquad (3.164)\\ &=\; (-2i)(\omega_1+\omega_2)\,\delta(\omega_1+\omega_2-\omega_3-\omega_4)\delta^2(x_\perp)\delta(x^+)\int\frac{dk^+}{2\pi}\,e^{-\frac{i}{2}k^+x^-}\\ &\quad\times\big[g_\perp^{\alpha\alpha'}\mathcal{J}_{1\omega_j}^{(2)}(k^+) + i\epsilon_\perp^{\alpha\alpha'}\mathcal{J}_{2\omega_j}^{(2)}(k^+)\big],\end{aligned}$$

and their imaginary parts are denoted by $\mathcal{J}_m^{(2)}(\omega_j k^+) = (-1/\pi)\mathrm{Im}\,\mathcal{J}_{m\omega_j}(k^+)$. Noting

the delta functions in Eqs. (3.161) and (3.164), we define the hard coefficients to be

$$
\begin{aligned}
h_i^{[2b]9}(z_1,z_2,\bar n\cdot p) &= \sum_{j,j'} B_{j'}^{(1)}(\omega_{3,4}) B_j^{(1)}(\omega_{1,2})\; g_\perp^{\alpha\alpha'}\,\frac{\bar n\cdot p}{m_b}\,\mathrm{Tr}\Big[\frac{P_v}{2}\,\overline{\Upsilon}^{(1)}_{j'\alpha'\mu}\,\frac{\bar{n}\!\!\!/}{2}\,\Upsilon^{(1)}_{j\alpha\nu}\Big] P_i^{\mu\nu}\,,\\
h_i^{[2b]10}(z_1,z_2,\bar n\cdot p) &= \sum_{j,j'} B_{j'}^{(1)}(\omega_{3,4}) B_j^{(1)}(\omega_{1,2})\; i\epsilon_\perp^{\alpha\alpha'}\,\frac{\bar n\cdot p}{m_b}\,\mathrm{Tr}\Big[\frac{P_v}{2}\,\overline{\Upsilon}^{(1)}_{j'\alpha'\mu}\,\frac{\bar{n}\!\!\!/}{2}\,\Upsilon^{(1)}_{j\alpha\nu}\Big] P_i^{\mu\nu}\,,
\end{aligned}
\tag{3.165}
$$

where $\omega_1 = z_1\bar n\cdot p$, $\omega_2 = (1-z_1)\bar n\cdot p$, $\omega_3 = z_2\bar n\cdot p$, $\omega_4 = (1-z_2)\bar n\cdot p$. This gives the factorization theorem

$$
\begin{aligned}
W_i^{(2b)} &= \int dz_1 dz_2\,\frac{h_i^{[2b]9}(z_1,z_2,\bar n\cdot p)}{m_b}\int_0^{p_X^+} dk^+\,\mathcal{J}_1^{(2)}(z_1,z_2,p_X^-\,k^+)\,f^{(0)}(k^+ + \overline{\Lambda} - p_X^+)\\
&+ \int dz_1 dz_2\,\frac{h_i^{[2b]10}(z_1,z_2,\bar n\cdot p)}{m_b}\int_0^{p_X^+} dk^+\,\mathcal{J}_2^{(2)}(z_1,z_2,p_X^-\,k^+)\,f^{(0)}(k^+ + \overline{\Lambda} - p_X^+).
\end{aligned}
\tag{3.166}
$$

For $\hat T^{(2c)}$ we have

$$
\begin{aligned}
\hat T^{(2c)} &= -i\sum_{j,j'}\sum_{\ell=c,d,e,f}\int[d\omega_n]\,\delta\big(\omega-\bar n\cdot p\big)\;C_{j'}(\omega)A_j^{(2\ell)}(\omega_n)\int d^4x\,e^{-ir\cdot x}\\
&\quad\times\mathrm{T}\left[J_{j'\mu}^{(0)\dagger}(\bar n\cdot p,x)\,J_{j\nu}^{(2\ell)}(\omega_n,0)+J_{j\mu}^{(2\ell)\dagger}(\omega_n,x)\,J_{j'\nu}^{(0)}(\bar n\cdot p,0)\right],
\end{aligned}
\tag{3.167}
$$

where we have $n=1$ for $\ell = c$ and $n = 1,2$ for $\ell = d,e,f$. For convenience we set $J_j^{(2\ell)}(\omega_n) = \overline{\mathcal{C}}^{(2\ell)}_{n,\omega_n}\Upsilon_j^{(2\ell)}\mathcal{H}_v$, so that $\mathcal{C}^{(2\ell)}$ contains the product of collinear fields in each current. Fierz transforming $\hat T^{(2c)}$ with Eq. (3.162) (again we need the first term only) and then reducing the Dirac structure using Eq. (3.73) gives

$$
\begin{aligned}
&J_{j'}^{(0)\dagger}J_j^{(2\ell)} + J_j^{(2\ell)\dagger}J_{j'}^{(0)} \qquad\qquad (3.168)\\
&= \frac{-1}{4}\,\mathrm{tr}\Big[\frac{P_v}{2}\bar\Upsilon_j^{(2\ell)}\frac{\bar{n}\!\!\!/}{2}P_R\Gamma_{j'}^{(0)}+\mathrm{h.c.}\Big]\Big[\bar{\mathcal{H}}_v(x)\mathcal{H}_v(0)\Big]\Big[\bar\chi_{n,\omega}(0)\frac{\bar{n}\!\!\!/P_L}{N_c}\mathcal{C}^{(2\ell)}_{n,\omega_{1,2}}(x)+(\mathrm{h.c.},\,x\leftrightarrow 0)\Big]\\
&+\frac{-1}{4}\,\mathrm{tr}\Big[\frac{P_v}{2}\bar\Upsilon_j^{(2\ell)}\frac{\bar{n}\!\!\!/}{2}P_R\Gamma_{j'}^{(0)}-\mathrm{h.c.}\Big]\Big[\bar{\mathcal{H}}_v(x)\mathcal{H}_v(0)\Big]\Big[\bar\chi_{n,\omega}(0)\frac{\bar{n}\!\!\!/P_L}{N_c}\mathcal{C}^{(2\ell)}_{n,\omega_{1,2}}(x)-(\mathrm{h.c.},\,x\leftrightarrow 0)\Big].
\end{aligned}
$$

The usoft operator here gives the leading-order shape function $f^{(0)}$. Next we define

the jet functions

$$
\begin{aligned}
&(-1)\langle 0|\bar\chi_{n,\omega}(0)\frac{\bar n\!\!\!/ P_L}{N_c}\Big(\Big[\frac{1}{\bar{\mathcal{P}}}ign\cdot\mathcal{B}_c\Big]\chi_n\Big)_{\omega_1}(x)\pm(\text{h.c.},\,x\leftrightarrow 0)|0\rangle \\
&\qquad=\frac{-2i}{\omega}\,\delta(\omega-\omega_1)\delta^2(x_\perp)\delta(x^+)\int\frac{dk^+}{2\pi}\,e^{-\frac{i}{2}k^+x^-}\,\mathcal{J}^{(2)}_{3\omega,4\omega}(k^+), \\
&\frac{1}{m_b}\langle 0|\bar\chi_{n,\omega}(0)\frac{\bar n\!\!\!/ P_L}{N_c}\big[(ign\cdot\mathcal{B}_c)_{-\omega_2}\chi_{n,\omega_1}\big](x)\pm(\text{h.c.},\,x\leftrightarrow 0)|0\rangle \\
&\qquad=\frac{-2i}{m_b}\,\delta(\omega-\omega_1-\omega_2)\delta^2(x_\perp)\delta(x^+)\int\frac{dk^+}{2\pi}\,e^{-\frac{i}{2}k^+x^-}\,\mathcal{J}^{(2)}_{5\omega_{1,2},6\omega_{1,2}}(k^+), \\
&\frac{-1}{m_b}\langle 0|\bar\chi_{n,\omega}(0)\frac{\bar n\!\!\!/ P_L}{N_c}\frac{1}{\omega_1}\big[ig\mathcal{B}^{\perp\alpha'}_{c,-\omega_2}\big(i\mathcal{D}^\alpha_{c\perp}\chi_n\big)_{\omega_1}\big](x)\pm(\text{h.c.},\,x\leftrightarrow 0)|0\rangle \\
&\qquad=\frac{-2i}{m_b}\,\delta(\omega-\omega_1-\omega_2)\delta^2(x_\perp)\delta(x^+)\int\frac{dk^+}{2\pi}\,e^{-\frac{i}{2}k^+x^-}\,\mathcal{J}^{(2)}_{7\omega_{1,2},8\omega_{1,2}}(k^+), \\
&\frac{1}{m_b}\langle 0|\bar\chi_{n,\omega}(0)\frac{\bar n\!\!\!/ P_L}{N_c}\frac{1}{\omega_2}\big[\big(ig\mathcal{B}^{\perp\alpha'}_c\,i\overleftarrow{\mathcal{D}}^\alpha_{c\perp}\big)_{\omega_2}\chi_{n,\omega_1}\big](x)\pm(\text{h.c.},\,x\leftrightarrow 0)|0\rangle \\
&\qquad=\frac{-2i}{m_b}\,\delta(\omega-\omega_1-\omega_2)\delta^2(x_\perp)\delta(x^+)\int\frac{dk^+}{2\pi}\,e^{-\frac{i}{2}k^+x^-}\,\mathcal{J}^{(2)}_{9\omega_{1,2},10\omega_{1,2}}(k^+),
\end{aligned}
\tag{3.169}
$$

and their imaginary parts $\mathcal{J}^{(2)}_m(\omega_j k^+)=(-1/\pi)\mathrm{Im}\,\mathcal{J}_{m\omega_j}(k^+)$, as well as the hard coefficients

$$
\begin{aligned}
h_i^{[2c]11,12}(\bar n\cdot p)&=\frac{m_b}{2\bar n\cdot p}\sum_{j,j'}C_{j'}(\bar n\cdot p)A_j^{(2c)}(\bar n\cdot p)\;\mathrm{Tr}\Big[\frac{P_v}{2}\,\overline{\Upsilon}^{(2c)}_{j\mu}\,\frac{\bar n\!\!\!/}{2}\,\Gamma^{(0)}_{j'\nu}\pm\text{h.c.}\Big]P_i^{\mu\nu}\,, \\
h_i^{[2c]13,14}(z_1,\bar n\cdot p)&=\frac{1}{2}\sum_{j,j'}C_{j'}(\bar n\cdot p)A_j^{(2d)}(\omega_{1,2})\;\mathrm{Tr}\Big[\frac{P_v}{2}\,\overline{\Upsilon}^{(2d)}_{j\mu}\,\frac{\bar n\!\!\!/}{2}\,\Gamma^{(0)}_{j'\nu}\pm\text{h.c.}\Big]P_i^{\mu\nu}\,, \\
h_i^{[2c]15,16}(z_1,\bar n\cdot p)&=\frac{1}{2}\sum_{j,j'}C_{j'}(\bar n\cdot p)A_j^{(2e)}(\omega_{1,2})\;\mathrm{Tr}\Big[\frac{P_v}{2}\,\overline{\Upsilon}^{(2e)}_{j\mu}\,\frac{\bar n\!\!\!/}{2}\,\Gamma^{(0)}_{j'\nu}\pm\text{h.c.}\Big]P_i^{\mu\nu}\,, \\
h_i^{[2c]17,18}(z_1,\bar n\cdot p)&=\frac{1}{2}\sum_{j,j'}C_{j'}(\bar n\cdot p)A_j^{(2f)}(\omega_{1,2})\;\mathrm{Tr}\Big[\frac{P_v}{2}\,\overline{\Upsilon}^{(2f)}_{j\mu}\,\frac{\bar n\!\!\!/}{2}\,\Gamma^{(0)}_{j'\nu}\pm\text{h.c.}\Big]P_i^{\mu\nu}\,,
\end{aligned}
\tag{3.170}
$$

where $\omega_1=z_1\bar n\cdot p$ and $\omega_2=(1-z_1)\bar n\cdot p$.

Putting all the pieces together we have

$$
\begin{aligned}
W_i^{(2c)}\;=\;&\sum_{m=3,4}\frac{h_i^{[2c]m+8}(\bar n\cdot p)}{m_b}\int_0^{p_X^+}dk^+\,\mathcal{J}^{(2)}_m(p_X^-\,k^+)\,f^{(0)}(k^++\overline{\Lambda}-p_X^+) \\
&+\sum_{m=5}^{10}\int dz_1\,\frac{h_i^{[2c]m+8}(z_1,\bar n\cdot p)}{m_b}\int_0^{p_X^+}dk^+\,\mathcal{J}^{(2)}_m(z_1,p_X^-\,k^+)\,f^{(0)}(k^++\overline{\Lambda}-p_X^+)\,.
\end{aligned}
\tag{3.171}
$$

Calculation of the remaining $\hat{T}^{(2)}$'s

The remaining $T^{(2)}$'s for which we have not yet defined hard, jet and soft functions include $T^{(2La)}$, $T^{(2Lb)}$, $T^{(2LL)}$ and $T^{(2Ga)}$. These time-ordered products all have jet functions that start at one-loop order and, unlike $T^{(2b,2c)}$, they also induce new shape functions, g_j. Factorization formulae can be derived for these contributions by following similar steps to the previous cases. Rather than going through this exercise, we instead list some of the soft operators and shape functions that would be required.

For $T^{(2La)}$ we have

$$\begin{aligned}
P_{8\lambda}^{\beta}(\ell_{1,2}^+) &= \int\frac{dx^-dy^-}{32\pi^2}\,e^{-\frac{i}{2}\ell_2^+x^-}e^{-\frac{i}{2}(\ell_1^+-\ell_2^+)y^-}\left[\overline{\mathcal{H}}_v(\tilde{x})i\overrightarrow{\mathcal{D}}_{us}^{\beta}(\tilde{y})\gamma_\lambda^T\gamma_5\mathcal{H}_v(0)\right],\\
P_{9\lambda}^{\beta}(\ell_{1,2}^+) &= \int\frac{dx^-dy^-}{32\pi^2}\,e^{-\frac{i}{2}\ell_2^+x^-}e^{-\frac{i}{2}(\ell_1^+-\ell_2^+)y^-}\left[\overline{\mathcal{H}}_v(\tilde{x})T^A i\overrightarrow{\mathcal{D}}_{us}^{\beta}(\tilde{y})T^A\gamma_\lambda^T\gamma_5\mathcal{H}_v(0)\right],\\
\langle\bar{B}_v|P_{8,9}^{\beta\lambda}(\ell_{1,2}^+)|\bar{B}_v\rangle &= \epsilon_\perp^{\beta\lambda}\,g_{11,12}^{(2)}(\ell_1^+,\ell_2^+),
\end{aligned}\tag{3.172}$$

while for $T^{(2Lb)}$ we find

$$\begin{aligned}
O_{8}^{\beta}(\ell_{1,2}^+) &= \int\frac{dx^-dy^-}{32\pi^2}\,e^{-\frac{i}{2}\ell_2^+x^-}e^{-\frac{i}{2}(\ell_1^+-\ell_2^+)y^-}\left[\overline{\mathcal{H}}_v(\tilde{x})i\overrightarrow{\mathcal{D}}_{us}^{\beta}(\tilde{y})\mathcal{H}_v(0)\right],\\
O_{9}^{\beta}(\ell_{1.2}^+) &= \int\frac{dx^-dy^-}{32\pi^2}\,e^{-\frac{i}{2}\ell_2^+x^-}e^{-\frac{i}{2}(\ell_1^+-\ell_2^+)y^-}\left[\overline{\mathcal{H}}_v(\tilde{x})T^A i\overrightarrow{\mathcal{D}}_{us}^{\beta}(\tilde{y})T^A\mathcal{H}_v(0)\right],\\
\langle\bar{B}_v|\bar{n}_\beta\,O_{8,9}^{\beta}(\ell_{1,2}^+)|\bar{B}_v\rangle &= g_{13,14}^{(2)}(\ell_1^+,\ell_2^+).
\end{aligned}\tag{3.173}$$

For both $T^{(2La)}$ and $T^{(2Lb)}$, the induced jet functions are of order λ^0.

For $T^{(2LL)}$ the necessary soft operators are

$$\begin{aligned}
O_{10}^{\alpha\beta}(\ell_{1,2,3}^+) &= i\int\frac{dx^-dy^-dz^-}{128\pi^3}e^{-\frac{i}{2}\{\ell_3x^-+(\ell_2^+-\ell_3^+)y^-+(\ell_1^+-\ell_2^+)z^-\}}\left[\overline{\mathcal{H}}_v(\tilde{x})i\mathcal{D}_{us}^{\perp\alpha}(\tilde{y})i\mathcal{D}_{us}^{\perp\beta}(\tilde{z})\mathcal{H}_v(0)\right],\\
P_{10\lambda}^{\alpha\beta}(\ell_{1.2.3}^+) &= i\int\frac{dx^-dy^-dz^-}{128\pi^3}e^{-\frac{i}{2}\{\cdots\}}\left[\overline{\mathcal{H}}_v(\tilde{x})i\mathcal{D}_{us}^{\perp\alpha}(\tilde{y})i\mathcal{D}_{us}^{\perp\beta}(\tilde{z})\gamma_\lambda^T\gamma_5\,\mathcal{H}_v(0)\right],
\end{aligned}\tag{3.174}$$

together with operators $O_{11-15}^{\alpha\beta}(\ell_{1.2,3}^+)$ and $P_{11-15\lambda}^{\alpha\beta}(\ell_{1,2,3}^+)$ that have different colour contractions between the gauge-invariant objects $\bar{\mathcal{H}}_v$, $i\mathcal{D}^{\perp\alpha}$, $i\mathcal{D}^{\perp\beta}$, and $\mathcal{H}_v$. The

shape functions are

$$\begin{aligned}\langle \bar{B}_v|O^{\alpha\beta}_{10-15}(\ell^+_{1,2,3})|\bar{B}_v\rangle &= g_\perp^{\alpha\beta}\, g^{(4)}_{15-20}(\ell_1^+,\ell_2^+,\ell_3^+)\,,\\ \langle \bar{B}_v|P^{\alpha\beta}_{10-15\lambda}(\ell^+_{1,2,3})|\bar{B}_v\rangle &= -\epsilon_\perp^{\alpha\beta}\Big(v_\lambda-\frac{n_\lambda}{n\cdot v}\Big)\, g^{(4)}_{21-26}(\ell_1^+,\ell_2^+,\ell_3^+)\,. \end{aligned} \tag{3.175}$$

For $T^{(2LL)}$ the jet functions are $\mathcal{O}(\lambda^{-2})$.

Finally, for $T^{(2Ga)}$ the time-ordered product has a structure that will produce the same soft operators, $O_3^{\alpha\beta}$ and $P_{4\lambda}^{\alpha\beta}$, as $T^{(2L)}$ and thus has shape functions $f_3^{(4)}(\ell_1^+,\ell_2^+)$ and $f_4^{(4)}(\ell_1^+,\ell_2^+)$. The jet functions for $T^{(2Ga)}$ are $\mathcal{O}(\lambda^{-2})$.

3.6.6 Summary of hard coefficients

To determine h_i^{1f-6f} we need to compute the traces in Eqs. (3.131), (3.145) and (3.157). Since there is no possibility of confusion, we shall now drop the bracketed factors, [2−], in the superscripts. For $B\to X_u e\bar{\nu}$ ($f=u$), expanding to leading order in $\bar{y}_H \gg u_H$ gives

$$\begin{aligned}
&h_1^{1u}=\frac{1}{8}\,, && h_2^{1u}=-\frac{(2-\bar{y}_H)}{2\bar{y}_H^2}\,, && h_3^{1u}=\frac{1}{4m_B\bar{y}_H}\,, && h_4^{1u}=\frac{-1}{m_B^2\bar{y}_H^2}\,, && h_5^{1u}=\frac{4-\bar{y}_H}{4m_B\bar{y}_H^2}\,,\\
&h_1^{2u}=\frac{-1}{4}\,, && h_2^{2u}=\frac{4\bar{y}_H-\bar{y}_H^2-2}{\bar{y}_H^3}\,, && h_3^{2u}=\frac{-1}{2m_B\bar{y}_H}\,, && h_4^{2u}=\frac{2\bar{y}_H-2}{m_B^2\bar{y}_H^3}\,, && h_5^{2u}=\frac{\bar{y}_H^2-6\bar{y}_H+4}{2m_B\bar{y}_H^3}\,,\\
&h_1^{3u}=\frac{-1}{4\bar{y}_H}\,, && h_2^{3u}=\frac{-1}{\bar{y}_H^2}\,, && h_3^{3u}=\frac{-1}{2m_B\bar{y}_H^2}\,, && h_4^{3u}=0\,, && h_5^{3u}=\frac{1}{2m_B\bar{y}_H^2}\,,\\
&h_1^{4u}=\frac{1}{4\bar{y}_H}\,, && h_2^{4u}=\frac{\bar{y}_H-2}{\bar{y}_H^3}\,, && h_3^{4u}=\frac{1}{2m_B\bar{y}_H^2}\,, && h_4^{4u}=\frac{-2}{m_B^2\bar{y}_H^3}\,, && h_5^{4u}=\frac{4-\bar{y}_H}{2m_B\bar{y}_H^3}\,,\\
&h_1^{5u}=\frac{-1}{2}\,, && h_2^{5u}=\frac{2-2\bar{y}_H}{\bar{y}_H^2}\,, && h_3^{5u}=\frac{-1}{m_B\bar{y}_H}\,, && h_4^{5u}=\frac{2}{m_B^2\bar{y}_H^2}\,, && h_5^{5u}=-\frac{(2-\bar{y}_H)}{m_B\bar{y}_H^2}\,,\\
&h_1^{6u}=0\,, && h_2^{6u}=\frac{2}{\bar{y}_H^2}\,, && h_3^{6u}=0\,, && h_4^{6u}=\frac{2}{m_B^2\bar{y}_H^2}\,, && h_5^{6u}=\frac{-2}{m_B\bar{y}_H^2}\,.
\end{aligned} \tag{3.176}$$

For $B \to X_s\gamma$ ($f = s$) we expand around $x_H = 1$, which gives

$$\begin{aligned}
h_1^{1s} &= -\frac{m_B^2}{8}, \quad h_2^{1s} = 0, \quad h_3^{1s} = -\frac{m_B}{4}, \quad h_4^{1s} = \frac{5}{8}, \quad h_5^{1s} = -\frac{m_B}{4}, \\
h_1^{2s} &= \frac{m_B^2}{4}, \quad h_2^{2s} = 0, \quad h_3^{2s} = \frac{m_B}{2}, \quad h_4^{2s} = -\frac{7}{4}, \quad h_5^{2s} = \frac{m_B}{2}, \\
h_1^{3s} &= -\frac{m_B^2}{4}, \quad h_2^{3s} = 0, \quad h_3^{3s} = -\frac{m_B}{2}, \quad h_4^{3s} = \frac{3}{4}, \quad h_5^{3s} = -\frac{m_B}{2}, \\
h_1^{4s} &= \frac{m_B^2}{4}, \quad h_2^{4s} = 0, \quad h_3^{4s} = \frac{m_B}{2}, \quad h_4^{4s} = -\frac{5}{4}, \quad h_5^{4s} = \frac{m_B}{2}, \\
h_1^{5s} &= -\frac{m_B^2}{2}, \quad h_2^{5s} = 0, \quad h_3^{5s} = -m_B, \quad h_4^{5s} = 2, \quad h_5^{5s} = -m_B, \\
h_1^{6s} &= h_2^{6s} = h_3^{6s} = 0, \quad h_4^{6s} = \frac{1}{2}, \quad h_5^{6s} = 0. \qquad (3.177)
\end{aligned}$$

3.7 Summary of Decay Rates to NLO

3.7.1 Discussion of NLO results

To facilitate the computation of the NLO corrections to the decay rates, they were divided into several pieces, as discussed at the beginning of Sec. 3.6. The full results at order Λ/m_b and all orders in α_s are quite complicated. However, now that factorization for the NLO rates has been achieved, we are able to expand consistently in factors of α_s evaluated at perturbative scales. In this section, we discuss which terms are kept for phenomenological purposes.

The most complicated contributions are the NLO correction to the W_i, namely $W_i^{(2)f}$, where $f = s$ for $B \to X_s\gamma$ and $f = u$ for $B \to X_u\ell\bar{\nu}$. From Eq. (3.105) in

Sec. 3.6, the NLO factorization theorem is

$$
\begin{aligned}
W_i^{(2)f} &= \frac{h_i^{0f}(\bar{n}\cdot p)}{2m_b} \int_0^{p_X^+} dk^+ \; \mathcal{J}^{(0)}(\bar{n}\cdot p\, k^+,\mu)\, f_0^{(2)}\big(k^+ + r^+,\mu\big) \\
&+ \sum_{r=1}^{2} \frac{h_i^{rf}(\bar{n}\cdot p)}{m_b} \int_0^{p_X^+} dk^+ \; \mathcal{J}^{(0)}(\bar{n}\cdot p\, k^+,\mu)\, f_r^{(2)}\big(k^+ + r^+,\mu\big) \\
&+ \sum_{r=3}^{4} \frac{h_i^{rf}(\bar{n}\cdot p)}{m_b} \int dk_1^+\, dk_2^+ \mathcal{J}^{(-2)}(\bar{n}\cdot p\, k_j^+,\mu)\, f_r^{(4)}\big(k_j^+ + r^+,\mu\big) \\
&+ \sum_{r=5}^{6} \frac{h_i^{rf}(\bar{n}\cdot p)}{\bar{n}\cdot p} \int dk_1^+ dk_2^+ dk_3^+ \; \mathcal{J}^{(-4)}(\bar{n}\cdot p\, k_{j'}^+,\mu)\, f_r^{(6)}\big(k_{j'}^+ + r^+,\mu\big) \\
&+ \ldots ,
\end{aligned}
\tag{3.178}
$$

where $j = 1,2$ and $j' = 1,2,3$. The ellipses denote terms given in Eq. (3.105) that have jet functions $\mathcal{J}$ that start at one-loop order. These additional terms are of order

$$
\frac{\alpha_s(\mu_0)}{\pi}\,\frac{\Lambda}{m_b}\,, \tag{3.179}
$$

where $\mu_0 \simeq \sqrt{m_b \Lambda_{\rm QCD}}$, so they are suppressed relative to the terms displayed in Eq. (3.178). They also induce dependence on new unknown shape functions, g_{0-26}, which makes it prohibitive to include them phenomenologically. Thus, throughout this section we shall stick to the terms displayed in Eq. (3.178), which enter at order Λ/m_b ($r = 0$–4) and $4\pi\alpha_s(\mu_0)\Lambda/m_b$ ($r = 5,6$). For convenience we drop the subscript 1 on $\mathcal{J}_1^{(-2,-4)}$ in this section, since there is no possibility of confusion. At tree level, the jet functions were computed in Sec. 3.6.3 and are

$$
\begin{aligned}
&\mathcal{J}^{(0)}(k^+) = \delta(k^+)\,, \qquad \mathcal{J}^{(-2)}(k_j^+) = \frac{\delta(k_1^+) - \delta(k_2^+)}{k_2^+ - k_1^+}\,, \\
&\mathcal{J}^{(-4)}(k_j^+) = 4\pi\alpha_s(\mu_0)\left[\frac{\delta(k_1^+)}{(k_2^+)(k_3^+)} + \frac{\delta(k_2^+)}{(k_1^+)(k_3^+)} + \frac{\delta(k_3^+)}{(k_1^+)(k_2^+)} - \pi^2\delta(k_1^+)\delta(k_2^+)\delta(k_3^+)\right].
\end{aligned}
\tag{3.180}
$$

The result for $\mathcal{J}^{(0)}$ at one-loop order can be found in Eq. (3.80). Examples of diagrams that contribute to Eq. (3.178) can be found in Table 3.4. Results for the hard functions h_i^{0f} were given in Eqs. (3.87) and (3.88) and for h_i^{1f-6f} in Eqs. (3.176) and (3.177). The running of the h_i^{rf}'s in Eq. (3.178) is the same as the running of the h_i^{0f}'s in

Eq. (3.87), and the h_i^{0f}'s depend only on the running of the C_i's computed in Ref. [23]. The shape functions $f_{0-6}^{(n)}$ are defined by Eqs. (3.119) and (3.120).

More $\mathcal{O}(\lambda^2)$ power corrections occur when one switches to hadronic variables in the LO factorization theorem; these were given in Eq. (3.100). For phenomenological purposes terms that start suppressed by the factor in Eq. (3.179) are not included, so we include the $(\lambda_1 + 3\lambda_2)$ term but not the $\overline{\Lambda}$ term.

Finally, the simplest source of power corrections is the kinematic expansion of the prefactors in the decay-rate formulae, which depend on which rate we consider (see Eqs. (3.39)-(3.41)).[13] In addition there are corrections from the expansion of $n\cdot q$ in the h_i's; these give the $h_i^{0'f}$'s in Eqs. (3.89) and (3.90). Both of these sources involve the same jet function and shape function as the LO contributions but different hard coefficients, which we shall denote by G^S, $G^T_{1a,1b}$, and G^D in the next section.

3.7.2 NLO Results for the Endpoint Decay Rates

In this section we combine the pieces to arrive at the NLO results for decay rates. The hadronic dimensionless variables that we use are

$$x_H^\gamma = \frac{2E_\gamma}{m_B}, \quad x_H = \frac{2E_\ell}{m_B}, \quad y_H = \frac{q^2}{m_B^2}, \quad s_H = \frac{m_X^2}{m_B^2}, \quad \overline{y}_H = \frac{\bar{n}\cdot p_X}{m_B}, \quad u_H = \frac{n\cdot p_X}{m_B}, \tag{3.181}$$

where only the first one is for $B \to X_s\gamma$ and the rest are for $B \to X_u\ell\bar{\nu}$. Note that $s_H = u_H\overline{y}_H$ and $y_H = (1-u_H)(1-\overline{y}_H)$, so these variables are not independent. The decay rates derived with SCET are valid for spectra dominated by the endpoint or SCET region, in which $u_H/\overline{y}_H \lesssim \lambda_H^2$ and $1-x_H^\gamma \lesssim \lambda_H^2$, where λ_H^2 is a small expansion parameter which one can choose to be ~ 0.2 or $\sim \Lambda/m_b \simeq 0.1$. In this region we write the decay rates as

$$\frac{1}{\Gamma}\frac{d\Gamma}{dZ} = \left(\frac{1}{\Gamma}\frac{d\Gamma}{dZ}\right)^{LO} + \left(\frac{1}{\Gamma}\frac{d\Gamma}{dZ}\right)^{NLO} + \dots, \tag{3.182}$$

[13] If one desires, he or she can straightforwardly treat x_H in the doubly and triply differential rates in a different manner from what we have done here, by using Eqs. (3.31) and (3.32) instead of Eqs. (3.41) and (3.40) and making the desired expansions.

where Z denotes a generic choice of phase-space variables. The doubly differential and triply differential decay rates that we consider were discussed in Secs. 3.2.2 and 3.2.3. We caution that if the SCET expansion is used for decay rates integrated over a larger region of phase space than the SCET region then it is important to check that sufficient smearing has occurred so that the contributions outside the SCET region do not cause the power expansion to break down. In Eq. (3.38) we proposed a method one could use to combine results from the local OPE with those from SCET even if a larger region of phase space was desired (which becomes relevant when radiative corrections are included). Note that the λ_H parameter provides a means of testing for cases where a pure SCET expansion is valid. Here we present results for arbitrary λ_H, and leave the investigation of the expansion in different decay rates to future work.

For convenience, we define a shorthand notation for the convolutions that appear at LO and NLO:

$$\big[\mathcal{J}\otimes f\big](p_X^+,p_X^-) \;=\; \int\! dk_j^+\; \mathcal{J}(p_X^-\,k_j^+,\mu)\; f\big(k_j^+ + \overline{\Lambda} - p_X^+,\mu\big)\,. \tag{3.183}$$

At LO we simply combine the h_i^{0s}'s and h_i^{0u}'s from Eqs. (3.87) and (3.88) and find

$$\begin{aligned}
\left(\frac{1}{\Gamma_0^s}\,\frac{d\Gamma^s}{dx_H^\gamma}\right)^{LO} &= H^S\,\big[\mathcal{J}^{(0)}\otimes f^{(0)}\big]\big(m_B(1-x_H^\gamma),m_B\big)\,, \qquad (3.184)\\
\left(\frac{1}{\Gamma_0^u}\,\frac{d^3\Gamma^u}{dx_H^{cut}\,d\overline{y}_H\,du_H}\right)^{LO} &= H^T(\overline{y}_H)\,\big[\mathcal{J}^{(0)}\otimes f^{(0)}\big](m_B u_H, m_B\overline{y}_H)\,,\\
\left(\frac{1}{\Gamma_0^u}\,\frac{d^2\Gamma^u}{d\overline{y}_H\,du_H}\right)^{LO} &= H^D(\overline{y}_H)\,\big[\mathcal{J}^{(0)}\otimes f^{(0)}\big](m_B u_H, m_B\overline{y}_H)\,,
\end{aligned}$$

where the convolution of the LO jet function and shape function is given by Eq. (3.183) (with one integration variable k^+) and the hard coefficients are

$$\begin{aligned}
H^S(\mu) &= m_B\big[C_1^{(t)} - \frac{1}{2}\,C_2^{(t)} - C_3^{(t)}\big]^2\,, \qquad (3.185)\\
H^T(\mu,\overline{y}_H) &= 12 m_B\,\overline{y}_H(1-\overline{y}_H)\big[C_1^{(v)}\big]^2\,,\\
H^D(\mu,\overline{y}_H) &= 2m_B\,\overline{y}_H^2\,\Big\{(3-2\overline{y}_H)(C_1^{(v)})^2 + 2C_1^{(v)}\big(C_3^{(v)} + \frac{\overline{y}_H}{2}C_2^{(v)}\big) + \big(C_3^{(v)} + \frac{\overline{y}_H}{2}C_2^{(v)}\big)^2\Big\}\,.
\end{aligned}$$

Note that we have suppressed the functional dependence of the coefficients, which once perturbative corrections are included is $C_i^{(t)}(\mu, m_B)$ and $C_i^{(v)}(\mu, m_B, \overline{y}_H)$. Our $W_i^{(0)}$'s for both $B \to X_u \ell \bar{\nu}$ and $B \to X_s \gamma$, and hence the corresponding LO triply and singly differential rates, respectively, agree with Ref. [27]. These results also match those of Ref. [47].

At NLO, combining all contributions, as discussed in Sec. 3.7.1, leads to the following expressions:

$$\begin{aligned}\left(\frac{1}{\Gamma_0^s}\frac{d\Gamma^s}{dx_H^\gamma}\right)^{NLO} &= -\frac{(\lambda_1+3\lambda_2)}{2m_B}\,H^S(m_b)\,\big[\mathcal{J}^{(0)}\otimes\widetilde{f^{(0)}}\big](m_B(1-x_H^\gamma),m_B)\\ &\quad+(1-x_H^\gamma)\,G^S\,\big[\mathcal{J}^{(0)}\otimes f^{(0)}\big](m_B(1-x_H^\gamma),m_B)\\ &\quad+\sum_{j=0}^{6}H_j^S(m_B)\,\big[\mathcal{J}^{(n_j)}\otimes f_j\big](m_B(1-x_H^\gamma),m_B)\,, \qquad (3.186)\end{aligned}$$

$$\begin{aligned}\left(\frac{1}{\Gamma_0^u}\frac{d^3\Gamma^u}{dx_H^{cut}\,d\overline{y}_H\,du_H}\right)^{NLO} &= -\frac{(\lambda_1+3\lambda_2)}{2m_B}H^T(\overline{y}_H)\;\big[\mathcal{J}^{(0)}\otimes\widetilde{f^{(0)}}\big](m_Bu_H,m_B\overline{y}_H)\\ &\quad+\Big[u_H\,G_{1a}^T(\overline{y}_H)+(u_H+x_H-1)\,G_{1b}^T(\overline{y}_H)\Big]\big[\mathcal{J}^{(0)}\otimes f^{(0)}\big](m_Bu_H,m_B\overline{y}_H)\\ &\quad+\sum_{j=0}^{6}H_j^T(\bar{y}_H)\,\big[\mathcal{J}^{(n_j)}\otimes f_j\big](m_Bu_H,m_B\overline{y}_H)\,, \qquad (3.187)\end{aligned}$$

$$\begin{aligned}\left(\frac{1}{\Gamma_0^u}\frac{d^2\Gamma^u}{d\overline{y}_H\,du_H}\right)^{NLO} &= -\frac{(\lambda_1+3\lambda_2)}{2m_B}H^D(\overline{y}_H)\;\big[\mathcal{J}^{(0)}\otimes\widetilde{f^{(0)}}\big](m_Bu_H,m_B\overline{y}_H)\\ &\quad+u_H\,G^D(\overline{y}_H)\,\big[\mathcal{J}^{(0)}\otimes f^{(0)}\big](m_Bu_H,m_B\overline{y}_H)\\ &\quad+\sum_{j=0}^{6}H_j^D(\bar{y}_H)\,\big[\mathcal{J}^{(n_j)}\otimes f_j\big](m_Bu_H,m_B\overline{y}_H)\,, \qquad (3.188)\end{aligned}$$

where $n_0 = n_1 = n_2 = 0$, $n_3 = n_4 = -2$, and $n_5 = n_6 = -4$, and the notation $\big[\mathcal{J}^{(n_j)}\otimes f_j\big]$ denotes the convolutions displayed in Eq. (3.178) (see also Eq. (3.101)). From the NLO phase-space factors in Eqs. (3.39), (3.41) and (3.40), and from the

NLO terms in the expansion of the h_i, i.e. Eqs. (3.90) and (3.89), we find that

$$\begin{aligned}
G^S(m_b) &= -3\,m_B\big(C_1^{(t)}-\frac{1}{2}\,C_2^{(t)}-C_3^{(t)}\big)^2\,, \qquad (3.189)\\
G_{1a}^T(\overline{y}_H) &= 12m_B(\overline{y}_H^2-1)(C_1^{(v)})^2\,,\\
G_{1b}^T(\overline{y}_H) &= 12m_B\Big\{2(1-\overline{y}_H)(C_1^{(v)})^2-\big[C_1^{(v)}+C_3^{(v)}+\frac{\overline{y}_H}{2}C_2^{(v)}\big]^2\Big\}\,,\\
G^D(\overline{y}_H) &= 2m_B\,\overline{y}_H\Big[(2\overline{y}_H^2-6)(C_1^{(v)})^2-\overline{y}_H(\overline{y}_H+3)(C_1^{(v)}+C_3^{(v)})\,C_2^{(v)}\\
&\qquad -\overline{y}_H^2(C_2^{(v)})^2-2(1+\overline{y}_H)(2C_1^{(v)}+C_3^{(v)})C_3^{(v)}\Big]\,.
\end{aligned}$$

By using Eqs. (3.176) and (3.177), we find that the hard coefficients for the terms with subleading shape functions are

$$\begin{aligned}
&H_0^S=\frac{H^S}{2m_B}\,,\quad H_1^S=-\frac{1}{2}\,,\quad H_2^S=1\,,\quad H_3^S=-1\,,\quad H_4^S=1\,,\quad H_5^S=-2\,,\quad H_6^S=0\,,\\
&H_0^T=\frac{H^T}{2m_B}\,,\quad H_1^T=6\overline{y}_H(1-\overline{y}_H)\,,\quad H_2^T=-12\overline{y}_H(1-\overline{y}_H)\,,\quad H_3^T=-12(1-\bar{y}_H)\,,\\
&H_4^T=12(1-\bar{y}_H)\,,\quad H_5^T=-24(1-\overline{y}_H)\,,\quad H_6^T=0\,,\\
&H_0^D=\frac{H^D}{2m_B}\,,\quad H_1^D=\overline{y}_H^2(1-2\overline{y}_H),\quad H_2^D=2\overline{y}_H(2\overline{y}_H^2+\overline{y}_H-2),\quad H_3^D=4\overline{y}_H^2-6\overline{y}_H\,,\\
&H_4^D=2\overline{y}_H-4\overline{y}_H^2\,,\quad H_5^D=8\overline{y}_H^2-8\overline{y}_H\,,\quad H_6^D=4\overline{y}_H\,. \qquad (3.190)
\end{aligned}$$

The H_{1-6} factors displayed here will be corrected by $\alpha_s(m_b)/\pi$ terms at one-loop order. Note that the shape functions $f_{5,6}$ depend on the flavour of the light quark in the four-quark operator and therefore differ for $B\to X_s$ and $B\to X_u$.

Equation (3.186) describes $B\to X_s\gamma$ in the endpoint region. In Eqs. (3.187) and (3.188), convergence of the SCET expansion requires $u_H\ll\bar{y}_H$. For Eq. (3.187), we have in addition made a cut on x_H such that $1-x_H\sim\lambda^2$. In contrast, for Eq. (3.188) the full range of x_H has been integrated over. We can also straightforwardly obtain the rate $d^2\Gamma^u/dq^2dm_X^2$, or equivalently $d^2\Gamma^u/ds_Hdy_H$, by changing variables from $\{\overline{y}_H,u_H\}$ to $\{y_H,s_H\}$ in the W_i and re-expanding. This is done by using $\bar{y}_H=\zeta-s_H/\zeta-\ldots$ and $u_H=s_H/\zeta+\ldots$, where $\zeta=1-y_H+s_H$ and the "..." terms are not needed at NLO in the power expansion. The result may then be substituted

into Eq. (3.42). Integration over y_H then gives the m_X^2 spectrum, $d\Gamma^u/ds_H$, for which restriction to the endpoint region requires $cut(s_H, y_H) \equiv \{s_H/\zeta^2 \leq \lambda_H^2/(1+\lambda_H^2)^2\}$.

3.7.3 Singly Differential Spectra

In this section we give results for singly differential spectra at NLO that are useful for measurements of $|V_{ub}|$. Since our goal is to explore the effect of the subleading shape functions, in this section we shall work at lowest order in α_s for the hard and jet functions, both at LO and NLO. For the shape functions we shall use $f_1^{(2)}(\omega) = 2\omega f^{(0)}(\omega)$ [26] and define

$$\begin{aligned} F(p^+) &= f^{(0)}(\bar\Lambda - p^+) + \frac{1}{2m_B} f_0^{(2)}(\bar\Lambda - p^+) - \frac{\lambda_1 + 3\lambda_2}{2m_B} f^{(0)\prime}(\bar\Lambda - p^+)\,, \quad (3.191) \\ F_2(p^+) &= f_2^{(2)}(\bar\Lambda - p^+)\,, \end{aligned}$$

where a prime denotes a derivative, as well as

$$\begin{aligned} F_{3,4}(p^+) &= \int dk_1^+\, dk_2^+ \left[\frac{\delta(k_1^+) - \delta(k_2^+)}{k_2^+ - k_1^+}\right] f_{3,4}^{(4)}(k_j^+ + \bar\Lambda - p^+), \quad (3.192) \\ F_{5,6}(p^+) &= \int dk_1^+\, dk_2^+\, dk_3^+ \left[\frac{\delta(k_1^+)}{(k_2^+)(k_3^+)} + \frac{\delta(k_2^+)}{(k_1^+)(k_3^+)} + \frac{\delta(k_3^+)}{(k_1^+)(k_2^+)} - \pi^2\delta(k_1^+)\delta(k_2^+)\delta(k_3^+)\right] \\ &\quad \times f_{5,6}^{(6)}(k_j^+ + \bar\Lambda - p^+)\,. \end{aligned}$$

We shall put an additional superscript s or u on $F_{5,6}(p^+)$ to distinguish the original four-quark operator with strange- and up-type quarks. For $B \to X_s\gamma$ the rate $d\Gamma^s/dx_H^\gamma$ in the endpoint region is equivalent to making a cut on x_H^γ. The necessary results already appear in Eqs. (3.184) and (3.186) and combining them gives

$$\begin{aligned} \frac{1}{\Gamma_0^s}\frac{d\Gamma^s}{dx_H^\gamma}\bigg|_{x_H^\gamma > x_H^c} &= m_B\big[1 - 3(1-x_H^\gamma)\big] F\big(m_B(1-x_H^\gamma)\big) + \big[m_B(1-x_H^\gamma) - \bar\Lambda\big] F\big(m_B(1-x_H^\gamma)\big) \\ &\quad + F_2\big(m_B(1-x_H^\gamma)\big) - F_3\big(m_B(1-x_H^\gamma)\big) + F_4\big(m_B(1-x_H^\gamma)\big) \\ &\quad - 8\pi\alpha_s(\mu_0)\; F_5^s\big(m_B(1-x_H^\gamma)\big)\,. \quad (3.193) \end{aligned}$$

where $1 - x_H^c \sim \lambda^2$. Here the $-3(1 - x_H^\gamma)$ term comes from expanding the kinematic prefactors, while the term that depends on $[m_B(1 - x_H) - \overline{\Lambda}]$ comes from reducing $f_1^{(2)}$ to $f^{(0)}$ (and we write it in terms of F for convenience, even though this includes some formally higher-order terms). The rate in Eq. (3.193) for $B \to X_s\gamma$ has been computed previously at NLO in Ref. [26]. The relation of our shape functions to those in Ref. [26] is shown in Table 3.7. Our result in Eq. (3.193) agrees with theirs, up to the $F_5^{(6)}$ term, which was computed here for the first time.[14]

To compute $d\Gamma^u/dx_H$ for $B \to X_u\ell\bar{\nu}$, we can use Eq. (3.31) and case i) of Table 3.2. Treating $r_\pi^2 = 0.026 \sim \lambda^4$, we can set $r_\pi = 0$ even at NLO. To ensure that the SCET expansion converges requires that one makes a cut on u_H. First consider the x_H spectrum. Since $u_H \leq 1 - x_H$, making a cut $x_H > x_H^c$ restricts u_H to the desired small values. However, at NLO accuracy this is not equivalent to our $u_H \leq \lambda_H^2 \overline{y}_H$ definition of the SCET region of phase space, and an additional term, $K(\lambda_H, x_H)$, is added to correct for this. Depending on the choice of other cuts, the error in including a larger region of phase space may be power suppressed. The parameter λ_H provides us with a way of testing this by comparing $\lambda_H = 0.2$ and $\lambda_H = 1$. We present our final results in a manner that makes it easy to take the $\lambda_H \to 1$ limit for situations where a large enough region has been smeared over that this is the case. For the x_H spectrum the result is

$$\begin{aligned}\frac{1}{\Gamma_0^u}\frac{d\Gamma^u}{dx_H}\bigg|_{\substack{x_H > x_H^c \\ \frac{u_H}{\overline{y}_H} < \lambda_H^2}} &= 2\int_0^{\min\{1-x_H,\lambda_H^2\}} du_H \Big\{ m_B(1-4u_H)F(m_B u_H) + (\overline{\Lambda} - m_B u_H)\, F(m_B u_H) \\ &\quad - F_2(m_B u_H) - 3F_3(m_B u_H) + 3F_4(m_B u_H) - 24\pi\alpha_s(\mu_0)\, F_5^u(m_B u_H) \Big\} \\ &\quad + K(\lambda_H, x_H)\,, \end{aligned} \tag{3.194}$$

[14] In making this comparison, note that Ref. [26] gave their result with partonic variables, whereas we have expressed ours in terms of hadronic variables here.

where

$$K(\lambda_H, x_H) = 2 \int_{(1-x_H)\lambda_H^2}^{\min\{1-x_H,\lambda_H^2\}} du_H \left\{ \frac{u_H^2}{\lambda_H^6} (2u_H - 3\lambda_H^2) \Big[m_B F(m_B u_H) \right. \tag{3.195}$$
$$\left. + (\overline{\Lambda} - m_B u_H) F(m_B u_H) - F_2(m_B u_H) \Big] \right.$$
$$- \frac{u_H}{\lambda_H^4} (u_H - 2\lambda_H^2) \Big[3F_3(m_B u_H) - 3F_4(m_B u_H) + 24\pi\alpha_s(\mu_0) F_5^u(m_B u_H) \Big]$$
$$\left. - \frac{2u_H(3u_H(1-x_H)\lambda_H^2 + u_H^3 - 3(1-x_H)\lambda_H^4 - 3u_H^2\lambda_H^2)}{\lambda_H^6} \Big[m_B F(m_B u_H) \Big] \right\}.$$

The λ_H-dependent term, $K(\lambda_H, x_H)$, arises when one writes the integral over $\bar{y}_H$ as $\int_{1-x_H}^1 d\bar{y}_H + \int_{u_H/\lambda_H^2}^{1-x_H} d\bar{y}_H \, \theta\left(\frac{u_H}{\lambda_H^2} - 1 + x_H\right)$, which is done to ensure that $u_H \leq \lambda_H^2 \bar{y}_H$. After inputting models for the shape functions one can use the $K(\lambda_H, x_H)$ term to check the consistency of the operator product expansion with this level of smearing.

The rate $d\Gamma^u/dx_H$ has been computed at NLO in Ref. [25] and we can compare our result with theirs. To do this we take $\lambda_H \to 1$, which sets $K(\lambda_H, x_H) \to 0$, since the restrictions we imposed on the phase space were not considered there. We also must convert back to partonic variables, which means dropping the $(\lambda_1 + 3\lambda_2)$ term in Eq. (3.191). After doing this, we find agreement with their Eq. (35) [15] on the coefficients of the LO F term and the F_2 and F_4 terms, but we disagree on the $u_H F$ term and the F_3 term. (Again the F_5 term is computed for the first time here, so no cross-check on this is possible.) The coefficient of our F_3 term also disagrees with the RPI constraint derived in Ref. [56], which predicted that it occurs in the combination $m_B F - F_3$.[16] We found that this combination occurs for $B \to X_s\gamma$, but not for $B \to X_u \ell \bar{\nu}$. In the next section, we present a non-trivial cross-check of the coefficients of our result in Eq. (3.194), namely that when re-expanded it correctly reproduces terms in the local OPE up to $1/m_b^3$.

Next we consider the p_X^- spectrum, namely $d\Gamma/d\bar{y}_H$. Integrating the doubly differ-

[15] We found that they have an overall 2 typographical error in this equation (see also [127]).

[16] Note that, from the point of view of the factorization theorem, such a reparameterization constraint would be very interesting, since it would give a relation between the jet functions $\mathcal{J}^{(-2)}$ and $\mathcal{J}^{(0)}$ to all orders in α_s, even though these operators appear to be defined by unrelated matrix elements. Eqs. (3.70) and (3.139).

ential rate from Eqs. (3.184) and (3.188) with a cut on u_H, i.e. $u_H \leq \lambda_H^2 \bar{y}_H$, restricts one to the triangular SCET region shown in Fig. 3-2 and gives

$$\begin{aligned}\frac{1}{\Gamma_0^u}\frac{d\Gamma^u}{d\bar{y}_H}\bigg|_{\bar{u}_H \leq \lambda_H^2 \bar{y}_H} &= 2\int_0^{\lambda_H^2 \bar{y}_H} du_H \Big\{ m_B\big[(3\bar{y}_H^2 - 2\bar{y}_H^3) + 2u_H(\bar{y}_H^3 - 3\bar{y}_H)\big] F(m_B u_H) \\ &+ (\overline{\Lambda} - m_B u_H)(\bar{y}_H^2 - 2\bar{y}_H^3) F(m_B u_H) + (2\bar{y}_H^3 + \bar{y}_H^2 - 2\bar{y}_H) F_2(m_B u_H) \\ &+ (2\bar{y}_H^2 - 3\bar{y}_H) F_3(m_B u_H) + (\bar{y}_H - 2\bar{y}_H^2) F_4(m_B u_H) \\ &+ 16\pi\alpha_s(\mu_0)(\bar{y}_H^2 - \bar{y}_H) F_5^u(m_B u_H) + 8\pi\alpha_s(\mu_0)\bar{y}_H F_6^u(m_B u_H) \Big\}. \end{aligned} \tag{3.196}$$

Another possibility is to consider the p_X^+ spectrum, which is $d\Gamma/du_H$, where we now integrate with the cut on $\bar{y}_H$, obtaining

$$\begin{aligned}\frac{1}{\Gamma_0^u}\frac{d\Gamma^u}{du_H}\bigg|_{\bar{y}_H \geq \frac{u_H}{\lambda_H^2}} &= \Big\{ m_B\big[(1 - 2\tilde{u}^3 + \tilde{u}^4) - u_H(5 - 6\tilde{u}^2 + \tilde{u}^4)\big] F(m_B u_H) \\ &- \frac{1}{3}(\overline{\Lambda} - m_B u_H)(1 + 2\tilde{u}^3 - 3\tilde{u}^4) F(m_B u_H) - \frac{1}{3}(1 - 6\tilde{u}^2 + 2\tilde{u}^3 + 3\tilde{u}^4) F_2(m_B u_H) \\ &- \frac{1}{3}(5 - 9\tilde{u}^2 + 4\tilde{u}^3) F_3(m_B u_H) - \frac{1}{3}(1 + 3\tilde{u}^2 - 4\tilde{u}^3) F_4(m_B u_H) \\ &- \frac{16\pi\alpha_s(\mu_0)}{3}(1 - 3\tilde{u}^2 + 2\tilde{u}^3) F_5^u(m_B u_H) + 8\pi\alpha_s(\mu_0)(1 - \tilde{u}^2) F_6^u(m_B u_H) \Big\}, \end{aligned} \tag{3.197}$$

where $\tilde{u} = u_H/\lambda_H^2$ is a parameter of order 1 for $\lambda_H \sim 0.2$. Given sufficient smearing, one can take $\lambda_H \to 1$ and the $\tilde{u}$ terms become subleading. The subleading terms in $d\Gamma^u/du_H$ provide power corrections to the phenomenological analysis using this spectrum in Ref. [48]. We leave the derivation of $d\Gamma^u/ds_H$ with phase-space cuts to future work, and so have not compared this rate with Ref. [55].

3.7.4 Comparison with the local OPE

A non-trivial check on our power-correction results can be obtained by expanding the subleading shape functions in a manner appropriate to the case where the local OPE

is valid. Essentially this means expanding

$$\delta(\ell^+ - in\cdot D) = \delta(\ell^+) - \delta'(\ell^+) in\cdot D + \dots . \tag{3.198}$$

The comparison will be made at the level of the partonic $d\Gamma^u/dx$ decay rate, and we define $w = m_B u_H - \overline{\Lambda}$. From Eq. (3.194) we have

$$\begin{aligned}
\frac{1}{\hat\Gamma_0^u}\frac{d\Gamma^u}{dx} &= 2\Big(\frac{m_B}{m_b}\Big)^4 \int_0^{1-x_H} du_H \Big\{ m_B(1-4u_H) f^{(0)}(\overline{\Lambda}-m_B u_H) + \frac{1}{2} f_0^{(2)}(\overline{\Lambda}-m_B u_H) \\
&\quad - \frac{(\lambda_1+3\lambda_2)}{2} f^{(0)\prime}(\overline{\Lambda}-m_B u_H) + (\overline{\Lambda}-m_B u_H)\, f^{(0)}(\overline{\Lambda}-m_B u_H) - f_2^{(2)}(\overline{\Lambda}-m_B u_H) \\
&\quad - 3F_3(m_B u_H) + 3F_4(m_B u_H) - 24\pi\alpha_s(\mu_0)\, F_5^u(m_B u_H) \Big\} + K(\lambda_H, x_H) \\
&= 2\Big(\frac{m_B}{m_b}\Big)^4 \int_{-\overline{\Lambda}}^{m_b(1-x)} dw \Big\{ \Big[1 - \frac{4w}{m_b} - \frac{4\overline{\Lambda}}{m_b}\Big] f^{(0)}(-w) + \frac{1}{2m_b} f_0^{(2)}(-w) - \frac{w}{m_b} f^{(0)}(-w) \\
&\quad - \frac{1}{m_b} f_2^{(2)}(-w) - \frac{3}{m_b} F_3(w+\overline{\Lambda}) + \frac{3}{m_b} F_4(w+\overline{\Lambda}) - \frac{24\pi\alpha_s(\mu_0)}{m_b}\, F_5^u(w+\overline{\Lambda}) \Big\} \\
&\quad + K(\lambda_H, x_H),
\end{aligned} \tag{3.199}$$

where $x = 2E_\ell/m_b$ and $\hat\Gamma_0^u = m_b^5/m_B^5\,\Gamma_0^u$. In writing the second equality, the $(\lambda_1+3\lambda_2)$ term was cancelled by the change in the upper limit of integration. The $-4\overline{\Lambda}/m_b$ term cancels the leading term in the expansion of $(m_B/m_b)^4$, while the terms that cancel higher terms are beyond order λ^2 in the SCET result. The F_5 term gives an α_s/m_b^3 term, which we shall drop below. In expanding the shape functions, we obtain singular functions peaking at $x = 1$, so it is safe to take $\lambda_H = 1$ and drop $K(\lambda_H, x_H)$. For the remaining shape functions, the local expansion gives [25]

$$\begin{aligned}
f^{(0)}(-w) &= \delta(w) - \frac{\lambda_1}{6}\,\delta''(w) - \frac{\rho_1}{18}\,\delta'''(w) + \dots , \\
f_0^{(2)}(-w) &= -(\lambda_1+3\lambda_2)\,\delta'(w) + \frac{\tau}{2}\,\delta''(w) + \dots , \\
f_2^{(2)}(-w) &= \lambda_2\,\delta'(w) + \frac{\rho_2}{2}\,\delta''(w) + \dots , \\
F_3(\overline{\Lambda}+w) &= -\frac{2}{3}\lambda_1\,\delta'(w) + \dots , \\
F_4(\overline{\Lambda}+w) &= -\lambda_2\,\delta'(w) + \dots ,
\end{aligned} \tag{3.200}$$

where λ_1, λ_2, ρ_1, ρ_2 are the standard HQET parameters, which are matrix elements of local operators, τ is a combination of time-ordered products of HQET operators, and terms beyond $1/m_b^3$ have been dropped. Substituting this result into Eq. (3.199) and integrating by parts using the relations [25] $\int dw[w\delta''(w)] = \int dw[-2\delta'(w)]$ and $\int dw[w\delta'''(w)] = \int dw[-3\delta''(w)]$, which are valid with smooth test functions, we find

$$\begin{aligned}\frac{1}{\hat{\Gamma}_0^u}\frac{d\Gamma^u}{dx} &= 2\theta(1-x) - \frac{\lambda_1}{3m_b^2}\,\delta'(1-x) - \frac{\lambda_1}{3m_b^2}\,\delta(1-x) - \frac{11\lambda_2}{m_b^2}\,\delta(1-x) \\ &\quad + \frac{\tau}{2m_b^3}\,\delta'(1-x) - \frac{\rho_1}{9m_b^3}\,\delta''(1-x) - \frac{5\rho_1}{3m_b^3}\,\delta'(1-x) - \frac{\rho_2}{m_b^3}\,\delta'(1-x)\,. \end{aligned} \tag{3.201}$$

This agrees exactly with the result obtained from the local OPE in Refs. [119, 79]. (Note that we do not compare the $1/m_b^3$ annihilation term, which does not arise from one of the shape functions appearing at order λ^2 in SCET.)

Of the terms in Eq. (3.201), it is those proportional to λ_1 and ρ_1 that test the difference between our results and those in Ref. [25]. Ref. [25] also obtained the λ_1 result in Eq. (3.201), and even though we disagree on the $u_H f^{(0)}$ and F_3 terms, the combination of the two gives the same λ_1 result. For the ρ_1 terms, their $\rho_1\delta''$ term agrees with Eq. (3.201), but the $\rho_1\delta'$ term does not. In the very recent paper [117] it was pointed out that from the local OPE the coefficient of the $\rho_1\delta'$ term should be $-5/3$, as in Eq. (3.201), rather than the $-1/3$ quoted in [25].

Ref. [117] went further to advocate a different approach to the shape-function region that involves using an unexpanded b-quark field, and doing this obtained a result with subleading shape functions whose expansion is consistent with the local OPE in Eq. (3.201). However, their result for the power-suppressed $d\Gamma^u/dx$ decay rate does not agree with the rate obtained here. In particular, our $-4u_H F$ term is not present there, and instead of our $-3F_3$ term they have the result "$4F_1 + 2G_2 - 3G_3$". Their "G_2" term is defined by operators that, in our analysis, can only show up suppressed by at least one factor of α_s through jet functions. In fact, the operator structure of our result actually agrees with the original one in Ref. [25], rather than the one in Ref. [117]. No proof of factorization has yet been achieved for this approach with the unexpanded b-quark field, and it is conceivable that this may help to explain

why a different structure of operators was obtained.

3.8 Conclusions and Discussion

In this chapter, we have computed a factorization theorem for the leading-order power corrections to inclusive $B \to X_s\gamma$ and $B \to X_u\ell\bar{\nu}$ decays in the endpoint region, where the X is jet-like. In particular, we have shown that these power corrections can be fully categorized and thus treated in a systematic fashion using the Soft-Collinear Effective Theory. A main result of our analysis is that perturbative power corrections to the decay rates can be systematically computed, and our result explicitly disentangles hard factors of $\alpha_s(m_b^2)$, collinear jet-induced factors of $\alpha_s(m_X^2)$, and soft ("$\alpha_s(\Lambda^2)$") non-perturbative QCD effects.

In addition, our results can be used as a starting point for the systematic resummation of Sudakov double logarithms in the power corrections. To achieve this, one needs to compute the anomalous dimensions of all the operators we have defined that appear in the subleading factorization theorem. Some of the terms here are already known. In the body of the chapter, we have shown that if we consider only subleading terms with non-vanishing jet functions at lowest order in α_s, then the logarithms that can be resummed into the hard function in these NLO contributions are *identical* to the analogous logarithms in the LO result. (These logs can be thought of as occurring between the scales m_b^2 and $m_b\Lambda$.) There are additional logarithms that are sensitive to the split between the jet and soft functions (logs between $m_b\Lambda$ and Λ^2), which require knowledge of the anomalous dimensions of subleading soft operators. The latter are very unlikely to be universal, and have not been computed here.

Our main final decay-rate formulae have been collected in Sec. 3.7. At lowest order in α_s, they include a derivation of the power corrections for the triply differential $B \to X_u\ell\bar{\nu}$ rate. Results have been derived in the literature for $d\Gamma/dE_\gamma$ in $B \to X_s\gamma$ [26] and the singly differential $B \to X_u\ell\bar{\nu}$ rate $d\Gamma/dE_\ell$ [108, 25, 117] (and $d\Gamma/dm_X^2$ [55]), and a comparison was given in Sec. 3.7.3. Agreement was found for $B \to X_s\gamma$, but for $d\Gamma/dE_\ell$ we found disagreement on two terms at subleading order. (A check on our

$d\Gamma/dE_\ell$ result was obtained by expanding it to compare with the local OPE, and full agreement was found up to $1/m_b^3$, as discussed in Sec. 3.7.4.) Using our results, we found it straightforward to present the power corrections to doubly differential rates, as well as other singly differential rates such as $d\Gamma/dp_X^-$ and $d\Gamma/dp_X^+$.

On the phenomenological side, a potentially interesting result is the identification of two new shape functions, which involve four-quark operators and have not been previously considered in the literature. They are denoted by $f_{5,6}$ ($F_{5,6}$), and definitions can be found in Eq. (3.120). In the endpoint decay rates they induce power-suppressed terms, which are quite large, of order

$$4\pi\alpha_s \frac{\Lambda}{m_b} \,. \tag{3.202}$$

Since $4\pi\alpha_s \sim 4$, these power corrections might numerically dominate over those that are simply of order $\alpha_s^0 \Lambda/m_b$. We have given results for the effect of these shape functions in all the considered decay rates. In our results for the decay rates, the numerical prefactors for $f_{5,6}$ turned out to be sizeable (e.g. $24\pi\alpha_s$ for f_5 in $d\Gamma/dE_\ell$), which justifies including the factor of 4 in Eq. (3.202). For the extraction of $|V_{ub}|$ from $d\Gamma/dE_\ell$, the important thing to consider is the difference between how these new shape functions affect $B \to X_u \ell\bar{\nu}$ and $B \to X_s\gamma$. In this case, comparing the combinations of F and F_5 in Eqs. (3.193) and (3.194), we see that the mismatch is

$$\simeq -8\pi\alpha_s(\mu_0)\big[3F_5^u - F_5^s\big] \,, \tag{3.203}$$

where the index u or s denotes the fact that these shape functions involve different flavours of light quark. To obtain a numerical estimate we approximate $F_5^u/(m_B F) \simeq F_5^s/(m_B F) \sim \Lambda/m_b\epsilon' \simeq 0.1\epsilon'$ and find that they can cause a deviation of

$$-16\pi\alpha_s(\mu_0)\, 0.1\epsilon' \simeq (180\%)\epsilon' \,, \tag{3.204}$$

where ϵ' denotes any additional dynamical suppression from the non-perturbative functions. This suggests that, even for $\epsilon' \sim 0.1 - 0.3$, these terms provide a size-

able new uncertainty for the cut spectrum $d\Gamma/dE_\ell$ approach to measuring $|V_{ub}|$. From Eq. (3.197) we see that the situation seems to be only slightly better for a cut $d\Gamma/dp_X^+$ spectrum. On the other hand, since the completion of the research described in this chapter, other groups have used model-dependent arguments, incorporating the vacuum-insertion approximation and numerical work, to estimate that the effects of $f_{5,6}$ are $\sim 5\%$ [128, 36]. One possible future direction is to derive experimental bounds on the new subleading shape-function effects by comparing endpoint-dependent methods with different spectra and different cuts on the phase space. It would also be useful to find model-independent ways of determining the size of the subleading shape functions that go beyond the simple dimensional analysis used here.

Theoretically, there are several avenues for future work on $B \to X_s\gamma$ and $B \to X_u\ell\bar{\nu}$. These include the calculation of perturbative corrections in the factorization theorems at subleading order, as well as a complete resummation of Sudakov logarithms. It would also be interesting to consider the structure of the subleading factorization theorems in moment space, as opposed to the momentum-space version considered here. Starting with our triply differential $B \to X_u\ell\bar{\nu}$ result, one could derive other doubly and singly differential decay spectra and consider their phenomenological implications. More formally, it remains to be checked that the convolutions that appear in our subleading factorization theorems actually converge when the functional forms of the jet functions are considered at higher orders in α_s. From a formal standpoint this is necessary for a complete "proof" of these results as factorization theorems. However, from a pragmatic standpoint this can be checked as each new phenomenologically relevant term is computed. We are not aware of any factorization formulae where convergence problems occur at higher orders in the perturbative expansion of the kernels when they are not present in the leading non-vanishing kernel results (the convergence of which we have checked). Finally, it should also be possible to extend the techniques used here to closely related physical cases such as deep inelastic scattering for $x \to 1$ (i.e. Bjorken $x \sim 1 - \Lambda/Q$).

Chapter 4

Shape-Function Effects and Split Matching in $B \to X_s \ell^+ \ell^-$

4.1 Introduction

In this chapter, we study $B \to X_s \ell^+ \ell^-$ ($\ell = e, \mu$) in the shape function region for the first time. We derive the proper theoretical expression for the leading-order triply differential decay rate, which incorporates non-perturbative effects that appear at this order and a correct treatment of the perturbative corrections at each of the scales. Using the Soft-Collinear Effective Theory (SCET) we prove that the non-perturbative dynamics governing the measurable low-q^2 spectra in $B \to X_s \ell^+ \ell^-$ is determined by the same universal shape function as in endpoint $B \to X_u \ell \bar{\nu}$ and $B \to X_s \gamma$ decays. We also prove that the decay rate can be split into a product of scale-invariant terms, capturing physics at scales above and below m_b. We show that this procedure, which we call "split matching", can be used to deal with a tension between the perturbative corrections that come from these two regions. Implications for relating the $B \to X_s \ell^+ \ell^-$ measurements with the m_X cut to the Wilson coefficients are presented in Chapter 5.

As stated previously, the inclusive rare decay $B \to X_s \ell^+ \ell^-$ is complementary to $B \to X_s \gamma$ in the search for physics beyond the Standard Model. Provided that one makes suitable phase-space cuts to avoid $c\bar{c}$ resonances, $B \to X_s \ell^+ \ell^-$ is dominated

by the quark-level process, which was calculated in Ref. [84]. Owing to the disparate scales, $m_b \ll m_W$, one encounters large logarithms of the form $\alpha_s^n(m_b)\log^n(m_b/m_W)$ (leading log [LL]), $\alpha_s^{n+1}(m_b)\log^n(m_b/m_W)$ (next-to-leading log [NLL]), etc., which should be summed. The NLL calculations were completed in Refs. [54, 121], and the NNLL analysis, although technically not fully complete, is at a level that the scale uncertainties have been substantially reduced, after the combined efforts of a number of groups [45, 63, 10, 8, 75, 9, 44, 77, 76].

Non-perturbative corrections to the quark-level result can also be calculated by means of a local operator product expansion (OPE) [131, 58, 43, 119], with non-perturbative matrix elements defined with the help of the Heavy Quark Effective Theory (HQET) [120]. As is the case for $B \to X_s\gamma$ and $B \to X_u\ell\bar{\nu}$, there are no $\mathcal{O}(1/m_b)$ corrections. The $\mathcal{O}(1/m_b^2)$ corrections and OPE were considered in Ref. [70] and subsequently corrected in Ref. [7]. The $\mathcal{O}(1/m_b^3)$ corrections were computed in Ref. [21, 20]. There are also non-perturbative contributions arising from the $c\bar{c}$ intermediate states. The largest $c\bar{c}$ resonances, i.e. the J/ψ and ψ', can be removed by suitable cuts in the dileptonic mass spectrum. It is generally believed that the operator product expansion holds for the computation of the dileptonic invariant mass as long as one avoids the region with the first two narrow resonances, although no complete proof of this (for the full operator basis) has been given. A picture for the structure of resonances can be obtained using the model of Krüger and Sehgal [101], which estimates factorizable contributions based on a dispersion relation and experimental data on $\sigma(e^+e^- \to c\bar{c} + \text{hadrons})$. Non-factorizable effects have been estimated in a model-independent way by means of an expansion in $1/m_c$ [61, 50] which is valid only away from the resonances.

Staying away from the resonance regions in the dileptonic mass spectrum leaves two perturbative windows, the low- and high-q^2 regions, corresponding to $q^2 \leq 6\,\text{GeV}^2$ and $q^2 \geq 14.4\,\text{GeV}^2$ respectively. These have complementary advantages and disadvantages [77]. For example, the latter has significant $1/m_b$ corrections but negligible scale and charm-mass dependence, whereas the former has small $1/m_b$ corrections but non-negligible scale and charm-mass dependence. The low-q^2 region has a high

rate compared to the high-q^2 region and so experimental spectra will become precise for this region first. However, at low q^2 an additional cut is required, making measurements less inclusive. In particular, a hadronic invariant-mass cut is imposed in order to eliminate the combinatorial background, which includes the semileptonic decay $b \to c(\to s e^+ \nu)\, e^- \bar{\nu} = b \to s e^+ e^-$ + missing energy. The latest analyses from *BABAR* and Belle impose cuts of $m_X \leq 1.8\,\text{GeV}$ and $m_X \leq 2.0\,\text{GeV}$ respectively [14, 91, 12, 95], which in the B-meson rest frame correspond to $q^0 \gtrsim 2.3\,\text{GeV}$ and put the decay rate in the shape function region. This cut dependence has so far been analyzed only in the Fermi-motion model [5, 6].

Existing calculations for $B \to X_s \ell^+ \ell^-$ are based on a local operator product expansion in Λ_{QCD}/m_b. When $m_X^2 \lesssim m_b \Lambda \sim (2\,\text{GeV})^2$, this operator product expansion breaks down, and, instead of depending on non-perturbative parameters $(\lambda_1, \lambda_2, \ldots)$ that are matrix elements of local operators, the decay rates depend on non-perturbative functions. Furthermore, in this region the standard perturbative α_s corrections to the partonic process $b \to s \ell^+ \ell^-$ do not apply, since some of these corrections become non-perturbative. Thus, even at leading order there does not exist in the literature a model-independent computation of the $B \to X_s \ell^+ \ell^-$ decay rate that can be compared directly with the data at low q^2.

As should be clear from Chapter 3, the endpoint region has been the focus of much work in the context of $B \to X_s \gamma$ and $B \to X_u \ell \bar{\nu}$ (see e.g. Refs. [125, 124, 41, 99, 30, 113, 112, 111, 116, 27, 47, 26, 108, 25, 106, 49, 36, 102]). Recall that in $B \to X_u \ell \bar{\nu}$ this is because of the cuts used to eliminate the dominant $b \to c$ background. In $B \to X_s \gamma$, it is known that cuts with $q^0 \gtrsim 2.1\,\text{GeV}$ put us in the shape function region.[1]

In the small-q^2 region of $B \to X_s \ell^+ \ell^-$ with $q^0 \geq 2.3\,\text{GeV}$, shape-function effects also dominate rather than the expansion in local operators. To see this, we note that the m_X cut causes $2 m_B E_X = m_B^2 + m_X^2 - q^2 \gg m_X^2$. Decomposing $2E_X = p_X^+ + p_X^-$ with

[1] In Ref. [129] it was pointed out that even a cut of $E_\gamma \geq E_0 = 1.8\,\text{GeV}$, corresponding to $m_X \lesssim 3\,\text{GeV}$, might not guarantee that a theoretical description in terms of the local OPE is sufficient, owing to sensitivity to the scale $\Delta = m_b - 2E_0$ in power and perturbative corrections. Using a multi-scale OPE with an expansion in Λ/Δ allows the shape function and local OPE regions to be connected [27, 47, 129].

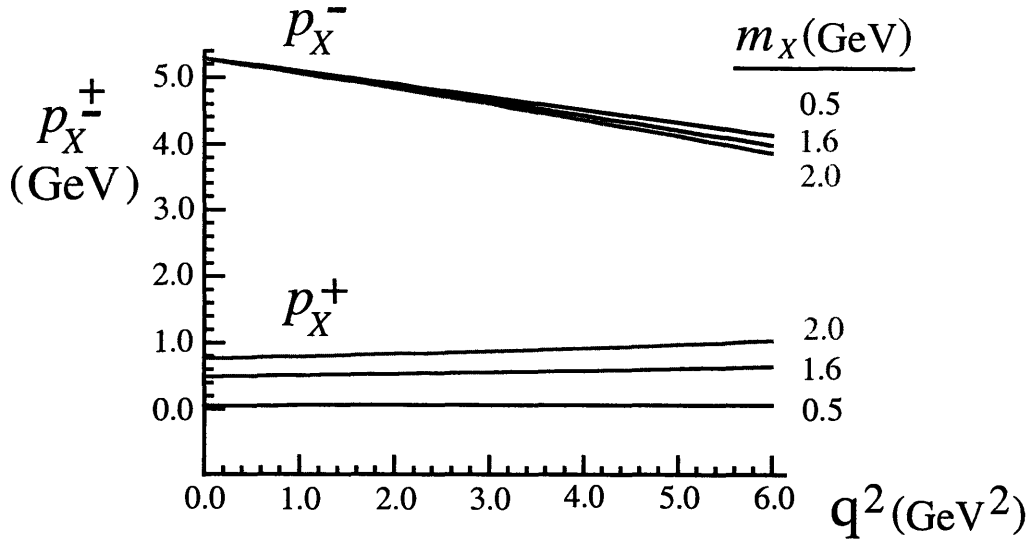

Figure 4-1: The kinematic range for p_X^- and p_X^+ given the experimental cuts of $q^2 < 6\,\mathrm{GeV}^2$ and $m_X \leq 2.0\,\mathrm{GeV}$ for $B \to X_s\ell^+\ell^-$.

$m_X^2 = p_X^- p_X^+$, we see that the X_s is jet-like with $p_X^- \gg p_X^+$, and the restricted sum over states in the X_s causes the non-perturbative shape functions to become important. For the experimental cuts on q^2 and m_X, values for $p_X^\pm$ are shown in Fig. 4-1. It should be clear from this figure that the measurable spectrum is dominated by decays for which $p_X^- \gg p_X^+$.

To compute $B \to X_s\ell^+\ell^-$ in the shape function region with renormalization-group evolution requires the following steps:

i) matching the Standard Model at $\mu \simeq m_W$ on to H_W,

ii) running H_W to $\mu \simeq m_b$,

iii) matching at $\mu \simeq m_b$ on to operators in SCET,

iv) running in SCET to $\mu \simeq \sqrt{m_b\Lambda}$,

v) computation of the imaginary part of forward-scattering time-ordered products in SCET at $\mu \simeq \sqrt{m_b\Lambda}$. This leads to a separation of scales in a factorization

theorem, which at LO takes the form[2]

$$d^3\Gamma^{(0)} = H \int dk\, \mathcal{J}^{(0)}(k)\, f^{(0)}(k)\,,$$

with perturbative H and $\mathcal{J}^{(0)}$, and the LO non-perturbative shape function $f^{(0)}$,

vi) evolution of the shape function $f^{(0)}$ from $\Lambda_{\rm QCD}$ up to $\mu \simeq \sqrt{m_b \Lambda_{\rm QCD}}$.

For the shape-function decay rate, steps i-ii) are the same as the local OPE results for $B \to X_s \ell^+ \ell^-$. Furthermore, based on the structure of leading-order SCET operators that we find for $B \to X_s \ell^+ \ell^-$, we demonstrate that results for other inclusive endpoint analyses can be used in steps iv) and vi) [22, 23, 47].[3] Because of this our computations focussed on steps iii) and v). In step iii) we show how to implement the split-matching procedure to formulate the perturbative corrections, which we elaborate on below. In step v) we derive a factorization theorem for $B \to X_s \ell^+ \ell^-$. This includes computing the hard coefficient functions H at NLL order and formulating the structure of these terms to all orders in α_s. It also includes a derivation of formulae for the decay rate and forward-backward asymmetry that properly take into account the effect of the current experimental cuts and the perturbative and non-perturbative corrections.

At leading order in the power expansion the result of steps i)-vi) takes the schematic form

$$\begin{aligned} d^3\Gamma^{(0)} \;&=\; \mathcal{E}(\mu_W) U_W(\mu_W,\mu_0) \mathcal{B}(\mu_0) U_H(\mu_0,\mu_i) \mathcal{J}(\mu_i) U_S(\mu_i,\mu_\Lambda) f^{(0)}(\mu_\Lambda)\,, \\ &\qquad \mu_W \simeq m_W\,,\ \mu_0 \simeq m_b\,,\ \mu_i \simeq (m_b\Lambda)^{1/2}\,,\ \mu_\Lambda \simeq 1\,\text{GeV}\,, \end{aligned} \tag{4.1}$$

where $\mathcal{E}$, $\mathcal{B}$ and $\mathcal{J}$ represent matching at various scales, and U_W, U_H and U_S represent the running between these scales. Eq. (4.1) shows only the scale dependence explicitly,

[2]Note that the operator product expansion used here occurs at $\mu \simeq \sqrt{m_b \Lambda}$, rather than at m_b^2, as in the standard local OPE.

[3]In step iv) we can run the hard functions down using results from Refs. [22, 23]. In step vi) we can run the shape function up to the intermediate scale using the simple result from Ref. [47]. An equally valid option would be to evolve the perturbative parts of the rate down to a scale $\mu \simeq 1$ GeV, as considered earlier [112, 113, 111, 27, 22].

not the kinematic dependences or the convolutions between $\mathcal{J}$, U_S, and $f^{(0)}$, which we describe later on.

In a standard application of renormalization-group-improved perturbation theory (LL, NLL, NNLL, etc.), the results at each stage of matching and running are tied together, as depicted in Eq. (4.1). Usually this would not be a problem, but for $B \to X_s \ell^+ \ell^-$ the nature of the perturbative expansion above and below $\mu \simeq m_b$ is different. Above $\mu \simeq m_b$ the series of $(\alpha_s \ln)^k$ terms are of the traditional form, with a basis of ~ 10 operators (including four-quark operators), whose mixing is crucial. Below $\mu \simeq m_b$ we demonstrate that the evolution is universal (to all orders in α_s) for the leading-order operators, but there are Sudakov double logarithms of the ratios of scales, which give a more complicated series. It turns out to be convenient to decouple these two stages of resummation so that one can consider working to different orders in the α_s expansion above and below $\mu = m_b$. There is a simple reason why this decoupling is important: for $\mu \geq m_b$ the power counting and running are for currents in the electroweak Hamiltonian and dictate treating $C_9 \sim 1/\alpha_s$ with $C_7 \sim 1$ and $C_{10} \sim 1$. However, at $\mu = m_b$ the coefficients C_9 and C_{10} are numerically comparable. For $\mu \leq m_b$ in the shape function region we must organize the power counting and running for time-ordered products of currents in SCET rather than amplitudes, and it would be vexing to have to include terms $\propto C_9^2$ to $\mathcal{O}(\alpha_s^2)$ before including the C_{10}^2 and C_7^2 terms at order $\mathcal{O}(\alpha_s^0)$. Thus, once we are below the scale m_b, a counting with $C_9 \sim C_{10} \sim C_7 \sim 1$ is more appropriate.

To decouple these two regions for $B \to X_s \ell^+ \ell^-$ decays we make use of two facts: i) for $\mu \geq m_b$ the operator $\mathcal{O}_{10}$ involves a conserved current and has no operators mixing into it, so it does not have an anomalous dimension, and ii) for $\mu \leq m_b$ all LO biquark operators in the Soft-Collinear Effective Theory have the same anomalous dimension [23]. We shall show that the operators for $B \to X_s \ell^+ \ell^-$ are related to these biquark operators. These properties ensure that we can separate the perturbative treatments in these two regions at any order in perturbation theory. This is done by introducing two matching scales, $\mu_0 \simeq m_b$ and $\mu_b \simeq m_b$. The two aforementioned

facts allow us to write

$$\begin{aligned} U_W(\mu_W,\mu_0)\mathcal{B}(\mu_0)U_H(\mu_0,\mu_i) &= U_W(\mu_W,\mu_0)\mathcal{B}(\mu_0,\mu_b)U_H(\mu_b,\mu_i) \\ &= U_W(\mu_W,\mu_0)B_1(\mu_0)B_2(\mu_b)U_H(\mu_b,\mu_i)\,, \end{aligned} \tag{4.2}$$

with well-defined B_1 and B_2. We define $B_2(\mu_b)$ by using the matching for the operator $\mathcal{O}_{10}$ and extend this to find B_2 matching coefficients for the other operators using property ii) above. The remaining contributions match on to B_1. Diagrams which are related to the anomalous dimension for $\mu \geq m_b$ end up being matched at the scale μ_0 on to B_1, while those related to anomalous dimensions for $\mu \leq m_b$ are matched at a different scale, μ_b, on to B_2. This leaves

$$d^3\Gamma^{(0)} = \Big[\mathcal{E}(\mu_W)U_W(\mu_W,\mu_0)B_1(\mu_0)\Big]\Big[B_2(\mu_b)U_H(\mu_b,\mu_i)\mathcal{J}(\mu_i)U_S(\mu_i,\mu_\Lambda)f^{(0)}(\mu_\Lambda)\Big]\,, \tag{4.3}$$

which is the product of two pieces that are separately μ-independent. We refer to this procedure as "split matching" because formally we match diagrams at two scales rather than at a single scale. The two matching μ's are "split" because they are parametrically similar in the power-counting sense.

We organize the remainder of this chapter as follows. We begin by using split matching to determine the hard matching functions, $\mathcal{B} = B_1 B_2$, for $B \to X_s\ell^+\ell^-$ in SCET; this is one of the main points of this chapter. It is discussed in Sec. 4.2.1 at leading power and one-loop order (including both bottom-, charm-, and light-quark loops and other virtual corrections). The extension to higher orders is also illustrated. Steps i) and ii) are summarized in Sec. 4.2.1, together with Appendix C. In Sec. 4.2.2 we discuss the running for step iv) and give a brief derivation of why the anomalous dimension is independent of the Dirac structure to all orders in α_s. In Sec. 4.2.3, we discuss the basic ingredients for the triply differential decay rate and the forward-backward asymmetry in terms of hadronic tensors. A second main point of this chapter is the SCET matrix-element computation for $B \to X_s\ell^+\ell^-$, step v), which is performed in Sec. 4.2.4. In Sec. 4.2.5 we review the running for the shape function,

step vi). In Sec. 4.3 we present our final results for the differential decay rates at leading order in the power expansion, including all the ingredients from Sec. 4.2 and incorporating the relevant experimental cuts. The triply differential spectrum and doubly differential spectra are derived in subsections 4.3.1-4.3.4. Readers interested only in our final results may skip directly to Sec. 4.3. We compare numerical results for matching coefficients at m_b with terms in the local OPE in subsection 4.3.5. In Appendix D we briefly comment on how our analysis will change if we assume a parametrically small dileptonic invariant mass, $q^2 \sim \lambda^2$, rather than the scaling $q^2 \sim \lambda^0$ used in the body of the chapter. (For the case $q^2 \sim \lambda^2$, the rate for $B \to X_s \ell^+ \ell^-$ would *not* be determined by a factorization theorem with the same structure as for $B \to X_u \ell \bar{\nu}$.)

4.2 Analysis in the Shape Function Region

4.2.1 Matching on to SCET

We begin by reviewing the form of the electroweak Hamiltonian obtained after evolution down to the scale $\mu \simeq m_b$, and then perform the leading-order matching of this Hamiltonian on to operators in SCET. For the treatment of γ_5 we use the NDR scheme throughout. Below the scale $\mu = m_W$, the effective Hamiltonian for $b \to s\ell^+\ell^-$ takes the form [84]

$$\mathcal{H}_W = -\frac{4G_F}{\sqrt{2}} V_{tb} V_{ts}^* \sum_{i=1}^{10} C_i(\mu) \mathcal{O}_i(\mu) \,, \tag{4.4}$$

where we have used unitarity of the CKM matrix to remove $V_{cb}V_{cs}^*$ dependence and have neglected the tiny $V_{ub}V_{us}^*$ terms. The operators $\mathcal{O}_1(\mu)$ to $\mathcal{O}_8(\mu)$ are the same ones we have already encountered in studying $B \to X_s\gamma$. The two additional operators are

$$\mathcal{O}_9 = \frac{e^2}{16\pi^2} \bar{s}_{L\alpha} \gamma^\mu b_{L\alpha} \bar{\ell} \gamma_\mu \ell, \qquad \mathcal{O}_{10} = \frac{e^2}{16\pi^2} \bar{s}_{L\alpha} \gamma^\mu b_{L\alpha} \bar{\ell} \gamma_\mu \gamma_5 \ell \,, \tag{4.5}$$

In the following, we shall once again neglect the mass of the strange quark in $\mathcal{O}_{7,8}$. For our analysis, m_s is not needed as a regulator for IR divergences, which are explicitly cut off by non-perturbative scales $\sim \Lambda_{\rm QCD}$. In the shape function region, the m_s dependence is small and was computed in Ref. [60]. Non-perturbative sensitivity to m_s shows up only at subleading power, while computable $\mathcal{O}(m_s^2/m_b\Lambda_{\rm QCD})$ jet-function corrections are numerically smaller than the $\Lambda_{\rm QCD}/m_b$ power corrections.

At NLL order, one requires the NLL Wilson coefficient of $\mathcal{O}_9$ and the LL coefficients of the other operators. For $\mathcal{O}_{7,9,10}$ these are given by [121, 54]

$$\begin{aligned}
C_7^{\rm NDR}(\mu) &= r_0^{-\frac{16}{23}}\, C_7(M_W) + \frac{8}{3}\left(r_0^{-\frac{14}{23}} - r_0^{-\frac{16}{23}}\right) C_8(M_W) + \sum_{i=1}^{8} t_i\, r_0^{-a_i}, \qquad (4.6)\\
C_9^{\rm NDR}(\mu) &= P_0^{NDR}(\mu) + \frac{Y(m_t^2/M_W^2)}{\sin^2\theta_W} - 4Z(m_t^2/M_W^2) + P_E(\mu)E(m_t^2/M_W^2),\\
C_{10}(\mu) &= C_{10}(M_W) = -\frac{Y(m_t^2/M_W^2)}{\sin^2\theta_W},
\end{aligned}$$

where $C_7(m_W)$, $C_8(m_W)$ and the Inami-Lim functions Y, Z, and E are obtained from matching at $\mu = m_W$, and are given in Appendix C. The μ-dependent factors include [121, 54]

$$\begin{aligned}
P_0^{NDR}(\mu) &= \frac{\pi}{\alpha_s(M_W)}\left(-0.1875 + \sum_{i=1}^{8} p_i\, r_0^{-a_i-1}\right) + 1.2468\\
&\quad + \sum_{i=1}^{8} r_0^{-a_i}\left(\rho_i^{NDR} + s_i\, r_0^{-1}\right),\\
P_E(\mu) &= 0.1405 + \sum_{i=1}^{8} q_i\, r_0^{-a_i-1}, \qquad r_0 = \frac{\alpha_s(\mu)}{\alpha_s(m_W)}. \qquad (4.7)
\end{aligned}$$

The numbers t_i, a_i, $\rho_i^{\rm NDR}$, s_i, q_i that appear here are listed in Appendix C. Results for the running coefficients of the four-quark operators, $C_{1-6}(\mu)$, can be found in Ref. [54]. We have modified the standard notation slightly (e.g. $r_0(\mu)$) to conform with additional stages of the RG evolution discussed in sections 4.2.2 and 4.2.5. Contributions beyond NLL will be mentioned below.

At a scale $\mu \approx m_b$, we need to match $b \to s\ell^+\ell^-$ matrix elements of $\mathcal{H}_{\rm W}$ on to

matrix elements of operators in SCET with a power expansion in the small parameter λ, where $\lambda^2 \sim \Lambda_{\rm QCD}/m_b$. For convenience, we refer to the resulting four-fermion scalar operators in SCET as "currents" and use the notation $J_{\ell\ell}$. In SCET we also need the effective Lagrangians. The heavy quark in the initial state is matched on to an HQET field h_v, and the light energetic strange quark is matched on to a collinear field ξ_n. For the leading-order analysis in Λ/m_b we need only the lowest-order terms,

$$\mathcal{H}_W = -\frac{G_F\alpha}{\sqrt{2}\pi}\,(V_{tb}V_{ts}^*)\,J_{\ell\ell}^{(0)}\,, \qquad \mathcal{L} = \mathcal{L}_{\rm HQET}^{(0)} + \mathcal{L}_{\rm SCET}^{(0)}\,, \tag{4.8}$$

where $J_{\ell\ell}^{(0)}$ is the LO operator.

To simplify the analysis we treat both m_c and m_b as hard scales and integrate out both charm and bottom loops at $\mu \simeq m_b$. At leading order in SCET, the currents that we match on to are

$$\begin{aligned} J_{\ell\ell}^{(0)} = & \sum_{i=a,b,c} C_{9i}(s)\,\big(\bar\chi_{n,p}\Gamma_i^{(v)\mu}\mathcal{H}_v\big)\big(\bar\ell\gamma_\mu\ell\big) + \sum_{i=a,b,c} C_{10i}(s)\,\big(\bar\chi_{n,p}\Gamma_i^{(v)\mu}\mathcal{H}_v\big)\big(\bar\ell\gamma_\mu\gamma_5\ell\big) \\ & - \sum_{j=a,\ldots,d} C_{7j}(s)\,2m_B\big(\bar\chi_{n,p}\Gamma_j^{(t)\mu}\mathcal{H}_v\big)\big(\bar\ell\gamma_\mu\ell\big)\,, \end{aligned} \tag{4.9}$$

where the sum is over Dirac structures to be discussed below. The simple structure of these LO SCET operators is quite important to our analysis: for example, by power counting there are no four-quark operators that need to be included in SCET at this order. The B momentum, total momentum of the leptons, and jet momentum (sum of the four-momenta of all the hadrons in X_s) are

$$p_B^\mu = m_B v^\mu\,, \qquad q^\mu = p_{\ell^+}^\mu + p_{\ell^-}^\mu\,, \qquad p_X^\mu = n\cdot p_X\,\frac{\bar n^\mu}{2} + \bar n\cdot p_X\,\frac{n^\mu}{2}\,, \tag{4.10}$$

respectively. As in the previous chapter, we shall use the hadronic dimensionless variables

$$x_H = \frac{2E_{\ell^-}}{m_B}\,, \qquad \overline{y}_H = \frac{\bar n\cdot p_X}{m_B}\,, \qquad u_H = \frac{n\cdot p_X}{m_B}\,, \qquad y_H = \frac{q^2}{m_B^2}\,. \tag{4.11}$$

In SCET the total partonic $\bar{n}\cdot p$ momentum of the jet is a hard momentum $\sim m_b$ and also appears in the SCET Wilson coefficients. At LO, $\bar{n}\cdot p = (m_b^2 - q^2)/m_b$ and demanding that $\bar{n}\cdot p$ is large means only that q^2 cannot be too close to m_b^2. For example, neither $q^2 \approx 0$ nor $q^2 \approx m_b^2/2$ modifies the power counting for $\bar{n}\cdot p$. Thus, there is no requirement to impose a scaling that q^2 be small. For convenience, in the hard coefficients we write

$$C\big(\bar{n}\cdot p, m_b, \mu_0, \mu_b\big) \to C\big(s, m_b, \mu_0, \mu_b\big)\,, \qquad\qquad s = \frac{q^2}{m_b^2}\,, \tag{4.12}$$

since the partonic variable s is a more natural choice in $b \to s\ell^+\ell^-$ and is equivalent at LO. For purposes of power counting in this chapter we count $s \sim \lambda^0$. We shall see in section 4.3.5 that varying s causes a very mild change in the coefficients. In Appendix D we briefly explore a different scenario, in which $s \sim \lambda^2$. A distinction between two matching scales μ_0 and μ_b is made in C in order to separate the decay rate into two μ-independent pieces, as displayed in Eq. (4.3). For power counting purposes, $\mu_0 \sim \mu_b \sim m_b$ and formally $\mu_0 \geq \mu_b$. For numerical work one can take $\mu_0 = \mu_b$.

In Eq. (4.9) we begin with a complete set of Dirac structures for the vector and tensor currents in SCET, namely

$$\Gamma^{(v)}_{a-c} = P_R\Big\{\gamma^\mu\,, v^\mu\,, \frac{n^\mu}{n\cdot v}\Big\}\,, \quad \Gamma^{(t)}_{a-d} = P_R\,\frac{q_\tau}{q^2}\,\Big\{i\sigma^{\mu\tau}\,, \gamma^{[\mu}v^{\tau]}\,, \frac{\gamma^{[\mu}n^{\tau]}}{n\cdot v}\,, \frac{n^{[\mu}v^{\tau]}}{n\cdot v}\Big\}\,. \tag{4.13}$$

These come with Wilson coefficients $C_{9a,b,c}$ and $C_{7a,b,c,d}$ respectively. This basis is over-complete for $B \to X_s\ell^+\ell^-$, but considering a redundant basis makes it easy to incorporate pre-existing perturbative calculations for the currents into our computations. Only the coefficients $C_{7a,9a}$ appear at tree level, but for heavy-to-light currents it is known that the other structures become relevant once perturbative corrections are included. For simplicity of notation, we treat the $1/q^2$ photon propagator in $\Gamma^{(t)}_j$ as part of the effective-theory operator.[4]

[4]If we instead demand that the momentum q^2 be collinear in the $\bar{n}$ direction, with $s \sim \lambda^2$, then the SCET operator with a photon field strength should be kept, and will then be contracted with

To reduce the basis in Eq. (4.13) further, we can use i) current conservation, $q^\mu \bar{\ell}\gamma_\mu \ell = 0$, ii) $q^\mu \bar{\ell}\gamma_\mu\gamma_5 \ell = 0$ for massless leptons, iii) a reduction of the tensor $\Gamma^{(t)}$ Dirac structures into vector structures, since they are all contracted with q_τ. Constraint ii) allows us to eliminate C_{10c}. Taken together, constraints i) and iii) allow us to reduce the seven terms C_{9i} and C_{7i} to two independent coefficients. For our new basis of operators we take

$$\begin{aligned} J_{\ell\ell}^{(0)} &= \mathcal{C}_9 \left(\bar{\chi}_{n,p} P_R \gamma^\mu \mathcal{H}_v\right)\left(\bar{\ell}\gamma_\mu \ell\right) - \mathcal{C}_7 \frac{2m_B\, q_\tau}{q^2}\left(\bar{\chi}_{n,p} P_R\, i\sigma^{\mu\tau} \mathcal{H}_v\right)\left(\bar{\ell}\gamma_\mu \ell\right) \\ &\quad + \mathcal{C}_{10a}\left(\bar{\chi}_{n,p} P_R \gamma^\mu \mathcal{H}_v\right)\left(\bar{\ell}\gamma_\mu\gamma_5 \ell\right) + \mathcal{C}_{10b}\left(\bar{\chi}_{n,p} P_R v^\mu \mathcal{H}_v\right)\left(\bar{\ell}\gamma_\mu\gamma_5 \ell\right), \quad (4.14) \end{aligned}$$

and find that

$$\begin{aligned} \mathcal{C}_9 &= C_{9a} + \frac{C_{9b}}{2} - \frac{m_B}{n\cdot q} C_{7b} + \frac{2m_B(C_{7c} - C_{7d}) + n\cdot q\, C_{9c}}{n\cdot q - \bar{n}\cdot q}, \quad (4.15) \\ \mathcal{C}_7 &= C_{7a} - \frac{C_{7b}}{2} - \frac{\bar{n}\cdot q}{4m_B} C_{9b} + \frac{1}{n\cdot q - \bar{n}\cdot q}\left[\frac{-q^2}{2m_B} C_{9c} - n\cdot q\, C_{7c} + \bar{n}\cdot q\, C_{7d}\right], \\ \mathcal{C}_{10a} &= C_{10a}, \\ \mathcal{C}_{10b} &= C_{10b} + \frac{2\, n\cdot q}{n\cdot q - \bar{n}\cdot q} C_{10c}. \end{aligned}$$

Our Dirac structures for the $\mathcal{C}_9$ and $\mathcal{C}_7$ terms in Eq. (4.14) were deliberately chosen, in order to make results for the decay rates appear as much as possible like those in the local OPE. The fact that the basis of SCET operators for $B \to X_s \ell^+ \ell^-$ involves only bilinear hadronic currents at LO means that in the leading-order factorization theorem we find the exact same non-perturbative shape function as for $B \to X_s\gamma$ and $B \to X_u \ell \bar{\nu}$. This is immediately evident from the operator-based proof of factorization in Ref. [30], for example. While the coefficients C_{9i}, C_{7i}, C_{10i} in Eq. (4.9) are functions only of $s = (n\cdot q)\,(\bar{n}\cdot q)/m_b^2$, the reduction of the basis of operators brings in additional kinematic dependence on $\bar{n}\cdot q$ and $n\cdot q$ for the $\mathcal{C}_i$'s (which is also the case in analyzing exclusive dileptonic decays [83]). At tree level we have $\mathcal{O}_{9,10}$ contributing to C_{9a} and

an operator with collinear leptons within SCET. In this case there will also be additional four-quark operators needed in the basis in Eq. (4.14).

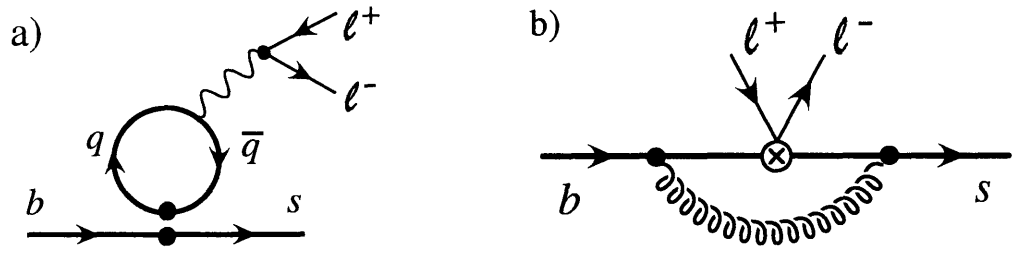

Figure 4-2: Graphs from H_W for matching on to SCET.

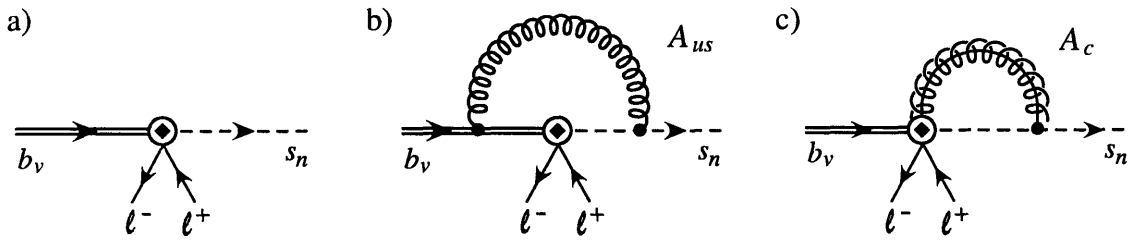

Figure 4-3: Graphs in SCET for the matching computation.

C_{10a}, and a contribution from $\mathcal{O}_7$ with the photon producing an $\ell^+\ell^-$ pair, which give

$$\mathcal{C}_9 = C_9^{\rm NDR}(\mu_0)\,, \quad \mathcal{C}_7 = \frac{\overline{m}_b(\mu_0)}{m_B}\, C_7^{\rm NDR}(\mu_0)\,, \quad \mathcal{C}_{10a} = C_{10}\,, \quad \mathcal{C}_{10b} = 0\,. \tag{4.16}$$

Beyond tree level there will be C_7 dependence in $\mathcal{C}_9$, and C_9 dependence in $\mathcal{C}_7$. Eq. (4.16) indicates that with our choice of basis the same short-distance dependence dominates in SCET: $\mathcal{C}_9 \approx C_9$, etc. We explore this further in Section 4.3.5. In Eq. (4.16) there is no distinction as to whether this matching is done at $\mu = \mu_0$ or $\mu = \mu_b$. The effective-theory operator in Eq. (4.14) was defined with a factor of m_B pulled out so that the μ-dependent factors $\overline{m}_b C_7^{\rm NDR}$ are contained in the coefficients $\mathcal{C}_7$.

At one-loop order, the full-theory diagrams needed for the matching are shown in Fig. 4-2 (plus wave-function renormalization, which is not shown). At this order the four-quark operators $\mathcal{O}_{1-6}$ contribute through Fig. 4-2a. The one-loop graphs in SCET with the operators in Eq. (4.14) are shown in Fig. 4-3 (plus wave-function renormalization, which is not shown). There are no graphs with four-quark operators within SCET since we treat $q^2 \sim \lambda^0$, so Fig. 4-2a matches directly on to $\mathcal{C}_9$.

As discussed in the introduction, we perform a split-matching procedure from the full theory above m_b on to SCET below m_b, making use of two matching scales μ_0 and μ_b. Contributions from this stage of matching therefore take the form

$$\mathcal{B}(\mu_0, \mu_b) = B_1(\mu_0) B_2(\mu_b) \,. \tag{4.17}$$

Since $\mathcal{O}_{10}$ has no anomalous dimension above m_b and there is a common universal anomalous dimension for all the operators in $J^{(0)}_{\ell\ell}$ below m_b, there is a well-defined prescription for carrying this out. We take all contributions that cause perturbative corrections to C_{10a} and C_{10b} to be at the scale μ_b, so for this operator $B_1(\mu_0) = C_{10}$, and at one-loop order $B_2(\mu_b)$ includes $\alpha_s(\mu_b)\ln^2(\mu_b)$, $\alpha_s(\mu_b)\ln(\mu_b)$, and $\alpha_s(\mu_b)$ terms from matching the vertex diagram Fig. 4-2b and wave-function diagrams on to SCET. The analogous contributions from vertex diagrams for C_9 and C_7 are also matched at $\mu = \mu_b$ to determine their $B_2(\mu_b)$'s (for C_7 the full-theory tensor current has a $\ln\mu$ that is matched at $\mu = \mu_0$). The universality of the anomalous dimensions in SCET guarantees that this procedure remains well defined at any order in perturbation theory and can be organized into the product structure displayed in Eq. (4.17). For C_9 and C_7 there are additional non-vertex-like contributions that are matched on to $B_1(\mu_0)$ at a scale $\mu_0 \geq \mu_b$. These include contributions from four-quark operators $\mathcal{O}_{1-6}$ in the full theory, which will match on to C_9 and C_7 in SCET.

The difference between the full-theory diagram in Fig. 4-2b and the SCET graphs in Fig. 4-3b,c is IR finite (where we must use the same IR regulator in both theories, as is always the case for matching computations). In the UV the full-theory graph in Fig. 4-2b plus wave-function renormalization is μ-independent since the current is conserved. The graphs in SCET induce a μ dependence and an anomalous dimension for the effective-theory currents. These terms are matched at $\mu = \mu_b$. We start with the basis in Eq. (4.9) and find

$$\begin{aligned} C_{10a}(\mu_0, \mu_b) &= C_{10}\Big[1 + \frac{\alpha_s(\mu_b)}{\pi}\,\omega_a^V(s, \mu_b)\Big] \,, \\ C_{10b,10c}(\mu_0, \mu_b) &= C_{10}\,\frac{\alpha_s(\mu_b)}{\pi}\,\omega_{b,c}^V(s) \,, \end{aligned} \tag{4.18}$$

with a constant μ_0-independent C_{10}. The perturbative coefficients were computed in Ref. [23], and setting $\bar{n}\cdot p/m_b = (1-s)$ we find

$$\begin{aligned}
\omega_a^V(s,\mu_b) &= -\frac{1}{3}\Big[2\ln^2(1-s) + 2\mathrm{Li}_2(s) + \ln(1-s)\Big(\frac{1-3s}{s}\Big) + \frac{\pi^2}{12} + 6 \\
&\qquad + 2\ln^2\Big(\frac{\mu_b}{m_b}\Big) + 5\ln\Big(\frac{\mu_b}{m_b}\Big) - 4\ln(1-s)\ln\Big(\frac{\mu_b}{m_b}\Big)\Big], \\
\omega_b^V(s) &= \frac{1}{3}\Big[\frac{2}{s} + \frac{2(1-s)}{s^2}\ln(1-s)\Big], \\
\omega_c^V(s) &= \frac{1}{3}\Big[\frac{(2s-1)(1-s)}{s^2}\ln(1-s) - \frac{(1-s)}{s}\Big].
\end{aligned} \tag{4.19}$$

For the matching on to $C_{9a,b,c}$ in the basis in Eq. (4.9) we have the same perturbative coefficients $\omega_{a,b,c}$ as for $C_{10a,b,c}$, because only the leptonic current differs:

$$\begin{aligned}
C_{9a}(\mu_0,\mu_b) &= C_9^{\rm mix}(\mu_0)\Big[1 + \frac{\alpha_s(\mu_b)}{\pi}\,\omega_a^V(s,\mu_b)\Big], \\
C_{9b,9c}(\mu_0,\mu_b) &= C_9^{\rm mix}(\mu_0)\Big[\frac{\alpha_s(\mu_b)}{\pi}\,\omega_{b,c}^V(s)\Big].
\end{aligned} \tag{4.20}$$

However, for C_{9i} there are additional contributions, $C_9^{\rm mix}(\mu_0)$, from the matching at $\mu = \mu_0$, which at one-loop order and $\mathcal{O}(\alpha_s^0)$ includes Fig. 4-2a:

$$\begin{aligned}
C_9^{\rm mix}(\mu_0) &= C_9^{NDR}(\mu_0) + \frac{2}{9}(3C_3 + C_4 + 3C_5 + C_6) - \frac{1}{2}h(1,s)(4C_3 + 4C_4 + 3C_5 + C_6) \\
&\quad + h\Big(\frac{m_c}{m_b},s\Big)(3C_1 + C_2 + 3C_3 + C_4 + 3C_5 + C_6) - \frac{1}{2}h(0,s)(C_3 + 3C_4) \\
&\quad + \frac{\alpha_s(\mu_0)}{\pi}\,C_9^{\rm mix(1)}(\mu_0).
\end{aligned} \tag{4.21}$$

where all running coefficients on the RHS are $C_i = C_i(\mu_0)$. We shall discuss the relation of $C_9^{\rm mix}$ to $\tilde{C}_9^{\rm eff}$ in in the local OPE analysis [121, 54] after Eq. (4.28). In Eq. (4.21) the functions $h(1,s)$, $h(z,s)$, and $h(0,s)$ for the b-quark, c-quark, and

light-quark penguin loops are [84, 121]

$$\begin{aligned} h(z,s) &= \frac{8}{9}\ln(\frac{\mu_0}{m_b}) - \frac{8}{9}\ln z + \frac{8}{27} + \frac{4}{9}\zeta - \frac{2}{9}(2+\zeta)\sqrt{|1-\zeta|} \\ &\quad \times\left[\theta(1-\zeta)\left(-i\pi + \ln\frac{1+\sqrt{1-\zeta}}{1-\sqrt{1-\zeta}}\right) + \theta(\zeta-1)\,2\arctan\frac{1}{\sqrt{\zeta-1}}\right], \\ h(0,s) &= \frac{8}{27} + \frac{8}{9}\ln(\frac{\mu_0}{m_b}) - \frac{4}{9}\ln s + \frac{4}{9}i\pi\,, \end{aligned} \tag{4.22}$$

with $\zeta = 4z^2/s$. Higher-order $\mathcal{O}(\alpha_s)$ corrections in Eq. (4.21) are denoted by the $C_9^{\mathrm{mix}(1)}$ term. An important class of these corrections from mixing can be determined from the NNLL analysis in Refs. [10, 8, 75, 9, 77, 76]:

$$C_9^{\mathrm{mix}(1)}(\mu_0) = C_8^{\mathrm{NDR}}\,\kappa_{8\to9}(s,\mu_0) + C_1\,\kappa_{1\to9}(s,\mu_0,\hat{m}_c) + C_2\,\kappa_{2\to9}(s,\mu_0,\hat{m}_c)\,. \tag{4.23}$$

To determine these terms one must be careful to separate out the factors in square brackets in Eq. (4.20). However we shall not attempt to include all NNLL terms consistently here. Contributions to $C_9^{\mathrm{mix}(1)}$ from the penguin coefficients C_{3-6} are unknown but expected to be small (at the $\sim 1\%$ level).

Lastly, we turn to the results for C_{7i}. From the vertex graphs we have

$$\begin{aligned} C_{7a}(\mu_0,\mu_b) &= C_7^{\mathrm{mix}}(\mu_0)\left[1 + \frac{\alpha_s(\mu_b)}{\pi}\,\omega_a^T(s,\mu_b)\right], \\ C_{7b,7c,7d}(\mu_0,\mu_b) &= C_7^{\mathrm{mix}}(\mu_0)\,\frac{\alpha_s(\mu_b)}{\pi}\,\omega_{b,c,d}^T(s)\,. \end{aligned} \tag{4.24}$$

The ω_i^T perturbative corrections are again determined from the SCET matching in Ref. [23], which (switching to s) gives

$$\begin{aligned} \omega_a^T(s,\mu_b) &= -\frac{1}{3}\Big[2\ln^2(1-s) + 2\mathrm{Li}_2(s) + \ln(1-s)\Big(\frac{2-4s}{s}\Big) + \frac{\pi^2}{12} + 6 \\ &\qquad + 2\ln^2\left(\frac{\mu_b}{m_b}\right) + 5\ln\left(\frac{\mu_b}{m_b}\right) - 4\ln(1-s)\ln\left(\frac{\mu_b}{m_b}\right)\Big], \\ \omega_b^T(s) &= \omega_d^T(s) = 0\,, \\ \omega_c^T(s) &= \frac{1}{3}\Big[\frac{-2(1-s)\ln(1-s)}{s}\Big]. \end{aligned} \tag{4.25}$$

Additional contributions from other diagrams are matched at the scale μ_0 into $C_7^{\rm mix}(\mu_0)$. Note that, unlike the vector currents, the tensor current for O_7 gets renormalized for $\mu > m_b$ and we must include the corresponding $\ln(\mu_0/m_b)$ in $C_7^{\rm mix}(\mu_0)$, i.e.

$$C_7^{\rm mix}(\mu_0) = \frac{\overline{m}_b(\mu_0)}{m_B}\left\{C_7^{\rm NDR}(\mu_0)\left[1-\frac{2\alpha_s(\mu_0)}{3\pi}\ln\left(\frac{\mu_0}{m_b}\right)\right] + \frac{\alpha_s(\mu_0)}{\pi}\,C_7^{\rm mix(1)}(\mu_0)\right\}, \tag{4.26}$$

where, much like in the case of $C_9^{\rm mix}$, we have

$$C_7^{\rm mix(1)}(\mu_0) = C_8^{\rm NDR}\,\kappa_a^8(s,\mu_0) + C_1\,\kappa_a^1(s,\mu_0,\hat{m}_c) + C_2\,\kappa_a^2(s,\mu_0,\hat{m}_c)\,, \tag{4.27}$$

and the results for $\kappa_{8\to7}(s,\mu_0)$, $\kappa_{1\to7}(s,\mu_0,\hat{m}_c)$, and $\kappa_{2\to7}(s,\mu_0,\hat{m}_c)$ can be found in Ref. [81]. Contributions to $C_7^{\rm mix(1)}$ from the penguin coefficients C_{3-6} can be found in Ref. [52].

Using Eq. (4.15), $\bar{n}\cdot q\, n\cdot q/m_B^2 = y_H$, and $n\cdot q/m_B = 1-u_H$, we can use the above results to give the final coefficients for our basis of operators with the minimal number of Dirac structures, namely

$$\begin{aligned}
\mathcal{C}_9 &= C_9^{\rm mix}(\mu_0)\left\{1+\frac{\alpha_s(\mu_b)}{\pi}\left[\omega_a^V(s,\mu_b)+\frac{1}{2}\,\omega_b^V(s)+\frac{(1-u_H)^2\,\omega_c^V(s)}{(1-u_H)^2-y_H}\right]\right\}\\
&\quad + C_7^{\rm mix}(\mu_0)\frac{\alpha_s(\mu_b)}{\pi}\left[\frac{2(1-u_H)[\omega_c^T(s)-\omega_d^T(s)]}{(1-u_H)^2-y_H}-\frac{\omega_b^T(s)}{(1-u_H)}\right],\\
\mathcal{C}_7 &= C_7^{\rm mix}(\mu_0)\left\{1+\frac{\alpha_s(\mu_b)}{\pi}\left[\omega_a^T(s,\mu_b)-\frac{1}{2}\,\omega_b^T(s)+\frac{y_H\,\omega_d^T(s)-(1-u_H)^2\omega_c^T(s)}{(1-u_H)^2-y_H}\right]\right\}\\
&\quad - C_9^{\rm mix}(\mu_0)\frac{\alpha_s(\mu_b)}{\pi}\left[\frac{y_H\,\omega_b^V(s)}{4(1-u_H)}+\frac{y_H\,(1-u_H)\omega_c^V(s)}{2[(1-u_H)^2-y_H]}\right],\\
\mathcal{C}_{10a} &= C_{10}\left\{1+\frac{\alpha_s(\mu_b)}{\pi}\,\omega_a^V(s,\mu_b)\right\},\\
\mathcal{C}_{10b} &= C_{10}\,\frac{\alpha_s(\mu_b)}{\pi}\left[\omega_b^V(s)+\frac{2(1-u_H)^2}{(1-u_H)^2-y_H}\,\omega_c^V(s)\right].
\end{aligned} \tag{4.28}$$

where the terms have the structure of a sum over products $B_1(\mu_0)B_2(\mu_b)$, as desired.

In using the results in Eq. (4.28) one can choose to work to different orders in

the μ_0- and μ_b-dependent terms, as shown in Eq. (4.3). For the μ_0 dependence, $C_9^{\rm mix}(\mu_0)$ and $C_7^{\rm mix}(\mu_0)$ include terms from matching at m_W and running to m_b, as well as matching contributions at m_b that cancel the μ_0 dependence from the other pieces. Thus, these coefficients have only a small residual μ_0 dependence, which is canceled at higher orders, just as in the local OPE. The C_i coefficients depend on μ_b, both through $\alpha_s(\mu_b)$ and through explicit μ_b dependence in ω_a^T and ω_a^V. The $\ln \mu_b$ dependence in ω_a^V and ω_a^T is identical, as expected from the known independence of the anomalous dimension on the Dirac structure in SCET. The μ_b dependence in $C_i(\mu_b, \mu_0)$ is universal, and will cancel against the universal μ_b dependence in the jet and shape functions, which they multiply in the decay rates. We consider the phenomenological organization of the perturbative series for μ_0 and μ_b terms in turn.

First consider the μ_0 terms. Because of mixing, the sizes of contributions to C_9^{NDR} are comparable at LL and NLL orders [121, 54], so a reasonable first approximation is to take the NLL result (just as for the local OPE decay rate). This entails dropping the $\mathcal{O}(\alpha_s)$ matching corrections $C_9^{\rm mix(1)}$ and $C_7^{\rm mix(1)}$, and running C_9 at NLL order with C_7 at LL order. As an improved approximation, we would then adopt the operationally well-defined NNLL approach [10, 8] of running both C_9 and C_7 to NLL order and keeping the $\mathcal{O}(\alpha_s)$ matching corrections at m_b.[5]

Below m_b there are Sudakov logarithms. For the μ_b dependence, the RG evolution in SCET sums these double-logarithmic series. As a first approximation we could take the LL and NLL running in $U_H(\mu_b, \mu_i)$ and $U_S(\mu_i, \mu_\Lambda)$ in Eq. (4.3), while using tree-level matching for $B_2(\mu_b)$ and $\mathcal{J}(\mu_i)$. This is consistent because the NLL running is equivalent to LL running in a single-log resummation. As a second approximation we could then take NNLL running in both terms and include one-loop matching for both $B_2(\mu_b)$ and $\mathcal{J}(\mu_i)$. However since the scales $m_b^2 \gg m_b\Lambda \gg 1\,\mathrm{GeV}^2$ are not as well separated as $m_W^2 \gg m_b^2$, we could instead consider the second approximation to include the one-loop matching for $B_2(\mu_b)$ and $\mathcal{J}(\mu_i)$ with NLL running, but without including the full NNLL running (for which parts remain unknown).

[5] We assume that matching at the high scale, m_W, is always done at the order appropriate to the running of $U_W(\mu_W, \mu_0)$ in Eq. (4.3).

Our procedure for split matching above was based on the non-renormalization of $\mathcal{O}_{10}$ in QCD. It can also be thought of as matching in two steps. First one matches at μ_0 on to the scale-invariant operators

$$\begin{aligned} J^{(0)} &= C_9^{\rm mix}\,(\bar{s}P_R\gamma^\mu b)(\bar{\ell}\gamma_\mu\ell) + C_{10}\,(\bar{s}P_R\gamma^\mu b)(\bar{\ell}\gamma_\mu\gamma_5\ell) \\ &\quad - C_7^{\rm mix}\,\frac{2m_B q_\tau}{q^2}\big[(\bar{s}P_R i\sigma^{\mu\tau} b)(\mu=m_b)\big](\bar{\ell}\gamma_\mu\ell), \end{aligned} \tag{4.29}$$

to determine the coefficients $C_{7,9}^{\rm mix}$. These coefficients are μ_0 independent at the order in perturbation theory to which the matching is done. Secondly, the operators in Eq. (4.29) are matched on to the SCET currents in Eq. (4.14) at the scale μ_b to determine the coefficients $\mathcal{C}_7$, $\mathcal{C}_9$, $\mathcal{C}_{10a,b}$. In Eq. (4.29) the operators for $C_9^{\rm mix}$ and C_{10} are conserved, but the tensor current has an anomalous dimension, and so we take $\mu = m_b$ as a reference point for matching on to a scale-invariant operator. This choice corresponds to the $\ln m_b$ factor in Eq. (4.26) for $C_7^{\rm mix}$. A different choice will affect the division of $\alpha_s(\mu_0)$ or $\alpha_s(\mu_b)$ terms. Note that Eq. (4.29) should be thought of only as an auxiliary step to facilitate the split matching; there is no sense in which the running of the tensor current is relevant by itself. In general the split-matching procedure could be carried out in a manner that gives different constant terms at a given order, but any such ambiguity will cancel order by order in $\mathcal{C}_7$ and $\mathcal{C}_9$ (and explicitly if $\mu_0 = \mu_b$).

Finally, note that our ω_a differs from the result for $\omega^{\rm OPE}$ identified in Ref. [121] for the partonic semileptonic decay rate when using the local OPE,

$$\begin{aligned} \omega_{semi}^{\rm OPE} = -\frac{1}{3}\bigg[&2\ln(s)\ln(1-s) + 4{\rm Li}_2(s) + \ln(1-s)\Big(\frac{5+4s}{1+2s}\Big) + \frac{2s(1+s)(1-2s)}{(1-s)^2(1+2s)}\,\ln(s) \\ &- \frac{(5+9s-6s^2)}{2(1-s)(1+2s)} + \frac{2\pi^2}{3}\bigg]. \end{aligned} \tag{4.30}$$

Here $\omega_{semi}^{\rm OPE}$ contains both vertex and bremsstrahlung contributions evaluated in the full theory. Grouping these contributions with the Wilson coefficient for $\mathcal{O}_9$ gives

$$C_9^{\rm local}(\mu) = C_9^{\rm mix}(\mu) + P_0^{NDR}(\mu)\,\frac{\alpha_s(\mu)}{\pi}\,\omega_{semi}^{\rm OPE}\,, \tag{4.31}$$

which is $\tilde{C}_9^{\rm eff}$ in the notation in Ref. [54]. At LO, the restricted phase space in the shape function region causes bremsstrahlung to contribute only to the jet and shape functions, and not at the scale $\mu \simeq m_b$. The shape function and jet function also modify the contributions from the vertex graphs. Thus, instead of $\omega_{semi}^{\rm OPE}$ the final results in the shape function region are given by our ω_i^V and ω_i^T factors appearing in C_{9i} and C_{7i}. Consequently, the main difference is in the terms we match at $\mu = \mu_b$, while the terms matched at $\mu = \mu_0$ that appear in $C_9^{\rm mix}$ and $C_7^{\rm mix}$ are identical to terms appearing in the local OPE analysis.

4.2.2 RG Evolution Between μ_b and μ_i

The running of the Wilson coefficients in SCET from the scale $\mu_b^2 \sim m_b^2$ to $\mu_i^2 \sim m_b \Lambda_{\rm QCD}$ involves double Sudakov logarithms and was derived in Refs. [22, 23] at NLL order. The SCET running is independent of the Dirac structure of the currents, which is a reflection of the spin symmetry structure of the current. We briefly outline a short argument for why this is true to all orders in perturbation theory. The leading-order currents in SCET have the structure

$$J = (\bar{\xi}_n W)_p \Gamma (Y^\dagger h_v)\,, \tag{4.32}$$

and we wish to see that their anomalous dimension is independent of Γ. The anomalous dimensions are computed from the UV structure of SCET loop diagrams, with the leading-order collinear- and heavy-quark Lagrangians. Soft gluon loops involve contractions between the Wilson line $Y^\dagger$ and the h_v and do not change the Dirac structure. Next consider the collinear loops. The attachment of a gluon from the Wilson line W to the collinear quark gives a factor of a projection matrix, which can be pushed through $\gamma_\perp$'s to give $\bar{\xi}_n \bar{n}\!\!\!/ n\!\!\!//4 = \bar{\xi}_n$. Thus it does not modify the Dirac structure, so only insertions from the $i\not{D}_c^\perp 1/(i\bar{n}\cdot D_c) i\not{D}_c^\perp$ term are of concern. These terms give structures of the form $\bar{u}_n^{(u)} \gamma_\perp^{\mu_1} \gamma_\perp^{\mu_2} \cdots \gamma_\perp^{\mu_{2k}} \Gamma u_v^{(b)}$, where all μ_i indices are contracted with each other. Using $\{\gamma_\perp^\mu, \gamma_\perp^\nu\} = 2g_\perp^{\mu\nu}$ and $\gamma_\perp^\mu \gamma_\mu^\perp = d-2$, we can reduce this product

to terms with zero $\gamma_\perp$'s since all vector indices are contracted. Hence all diagrams reduce to having the Dirac structure that was present at tree level, $\bar{u}_n^{(u)}\Gamma u_v^{(b)}$.

Thus, all the LO coefficients obey the same homogeneous anomalous dimension equation,

$$\begin{aligned}\mu\frac{d}{d\mu}\mathcal{C}_i(\mu) &= \Big[-\Gamma_{\rm cusp}(\alpha_s)\ln\Big(\frac{\mu}{\bar{\mathcal{P}}}\Big)+\tilde{\gamma}(\alpha_s)\Big]\mathcal{C}_i(\mu) \\ &= \Big[-\Gamma_{\rm cusp}(\alpha_s)\ln\Big(\frac{\mu}{\mu_b}\Big)+\Big\{\tilde{\gamma}(\alpha_s)+\Gamma_{\rm cusp}(\alpha_s)\ln\Big(\frac{\bar{n}\cdot p}{\mu_b}\Big)\Big\}\Big]\mathcal{C}_i(\mu)\,.\end{aligned} \tag{4.33}$$

This must be integrated together with the beta function $\beta = \mu d/d\mu\,\alpha_s(\mu)$ to solve for U_H in

$$\mathcal{C}_i(\mu_i) = \sqrt{U_H(\mu_i,\mu_b)}\,\mathcal{C}_i(\mu_b)\,. \tag{4.34}$$

In the second line of Eq. (4.33) we used the fact that $\bar{\mathcal{P}}$ gives the total partonic $\bar{n}\cdot p$ momentum of the jet X_s in the $B\to X_s\ell^+\ell^-$ matrix element, and we introduced artificial dependence on the matching scale μ_b in order to make the $\bar{n}\cdot p$ dependence appear in a small logarithm. Here $\bar{n}\cdot p = m_b - \bar{n}\cdot q$. We write

$$\Gamma^{\rm cusp} = \sum_{n=0}^{\infty}\Gamma_n^{\rm cusp}\Big(\frac{\alpha_s}{4\pi}\Big)^{n+1}\,,\quad \tilde{\gamma} = \sum_{n=0}^{\infty}\tilde{\gamma}_n\Big(\frac{\alpha_s}{4\pi}\Big)^{n+1}\,,\quad \beta = -2\alpha_s\sum_{n=0}^{\infty}\beta_n\Big(\frac{\alpha_s}{4\pi}\Big)^{n+1}\,. \tag{4.35}$$

At NLL order we need $\beta_0 = 11C_A/3 - 2n_f/3$, $\beta_1 = 34C_A^2/3 - 10C_An_f/3 - 2C_Fn_f$ and

$$\Gamma_0^{\rm cusp} = 4C_F\,,\quad \Gamma_1^{\rm cusp} = 8C_FB = 8C_F\Big[C_A\Big(\frac{67}{18}-\frac{\pi^2}{6}\Big)-\frac{5}{9}n_f\Big]\,,\quad \tilde{\gamma}_0 = -5C_F\,, \tag{4.36}$$

where $C_A = 3$ and $C_F = 4/3$ for SU(3). For the number of active flavours we take $n_f = 4$ since we're running below m_b. The cusp anomalous dimension $\Gamma_1^{\rm cusp}$ was computed in Ref. [98, 96], and the result for $\Gamma_2^{\rm cusp}$ was recently found in Ref. [122]. RG evolution in SCET at NNLL order has been considered in Refs. [129, 104]. For the NNLL result one needs $\Gamma_2^{\rm cusp}$, $\tilde{\gamma}_1$, and β_2. For $\tilde{\gamma}_1$ an independent calculation does

not exist, but a conjecture for its value was given in Ref. [129] based on the structure of the three-loop splitting function [122]. For the sake of clarity we stick to NLL order here. The result is

$$U_H(\mu_i,\mu_b) = \exp\left[\frac{2g_0(r_1)}{\alpha_s(\mu_b)} + 2g_1(r_1,\bar{n}\cdot p)\right], \tag{4.37}$$

where the independent variable is μ_i and

$$r_1(\mu_i) = \frac{\alpha_s(\mu_i)}{\alpha_s(\mu_b)} = \frac{2\pi}{2\pi + \beta_0\alpha_s(\mu_b)\ln(\mu_i/\mu_b)}, \tag{4.38}$$

with

$$\begin{aligned} g_0(r_1) &= -\frac{4\pi C_F}{\beta_0^2}\left[\frac{1}{r_1} - 1 + \ln r_1\right], \\ g_1(r_1,\bar{n}\cdot p) &= -\frac{C_F\beta_1}{\beta_0^3}\left[1 - r_1 + r_1\ln r_1 - \frac{1}{2}\ln^2 r_1\right] \\ &\quad + \frac{C_F}{\beta_0}\left[\frac{5}{2} - 2\ln\left(\frac{\bar{n}\cdot p}{\mu_b}\right)\right]\ln r_1 - \frac{2C_F B}{\beta_0^2}\left[r_1 - 1 - \ln r_1\right]. \end{aligned} \tag{4.39}$$

This is the form for the universal running of the LO SCET currents found in Ref. [23]. Switching to $\alpha_s(\mu_i)$ as the independent variable, with $r_1 = \alpha_s(\mu_i)/\alpha_s(\mu_b)$, gives

$$U_H(\mu_i,\mu_b) = \left(\frac{\bar{n}\cdot p}{\mu_b}\right)^{-\frac{4C_F}{\beta_0}\ln r_1} \exp\left[\frac{2g_0(r_1)}{\alpha_s(\mu_b)} + 2\tilde{g}_1(r_1)\right], \tag{4.40}$$

where $g_0(r_1)$ is as in Eq. (4.39) and

$$\tilde{g}_1(r_1) = \frac{C_F\beta_1}{2\beta_0^3}\ln^2 r_1 + \frac{5C_F}{2\beta_0}\ln r_1 + \frac{C_F}{\beta_0^3}\left(2B\beta_0 - \beta_1\right)\left(1 - r_1 + \ln r_1\right). \tag{4.41}$$

This form of the evolution with $\alpha_s(\mu)$ as the variable was used in Ref. [47], and is also the one we adopt here. The decay rate is computed from a time-ordered product of currents and so at the intermediate scale $\mu_i^2 \sim m_b\Lambda$ will involve products

$$C_i(\mu_i,\mu_0)\,C_j(\mu_i,\mu_0) = U_H(\mu_i,\mu_b)\,C_i(\mu_b,\mu_0)\,C_j(\mu_b,\mu_0), \tag{4.42}$$

explaining why we used a notation with $\sqrt{U_H}$ in Eq. (4.34).

4.2.3 Hadronic Tensor and Decay Rates

In the last two sections we constructed the required basis of SCET current operators with matching at $\mu_0^2 \sim \mu_b^2 \sim m_b^2$ and evolution to $\mu_i^2 \sim m_b\Lambda$. At the scale μ_i we take time-ordered products of the SCET currents and compute the decay rates using the optical theorem. In this section we discuss the tensor decomposition of the time-ordered products and results for differential decay rates.

In order to simplify the computation of decay rates it is useful to write the sum of hadronic operators as a sum of left-handed and right-handed terms since for massless leptons we have only LL or RR contributions [7]. Doing this for our current, we have

$$\begin{aligned}
\mathcal{J}_{\ell\ell}^{(0)} &= \big[\mathcal{C}_9 - \mathcal{C}_{10a}\big]\big(\bar\chi_n\,\gamma_\mu P_L\,\mathcal{H}_v\big)\big(\bar\ell\,\gamma^\mu P_L\,\ell\big) + \big[\mathcal{C}_9 + \mathcal{C}_{10a}\big]\big(\bar\chi_n\,\gamma_\mu P_L\,\mathcal{H}_v\big)\big(\bar\ell\,\gamma^\mu P_R\,\ell\big) \\
&\quad + \mathcal{C}_{10b}\big(\bar\chi_n\,v_\mu P_R\,\mathcal{H}_v\big)\big(\bar\ell\,\gamma^\mu\gamma_5\,\ell\big) - \mathcal{C}_7\,\frac{2m_B q^\tau}{q^2}\big(\bar\chi_n\,i\sigma_{\mu\tau}\,\mathcal{H}_v\big)\big(\bar l\,\gamma^\mu\,l\big) \\
&= \big(J_{L\mu}\,L_L^\mu + J_{R\mu}\,L_R^\mu\big)\,, \qquad (4.43)
\end{aligned}$$

where

$$\begin{aligned}
L_L^\mu &= \bar\ell\,\gamma^\mu\,P_L\,\ell\,, \qquad L_R^\mu = \bar\ell\,\gamma^\mu\,P_R\,\ell\,, \qquad (4.44)\\
J_{L(R)}^\mu &= \bar\chi_n\,P_R\Big[\big(\mathcal{C}_9 \mp \mathcal{C}_{10a}\big)\gamma^\mu + \mathcal{C}_7\,\frac{2m_B\gamma^\mu\,\not{q}}{q^2} \mp \mathcal{C}_{10b}\,v^\mu\Big]\mathcal{H}_v \\
&\equiv \bar\chi_n\,\Gamma_{L(R)}^\mu\,\mathcal{H}_v\,.
\end{aligned}$$

Thus, the inclusive decay rate for $\bar B \to X_s\ell^+\ell^-$ is proportional to $(W_{\mu\nu}^L L_L^{\mu\nu} + W_{\mu\nu}^R L_R^{\mu\nu})$, where the leptonic parts $L_{L(R)}^{\mu\nu}$ and hadronic parts $W_{L(R)}^{\mu\nu}$ are given by

$$\begin{aligned}
L_{L(R)}^{\mu\nu} &= \sum_{\text{spin}} \big[\bar l_{L(R)}(p_+)\,\gamma^\mu\,l_{L(R)}(p_-)\big]\,\big[\bar l_{L(R)}(p_-)\,\gamma^\nu\,l_{L(R)}(p_+)\big] \\
&= 2\left[p_+^\mu\,p_-^\nu + p_-^\mu\,p_+^\nu - g^{\mu\nu}\,p_+\cdot p_- \mp i\epsilon^{\mu\nu\alpha\beta}\,p_{+\alpha}\,p_{-\beta}\right], \qquad (4.45)
\end{aligned}$$

and

$$
\begin{aligned}
W_{\mu\nu}^{L(R)} &= \frac{1}{2m_B}\sum_X (2\pi)^3\delta^4(p_B - q - p_X)\langle \bar{B}|J_\mu^{L(R)\dagger}|X\rangle\langle X|J_\nu^{L(R)}|\bar{B}\rangle \qquad (4.46)\\
&= -g_{\mu\nu}W_1^{L(R)} + v_\mu v_\nu W_2^{L(R)} + i\epsilon_{\mu\nu\alpha\beta}v^\alpha q^\beta W_3^{L(R)} + q_\mu q_\nu W_4^{L(R)}\\
&\quad +(v_\mu q_\nu + v_\nu q_\mu)W_5^{L(R)}\,.
\end{aligned}
$$

The optical theorem relates $W_{\mu\nu}^{L(R)}$ to the forward scattering amplitude defined as

$$
\begin{aligned}
T_{\mu\nu}^{L} &= \frac{-i}{2m_B}\int d^4x\, e^{-iq\cdot x}\,\langle \bar{B}|T J_\mu^{L\dagger}(x) J_\nu^{L}(0)|\bar{B}\rangle \qquad (4.47)\\
&= -g_{\mu\nu}T_1^L + v_\mu v_\nu T_2^L + i\epsilon_{\mu\nu\alpha\beta}v^\alpha q^\beta T_3^L + q_\mu q_\nu T_4^L + (v_\mu q_\nu + v_\nu q_\mu)T_5^L\,,
\end{aligned}
$$

with an analogous definition for $T_{\mu\nu}^R$, giving

$$
W_i^L = -\frac{1}{\pi}\,\mathrm{Im}\,T_i^L\,, \qquad W_i^R = -\frac{1}{\pi}\,\mathrm{Im}\,T_i^R\,. \qquad (4.48)
$$

Contracting the lepton tensor $L_{L(R)}^{\mu\nu}$ with $W_{L(R)}^{\mu\nu}$ and neglecting the mass of the leptons give the differential decay rate

$$
\frac{d^3\Gamma}{dq^2 dE_- dE_+} = \Gamma_0\,\frac{96}{m_B^5}\Big[q^2 W_1 + (2E_-E_+ - q^2/2)W_2 + q^2(E_- - E_+)W_3\Big]\theta(4E_-E_+ - q^2)\,, \qquad (4.49)
$$

where $E_\pm = v\cdot p_\pm$, $W_1 = W_1^L + W_1^R$, $W_2 = W_2^L + W_2^R$, $W_3 = W_3^L - W_3^R$ and the normalization factor is

$$
\Gamma_0 = \frac{G_F^2\, m_B^5}{192\pi^3}\,\frac{\alpha^2}{16\pi^2}\,|V_{tb}V_{ts}^*|^2\,. \qquad (4.50)
$$

The W_i are functions of q^2 and $v\cdot q = v\cdot(p_+ + p_-)$. Another quantity of interest is the forward-backward asymmetry in the variable

$$
\cos\theta = \frac{v\cdot p_- - v\cdot p_+}{\sqrt{(v\cdot q)^2 - q^2}}. \qquad (4.51)
$$

where θ is the angle between the B and ℓ^+ in the CM frame of the $\ell^+\ell^-$ pair:

$$\frac{d^2A_{\rm FB}}{dv\cdot q\,dq^2} \equiv \int_{-1}^{1} d(\cos\theta)\,\frac{\mathrm{sign}(\cos\theta)}{\Gamma_0}\,\frac{d^3\Gamma}{dv\cdot q\,dq^2\,d\cos\theta} = \frac{48\,q^2}{m_B^5}\big[(v\cdot q)^2 - q^2\big]\,W_3\,. \quad (4.52)$$

In terms of the dimensionless variables

$$x_H = \frac{2E_{\ell^-}}{m_B}\,, \qquad \overline{y}_H = \frac{\bar{n}\cdot p_X}{m_B}\,, \qquad u_H = \frac{n\cdot p_X}{m_B}\,, \quad (4.53)$$

the triply differential decay rate is

$$\begin{aligned}\frac{1}{\Gamma_0}\frac{d^3\Gamma}{dx_H\,d\overline{y}_H\,du_H} = {}& 24m_B(\overline{y}_H-u_H)\Big\{(1-u_H)(1-\overline{y}_H)W_1 \\ &+\frac{1}{2}(1-x_H-u_H)(x_H+\overline{y}_H-1)W_2 \\ &+\frac{m_B}{2}(1-u_H)(1-\overline{y}_H)\big(2x_H+u_H+\overline{y}_H-2\big)W_3\Big\}\,,\end{aligned} \quad (4.54)$$

where $W_i = W_i(u_H, \overline{y}_H)$. For a strict SCET expansion we want $n\cdot p_X \ll \bar{n}\cdot p_X$ i.e. $u_H \ll \overline{y}_H$. However, it is useful to keep the full dependence on the phase-space prefactors rather than expanding them, because it is then simpler to make contact with the total rate in the local OPE, as emphasized recently in Refs. [135, 104], and so we keep these factors here. We shall also keep the formally subleading kinematic prefactors in our hard functions rather than expanding them as we did in Ref. [106]. Other variables of interest include the dileptonic and hadronic invariant masses,

$$y_H = \frac{q^2}{m_B^2}\,, \qquad s_H = \frac{m_X^2}{m_B^2}\,, \quad (4.55)$$

where

$$s_H = u_H\overline{y}_H\,, \qquad y_H = (1-u_H)(1-\overline{y}_H)\,, \quad (4.56)$$

so that $[\overline{y}_H \geq u_H]$

$$\{\overline{y}_H, u_H\} = \frac{1}{2}\Big[1 - y_H + s_H \pm \sqrt{(1-y_H+s_H)^2 - 4s_H}\,\Big]\,. \quad (4.57)$$

A few interesting doubly differential spectra are

$$\begin{aligned}
\frac{1}{\Gamma_0}\frac{d^2\Gamma}{d\bar{y}_H\,du_H} &= 24m_B(\bar{y}_H-u_H)^2\Big\{(1-u_H)(1-\bar{y}_H)W_1+\frac{1}{12}(\bar{y}_H-u_H)^2W_2\Big\}\,, \qquad (4.58)\\
\frac{1}{\Gamma_0}\frac{d^2\Gamma}{dy_H\,ds_H} &= 2m_B\sqrt{(1-y_H+s_H)^2-4\,s_H}\,\Big\{12y_HW_1+\big[(1-y_H+s_H)^2-4s_H\big]W_2\Big\}\,,\\
\frac{1}{\Gamma_0}\frac{d^2\Gamma}{dy_H\,du_H} &= \frac{2m_B}{(1-u_H)^3}\big[(1-u_H)^2-y_H\big]^2\Big\{12y_HW_1+\Big[\frac{(1-u_H)^2-y_H}{(1-u_H)}\Big]^2W_2\Big\}\,,\\
\frac{1}{\Gamma_0}\frac{d^2\Gamma}{ds_H\,du_H} &= \frac{2m_B(s_H-u_H^2)^2}{u_H^5}\Big\{12u_H(1-u_H)(u_H-s_H)W_1+(s_H-u_H^2)^2\,W_2\Big\}\,.
\end{aligned}$$

For doubly differential forward-backward asymmetries we find

$$\begin{aligned}
\frac{d^2A_{\rm FB}}{d\bar{y}_H\,du_H} &= 6m_B^2\,(\bar{y}_H-u_H)^3(1-u_H)(1-\bar{y}_H)\,W_3\,, \qquad (4.59)\\
\frac{d^2A_{\rm FB}}{dy_H\,ds_H} &= 6m_B^2\,y_H\big[(1-y_H+s_H)^2-4s_H\big]W_3\,,\\
\frac{d^2A_{\rm FB}}{dy_H\,du_H} &= 6m_B^2\,\frac{y_H\,[(1-u_H)^2-y_H]^3}{(1-u_H)^4}\,W_3\,,\\
\frac{d^2A_{\rm FB}}{ds_H\,du_H} &= 6m_B^2\,\frac{(s_H-u_H^2)^3(u_H-s_H)(1-u_H)}{u_H^5}\,W_3\,.
\end{aligned}$$

4.2.4 LO Matrix Elements in SCET

At lowest order in the Λ/m_b expansion, the only time-ordered product consists of two lowest-order currents $\mathcal{J}_{\ell\ell}^{(0)}$ as shown in Fig. 4-4. The factorization of hard contributions into the SCET Wilson coefficients and the decoupling of soft and collinear gluons at lowest order are identical to the steps for $B\to X_s\gamma$ and $B\to X_u\ell\bar{\nu}$, and directly give the factorization theorem for these time-ordered products [30]. The SCET result agrees with the factorization theorem of Korchemsky and Sterman [99]. However, the structure of $\alpha_s(\sqrt{m_b\Lambda})$ and $\alpha_s(m_b)$ corrections differs from the parton-model rate, as mentioned in Refs. [27, 47]. Beyond lowest order in $\alpha_s(m_b)$ the kinematic dependences also differ, as mentioned in Ref. [106]. For $B\to X_u\ell\bar{\nu}$, the final triply differential rate with perturbative corrections at $\mathcal{O}(\alpha_s)$ can be found in Refs. [27, 47].

The factorization and use of the optical theorem is carried out at the scale $\mu=\mu_i$,

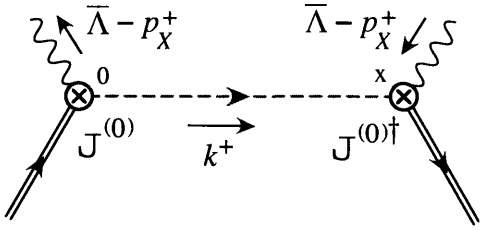

Figure 4-4: Time-ordered product for the leading-order factorization theorem.

and we expand $W_i = W_i^{(0)} + W_i^{(2)} + \ldots$ in powers of $\lambda \sim (\Lambda_{\rm QCD}/m_b)^{1/2}$ (with no linear term). For $B \to X_s \ell^+ \ell^-$ we have bilinear hadronic current operators in SCET in Eq. (4.14) and so, as is the case for $B \to X_u \ell \bar{\nu}$, we find

$$W_i^{(0)} = h_i(p_X^+, p_X^-, \mu_i) \int_0^{p_X^+} dk^+ \, \mathcal{J}^{(0)}(p^-, k^+, \mu_i) \, f^{(0)}(k^+ + \overline{\Lambda} - p_X^+, \mu_i) \,. \quad (4.60)$$

This result is important, since it states that the same shape function $f^{(0)}$ appears in $B \to X_s \ell^+ \ell^-$ as appears in $B \to X_s \gamma$ and $B \to X_u \ell \bar{\nu}$. This formula relies on the power counting $s \sim y_H \sim \lambda^0$ that we adopted (and would not be true for the counting $s \sim \lambda^2$ discussed in Appendix D). At tree level the structure of this factorization theorem is illustrated by Fig. 4-4. The hard coefficients here are

$$\begin{aligned}
h_1(p_X^+, p_X^-, \mu_i) &= \frac{1}{4}\mathrm{Tr}\Big[P_v \, \overline{\Gamma}_\mu^L \, \not{n} \, \Gamma_\nu^L\Big] P_1^{\mu\nu} + \frac{1}{4}\mathrm{Tr}\Big[P_v \, \overline{\Gamma}_\mu^R \, \not{n} \, \Gamma_\nu^R\Big] P_1^{\mu\nu} \,, \\
h_2(p_X^+, p_X^-, \mu_i) &= \frac{1}{4}\mathrm{Tr}\Big[P_v \, \overline{\Gamma}_\mu^L \, \not{n} \, \Gamma_\nu^L\Big] P_2^{\mu\nu} + \frac{1}{4}\mathrm{Tr}\Big[P_v \, \overline{\Gamma}_\mu^R \, \not{n} \, \Gamma_\nu^R\Big] P_2^{\mu\nu} \,, \\
h_3(p_X^+, p_X^-, \mu_i) &= \frac{1}{4}\mathrm{Tr}\Big[P_v \, \overline{\Gamma}_\mu^L \, \not{n} \, \Gamma_\nu^L\Big] P_3^{\mu\nu} - \frac{1}{4}\mathrm{Tr}\Big[P_v \, \overline{\Gamma}_\mu^R \, \not{n} \, \Gamma_\nu^R\Big] P_3^{\mu\nu} \,,
\end{aligned} \quad (4.61)$$

with $P_v = (1 + \not{v})/2$ and $\overline{\Gamma} = \gamma^0 \Gamma^\dagger \gamma^0$. In Eq. (4.60) we have the same leading-order shape function as in $B \to X_s \gamma$ and $B \to X_u \ell \bar{\nu}$.

4.2.5 RG Evolution Between μ_Λ and μ_i

The function $f^{(0)}$ cannot be computed in perturbation theory and must therefore be extracted from data. This same function appears at LO in the $B \to X_s \gamma$, $B \to X_u \ell \bar{\nu}$ and $B \to X_s \ell^+ \ell^-$ decay rates. In practice, a model for $f^{(0)}$ is written down with a few parameters, which are fitted to the data. The support of $f^{(0)}(\overline{\Lambda} - r^+)$ is $-\infty$ to $\overline{\Lambda}$

since $r^+ \in [0,\infty)$. It is often convenient to switch variables to $\hat{f}^{(0)}(r^+) = f^{(0)}(\overline{\Lambda} - r^+)$ which has support from 0 to ∞, although we shall keep using $f^{(0)}$ here. A typical three-parameter model is [108, 103]

$$f^{(0)}(\overline{\Lambda} - r^+, \mu_\Lambda) = \hat{f}^{(0)}(r^+, \mu_\Lambda) = \frac{a^b\,(r^+)^{b-1}}{\Gamma(b)\,L^b} \exp\Big(\frac{-ar^+}{L}\Big)\theta(r^+)\,, \tag{4.62}$$

where a, b are dimensionless and $L \sim \Lambda_{\rm QCD}$. These parameters can be fitted to the $B \to X_s\gamma$ photon spectrum and the function $f^{(0)}$ can then be used elsewhere. The most natural scale to fix this model at is $\mu = \mu_\Lambda \sim 1\,\text{GeV}$, at which it contains no large logarithms. The result of evolving the shape function to the intermediate scale is then [47]

$$f^{(0)}(\overline{\Lambda}-r^+, \mu_i) \;=\; e^{V_S(\mu_i,\mu_\Lambda)}\,\frac{1}{\Gamma(\eta)}\int_0^{r^+} dr^{+\prime}\,\frac{f^{(0)}(\overline{\Lambda}-r^{+\prime},\mu_\Lambda)}{\mu_\Lambda^\eta\,(r^+ - r^{+\prime})^{1-\eta}}\,. \tag{4.63}$$

(The structure of this result also applies at higher orders in RG-improved perturbation theory [129], and at one-loop order a similar structure was considered earlier, in Ref. [17].) At NLL order

$$\begin{aligned} V_S(\mu_i,\mu_\Lambda) &= \frac{\Gamma_0^{\rm cusp}}{2\beta_0^2}\left[\frac{-4\pi}{\alpha_s(\mu_\Lambda)}\,(r_2 - 1 - \ln r_2) + \frac{\beta_1}{2\beta_0}\,\ln^2 r_2 + \left(\frac{\Gamma_1^{\rm cusp}}{\Gamma_0^{\rm cusp}} - \frac{\beta_1}{\beta_0}\right)\left(1 - \frac{1}{r_2} - \ln r_2\right)\right] \\ &\quad - \frac{\Gamma_0^{\rm cusp}}{\beta_0}\,\gamma_E\,\ln r_2 - \frac{\gamma_0}{\beta_0}\,\ln r_2\,, \\ \eta &= \frac{\Gamma_0^{\rm cusp}}{\beta_0}\,\ln r_2\,. \end{aligned} \tag{4.64}$$

Here, $r_2 = \alpha_s(\mu_\Lambda)/\alpha_s(\mu_i)$, $\Gamma_0^{\rm cusp}$ and $\Gamma_1^{\rm cusp}$ are the same as in Section 4.2.2 and $\gamma_0 = -2C_F$. For numerical integration this can be rewritten in the form

$$f^{(0)}(\overline{\Lambda}-r^+, \mu_i) \;=\; \frac{e^{V_S(\mu_i,\mu_\Lambda)}}{\Gamma(1+\eta)}\left(\frac{r^+}{\mu_\Lambda}\right)^\eta \int_0^1 dt\, f^{(0)}\left(\overline{\Lambda}-r^+(1-t^{1/\eta}), \mu_\Lambda\right)\,. \tag{4.65}$$

4.3 $B \to X_s \ell^+ \ell^-$ Spectra in the Shape Function Region

4.3.1 Triply Differential Spectrum

At lowest order in the power expansion, Eqs. (3.17) and (4.60) give the result

$$W_i^{(0)} = h_i(p_X^-, p_X^+, m_b, \mu_i) \int_0^{p_X^+} dk^+ \, \mathcal{J}^{(0)}(p^-, k^+, \mu_i) \, f^{(0)}(k^+ + \overline{\Lambda} - p_X^+, \mu_i) \,, \quad (4.66)$$

where RG evolution from the hard scale to the intermediate scale gives

$$h_i(p_X^-, p_X^+, \mu_i) = U_H(\mu_i, \mu_b) \, h_i(p_X^-, p_X^+, \mu_b) \,, \quad (4.67)$$

and the results at $\mu = \mu_b$ are determined from the traces in Eq. (4.61):

$$\begin{aligned}
h_1(p_X^-, p_X^+, \mu_b) &= \frac{1}{2}\Big(|C_9|^2 + |C_{10a}|^2\Big) + \frac{2\,\mathrm{Re}[C_7 C_9^*]}{(1-\bar{y}_H)} + \frac{2\,|C_7|^2}{(1-\bar{y}_H)^2} \,, \quad (4.68)\\
h_2(p_X^-, p_X^+, \mu_b) &= \frac{2\,(1-u_H)}{(\bar{y}_H - u_H)}\Big(|C_9|^2 + |C_{10a}|^2 + \mathrm{Re}[C_{10a} C_{10b}^*]\Big) + \frac{|C_{10b}|^2}{2} \\
&\quad - \frac{8|C_7|^2}{(1-\bar{y}_H)(\bar{y}_H - u_H)} \,, \\
h_3(p_X^-, p_X^+, \mu_b) &= \frac{-4\,\mathrm{Re}[C_{10a} C_7^*]}{m_B(1-\bar{y}_H)(\bar{y}_H - u_H)} - \frac{2\,\mathrm{Re}[C_{10a} C_9^*]}{m_B(\bar{y}_H - u_H)} \,.
\end{aligned}$$

Here $C_i = C_i(p_X^-, p_X^+, \mu_b, \mu_0, m_b)$, so these hard coefficients also depend on m_b and have residual μ_0 scale dependence. Explicit formulae are given in Eq. (4.28). For convenience we define

$$\begin{aligned}
F^{(0)}(p_X^+, p_X^-) &= U_H(\mu_i, \mu_b) \int_0^{p_X^+} dk^+ \, \mathcal{J}^{(0)}(p^-, k^+, \mu_i) \, f^{(0)}(k^+ + \overline{\Lambda} - p_X^+, \mu_i) \\
&= p_X^+ \, U_H(\mu_i, \mu_b) \int_0^1 dz \, \mathcal{J}^{(0)}(p^-, z\, p_X^+, \mu_i) \, f^{(0)}\big(\overline{\Lambda} - p_X^+(1-z), \mu_i\big) \,. \quad (4.69)
\end{aligned}$$

where $p_X^- = p^- + \bar{\Lambda}$. In terms of this function,

$$W_i^{(0)} = h_i(p_X^+, p_X^-, \mu_b)\, F^{(0)}(p_X^+, p_X^-)\,. \tag{4.70}$$

We find that to NLL order

$$\begin{aligned} F^{(0)}(p_X^+, p_X^-) &= U_H(\mu_i,\mu_b) f^{(0)}\big(\overline{\Lambda} - p_X^+, \mu_i\big) \\ &\quad + U_H(\mu_i,\mu_b)\frac{\alpha_s(\mu_i) C_F}{4\pi}\bigg\{\Big(2\ln^2\frac{p^- p_X^+}{\mu_i^2} - 3\ln\frac{p^- p_X^+}{\mu_i^2} + 7 - \pi^2\Big) f^{(0)}\big(\overline{\Lambda} - p_X^+, \mu_i\big) \\ &\qquad + \int_0^1 \frac{dz}{z}\left[4\ln\frac{z\, p^- p_X^+}{\mu_i^2} - 3\right]\Big[f^{(0)}\big(\overline{\Lambda} - p_X^+(1-z), \mu_i\big) - f^{(0)}\big(\overline{\Lambda} - p_X^+, \mu_i\big)\Big]\bigg\}. \end{aligned} \tag{4.71}$$

Note that, until we include the α_s corrections from the jet function, $F^{(0)}$ is independent of p_X^-, so that all of this dependence is in the $h_i(p_X^+, p_X^-, \mu_b)$ functions.

Now, the triply differential decay rate in Eq. (4.54) becomes

$$\begin{aligned} \frac{1}{\Gamma_0}\frac{d^3\Gamma}{dx_H\, d\overline{y}_H\, du_H} &= 24 m_B(\overline{y}_H - u_H)\Big\{(1-u_H)(1-\overline{y}_H)h_1 + \frac{1}{2}(1-x_H-u_H)(x_H+\overline{y}_H-1)h_2 \\ &\quad + \frac{m_B}{2}(1-u_H)(1-\overline{y}_H)\big(2x_H+u_H+\overline{y}_H-2\big)h_3\Big\} F^{(0)}(m_B u_H, m_B\overline{y}_H)\,, \end{aligned} \tag{4.72}$$

with $h_{1,2,3}$ from Eq. (4.68). As a check on this result, one can make the substitutions

$$\begin{aligned} \mathcal{C}_{9a} = -\mathcal{C}_{10a} &= 1/2\,,\ \ \mathcal{C}_7 = \mathcal{C}_{10b} = 0\,, \\ \frac{G_F\alpha}{\sqrt{2}\pi} V_{tb} V_{ts}^* &\to \frac{4G_F}{\sqrt{2}} V_{ub}\,, \end{aligned} \tag{4.73}$$

after which the h_1 and h_2 terms in Eq. (4.72) agree with terms in the leading-order shape-function spectrum for $B \to X_u \ell\bar{\nu}$ [27, 55]. The h_3 term for $B \to X_s \ell\ell$ was the difference of products of left- and right-handed currents and so should not agree in this limit.

4.3.2 $d^2\Gamma/dq^2dm_X^2$ Spectrum with q^2 and m_X Cuts

Next we discuss doubly differential rates and forward-backward (F.B.) asymmetries. For $d^2\Gamma/dq^2dm_X^2$ the rate is obtained from Eq. (4.72) by integrating over x_H and changing variables. In terms of dimensionless variables $y_H = q^2/m_B^2$ and $s_H = m_X^2/m_B^2$ we have

$$\begin{aligned}\frac{1}{\Gamma_0}\frac{d^2\Gamma}{dy_H ds_H} &= H^{ys}(y_H,s_H)\, m_B F^{(0)}\Big(m_B u_H(y_H,s_H), m_B\overline{y}_H(y_H,s_H)\Big)\,, \quad (4.74)\\ \frac{1}{\Gamma_0}\frac{d^2A_{\rm FB}}{dy_H ds_H} &= K^{ys}(y_H,s_H)\, m_B F^{(0)}\Big(m_B u_H(y_H,s_H), m_B\overline{y}_H(y_H,s_H)\Big)\,,\end{aligned}$$

where

$$\begin{aligned}H^{ys}(y_H,s_H) &= 2\sqrt{(1-y_H+s_H)^2-4\,s_H}\,\Big\{12y_H h_1 + \big[(1-y_H+s_H)^2-4s_H\big]h_2\Big\}\,, \quad (4.75)\\ K^{ys}(y_H,s_H) &= 6y_H\big[(1-y_H+s_H)^2-4s_H\big]h_3\end{aligned}$$

and we need to substitute $h_{1,2,3}$ from Eq. (4.68) and $u_H(y_H,s_H)$ and $\overline{y}_H(y_H,s_H)$, as given in Eq. (4.57). When one takes experimental cuts on q^2 and m_X^2,

$$y_H^{\rm min} < y_H < y_H^{\rm max}\,, \qquad 0 < s_H < s_H^0\,, \quad (4.76)$$

the limits on the doubly differential rate and F.B. asymmetry in Eq. (4.74) are

$$\begin{aligned}&1)\qquad y_H^{\rm min} \le y_H \le y_H^{\rm max}\,, \qquad 0 \le s_H \le \min\big\{s_H^0\,,(1-\sqrt{y_H})^2\big\}\,,\\ &2)\qquad 0 \le s_H \le s_H^0\,, \qquad y_H^{\rm min} \le y_H \le \min\big\{y_H^{\rm max}\,,(1-\sqrt{s_H})^2\big\}\,, \quad (4.77)\end{aligned}$$

depending on the desired order of integration.

4.3.3 $d^2\Gamma/dm_X^2 dp_X^+$ Spectrum with q^2 and m_X Cuts

The hadronic invariant-mass spectrum and forward-backward asymmetry can be obtained by integrating the doubly differential spectra

$$\begin{aligned}
\frac{1}{\Gamma_0}\,\frac{d^2\Gamma}{ds_H du_H} &= H^s(s_H,u_H)\, m_B F^{(0)}\Big(m_B u_H, m_B\frac{s_H}{u_H}\Big)\,,\\
\frac{1}{\Gamma_0}\,\frac{d^2 A_{\rm FB}}{ds_H du_H} &= K^s(s_H,u_H)\, m_B F^{(0)}\Big(m_B u_H, m_B\frac{s_H}{u_H}\Big)
\end{aligned} \tag{4.78}$$

over u_H. Here

$$\begin{aligned}
H^s(s_H,u_H) = \frac{4(s_H-u_H^2)^2}{(u_H-s_H)u_H^4}\Big\{&(1-u_H)(u_H-s_H)(3u_H-2s_H-u_H^2)\big(|\mathcal{C}_9|^2+|\mathcal{C}_{10a}|^2\big)\\
&+4\,u_H(3u_H-s_H-2u_H^2)|\mathcal{C}_7|^2+12u_H(1-u_H)(u_H-s_H)\mathrm{Re}\big[\mathcal{C}_7\,\mathcal{C}_9^*\big]\\
&+(1-u_H)(u_H-s_H)(s_H-u_H^2)\mathrm{Re}\big[\mathcal{C}_{10a}\,\mathcal{C}_{10b}^*\big]+\frac{(u_H-s_H)(s_H-u_H^2)^2}{4u_H}\,|\mathcal{C}_{10b}|^2\Big\}\,,\\
K^s(s_H,u_H) = \frac{-12(s_H-u_H^2)^2(u_H-s_H)(1-u_H)}{u_H^4}&\left\{\mathrm{Re}\big[\mathcal{C}_9\,\mathcal{C}_{10a}^*\big]+\frac{2u_H}{u_H-s_H}\,\mathrm{Re}\big[\mathcal{C}_7\,\mathcal{C}_{10a}^*\big]\right\},
\end{aligned} \tag{4.79}$$

and the limits with q^2 and m_X cuts are

$$\begin{aligned}
&0\le s_H\le s_H^0\,,\qquad \max\Big\{s_H\,,u_1(s_H)\Big\}\le u_H\le \min\Big\{\sqrt{s_H}\,,u_2(s_H)\Big\}\,,\\
&u_1(s_H)=\frac{1+s_H-y_H^{\rm min}-\sqrt{(1+s_H-y_H^{\rm min})^2-4s_H}}{2}\,,\\
&u_2(s_H)=\frac{1+s_H-y_H^{\rm max}-\sqrt{(1+s_H-y_H^{\rm max})^2-4s_H}}{2}\,.
\end{aligned} \tag{4.80}$$

4.3.4 $d^2\Gamma/dq^2 dp_X^+$ Spectrum with q^2 and m_X Cuts

From Eqs. (4.58) and the above results, we can obtain the dileptonic invariant-mass spectrum and forward-backward asymmetry, for example by integrating the doubly

differential spectra

$$\begin{aligned}\frac{1}{\Gamma_0}\,\frac{d^2\Gamma}{dy_H du_H} &= H^y(y_H,u_H)\, m_B F^{(0)}\Big(m_B u_H, m_B\,\frac{1-y_H-u_H}{1-u_H}\Big), \qquad (4.81)\\ \frac{1}{\Gamma_0}\,\frac{d^2 A_{\rm FB}}{dy_H du_H} &= K^y(y_H,u_H)\, m_B F^{(0)}\Big(m_B u_H, m_B\,\frac{1-y_H-u_H}{1-u_H}\Big)\end{aligned}$$

over u_H. Here

$$\begin{aligned}H^y(y_H,u_H) = \frac{4[(1-u_H)^2-y_H]^2}{y_H(1-u_H)^3}\Big\{& y_H[(1-u_H)^2+2y_H]\,\big(|C_9|^2+|C_{10a}|^2\big) \qquad (4.82)\\ &+ [8(1-u_H)^2+4y_H]\,|C_7|^2 + 12y_H(1-u_H)\mathrm{Re}\big[C_7 C_9^*\big]\\ &+ y_H[(1-u_H)^2-y_H]\,\mathrm{Re}\big[C_{10a}C_{10b}^*\big] + \frac{y_H[(1-u_H)^2-y_H]^2}{4(1-u_H)^2}\,|C_{10b}|^2\Big\},\\ K^y(y_H,u_H) = \frac{-12y_H\,[(1-u_H)^2-y_H]^2}{(1-u_H)^3}&\left\{\mathrm{Re}\big[C_9\,C_{10a}^*\big] + \frac{2(1-u_H)}{y_H}\,\mathrm{Re}\big[C_7\,C_{10a}^*\big]\right\},\end{aligned}$$

and the limits of integration with cuts are

$$y_H^{\rm min} < y_H < y_H^{\rm max}\,, \quad 0 \le u_H \le \min\left\{1-\sqrt{y_H}\,,\, \frac{1+s_H^0-y_H-\sqrt{(1+s_H^0-y_H)^2-4s_H^0}}{2}\right\}. \qquad (4.83)$$

The opposite order of integration is also useful:

$$\begin{aligned}&0 \le u_H \le 1\,, \quad y_1(u_H) < y_H < y_2(u_H)\,,\\ &y_1(u_H) = \max\left\{y_H^{\rm min}, \frac{(1-u_H)(u_H-s_H^0)}{u_H}\right\}, \quad y_2(u_H) = \min\Big\{y_H^{\rm max}, (1-u_H)^2\Big\}. \qquad (4.84)\end{aligned}$$

The doubly differential rate can also be expressed in terms of the coefficients $C_9^{\rm mix}$, $C_7^{\rm mix}$, and C_{10}. This is one step closer to the short-distance coefficients C_9, C_7, and C_{10} of H_W, which we wish to measure in order to test the Standard Model predictions for

the corresponding FCNC interactions. Substituting Eq. (4.28) into Eq. (4.82) gives

$$
\begin{aligned}
H^y(y_H,u_H) &= \frac{4\big[(1-u_H)^2-y_H\big]^2}{(1-u_H)^3}\Bigg\{\big|C_7^{\rm mix}(s,\mu_0)\big|^2\Big[4\Omega_C^2(s,\mu_b)+\frac{8(1-u_H)^2}{y_H}\,\Omega_D^2(s,\mu_b)\Big] \\
&\quad+\Big[\big|C_9^{\rm mix}(s,\mu_0)\big|^2+C_{10}^2\Big]\Big[2y_H\,\Omega_A^2(s,\mu_b)+(1-u_H)^2\,\Omega_B^2(y_H,u_H,s,\mu_b)\Big] \\
&\quad+{\rm Re}\big[C_7^{\rm mix}(s,\mu_0)C_9^{\rm mix}(s,\mu_0)^*\big]\Big[12(1-u_H)\Omega_E(s,\mu_b)\Big]\Bigg\} \\
K^y(y_H,u_H) &= \frac{-12y_H\,[(1-u_H)^2-y_H]^2}{(1-u_H)^3}\,\Bigg\{{\rm Re}\big[C_9^{\rm mix}(s,\mu_0)\,C_{10}^*\big]\Omega_A^2(s,\mu_b) \\
&\quad+\frac{2(1-u_H)}{y_H}\,{\rm Re}\big[C_7^{\rm mix}(s,\mu_0)\,C_{10}^*\big]\Omega_A(s,\mu_b)\Omega_D(s,\mu_b)\Bigg\}\,,
\end{aligned}
\tag{4.85}
$$

where $s=q^2/m_b^2$ and

$$
\begin{aligned}
\Omega_A &= 1+\frac{\alpha_s(\mu_b)}{\pi}\,\omega_a^V(s,\mu_b)\,, \\
\Omega_B &= 1+\frac{\alpha_s(\mu_b)}{\pi}\Big[\omega_a^V(s,\mu_b)+\omega_c^V(s,\mu_b)+\frac{(1-u_H)^2-y_H}{2(1-u_H)^2}\omega_b^V(s,\mu_b)\Big]\,, \\
\Omega_C &= 1+\frac{\alpha_s(\mu_b)}{\pi}\Big[\omega_a^T(s,\mu_b)-\omega_b^T(s,\mu_b)-\omega_d^T(s,\mu_b)\Big]\,, \\
\Omega_D &= 1+\frac{\alpha_s(\mu_b)}{\pi}\Big[\omega_a^T(s,\mu_b)-\omega_c^T(s,\mu_b)-\frac{(1-u_H)^2+y_H}{2(1-u_H)^2}\omega_b^T(s,\mu_b)\Big]\,, \\
\Omega_E &= \big(2\Omega_A\Omega_D+\Omega_B\Omega_C\big)/3\,.
\end{aligned}
\tag{4.86}
$$

This is the form that turns out to be the most useful for the analysis in Chapter 5.

4.3.5 Numerical Analysis of Wilson Coefficients

As shown in Fig. 4-1, for the small-q^2 window ($q^2 < 6\,{\rm GeV}^2$) we have $p_X^+ \ll p_X^-$. Generically, the hard contributions in $\mathcal{C}_9$, $\mathcal{C}_7$, and $\mathcal{C}_{10a,10b}$ from our split-matching procedure depend on the variable q^2. In Fig. 4-5 we plot the q^2 dependence of the real part of the coefficients and see that there is in fact very little numerical change over the low-q^2 window. Here ${\rm Re}\big[C_9^{\rm local}\big]$ varies by $\pm1.5\%$, ${\rm Re}\big[C_9^{\rm mix}\big]$ by $\pm1\%$, and the real parts of $\{\mathcal{C}_9,\mathcal{C}_7,\mathcal{C}_{10a},\mathcal{C}_{10b}\}$ by $\{\pm1\%,\pm5\%,\pm2\%,\pm3\%\}$. The imaginary parts are either very small or also change by only a few percent over the low-q^2 window. The

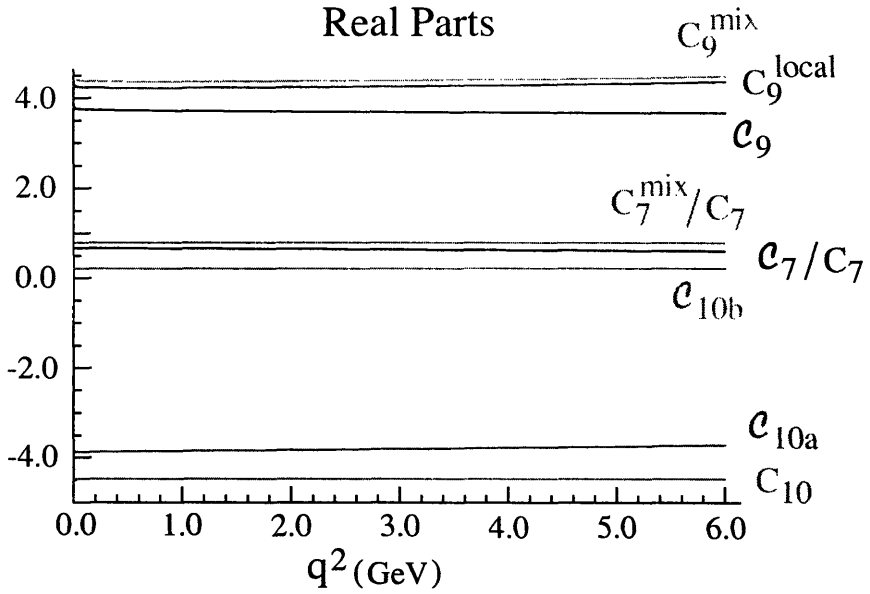

Figure 4-5: Comparison of the real part of Wilson coefficients at $\mu_0 = \mu_b = 4.8\,\text{GeV}$ with $m_c/m_b = 0.292$, $\overline{m_b}(\mu_0) = 4.17\,\text{GeV}$, and $m_b = 4.8\,\text{GeV}$. For $\mathcal{C}_9$, $\mathcal{C}_7$, and $\mathcal{C}_{10b}$ we take $p_X^+ = 0$.

analytic formulae for the q^2 dependence mean that there is no problem keeping the exact dependence, but this does make it necessary to perform integrals over regions in q^2 numerically. A reasonable first approximation can actually be obtained by fixing a constant q^2 in the hard coefficients, while keeping the full q^2 dependence elsewhere.

Since the coefficients change very little with q^2 we continue our numerical analysis by fixing $q^2 = 3\,\text{GeV}^2$. If we then take $\mu_0 = \mu_b = m_b = 4.8\,\text{GeV}$, $\overline{m_b}(\mu_0) = 4.17\,\text{GeV}$, $m_c/m_b = 0.292$ and $p_X^+ = 0$ we find that Eq. (4.28) gives

$$\begin{aligned}
\mathcal{C}_9 &= 0.826\, C_9^{\text{mix}} + 0.097\, C_7^{\text{mix}} = 3.448\, \frac{C_9^{\text{mix}}}{C_9^{\text{NDR}}} - 0.030\, \frac{C_7^{\text{mix}}}{C_7^{\text{NDR}}}\,, \\
\mathcal{C}_7 &= 0.823\, C_7^{\text{mix}} + 0.001\, C_9^{\text{mix}} = -0.239\, \frac{C_7^{\text{mix}}}{C_7^{\text{NDR}}} + 0.005\, \frac{C_9^{\text{mix}}}{C_9^{\text{NDR}}}\,.
\end{aligned} \tag{4.87}$$

These numbers indicate that, despite the entanglement of $C_{7,9}^{\text{mix}}$ in $\mathcal{C}_{7,9}$ due to $\alpha_s(m_b)$ corrections, numerically $\mathcal{C}_9$ is dominated by C_9 and $\mathcal{C}_7$ is dominated by C_7 in the Standard Model.

For the coefficients at $q^2 = 3.0\,\mathrm{GeV}^2$, with the other parameters as above, we have

$$\begin{aligned}
C_9^{\rm mix} &= 4.487 + 0.046i\,, & C_7^{\rm mix} &= -0.248\,,\\
\mathcal{C}_9(u_H = 0) &= 3.683 + 0.038i\,, & \mathcal{C}_7(u_H = 0) &= -0.198 + 6\times 10^{-5} i\,,\\
\mathcal{C}_9(u_H = 0.2) &= 3.663 + 0.038i & \mathcal{C}_7(u_H = 0.2) &= -0.193 + 10^{-4} i\,,\\
\mathcal{C}_{10a} &= -3.809\,, & \mathcal{C}_{10b}(u_H = 0) &= 0.214\,,\\
& & \mathcal{C}_{10b}(u_H = 0.2) &= 0.237\,. \qquad (4.88)
\end{aligned}$$

The relevant range of p_X^+ in Fig. 4-1 gives $0 \le u_H \le 0.2$. From the above numbers it is easy to see that the u_H dependence of $\mathcal{C}_9$, $\mathcal{C}_7$, and C_{10b} is very mild over the range of interest. The perturbative α_s corrections due to $\omega_i^{V,T}$ reduce both $\mathcal{C}_9$ and $\mathcal{C}_7$ by 17% relative to $C_9^{\rm mix}$ and $C_7^{\rm mix}$ respectively, and $\mathcal{C}_{10a}$ by 15%. This can be seen both in Fig. 4-5 and in Eq. (4.88), when one notes that $C_{10} = -4.480$. Comparing with coefficients in the local OPE, we note that the ω_{semi}^{OPE} factor, which accounts for the difference between $C_9^{\rm local}$ and $C_9^{\rm mix}$, is significantly smaller than the combination of α_s corrections in the ω_i^V terms that shifts $\mathcal{C}_9$ from its lowest-order value.

In quoting the above numbers, we have not varied the scales μ_0 and μ_b. The main point was to compare the size of the hard corrections in the shape function and local OPE regions, and to see how much deviation from $C_{7,9}^{\rm mix}$ they cause. The dependence on μ_0 for the $\mathcal{C}_i$ is similar to that in the local OPE analysis at NLL [121, 54] and will be reduced by a similar amount when the full NNLL expressions are included in $C_{7,9}^{\rm mix}$. The μ_b dependence of the $\mathcal{C}_i$ is fairly strong because of the appearance of double logarithms, but it is canceled by the μ_b dependence in the function $F^{(0)}$, which contains the NLL jet and shape functions.

4.4 Conclusion

In this chapter we have performed a model-independent analysis of $B \to X_s\ell^+\ell^-$ decays with cuts giving the small-q^2 window and an m_X cut to remove $b \to c$ backgrounds. These cuts put us in the shape function region. We analyzed the rate for

the formal counting with $q^2 \sim \lambda^0$ and $m_X^2 \sim \lambda^2$ and showed that the same universal shape function as in $B \to X_u \ell \bar{\nu}$ and $B \to X_s \gamma$ is the only non-perturbative input needed for these decays. We also developed a new effective-theory technique of split matching. Split matching between two effective theories is done not at a single scale μ, but rather at two nearby scales. For $B \to X_s \ell^+ \ell^-$ this allowed us to decouple the perturbation-theory analysis above and below m_b, which simplifies the organization of the α_s contributions.

In Section 4.3 we presented the leading-power triply differential spectrum and doubly differential forward-backward asymmetry with renormalization-group evolution and matching to $\mathcal{O}(\alpha_s)$. Above the scale m_b, we restricted our analysis to include the standard NLL terms from the local OPE, but illustrated how terms from NNLL can be incorporated. Below m_b we considered running to NLL and matching at one-loop (NNLL evolution will be straightforward to incorporate if desired). We then computed several phenomenologically relevant doubly differential spectra with phase-space cuts on q^2 and m_X (from which the singly differential spectra can be obtained by numerical integration). In section 4.3.5 we discussed the numerical size of our perturbative hard coefficients and compared them to the local OPE results.

Our results for the doubly differential rate in Eqs. (4.81) and (4.82), together with $F^{(0)}$ from Eq. (4.71), determine the shape-function-dependent rate for $B \to X_s \ell^+ \ell^-$. Using as input a result for the non-perturbative shape function $f^{(0)}$ from a fit to the $B \to X_s \gamma$ spectrum or from $B \to X_u \ell \bar{\nu}$ gives a model-independent result for $B \to X_s \ell^+ \ell^-$ with phase-space cuts.

Chapter 5

Universality and m_X-cut Effects in $B \to X_s \ell^+ \ell^-$

5.1 Introduction

In this chapter we compute the $B \to X_s \ell^+ \ell^-$ rate with an m_X cut in the low-q^2 region in a model-independent framework, using the results of Chapter 4. This enables us to carry out a full investigation of the m_X-cut dependence and phenomenology. An intriguing universality of the cut dependence is found, which makes the experimental extraction of short-distance Wilson coefficients in the presence of cuts much simpler.

To be more specific, we shall compute

$$\begin{aligned} \Gamma_{ij}^{\rm cut} &= \int_{q_1^2}^{q_2^2} {\rm d}q^2 \int_0^{m_X^{\rm cut}} {\rm d}m_X \, {\rm Re}(c_i c_j^*) \, \frac{{\rm d}^2\Gamma_{ij}}{{\rm d}q^2 {\rm d}m_X} \\ &= \eta_{ij}(m_X^{\rm cut}, q_1^2, q_2^2) \frac{\Gamma_0}{m_B^5} \int_{q_1^2}^{q_2^2} {\rm d}q^2 \, {\rm Re}(c_i c_j^*) \frac{(m_b^2 - q^2)^2}{m_b^3} \, G_{ij} \,, \end{aligned} \tag{5.1}$$

where $ij = \{77, 99, 00, 79\}$ label contributions of time-ordered products $T\{O_j^\dagger, O_i\}$. The η_{ij}'s contain the effects of the m_X cut, and the short-distance coefficients $c_{7,9,0}$ track the $C_{7,9,10}$ dependence in the effective Hamiltonian. Here $c_7 = C_7^{\rm mix}(q^2)$, $c_9 = C_9^{\rm mix}(q^2)$, and $c_0 = C_{10}$ can be obtained from local OPE calculations [54, 121] at each

order, as discussed in Ref. [107]. The functions

$$\begin{aligned} G_{99,00} &= (2q^2 + m_b^2)\,, \\ G_{77} &= 4m_B^2(1 + 2m_b^2/q^2)\,, \\ G_{79} &= 12 m_B m_b \end{aligned} \tag{5.2}$$

arise from kinematics. Here and below, m_b is a short-distance mass, such as m_b^{1S} [89, 88], and $\Gamma_0 = [G_F^2 m_B^5/(192\pi^3)]\,[\alpha_{\rm em}^2/(4\pi^2)]\,|V_{tb}V_{ts}^*|^2$. We also study $\eta'_{ij}(p_X^{+\rm cut}, q_1^2, q_2^2)$, which are defined by

$$\begin{aligned} \Gamma_{ij}^{\rm cut} &= \int_{q_1^2}^{q_2^2} {\rm d}q^2 \int_0^{p_X^{+\rm cut}} {\rm d}p_X\, {\rm Re}(c_i c_j^*)\, \frac{{\rm d}^2\Gamma_{ij}}{{\rm d}q^2 {\rm d}p_X} \\ &= \eta'_{ij}\big(p_X^{+\rm cut}, q_1^2, q_2^2\big) \frac{\Gamma_0}{m_B^5} \int_{q_1^2}^{q_2^2} {\rm d}q^2\, {\rm Re}(c_i c_j^*) \frac{(m_b^2 - q^2)^2}{m_b^3}\, G_{ij}\,. \end{aligned} \tag{5.3}$$

At leading order in $\Lambda_{\rm QCD}/m_b$ and α_s, $\eta_{ij} = 1$ for $m_X^{\rm cut} = m_B$, and η_{ij} give the fraction of events with $m_X < m_X^{\rm cut}$. This is altered at subleading order by α_s corrections, but η_{ij} still determine the total rate with cuts,

$$\Gamma^{\rm cut} = \sum_{ij} \Gamma_{ij}^{\rm cut}\,. \tag{5.4}$$

In principle, η_{ij} depend in a non-trivial way on ij (and q_1^2 and q_2^2) because of their different dependence on kinematic variables, α_s corrections, etc. At leading order in $\Lambda_{\rm QCD}/m_b$, we demonstrate that η_{ij} are independent of the choice of ij; this is what we mean by "universality". We first show this formally at leading order in $p_X^+/m_B \ll 1$ for $\eta'(p_X^{+\rm cut})$ and then numerically for the experimentally relevant $\eta(m_X^{\rm cut})$, including the α_s corrections and phase-space effects. Since the same shape function occurs in $B \to X_s\ell^+\ell^-$, $X_u\ell\bar\nu$, and $X_s\gamma$, the $m_X^{\rm cut}$ or $p_X^{+\rm cut}$ dependence in one can be accurately determined from the others. For current experimental cuts this is a 10–30% effect. We shall also discuss another possibility: because of universality, normalizing the $B \to X_s\ell^+\ell^-$ rate to $B \to X_u\ell\bar\nu$ with the same cuts removes the main uncertainties.

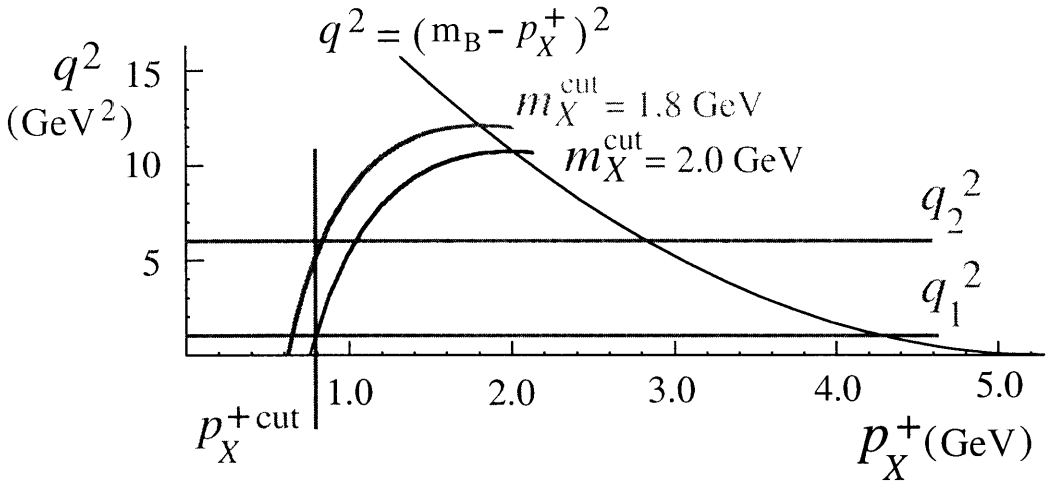

Figure 5-1: Phase-space cuts. A substantial part of the rate for $q_1^2 < q^2 < q_2^2$ falls in the rectangle bounded by $p_X^+ < p_X^{+\mathrm{cut}}$.

5.2 m_X-cut Effects at leading order

The phase-space cuts are shown in Fig. 5-1. Recall from Chapter 4 that, of the variables symmetric in p_{ℓ^+} and p_{ℓ^-} ($p_X^\pm$, E_X, q^2, m_X^2), only two are independent: we work with q^2 and p_X^+ or m_X. As discussed in Chapter 3, for the $p_X^+ \ll p_X^-$ region, factorization of the form $\mathrm{d}\Gamma = HJ \otimes \hat{f}^{(0)}$ (where H contains perturbative physics at $\mu_b \sim m_b$, J at $\mu_i \sim \sqrt{\Lambda_{\mathrm{QCD}} m_b}$, and $\hat{f}^{(0)}(\omega)$ is a universal non-perturbative shape function) has been shown for semileptonic and radiative B decays. In Chapter 4, we found that this factorization also applies for $B \to X_s \ell^+ \ell^-$ with the same $\hat{f}^{(0)}$, as long as q^2 is not parametrically small [107].

In the $q^2 < 6\,\mathrm{GeV}^2$ region, $|C_9^{\mathrm{mix}}(q^2, \mu_0 = 4.8\,\mathrm{GeV})| = 4.52$ to better than 1%, and can be taken to be constant. We neglect α_s corrections in this section, using Eq. (4.81) with $F^{(0)} \to \hat{f}^{(0)}$:

$$\begin{aligned}
\frac{\mathrm{d}\Gamma}{\mathrm{d}p_X^+ \mathrm{d}q^2} &= \hat{f}^{(0)}(p_X^+)\,\frac{\Gamma_0}{m_B^5}\,\frac{[(m_B - p_X^+)^2 - q^2]^2}{(m_B - p_X^+)^3} \\
&\quad \times \Big\{ (|C_9^{\mathrm{mix}}|^2 + C_{10}^2)\big[2q^2 + (m_B - p_X^+)^2\big] \\
&\quad + 4m_B^2\,|C_7^{\mathrm{mix}}|^2 \Big[1 + \frac{2(m_B - p_X^+)^2}{q^2}\Big] \\
&\quad + 12 m_B\,\mathrm{Re}\big[C_7^{\mathrm{mix}} C_9^{\mathrm{mix}*}\big](m_B - p_X^+)\Big\}. \qquad (5.5)
\end{aligned}$$

where $\hat{f}^{(0)}(\omega)$ has support in $\omega \in [0,\infty)$. As a function of p_X^+, the kinematic terms in Eq. (5.5) vary *only* on a scale m_B, while $\hat{f}^{(0)}(p_X^+)$ varies on a scale $\Lambda_{\rm QCD}$. Writing $m_B = m_b + \bar{\Lambda}$ and expanding in $(p_X^+ - \bar{\Lambda})/m_B$ decouple the p_X^+ and q^2 dependences in Eq. (5.5):

$$\begin{aligned}\frac{d\Gamma}{dp_X^+ dq^2} \;\to\; \hat{f}^{(0)}(p_X^+)\,\frac{\Gamma_0}{m_B^5}\,\frac{[m_b^2-q^2]^2}{m_b^3}\,\Big\{&(|C_9^{\rm mix}|^2 + C_{10}^2)\big[2q^2+m_b^2\big] \\ &+ 4m_B^2\,|C_7^{\rm mix}|^2\Big[1+\frac{2m_b^2}{q^2}\Big] + 12 m_B\, m_b {\rm Re}\big[C_7^{\rm mix} C_9^{\rm mix *}\big]\Big\}. \end{aligned} \tag{5.6}$$

Hence, we obtain the local OPE prefactors, $(m_b^2 - q^2)^2\, G_{ij}(q^2)$, in Eq. (5.1). For $\eta'_{ij}(p_X^{+\rm cut}, q_1^2, q_2^2)$, the p_X^+ integration is over a rectangle in Fig. 5-1, whose boundaries do not couple p_X^+ and q^2. Thus,

$$\eta' = \int dp_X^+\, \hat{f}^{(0)}(p_X^+)\,, \tag{5.7}$$

which is independent of ij and $q_{1,2}^2$. While the m_X cut retains more events than the p_X^+ cut, the latter may give theoretically cleaner constraints on short-distance physics when statistical errors become small.

The effect of the m_X cut is q^2 dependent, because the upper limit of the p_X^+ integration is q^2-dependent, as shown in Fig. 5-1. When one includes the full p_X^+ dependence in Eq. (5.5), the universality of $\eta_{ij}(m_X^{\rm cut}, q_1^2, q_2^2)$ is maintained to better than 3% for $1\,{\rm GeV}^2 \le q_1^2 \le 2\,{\rm GeV}^2$, $5\,{\rm GeV}^2 \le q_2^2 \le 7\,{\rm GeV}^2$, and $m_X^{\rm cut} \ge 1.7\,{\rm GeV}$, because the region where the p_X^+ and q^2 integration limits are coupled has a small effect on the ij dependence. This is exhibited in Fig. 5-2, where the solid curves show $\eta_{ij}(m_X^{\rm cut}, 1\,{\rm GeV}^2, 6\,{\rm GeV}^2)$ with the shape function set to model 1 of Ref. [135], with $m_b^{1S} = 4.68\,{\rm GeV}$ and λ_1 from Ref. [24]. (Taking $q_1^2 = 1\,{\rm GeV}^2$ instead of $4m_\ell^2$ increases the sensitivity to $C_{9,10}$, but one may be concerned by local duality / resonances near $q^2 = 1\,{\rm GeV}^2$. To estimate this uncertainty, assume the ϕ is just below the cut and $\mathcal{B}(B \to X_s\phi) \approx 10 \times \mathcal{B}(B \to K^{(*)}\phi)$. Then $B \to X_s\phi \to X_s\ell^+\ell^-$ is $\sim 2\%$ of the $X_s\ell^+\ell^-$ rate.)

The LO local OPE results for $\eta_{ij}(m_X^{\rm cut}, q_1^2, q_2^2)$ are obtained by replacing $\hat{f}^{(0)}(p_X^+)$

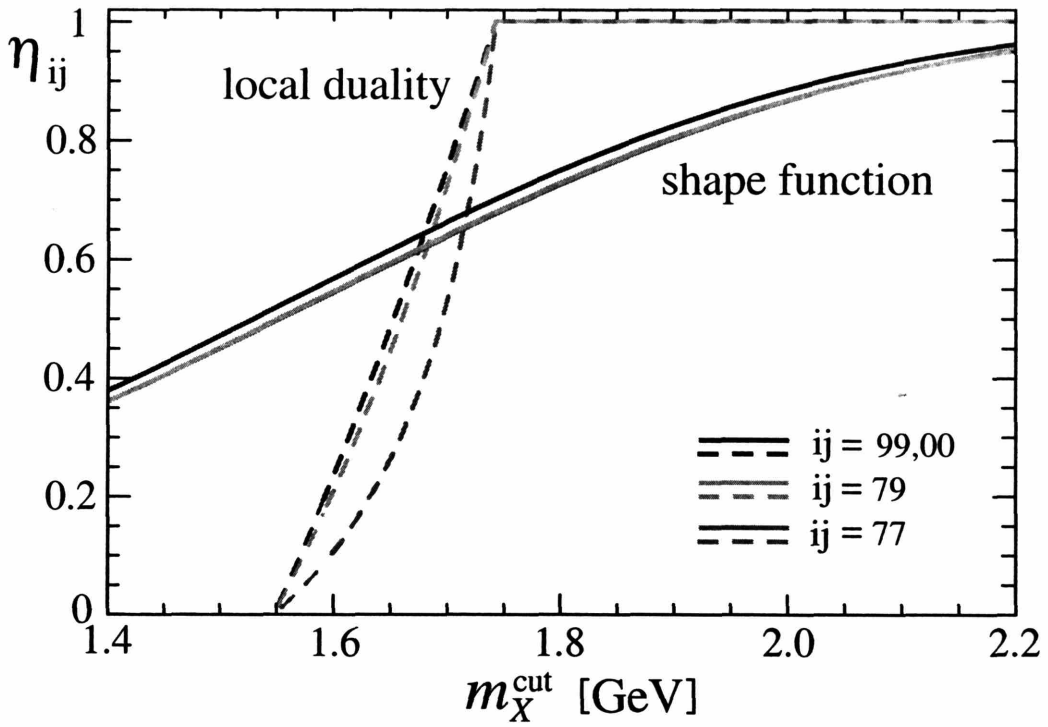

Figure 5-2: $\eta_{ij}(m_X^{\rm cut}, 1\,{\rm GeV}^2, 6\,{\rm GeV}^2)$ as functions of $m_X^{\rm cut}$. The dashed curves show the local OPE result, the solid curves include the leading shape-function effects. The uppermost, middle, and lowest curves are $\eta_{00,99}$, η_{79}, and η_{77}, respectively.

by $\delta(\bar\Lambda - p_X^+)$ in Eq. (5.5). Performing the p_X^+ integral sets $(m_B - p_X^+) = m_b$ and implies that $m_X^2 > \bar\Lambda(m_B - q^2/m_b)$. This makes the lower limit on q^2 equal $\max\{q_1^2,\, m_b[m_B - (m_X^{\rm cut})^2/\bar\Lambda]\}$, and so the η_{ij}'s depend on the shape of $d\Gamma_{ij}$. In Fig. 5-2 the local OPE results are shown by dashed lines, and clearly $\eta_{77} \neq \eta_{99}$. However, the local OPE is not applicable for $p_X^+ \sim \Lambda_{\rm QCD}$.

The universality of η_{ij} found here could be broken by α_s corrections in the H or J functions, or by renormalization-group evolution, since these effects couple p_X^+ and q^2 and have been neglected so far. We consider these next.

5.3 Calculation and Results at $\mathcal{O}(\alpha_s)$

The shape function model is specified at μ_Λ, and we now implement the convolution of jet and shape functions at NLL order, including α_s corrections, using Eqs. (4.71) and (4.65). The hard α_s corrections are included by using Eqs. (4.85) and (4.86).

The model we use for $\hat{f}^{(0)}$ is a generalization of model 1 of Ref. [135]:

$$\begin{aligned}\hat{f}_{\rm mod}(r^+; a, b, c, p, q) &= \tilde{f}_{\rm mod}\big(r^+;\, c\,a,\, b\,n(p,q),\, p,\, q\big) \\ &\quad + \tilde{f}_{\rm mod}\big(r^+,\, c(1-a),\, b\;n(p+1,q),\, p+1,\, q\big)\,, \\ \tilde{f}_{\rm mod}(r^+; a',\, b',\, p',\, q') &= \frac{a'}{\Gamma\big((p'+1)/q'\big)}\frac{q'}{b'}\left(\frac{r^+}{b'}\right)^{p'}\exp\left[-\left(\frac{r^+}{b'}\right)^{q'}\right], \\ n(x,y) &= \frac{\Gamma\big((x+1)/y\big)}{\Gamma\big((x+2)/y\big)}\,.\end{aligned} \tag{5.8}$$

The model parameters (a, b, c) are determined (in terms of the remaining parameters, p and q) by the known constraints on the first three moments of the shape function [47] converted to the $1S$ mass scheme. We estimate the shape-function uncertainties by varying p and q to obtain five different models, each chosen to be consistent with $B \to X_s\gamma$ data. Since we also use two different values of μ_Λ, this results in a total of ten functional forms for $\hat{f}^{(0)}$ for each value of m_b^{1S}.

For each shape-function model, the deviations of the η_{ij}'s from being universal when we include all NLL corrections are still below 3%. Thus, the picture of universality in Fig. 5-2 remains valid at NLL order. This means we can explore the overall shift by just studying η_{00}.

In Fig. 5-3, we plot $\eta_{00}(m_X^{\rm cut}, 1\,{\rm GeV}^2, 6\,{\rm GeV}^2)$, including the α_s corrections. The ten orange, green and purple (medium, light, dark) curves correspond to $m_b^{1S} = 4.68\,{\rm GeV}$, $4.63\,{\rm GeV}$, and $4.73\,{\rm GeV}$, respectively, where the central values $\mu_0 = \mu_b = 4.8\,{\rm GeV}$ and $\mu_i = 2.5\,{\rm GeV}$ have been used. The curves with slightly lower (higher) values of η_{00} at large $m_X^{\rm cut}$ correspond to $\mu_\Lambda = 1.5\,{\rm GeV}$ ($2\,{\rm GeV}$). For $m_X^{\rm cut} = 2\,{\rm GeV}$, varying μ_b in the range $3.5\,{\rm GeV} < \mu_b < 7.5\,{\rm GeV}$ changes η_{00} by $\pm 6\%$. We find a $\pm 5\%$ variation for $2\,{\rm GeV} < \mu_i < 3\,{\rm GeV}$.

Using the c_i's at NLL order, for $1\,{\rm GeV}^2 < q^2 < 6\,{\rm GeV}^2$ and $m_X^{\rm cut} = 1.8$ and $2.0\,{\rm GeV}$, we obtain $\Gamma^{\rm cut}\,\tau_B = (1.20\pm0.15)\times10^{-6}$ and $(1.48\pm0.14)\times10^{-6}$, respectively, where uncertainties from m_b, μ_b, μ_i, and $\hat{f}^{(0)}$ are included. Changing μ_0 to $3.5\,{\rm GeV}$ ($10\,{\rm GeV}$) changes both of these rates by -2% ($+7\%$), and this uncertainty will be

reduced by including NNLL corrections [45, 10, 44, 75, 9, 77].

The largest source of universality breaking in the η_{ij}'s and one of the largest uncertainties in the rate is the subleading shape functions, which affect the rate by $\sim 5\%$ for $m_X^{\rm cut} = 2\,{\rm GeV}$ and by $\sim 10\%$ for $m_X^{\rm cut} = 1.8\,{\rm GeV}$.

If the $m_X^{\rm cut}$ dependence were not universal, it would modify the zero of the forward-backward asymmetry, $A_{\rm FB}(q_0^2) = 0$. The quantity q_0^2 is interesting because at LO in the local OPE it is determined by the equation

$$\frac{q_0^2}{m_b^2}{\rm Re}\big[C_9^{\rm local}(q_0^2)\big] + 2C_7^{NDR} = 0\,, \tag{5.9}$$

which makes it sensitive to physics beyond the Standard Model. We find that imposing the cut $m_X^{\rm cut} = 2\,{\rm GeV}$ shifts the zero at NLL by $\Delta q_0^2 \approx -0.04\,{\rm GeV}^2$, which is much less than the higher-order uncertainties [75, 9, 77]. We obtain the central value $q_0^2 = 2.8\,{\rm GeV}^2$, which is lower than earlier results [75, 9]. The reason is that in the SCET calculation of $A_{\rm FB}$, using K in Eq. (4.85), the pole mass $m_b^{\rm pole}$ never occurs, only $m_B - p_X^+$ and $\overline{m}_b$ (at this order, $C_7^{\rm mix} = (\overline{m}_b/m_B)C_7^{\rm eff}$ [107]). Thus, schematically, $q_0^2 \sim 2m_b^{1S}[\overline{m}_b(\mu_0)C_7(\mu_0)]/{\rm Re}[C_9(q_0^2)]$, and there is no reason to expand $\overline{m}_b$ in terms of $m_b^{\rm pole}$. Using $m_b^{\rm pole}$ in Eq. (5.9) would give large central values for q_0^2.

Let's now consider how one might best minimize the hadronic uncertainties. We previously mentioned that one strategy is to extract the incalculable shape function $f^{(0)}$ from the $B \to X_s\gamma$ data and use it as an input to our $B \to X_s\ell^+\ell^-$ results. In the latter process, the theoretical uncertainties are reduced by raising the value of $m_X^{\rm cut}$. Another possibility is to keep $m_X^{\rm cut} < m_D$ and measure

$$R = \frac{\Gamma^{\rm cut}(B \to X_s\ell^+\ell^-)}{\Gamma^{\rm cut}(B \to X_u\ell\bar{\nu})}\,, \tag{5.10}$$

with the same cuts used in numerator and denominator. The point of this approach is that we have found that the m_X-cut effects are universal (to a good approximation) for all short-distance contributions. The semileptonic decay essentially corresponds to the $|C_{10}|^2$ term (refer to Eq. (4.73)). Thus, the effects of $m_X^{\rm cut}$, as well as the m_b dependence, are drastically reduced in the ratio R.

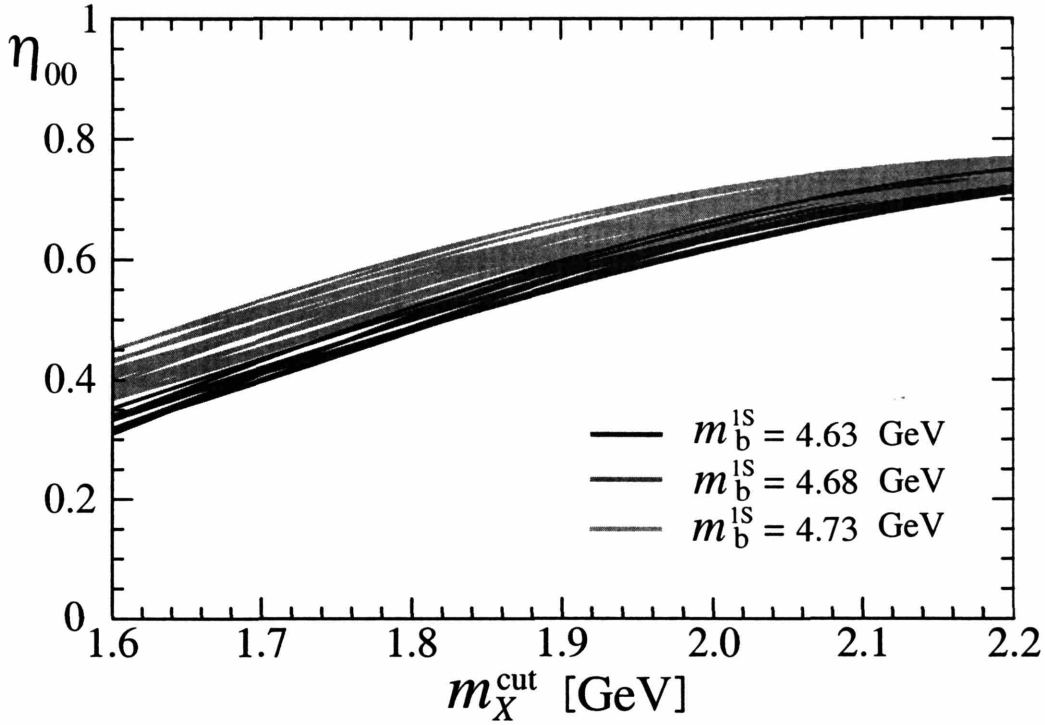

Figure 5-3: $\eta_{00}(m_X^{\rm cut}, 1\,{\rm GeV}^2, 6\,{\rm GeV}^2)$ as a function of $m_X^{\rm cut}$. The orange, green and purple (medium, light, dark) curves show $m_b^{1S} = 4.68\,{\rm GeV}$, $4.63\,{\rm GeV}$, and $4.73\,{\rm GeV}$, respectively.

In conclusion, we pointed out that the experimentally used upper cut on m_X makes the observed $B \to X_s \ell^+ \ell^-$ rate in the low-q^2 region sensitive to the shape function. We found that the η's for the different operators' contributions are universal to a good approximation. Thus, one can either use the shape function measured in other processes or use the ratio R above, with the result that the sensitivity to new physics is not reduced. These results also apply for $B \to X_d \ell^+ \ell^-$, which may be studied at a higher-luminosity B factory. Subleading $\Lambda_{\rm QCD}/m_b$ as well as NNLL corrections to the rate and the forward-backward asymmetry will be studied in the future.

Chapter 6

Conclusions

Heavy-quark physics plays a crucial role in the study of physics both within and beyond the Standard Model. Within the Standard Model, QCD and the flavour sector can be probed rigorously. The search for new physics is aided by the examination of FCNC processes, which are absent at tree level in the Standard Model.

On the theoretical side, effective field theories are a powerful technique. The basic idea is that, in order to describe a physical system, one should determine the relevant degrees of freedom, exploit the symmetries to constrain the possible interactions, and identify a suitable expansion parameter. This enables one to provide a lowest-order description and incorporate higher-order corrections systematically, while avoiding any *ad hoc* models or assumptions.

In this thesis, we have focussed on inclusive semileptonic and rare decays in the shape function region, to which one is restricted by experimentally required cuts. Here, the operator product expansion is invalid. The relevant degrees of freedom include collinear and ultrasoft modes and the appropriate effective field theory is $\mathrm{SCET_I}$, which has an expansion in $\lambda \sim \sqrt{\Lambda_{\mathrm{QCD}}/m_b}$.

In order to make predictions, one has to disentangle short- and long-distance effects, a process known as factorization. One can then treat the hard and soft effects separately, using whatever tool is appropriate for each. In endpoint decays, there are three scales. The contributions at the hard and intermediate scales are both calculable perturbatively, whereas the long-distance hadronic physics is described by

non-perturbative but universal shape functions. SCET helps to simplify the derivation of factorization theorems. We used it in Chapter 3 to derive a factorization theorem, at order λ^2 and all orders in α_s, for the processes $B \to X_u \ell \bar{\nu}$ and $B \to X_s \gamma$ in the endpoint region. This involved constructing all $\mathcal{O}(\lambda^2)$ time-ordered products of the form $J^{(n_1)\dagger} \mathcal{L}^{(n_2)} \cdots \mathcal{L}^{(n_{j-1})} J^{(n_j)}$, with $\sum_i n_i = 2$, a task made possible by the transparent power counting of SCET. We obtained the complete list of subleading shape functions and the triply differential rate at this order for the first time. If one works at tree level in the jet function, the relevant subleading shape functions are $f_0^{(0)}$, $f_{1,2}^{(2)}$, $f_{3,4}^{(4)}$ and $f_{5,6}^{(6)}$, the last two of which are due to four-quark operators. Now, $f_0^{(0)}$ can be absorbed into the leading-order shape function, $f^{(0)}$, and $f_1^{(2)}$ can be expressed in terms of $f^{(0)}$; this leaves five independent subleading shape functions. However, if one includes one-loop corrections to the jet function, then prohibitively many shape functions appear.

We next considered the decay $B \to X_s \ell^+ \ell^-$, in which the small-q^2 region is important for achieving sensitivity to new physics, but the experimentally used cut on m_X leads to shape-function effects being significant. Here, we encountered a problem in the perturbative power counting. Above the scale m_b, one usually expands in α_s, with $\alpha_s \log(m_W/m_b) = \mathcal{O}(1)$. Because of mixing with $\mathcal{O}_{1,2}$, $C_9 \sim \log(m_W/m_b) \sim \frac{1}{\alpha_s}$, whereas $C_{7,10} \sim 1$. This power counting is important for cancelling scheme and scale dependence in the running. However, numerically $|C_9(m_b)| \sim C_{10}$. This conflict is exacerbated by the fact that in the shape function region only the rate is calculable, not the amplitude. It would not make sense to have to count $\langle \bar{B}|\mathcal{O}_9^\dagger \mathcal{O}_9|\bar{B}\rangle \sim \frac{1}{\alpha_s^2}$, but $\langle \bar{B}|\mathcal{O}_{10}^\dagger \mathcal{O}_{10}|\bar{B}\rangle \sim 1$. The solution to this problem was to use "split matching", which decouples the scale dependence above and below $\mu = m_b$ and thereby allows one to use different perturbative power counting in these two regions.

The decay spectra derived were used to calculate the effect of the m_X cut on the $B \to X_s \ell^+ \ell^-$ rate. We found approximate universality, i.e. the contributions from different operators were affected in approximately the same way. Consequently, one can minimize uncertainties and maintain sensitivity to new physics either by using $B \to X_s \gamma$ data to determine the leading-order shape function or by normalizing with

respect to the $B \rightarrow X_u \ell \bar{\nu}$ rate with the same cuts.

Appendix A

Expansion of the heavy quark field and derivation of the currents

To derive the power expansion of the heavy-to-light current $J = \bar{\psi}^{(q)}\Gamma\psi^{(b)}$ at tree level we just need the expansion of the light- and heavy-quark full-theory fields, $\psi^{(q)}$ and $\psi^{(b)}$, in terms of SCET collinear fields (ξ_n) and soft heavy fields (h_v) respectively. $\psi^{(q)}$ also contains terms with usoft light quark fields, but they do not contribute for inclusive processes until higher order, and so we neglect these terms here. For the light quark field we have [118]

$$\begin{aligned}\psi^{(q)} &= \left[1+\frac{1}{i\bar{n}\cdot D_c + Wi\bar{n}\cdot D_{us}W^\dagger}(i\not{D}_c^\perp + Wi\not{D}_{us}^\perp W^\dagger)\frac{\not{\bar{n}}}{2}\right]\xi_n \qquad (A.1)\\ &= \xi_n + \frac{1}{i\bar{n}\cdot D_c} i\not{D}_c^\perp \frac{\not{\bar{n}}}{2}\xi_n + W\frac{1}{\bar{\mathcal{P}}} i\not{D}_{us}^\perp \frac{\not{\bar{n}}}{2}W^\dagger\xi_n - W\frac{i\bar{n}\cdot D_{us}}{\bar{\mathcal{P}}^2}W^\dagger i\not{D}_c^\perp\frac{\not{\bar{n}}}{2}\xi_n + \mathcal{O}(\lambda^4)\,.\end{aligned}$$

Here we have used the collinear fields [32]

$$\begin{aligned} in\cdot D &= in\cdot\partial + gn\cdot A_c + gn\cdot A_{us}\,, \qquad iD^\perp = iD_c^\perp + WiD_{us}^\perp W^\dagger\,,\\ i\bar{n}\cdot D &= i\bar{n}\cdot D_c + Wi\bar{n}\cdot D_{us}W^\dagger\,, \end{aligned} \qquad (A.2)$$

which obviously will give an expansion with terms that are individually usoft and collinear gauge covariant at each order in λ.

For the heavy quark fields we start with the QCD Lagrangian $\mathcal{L} = \bar{\psi}^{(b)}(i\not{D} -$

$m_b)\psi^{(b)}$. We then divide the quark fields into on-shell and off-shell terms, $\psi^{(b)} = \exp(-imv\cdot x)(h_v + \psi_B)$, where $\not{v}h_v = h_v$. Unlike in HQET, the off-shell field ψ_B does not satisfy $\not{v}\psi_B = -\psi_B$, since collinear gluons give off-shell quark fields that have quark components, $\not{v}\psi_B = \psi_B$. This gives the Lagrangian

$$\mathcal{L} = \bar{h}_v iv\cdot D_{us} h_v + \bar{\psi}_B[i\not{D} + m_b(\not{v} - 1)]\psi_B + \bar{h}_v(i\not{D} - \not{\mathcal{P}})\psi_B + \bar{\psi}_B(i\not{D} - \not{\mathcal{P}})h_v\,, \quad \text{(A.3)}$$

where the subtraction in $(i\not{D} - \not{\mathcal{P}})$ removes the terms that vanish by momentum conservation. Varying with respect to $\bar{\psi}_B$ gives

$$[i\not{D} + m_b(\not{v} - 1)]\psi_B = -(i\not{D} - \not{\mathcal{P}})h_v\,, \quad \text{(A.4)}$$

which is a higher-order version of the LO equation for ψ_B derived in Ref. [30]. To solve for ψ_B in terms of h_v at higher orders we use a strategy proposed in Ref. [37], namely expanding $\psi_B = \psi_B^{(3)} + \psi_B^{(4)} + \ldots$, and considering the solutions order by order in λ (noting that $h_v \sim \lambda^3$). To facilitate this we rewrite Eq. (A.4) as

$$\Big[\Delta^{(0)} + i\not{D}_c^\perp + \Delta^{(2)}\Big](\psi_B^{(3)} + \psi_B^{(4)} + \ldots) = -\Big[\frac{\not{n}}{2} g\bar{n}\cdot A_c + g\not{A}_c^\perp + \Delta^{(2)}\Big]h_v\,, \quad \text{(A.5)}$$

$$\Delta^{(0)} = \frac{\not{n}}{2} i\bar{n}\cdot D_c + m_b(\not{v} - 1)\,, \qquad \Delta^{(2)} = W\Big(\frac{\not{n}}{2} i\bar{n}\cdot D_{us} + i\not{D}_{us}^\perp\Big)W^\dagger + \frac{\bar{\not{n}}}{2} in\cdot D\,.$$

The complete set of equations to solve is then

$$\begin{aligned}
\Delta^{(0)}\psi_B^{(3)} &= -\frac{\not{n}}{2} g\bar{n}\cdot A_c h_v\,, \quad \text{(A.6)}\\
\Delta^{(0)}\psi_B^{(4)} &= -i\not{D}_\perp^c \psi_B^{(3)} - g\not{A}_c^\perp h_v\,,\\
\Delta^{(0)}\psi_B^{(5)} &= -i\not{D}_\perp^c \psi_B^{(4)} - \Delta^{(2)}(\psi_B^{(3)} + h_v)\,,\\
\Delta^{(0)}\psi_B^{(n)} &= -i\not{D}_\perp^c \psi_B^{(n-1)} - \Delta^{(2)}\psi_B^{(n-2)}\,,
\end{aligned}$$

where $n \geq 6$. Obviously, the crucial point is to invert the operator $\Delta^{(0)}$. When acting

on a collinear field, the inverse $[\Delta^{(0)}]_c^{-1}$ is simply given by

$$[\Delta^{(0)}]_c^{-1} = \frac{\bar{n}\!\!\!/}{2m_b\, n\cdot v} + \frac{(1+v\!\!\!/)}{n\cdot v\, i\bar{n}\cdot D_c}\,. \tag{A.7}$$

Owing to the $1/(i\bar{n}\cdot D_c)$, this solution is ill-defined when acting on an ultrasoft field and will not suffice to solve for $\psi_B^{(n\geq 5)}$. For the solution to the first equation we find

$$\psi_B^{(3)} = -\frac{1}{i\bar{n}\cdot D_c} g\bar{n}\cdot A_c h_v = (W-1)h_v\,, \tag{A.8}$$

which, as expected, is in agreement with the LO solution in the appendix of Ref. [30]. Thus, at lowest order the solution for the full-theory field is $\psi = h_v + \psi_B^{(3)} = W h_v$. At the next order, we find that

$$\begin{aligned}\psi_B^{(4)} &= -[\Delta^{(0)}]_c^{-1}(i\not{D}_c^{\perp} W - \not{\mathcal{P}}_\perp)h_v = -[\Delta^{(0)}]_c^{-1}\frac{1}{i\bar{n}\cdot D_c} ig\not{B}_\perp^c W h_v \\ &= -\frac{1}{m_b\, n\cdot v}\frac{\bar{n}\!\!\!/}{2} W\Big[\frac{1}{\bar{\mathcal{P}}} W^\dagger ig\not{B}_\perp^c W\Big]h_v - \frac{2}{n\cdot v} W\Big[\frac{1}{\bar{\mathcal{P}}^2} W^\dagger igv\cdot B_\perp^c W\Big]h_v\,,\end{aligned} \tag{A.9}$$

where

$$igB_\perp^{c\mu} = [i\bar{n}\cdot D^c, iD_c^{\perp\mu}]. \tag{A.10}$$

The result agrees with Refs. [37, 130], except that we have written the last term as $v\cdot B_\perp^c$ to emphasize that it must start with at least one collinear gluon.

To proceed we let

$$\psi_B^{(n)} = W\tilde{\psi}_B^{(n)}\,, \qquad \Delta^{(0)} W = W\tilde{\Delta}^{(0)}\,, \tag{A.11}$$

and then write the remaining equations for $\tilde{\psi}_B^{(n)}$. Using the equation of motion for W gives

$$\tilde{\Delta}^{(0)} = \frac{\bar{n}\!\!\!/}{2}\bar{\mathcal{P}} + m_b(v\!\!\!/ - 1)\,, \qquad [\tilde{\Delta}^{(0)}]_c^{-1} = \frac{\bar{n}\!\!\!/}{2m_b\, n\cdot v} + \frac{(1+v\!\!\!/)}{n\cdot v\,\bar{\mathcal{P}}}\,, \tag{A.12}$$

and so, after we multiply on the left by $W^\dagger$, the remaining equations become

$$\begin{aligned}
\tilde{\Delta}^{(0)}\tilde{\psi}_B^{(5)} &= -\tilde{\Delta}^{(1)}\tilde{\psi}_B^{(4)} - \tilde{\Delta}^{(2)}h_v - i\not{D}_{us}h_v\,, \\
\tilde{\Delta}^{(0)}\tilde{\psi}_B^{(n)} &= -\tilde{\Delta}^{(1)}\tilde{\psi}_B^{(n-1)} - \tilde{\Delta}^{(2)}\tilde{\psi}_B^{(n-2)} - i\not{D}_{us}\tilde{\psi}_B^{(n-2)}\,, \\
\tilde{\Delta}^{(1)} &= (W^\dagger i\not{D}_\perp^c W)\,, \qquad \tilde{\Delta}^{(2)} = \frac{\bar{n}\!\!\!/}{2}(W^\dagger in\cdot DW - in\cdot D_{us})\,,
\end{aligned} \tag{A.13}$$

where $n \geq 5$.

To solve Eqs. (A.13) we invert $\tilde{\Delta}^{(0)}$. For terms with at least one collinear gluon field, such as $\tilde{\Delta}^{(1,2)}$, we can use the inverse $[\tilde{\Delta}^{(0)}]_c^{-1}$ from Eq. (A.12). Only terms that are purely usoft, including $i\not{D}_{us}h_v$ and possibly $i\not{D}_{us}\tilde{\psi}_B^{(n-2)}$, need to be handled with care. For these terms a purely usoft $\psi_B^{(n)}$ suffices, in which case $\tilde{\Delta}^{(0)} = m(\not{v} - 1)$. The subset of purely usoft terms in Eqs. (A.13) is given uniquely by the terms $m(\not{v} - 1)\psi_B^{(5)} = -i\not{D}_{us}h_v$ and $m(\not{v}-1)\psi_B^{(n)} = -i\not{D}_{us}\psi_B^{(n-2)}$, which are the same as we would find in pure HQET. Thus, the solution for the pure usoft terms is

$$\psi_B^{us} = \frac{1}{2m_b + iv\cdot D_{us}} i\not{D}_{us}^T h_v\,, \qquad [\tilde{\Delta}^{(0)}]_{us}^{-1} = -\frac{1}{2m_b}\frac{(1-\not{v})}{2}\,, \tag{A.14}$$

where it is sufficient to use this $[\tilde{\Delta}^{(0)}]_{us}^{-1}$ since $(1-\not{v})/2\,\psi_B^{us} = \psi_B^{us}$. From Eq. (A.13), the solution for $\psi_B^{(5)}$ is then

$$\begin{aligned}
\psi_B^{(5)} &= W\frac{i\not{D}_{us}^T}{2m_b}h_v - W[\tilde{\Delta}^{(0)}]_c^{-1}\tilde{\Delta}^{(1)}\tilde{\psi}_B^{(4)} - W[\tilde{\Delta}^{(0)}]_c^{-1}\tilde{\Delta}^{(2)}h_v \\
&= W\frac{i\not{D}_{us}^T}{2m_b}h_v - W\frac{\not{n}\bar{\not{n}}}{4m_b\, n\cdot v}\Big[\frac{1}{\bar{\mathcal{P}}}W^\dagger ign\cdot B_c W\Big]h_v - W\frac{\bar{n}\cdot v}{n\cdot v\,\bar{\mathcal{P}}}\Big[\frac{1}{\bar{\mathcal{P}}}W^\dagger ign\cdot B_c W\Big]h_v \\
&\quad - W\frac{1}{m_b\, n\cdot v}\Big[\frac{1}{\bar{\mathcal{P}}}W^\dagger i\not{D}_c^\perp W\Big]\Big[\frac{1}{\bar{\mathcal{P}}}W^\dagger ig\not{B}_\perp^c W\Big]h_v \\
&\quad + W\frac{\not{n}}{m_b\,(n\cdot v)^2}\Big[\frac{1}{\bar{\mathcal{P}}}W^\dagger iv\cdot D_c^\perp W\Big]\Big[\frac{1}{\bar{\mathcal{P}}}W^\dagger ig\not{B}_\perp^c W\Big]h_v \\
&\quad + W\frac{\not{n}}{m_b\,(n\cdot v)^2}\Big[\frac{1}{\bar{\mathcal{P}}}W^\dagger ig\not{B}_\perp^c W\Big]\Big[\frac{1}{\bar{\mathcal{P}}^2}W^\dagger igv\cdot B_\perp^c W\Big]h_v \\
&\quad + W\frac{4}{(n\cdot v)^2}\Big[\frac{1}{\bar{\mathcal{P}}}W^\dagger iv\cdot D_c^\perp W\Big]\Big[\frac{1}{\bar{\mathcal{P}}^2}W^\dagger igv\cdot B_\perp^c W\Big]h_v\,.
\end{aligned} \tag{A.15}$$

From the expansion of the fields we obtain the expansion of the currents at tree

level,

$$
\begin{aligned}
J &= \left[\bar{\xi}_n + \bar{\psi}_L^{(2)} + \bar{\psi}_L^{(3)} + \ldots\right] \Gamma \left[W h_v + \psi_B^{(4)} + \psi_B^{(5)} \ldots\right] \qquad \text{(A.16)} \\
&= \left[\bar{\xi}_n \Gamma W h_v\right] + \left[\bar{\xi}_n \Gamma \psi_B^{(4)} + \bar{\psi}_L^{(2)} \Gamma W h_v\right] + \left[\bar{\xi}_n \Gamma \psi_B^{(5)} + \bar{\psi}_L^{(3)} \Gamma W h_v + \bar{\psi}_L^{(2)} \Gamma \psi_B^{(4)}\right] + \ldots .
\end{aligned}
$$

The leading-order SCET heavy-to-light current is

$$
J^{(0)}(\omega) = (\bar{\xi}_n W)_\omega \Gamma h_v . \qquad \text{(A.17)}
$$

For the currents suppressed by λ we obtain

$$
\begin{aligned}
J^{(1)} &= -\bar{\xi}_n \, i\overleftarrow{\not{D}}_c^\perp \frac{\not{\bar{n}}}{2} \frac{1}{i\bar{n}\cdot\overleftarrow{D}_c} \Gamma W h_v - \frac{1}{n\cdot v m} \bar{\xi}_n \Gamma \frac{\not{n}}{2} \frac{1}{i\bar{n}\cdot D_c} ig \not{B}_\perp^c W h_v \\
&\quad - \frac{2}{n\cdot v} \bar{\xi}_n \Gamma \frac{1}{(i\bar{n}\cdot D_c)^2} ig v\cdot B_\perp^c W h_v .
\end{aligned}
$$

Making the field redefinition and putting in the most general ω_i dependence consistent with RPI gives [130][1]

$$
\begin{aligned}
J^{(1a)}(\omega) &= \frac{1}{\omega} \left(\bar{\xi}_n \, i\overleftarrow{\not{D}}_c^\perp W\right)_\omega \frac{\not{\bar{n}}}{2} \Gamma (Y^\dagger h_v) , \qquad \text{(A.18)} \\
J^{(1b)}(\omega_1, \omega_2) &= -\frac{1}{m_b \, n\cdot v} (\bar{\xi}_n W)_{\omega_1} \Gamma \frac{\not{n}}{2} \left(ig \not{B}_c^\perp\right)_{\omega_2} (Y^\dagger h_v) , \\
J^{(1c)}(\omega) &= -\frac{2}{n\cdot v} \left(\bar{\xi}_n \frac{1}{(i\bar{n}\cdot D_c)^2} ig v\cdot B_\perp^c W\right)_\omega \Gamma (Y^\dagger h_v) ,
\end{aligned}
$$

[1]Note that for $J^{(1c)}$ we find a field strength $B_\perp^c$ rather than a $v\cdot D_\perp^c$ acting on W.

where $\mathcal{B}_c^\perp$ is defined in Eq. (2.70). For the currents suppressed by λ^2 we find

$$
\begin{aligned}
J^{(2)} &= \bar\xi_n \Gamma W \frac{i\not{\mathcal{D}}_{us}}{2m} h_v - \frac{1}{n\cdot v}\bar\xi_n\Gamma\left(\frac{\not n\not{\bar n}}{4m} + \frac{\bar n\cdot v}{i\bar n\cdot D_c}\right)\frac{1}{i\bar n\cdot D_c} ign\cdot MWh_v \qquad \text{(A.19)}\\
&+ \frac{1}{n\cdot v}\bar\xi_n \overleftarrow{i\not{\mathcal{D}}}_c^\perp \frac{\not{\bar n}}{2}\frac{1}{i\bar n\cdot \overleftarrow{D}_c}\Gamma\left(\frac{\not n}{2m}\frac{1}{i\bar n\cdot D_c} ig\not{\mathcal{B}}_\perp^c + \frac{2}{(i\bar n\cdot D_c)^2} igv\cdot B_\perp^c\right) Wh_v\\
&- \bar\xi_n W i\overleftarrow{\not{\mathcal{D}}}_{us}^\perp W^\dagger \frac{\not{\bar n}}{2}\frac{1}{i\bar n\cdot\overleftarrow{D}_c}\Gamma W h_v - \frac{1}{n\cdot vm}\bar\xi_n\Gamma\frac{1}{i\bar n\cdot D_c} i\not{\mathcal{D}}_\perp^c \frac{1}{i\bar n\cdot D_c} ig\not{\mathcal{B}}_\perp^c W h_v\\
&+ \frac{1}{(n\cdot v)^2 m}\bar\xi_n\Gamma\frac{1}{i\bar n\cdot D_c} iv\cdot D_c^\perp \not n\frac{1}{i\bar n\cdot D_c} ig\not{\mathcal{B}}_\perp^c W h_v\\
&+ \frac{4}{(n\cdot v)^2}\bar\xi_n\Gamma\frac{1}{i\bar n\cdot D_c} iv\cdot D_c^\perp \frac{1}{(i\bar n\cdot D_c)^2} igv\cdot B_\perp^c W h_v\\
&+ \frac{1}{(n\cdot v)^2 m}\bar\xi_n\Gamma\not n\left(i\not{\mathcal{D}}_\perp^c\frac{1}{i\bar n\cdot D_c} - \frac{1}{i\bar n\cdot D_c} i\not{\mathcal{D}}_\perp^c\right)\frac{1}{i\bar n\cdot D_c} igv\cdot B_\perp^c W h_v\,,
\end{aligned}
$$

where

$$
ign\cdot M = [i\bar n\cdot D^c, in\cdot D]. \qquad \text{(A.20)}
$$

It will be convenient for us to label the terms as follows:

$$
\begin{aligned}
J^{(2a)} &= \bar\xi_n\Gamma W\frac{i\not{\mathcal{D}}_{us}}{2m}h_v\,, \qquad J^{(2b)} = -\bar\xi_n W i\overleftarrow{\not{\mathcal{D}}}_{us}^\perp W^\dagger\frac{\not{\bar n}}{2}\frac{1}{i\bar n\cdot\overleftarrow{D}_c}\Gamma W h_v\,,\\
J^{(2c)} &= -\frac{\bar n\cdot v}{n\cdot v}\bar\xi_n\Gamma\frac{1}{(i\bar n\cdot D_c)^2} ign\cdot MWh_v\,,\\
J^{(2d)} &= -\frac{1}{n\cdot v\, m}\bar\xi_n\Gamma\frac{\not n\not{\bar n}}{4}\frac{1}{i\bar n\cdot D_c} ign\cdot MWh_v\,,\\
J^{(2e)} &= \frac{1}{n\cdot v\, m}\bar\xi_n\overleftarrow{i\not{\mathcal{D}}}_c^\perp\frac{\not{\bar n}}{2}\frac{1}{i\bar n\cdot\overleftarrow{D}_c}\Gamma\frac{\not n}{2}\frac{1}{i\bar n\cdot D_c} ig\not{\mathcal{B}}_\perp^c W h_v\,,\\
J^{(2f)} &= -\frac{1}{n\cdot v\, m}\bar\xi_n\Gamma\frac{1}{i\bar n\cdot D_c} i\not{\mathcal{D}}_\perp^c\frac{1}{i\bar n\cdot D_c} ig\not{\mathcal{B}}_\perp^c W h_v\,,\\
J^{(2g)} &= \frac{1}{(n\cdot v)^2\, m}\bar\xi_n\Gamma\frac{1}{i\bar n\cdot D_c} iv\cdot D_c^\perp\not n\frac{1}{i\bar n\cdot D_c} ig\not{\mathcal{B}}_\perp^c W h_v\,,\\
J^{(2h)} &= \frac{1}{(n\cdot v)^2\, m}\bar\xi_n\Gamma\not n\frac{1}{i\bar n\cdot D_c} ig\not{\mathcal{B}}_\perp^c\frac{1}{(i\bar n\cdot D_c)^2} igv\cdot B_\perp^c W h_v\,,\\
J^{(2i)} &= \frac{2}{n\cdot v}\bar\xi_n\overleftarrow{i\not{\mathcal{D}}}_c^\perp\frac{\not{\bar n}}{2}\frac{1}{i\bar n\cdot\overleftarrow{D}_c}\Gamma\frac{1}{(i\bar n\cdot D_c)^2} igv\cdot B_\perp^c W h_v\,,\\
J^{(2j)} &= \frac{4}{(n\cdot v)^2}\bar\xi_n\Gamma\frac{1}{i\bar n\cdot D_c} iv\cdot D_c^\perp\frac{1}{(i\bar n\cdot D_c)^2} igv\cdot B_\perp^c W h_v\,. \qquad \text{(A.21)}
\end{aligned}
$$

The terms $J^{(2a)}$ to $J^{(2f)}$ agree with those found in Refs. [37, 38], which use the

position-space formulation of SCET. $J^{(2a)}$, $J^{(2b)}$ and $J^{(2c)}$ correspond to the third, last and fourth terms, respectively, of Eq. (41) in Ref. [38], while $J^{(2d)}$, $J^{(2e)}$ and $J^{(2f)}$ correspond to the second, last and third terms, respectively, of their Eq. (43). The rest of their second-order terms correspond to Lagrangian insertions in our SCET calculation. The terms $J^{(2g)}$ to $J^{(2j)}$ do not appear in Refs. [37, 38], because they set $v_\perp^\mu \sim \lambda$ (more generally, the assignment $v_\perp^\mu \sim 1$ used here is allowed). We follow the common practice of dropping the $v_\perp$ terms in our analysis of the factorization theorems by picking a frame where $v_\perp = 0$.

Appendix B

Reparameterization invariance for the currents

It is useful to separate the RPI transformations according to the power suppression in λ that they cause. We shall denote this by a bracketed superscript. For type-I transformations we have, at the same order in λ,

$$\begin{aligned}
&\delta_{\rm I}(\bar{n}\cdot D) = \delta_I(W) = 0\,,\\
&\delta_{\rm I}^{(\lambda^0)}(n\cdot D) = \Delta^\perp\cdot D_c^\perp\,, \qquad \delta_{\rm I}^{(\lambda^0)}(D_{c\mu}^\perp) = -\frac{\Delta_\mu^\perp}{2}\bar{n}\cdot D_c\,,\\
&\delta_{\rm I}^{(\lambda^0)}(\xi_n) = 0\,.
\end{aligned} \tag{B.1}$$

Type-I transformations one order higher in λ are

$$\begin{aligned}
&\delta_{\rm I}^{(\lambda^1)}(D_{c\mu}^\perp) + \delta_{\rm I}^{(\lambda^0)}(W D_{us,\mu}^\perp W^\dagger) = -\frac{\bar{n}_\mu}{2}\Delta^\perp\cdot D_c^\perp\,,\\
&\delta_{\rm I}^{(\lambda^1)}(\bar{\xi}_n) = \bar{\xi}_n\frac{\bar{n}\!\!\!/\Delta^\perp}{4}\,.
\end{aligned} \tag{B.2}$$

For type-II transformations we have, at the same order in λ,

$$\begin{aligned}
\delta_{\rm II}(n\cdot D) &= 0\,, \\
\delta_{\rm II}^{(\lambda^0)}(D_{c\mu}^\perp) &= -\frac{n_\mu}{2}\varepsilon^\perp\cdot D_c^\perp\,, \\
\delta_{\rm II}^{(\lambda^0)}(\xi_n) &= \delta_{\rm II}^{(\lambda^0)}(W) = 0\,.
\end{aligned} \tag{B.3}$$

Type-II transformations one order higher in λ are

$$\begin{aligned}
&\delta_{\rm II}^{(\lambda^1)}(D_{c\mu}^\perp) + \delta_{\rm II}^{(\lambda^0)}(WD_{us,\mu}^\perp W^\dagger) = -\frac{\varepsilon_\mu^\perp}{2} n\cdot D - \frac{n_\mu}{2} W\varepsilon^\perp\cdot D_{us}^\perp W^\dagger\,, \\
&\delta_{\rm II}^{(\lambda^1)}(\bar\xi_n) = \bar\xi_n \overleftarrow{\not{D}}_c^\perp \frac{1}{\bar n\cdot\overleftarrow{D}_c}\frac{\not{\bar n}_\perp}{2}\,, \qquad \delta_{\rm II}^{(\lambda^1)}(W) = \left[-\frac{1}{\bar n\cdot D_c}\,\varepsilon^\perp\cdot D_c^\perp W\right]\,,
\end{aligned} \tag{B.4}$$

where the differential operators do not act outside the square brackets. Furthermore,

$$\delta_{\rm II}^{(\lambda^2)}(\bar\xi_n) = \bar\xi_n W \overleftarrow{\not{D}}_{us}^\perp W^\dagger \frac{1}{\bar n\cdot\overleftarrow{D}_c}\frac{\not{\bar n}_\perp}{2}\,. \tag{B.5}$$

Note that Table I of Ref. [118] seems to suggest that the transformation of W involves the full covariant derivative with both collinear and usoft parts. However, the Wilson line referred to in that table is constructed from $\bar n\cdot(A_c + A_{us})$; for the Wilson line built out of $\bar n\cdot A_c$ alone, the equation of motion is $i\bar n\cdot D_c W = 0$, and hence $\delta_{\rm II}(W) = \delta_{\rm II}^{(\lambda)}(W)$.

Using the above transformations and the definitions (A.10) and (A.20), we obtain

$$\begin{aligned}
\delta_{\rm I}^{(\lambda^1)}(igB_\perp^{c\mu}) &= -\frac{1}{2}\bar n^\mu \Delta_\alpha^\perp [i\bar n\cdot D_c, iD_c^{\perp\alpha}] + [\delta_{\rm I}^{(\lambda^0)}(WiD_{us}^{\perp\mu}W^\dagger), i\bar n\cdot D_c] \\
&= -\frac{1}{2}\bar n^\mu ig\Delta^\perp\cdot B_\perp^c\,.
\end{aligned} \tag{B.6}$$

since the second commutator in the first line above equals $[W\delta_{\rm I}^{(\lambda^0)}(iD_{us}^{\perp\mu})W^\dagger, W\bar{\mathcal{P}}W^\dagger] = W[\delta_{\rm I}^{(\lambda^0)}(iD_{us}^{\perp\mu}), \bar{\mathcal{P}}]W^\dagger = 0$. Similarly, we find that

$$\delta_{\rm I}^{(\lambda^0)}(igB_\perp^{c\mu}) = 0\,, \qquad \delta_{\rm I}^{(\lambda^0)}(ign\cdot M) = ig\Delta^\perp\cdot B_\perp^c\,. \tag{B.7}$$

Then, it is straightforward to show that

$$\begin{aligned}
\delta_{\rm I}^{(\lambda^1)} J^{(1a)} + \delta_{\rm I}^{(\lambda^0)} J^{(2b)} &= 0\,, \\
\delta_{\rm I}^{(\lambda^1)} J^{(1b)} + \delta_{\rm I}^{(\lambda^0)} J^{(2d)} + \delta_{\rm I}^{(\lambda^0)} J^{(2e)} + \delta_{\rm I}^{(\lambda^0)} J^{(2f)} + \delta_{\rm I}^{(\lambda^0)} J^{(2g)} &= 0\,, \\
\delta_{\rm I}^{(\lambda^1)} J^{(1c)} + \delta_{\rm I}^{(\lambda^0)} J^{(2c)} + \delta_{\rm I}^{(\lambda^0)} J^{(2i)} + \delta_{\rm I}^{(\lambda^0)} J^{(2j)} &= 0\,. \qquad \text{(B.8)}
\end{aligned}$$

It follows that $\delta_{\rm I}^{(\lambda^1)} J^{(1)} + \delta_{\rm I}^{(\lambda^0)} J^{(2)} = 0$.

Repeating the process for type-II transformations, we obtain

$$\begin{aligned}
\delta_{\rm II}^{(\lambda^1)}(igB_\perp^{c\mu}) &= \varepsilon_\nu^\perp [iD_c^{\perp\nu}, iD_c^{\perp\mu}] - \frac{\varepsilon_\perp^\mu}{2}[i\bar{n}\cdot D_c, in\cdot D] \\
&\quad -\frac{n^\mu}{2}[i\bar{n}\cdot D_c, Wi\varepsilon^\perp\cdot D_{us}^\perp W^\dagger] - [i\bar{n}\cdot D_c, \delta_{\rm II}^{(\lambda^0)}(WiD_{us}^{\perp\mu}W^\dagger)] \\
&= ig\varepsilon_\nu^\perp\cdot G_{c\perp}^{\mu\nu} - \frac{\varepsilon_\perp^\mu}{2} ign\cdot M\,, \qquad \text{(B.9)}
\end{aligned}$$

where $gG_{c\perp}^{\mu\nu} = i[iD_c^{\perp\mu}, iD_c^{\perp\nu}]$. Similarly, we find that

$$\delta_{\rm II}^{(\lambda^0)}(igB_\perp^{c\mu}) = \frac{n^\mu}{2} ig\varepsilon^\perp\cdot B_\perp^c\,, \qquad \delta_{\rm II}^{(\lambda^0)}(ign\cdot M) = 0\,. \qquad \text{(B.10)}$$

Then,

$$\begin{aligned}
&\delta_{\rm II}^{(\lambda^2)} J^{(0)} + \delta_{\rm II}^{(\lambda^1)} J^{(1a)} + \delta_{\rm II}^{(\lambda^1)} J^{(1c)} + \delta_{\rm II}^{(\lambda^0)} J^{(2b)} + \delta_{\rm II}^{(\lambda^0)} J^{(2c)} + \delta_{\rm II}^{(\lambda^0)} J^{(2i)} + \delta_{\rm II}^{(\lambda^0)} J^{(2j)} \\
&= -\bar{\xi}_n i\overleftarrow{\not{D}}_c^\perp \frac{1}{i\bar{n}\cdot\overleftarrow{D}_c}\frac{\not{\varepsilon}_\perp}{2} i\overleftarrow{\not{D}}_c^\perp \frac{\not{\bar{n}}}{2}\frac{1}{i\bar{n}\cdot\overleftarrow{D}_c}\Gamma W h_v + \bar{\xi}_n \frac{\not{\varepsilon}_\perp}{2} in\cdot\overleftarrow{D}\frac{\not{\bar{n}}}{2}\frac{1}{i\bar{n}\cdot\overleftarrow{D}_c}\Gamma W h_v \\
&\quad + \bar{\xi}_n i\overleftarrow{\not{D}}_c^\perp \frac{\not{\bar{n}}}{2}\frac{1}{i\bar{n}\cdot\overleftarrow{D}_c} i\varepsilon^\perp\cdot\overleftarrow{D}_c \frac{1}{i\bar{n}\cdot\overleftarrow{D}_c}\Gamma W h_v + \bar{\xi}_n i\overleftarrow{\not{D}}_c^\perp \frac{\not{\bar{n}}}{2}\frac{1}{i\bar{n}\cdot\overleftarrow{D}_c}\Gamma\left[\frac{1}{i\bar{n}\cdot D_c}\, i\varepsilon^\perp\cdot D_c^\perp W\right] h_v \\
&\quad + \frac{2}{n\cdot v}\bar{\xi}_n\Gamma\frac{1}{(i\bar{n}\cdot D_c)^2}\left(i\varepsilon^\perp\cdot D_c^\perp\frac{1}{i\bar{n}\cdot D_c} igv\cdot B_\perp^c W h_v - v_\mu\varepsilon_\nu^\perp igG_{c\perp}^{\mu\nu} W h_v\right. \\
&\quad \left. + igv\cdot B_\perp^c\left[\frac{1}{i\bar{n}\cdot D_c}\, i\varepsilon^\perp\cdot D_c^\perp W\right] h_v\right) - \frac{2}{n\cdot v}\bar{\xi}_n\Gamma\frac{1}{i\bar{n}\cdot D_c} iv\cdot D_c^\perp\frac{1}{(i\bar{n}\cdot D_c)^2} ig\varepsilon^\perp\cdot B_\perp^c W h_v \\
&\quad - \bar{\xi}_n i\overleftarrow{\not{D}}_c^\perp\frac{\not{\bar{n}}}{2}\frac{1}{i\bar{n}\cdot\overleftarrow{D}_c}\Gamma\frac{1}{(i\bar{n}\cdot D_c)^2} ig\varepsilon^\perp\cdot B_\perp^c W h_v\,. \qquad \text{(B.11)}
\end{aligned}$$

Now, since $(i\bar{n}\cdot D_c)^{-1} ig\varepsilon^\perp\cdot B_\perp^c W h_v = \varepsilon^\perp\cdot(iD_c^\perp W - \mathcal{P}_\perp)h_v$, we can write

$$\left[\frac{1}{i\bar{n}\cdot D_c}\, i\varepsilon^\perp\cdot D_c^\perp W\right] h_v = \frac{1}{i\bar{n}\cdot D_c}\varepsilon^\perp\cdot(iD_c^\perp W - \mathcal{P}_\perp)h_v = \frac{1}{(i\bar{n}\cdot D_c)^2} ig\varepsilon^\perp\cdot B_\perp^c W h_v\,. \quad \text{(B.12)}$$

Substituting this into Eq. (B.11) and combining the first and third terms, we obtain

$$\begin{aligned}
&\delta_{\rm II}^{(\lambda^2)} J^{(0)} + \delta_{\rm II}^{(\lambda^1)} J^{(1a)} + \delta_{\rm II}^{(\lambda^1)} J^{(1c)} + \delta_{\rm II}^{(\lambda^0)} J^{(2b)} + \delta_{\rm II}^{(\lambda^0)} J^{(2c)} + \delta_{\rm II}^{(\lambda^0)} J^{(2i)} + \delta_{\rm II}^{(\lambda^0)} J^{(2j)} \\
&\quad = \bar{\xi}_n\, i\overleftarrow{\not{D}}_c^\perp \frac{1}{i\bar{n}\cdot\overleftarrow{D}_c}\, i\overleftarrow{\not{D}}_c^\perp \frac{\not{\varepsilon}_\perp}{2}\frac{\not{\bar{n}}}{2}\frac{1}{i\bar{n}\cdot\overleftarrow{D}_c}\Gamma W h_v + \bar{\xi}_n \frac{\not{\varepsilon}_\perp}{2} in\cdot\overleftarrow{D}\frac{\not{\bar{n}}}{2}\frac{1}{i\bar{n}\cdot\overleftarrow{D}_c}\Gamma W h_v \\
&\qquad + \frac{2}{n\cdot v}\bar{\xi}_n\Gamma\frac{1}{(i\bar{n}\cdot D_c)^2}\Big(i\varepsilon^\perp\cdot D_c^\perp\, v\cdot(iD_c^\perp W - \mathcal{P}_\perp)h_v \\
&\qquad\quad -\big\{i\varepsilon^\perp\cdot D_c^\perp\, v\cdot(iD_c^\perp W - \mathcal{P}_\perp) - (iv\cdot D_c^\perp i\varepsilon^\perp\cdot D_c^\perp W - i\varepsilon^\perp\cdot D_c^\perp v\cdot\mathcal{P}_\perp)\big\}h_v \\
&\qquad\quad -iv\cdot D_c^\perp\,\varepsilon^\perp\cdot(iD_c^\perp W - \mathcal{P}_\perp)h_v\Big) \\
&\quad = -\bar{\xi}_n\left(i\overleftarrow{\not{D}}_c^\perp\frac{1}{i\bar{n}\cdot\overleftarrow{D}_c}\, i\overleftarrow{\not{D}}_c^\perp + in\cdot\overleftarrow{D}\right)\frac{\not{\bar{n}}\not{\varepsilon}_\perp}{4}\frac{1}{i\bar{n}\cdot\overleftarrow{D}_c}\Gamma W h_v \\
&\qquad + \frac{2}{n\cdot v}\bar{\xi}_n\Gamma\frac{1}{(i\bar{n}\cdot D_c)^2}(iv\cdot D_c^\perp\varepsilon^\perp\cdot\mathcal{P}_\perp - i\varepsilon^\perp\cdot D_c^\perp v\cdot\mathcal{P}_\perp)h_v \\
&\quad = 0\,. \qquad\qquad\qquad\qquad\qquad\qquad\qquad\qquad\qquad\qquad\qquad\qquad \text{(B.13)}
\end{aligned}$$

The first term of the second-last equality above is zero, owing to the equation of motion obtained from Eq. (2.45). In the second term, the expression in brackets begins at one collinear gluon, ensuring that the $1/(i\bar{n}\cdot D_c)$ does not cause any singularities. Thus the label operators make this term zero.

Using completely analogous manipulations, we also find the closure relation that involves the $J^{(1b)}$ current. Thus the type-II constraints are

$$\begin{aligned}
&\delta_{\rm II}^{(\lambda^2)} J^{(0)} + \delta_{\rm II}^{(\lambda^1)} J^{(1a)} + \delta_{\rm II}^{(\lambda^1)} J^{(1c)} + \delta_{\rm II}^{(\lambda^0)} J^{(2b)} + \delta_{\rm II}^{(\lambda^0)} J^{(2c)} + \delta_{\rm II}^{(\lambda^0)} J^{(2i)} + \delta_{\rm II}^{(\lambda^0)} J^{(2j)} = 0\,, \\
&\delta_{\rm II}^{(\lambda^1)} J^{(1b)} + \delta_{\rm II}^{(\lambda^0)} J^{(2d)} + \delta_{\rm II}^{(\lambda^0)} J^{(2e)} + \delta_{\rm II}^{(\lambda^0)} J^{(2f)} + \delta_{\rm II}^{(\lambda^0)} J^{(2g)} + \delta_{\rm II}^{(\lambda^0)} J^{(2h)} = 0\,. \qquad \text{(B.14)}
\end{aligned}$$

It then follows that $\delta_{\rm II}^{(\lambda^2)} J^{(0)} + \delta_{\rm II}^{(\lambda^1)} J^{(1)} + \delta_{\rm II}^{(\lambda^0)} J^{(2)} = 0$. Dropping the $J^{(2g)-(2j)}$ currents, these relations agree with Ref. [37].

From the results in Eqs. (B.8) and (B.14) we see that the currents split into two

sets:

$$J^{(0)} + J^{(1a)} + J^{(1c)} + J^{(2b)} + J^{(2c)} + J^{(2i)} + J^{(2j)}\,,$$
$$J^{(1b)} + J^{(2d)} + J^{(2e)} + J^{(2f)} + J^{(2g)} + J^{(2h)}\,. \qquad \text{(B.15)}$$

When we add non-trivial Wilson coefficients to all the currents, the number of ω_i parameters they depend on is restricted by RPI, i.e. in the set with $J^{(0)}$ they have one parameter ω and in the second set with $J^{(1b)}$ they have two parameters, $\omega_{1,2}$. In the second set the combination of fields restricted to have momentum ω_1 and ω_2 is determined by the manner in which the terms in the RPI-transformed currents cancel. Making the Y field redefinition in Eq. (2.48) and putting in the most general ω_i dependence consistent with RPI, we find

$$\begin{aligned}
J^{(2a)}(\omega) &= \frac{1}{2m_b}\,(\bar\xi_n W)_\omega \Gamma\Big(Y^\dagger i\not{D}^T_{us} h_v\Big)\,,\\
J^{(2b)}(\omega) &= \frac{1}{\omega}\,(\bar\xi_n W)_\omega \Big(Y^\dagger\, i\overleftarrow{\not{D}}^\perp_{us}\frac{\not{\bar n}}{2}\Gamma h_v\Big)\,,\\
J^{(2c)}(\omega) &= -\frac{\bar n\cdot v}{n\cdot v}\Big(\bar\xi_n\Gamma\frac{1}{(i\bar n\cdot D_c)^2} ign\cdot B_c W\Big)_\omega (Y^\dagger h_v)\,,\\
J^{(2d)}(\omega_1,\omega_2) &= -\frac{1}{m_b\, n\cdot v}\,(\bar\xi_n W)_{\omega_1}\Gamma\frac{\not{n}\not{\bar n}}{4}\Big(\frac{1}{\bar{\mathcal P}} W^\dagger ign\cdot B_c W\Big)_{\omega_2}(Y^\dagger h_v)\,,\\
J^{(2e)}(\omega_1,\omega_2) &= -\frac{1}{m_b\, n\cdot v\,\omega_1}\,(\bar\xi_n\, i\overleftarrow{\not{D}}^\perp_c W)_{\omega_1}\frac{\not{\bar n}}{2}\Gamma\frac{\not{n}}{2}\,(ig\not{B}^\perp_c)_{\omega_2}(Y^\dagger h_v)\,,\\
J^{(2f)}(\omega_1,\omega_2) &= -\frac{1}{m_b\, n\cdot v}\,(\bar\xi_n W)_{\omega_1}\Gamma\Big(\frac{1}{\bar{\mathcal P}} W^\dagger i\not{D}^c_\perp\frac{1}{i\bar n\cdot D_c} ig\not{B}^c_\perp W\Big)_{\omega_2}(Y^\dagger h_v)\,,\\
J^{(2g)}(\omega_1,\omega_2) &= \frac{1}{m_b (n\cdot v)^2}\,(\bar\xi_n W)_{\omega_1}\Gamma\not{n}\Big(\frac{1}{\bar{\mathcal P}} W^\dagger iv\cdot D^\perp_c\frac{1}{i\bar n\cdot D_c} ig\not{B}^c_\perp W\Big)_{\omega_2}(Y^\dagger h_v)\,,\\
J^{(2h)}(\omega_1,\omega_2) &= \frac{1}{m_b\,(n\cdot v)^2}\,(\bar\xi_n W)_{\omega_1}\Gamma\not{n}\Big(\frac{1}{\bar{\mathcal P}} W^\dagger ig\not{B}^c_\perp\frac{1}{(i\bar n\cdot D_c)^2} igv\cdot B^c_\perp W\Big)_{\omega_2}(Y^\dagger h_v)\,,\\
J^{(2i)}(\omega) &= \frac{2}{n\cdot v}\Big(\bar\xi_n\, i\overleftarrow{\not{D}}^\perp_c\frac{1}{i\bar n\cdot\overleftarrow{D}_c}\frac{1}{(i\bar n\cdot D_c)^2} igv\cdot B^c_\perp W\Big)_\omega\frac{\not{\bar n}}{2}\Gamma(Y^\dagger h_v)\,,\\
J^{(2j)}(\omega) &= \frac{4}{(n\cdot v)^2}\Big(\bar\xi_n\Gamma\frac{1}{i\bar n\cdot D_c} iv\cdot D^\perp_c\frac{1}{(i\bar n\cdot D_c)^2} igv\cdot B^c_\perp W\Big)_\omega (Y^\dagger h_v)\,, \qquad \text{(B.16)}
\end{aligned}$$

where

$$igB^\mu_{c\perp} = [i\bar n\cdot D_c, iD^\mu_{c\perp}]\,. \qquad ign\cdot B_c = [i\bar n\cdot D_c, in\cdot\partial + gn\cdot A_n]\,. \qquad \text{(B.17)}$$

Appendix C

Wilson Coefficients

The coefficients and functions that appear in Eq. (4.6) are defined as follows [54].

$$
\begin{aligned}
C_7(M_W) &= -\frac{1}{2}A(m_t^2/M_W^2)\,, \qquad \text{(C.1)}\\
C_8(M_W) &= -\frac{1}{2}F(m_t^2/M_W^2)\,,\\
Y(x) &= C(x) - B(x)\,,\\
Z(x) &= C(x) + \frac{1}{4}D(x)\,,\\
A(x) &= \frac{x(8x^2+5x-7)}{12(x-1)^3} + \frac{x^2(2-3x)}{2(x-1)^4}\ln x\,,\\
B(x) &= \frac{x}{4(1-x)} + \frac{x}{4(x-1)^2}\ln x\,,\\
C(x) &= \frac{x(x-6)}{8(x-1)} + \frac{x(3x+2)}{8(x-1)^2}\ln x\,,\\
D(x) &= \frac{-19x^3+25x^2}{36(x-1)^3} + \frac{x^2(5x^2-2x-6)}{18(x-1)^4}\ln x - \frac{4}{9}\ln x\,,\\
E(x) &= \frac{x(18-11x-x^2)}{12(1-x)^3} + \frac{x^2(15-16x+4x^2)}{6(1-x)^4}\ln x - \frac{2}{3}\ln x\,,\\
F(x) &= \frac{x(x^2-5x-2)}{4(x-1)^3} + \frac{3x^2}{2(x-1)^4}\ln x\,,
\end{aligned}
$$

and

$$
\begin{aligned}
t_i &= (\ 2.2996, -1.0880, -\tfrac{3}{7}, -\tfrac{1}{14}, -0.6494, -0.0380, -0.0186, -0.0057\ ), \\
a_i &= (\ \tfrac{14}{23}, \tfrac{16}{23}, \tfrac{6}{23}, -\tfrac{12}{23}, 0.4086, -0.4230, -0.8994, 0.1456\ ), \\
p_i &= (\ 0, 0, -\tfrac{80}{203}, \tfrac{8}{33}, 0.0433, 0.1384, 0.1648, -0.0073\ ), \\
\rho_i^{NDR} &= (\ 0, 0, 0.8966, -0.1960, -0.2011, 0.1328, -0.0292, -0.1858\ ), \\
s_i &= (\ 0, 0, -0.2009, -0.3579, 0.0490, -0.3616, -0.3554, 0.0072\ ), \\
q_i &= (\ 0, 0, 0, 0, 0.0318, 0.0918, -0.2700, 0.0059\ ).
\end{aligned}
\tag{C.2}
$$

Appendix D

The Case of Collinear q^2

In the body of the chapter we used $q^2 \sim \lambda^0$. We were free to choose this counting since the power counting for the leptonic variable q^2 does not affect the counting for $p_X^{\pm}$ in the shape function region. (The only restriction was not to have q^2 too close to m_b^2.) However, we are free to consider other choices. In this appendix we consider how our analysis will change if we instead take $q^2 \sim \lambda^2$. With this scaling, new physical degrees of freedom are needed at leading order in SCET, making the analysis more complicated. In particular we must consider graphs with quark fields that are collinear to the collinear photon (or dilepton pair), since with this power counting we have $(q^0)^2 \gg q^2$.

An example of a new *nonzero* graph is the one generated by four-quark operators within SCET, as shown in Fig. D-1, which involve these additional degrees of freedom. In this graph we have a light-quark loop of collinear-$\bar{n}$ fields that are collinear to the virtual photon. The presence of this type of diagram changes the hard matching at $\mu_b = m_b$. It also means that we have a more complicated pattern of operator mixing within SCET, since divergences in the displayed diagram will cause an evolution for C_9, etc. Therefore, the running below m_b will no longer be universal. In the presence of these diagrams the jet function will also no longer be given by a single bilinear operator, since it will also involve some contributions with a factorized matrix element of $\bar{n}$-fields, which are also integrated out at $p^2 \sim m_b \Lambda_{\rm QCD}$. Finally, the appearance of these additional degrees of freedom might also affect the number of non-perturbative

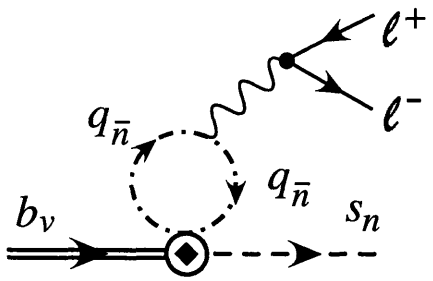

Figure D-1: Additional graphs in SCET for the matching computation for the case where $q^2 \sim \lambda^2$.

shape functions that appear in the factorization theorem. It would be interesting to carry out a detailed analysis of this $q^2 \sim \lambda^2$ case in the future.

In $B \to X_s\gamma$ at lowest order, the analog of the graph in Fig. D-1 vanishes at one-loop order, and this argument can be extended to include higher orders in α_s [129]. This relies on the fact that here $q^2 = 0$ and does not generate a scale. We find that the same reasoning does not apply for $B \to X_s\ell\ell$ for parametrically small but finite q^2.

Finally, we comment on the possibility of penguin charm-loop effects. In our analysis we integrated out the charm loops at the same time as the bottom loops. This is reasonable when treating $q^2 \sim \lambda^0$. One could also consider the case $m_c^2 \sim m_b\Lambda$, which is also reasonable numerically. This type of power counting was considered for the simpler case of $B \to X_c\ell\bar{\nu}$ decays with energetic X_c in Ref. [46] and it would be interesting to extend this to $B \to X_s\ell\ell$. We remark that the problematic region for $B \to \pi\pi$ factorization theorems [28, 71, 35, 29], which is near the charm threshold, $q^2 \sim 4m_c^2$, is not relevant for our analysis. The experimental cuts on q^2 explicitly remove the known large contributions from this region.

Bibliography

[1] K. Abe et al. A measurement of the branching fraction for the inclusive $B \to X_s\gamma$ decays with the Belle detector. *Phys. Lett.*, B511:151–158, 2001.

[2] K. Abe et al. Measurement of the inclusive semileptonic branching fraction of B mesons and $|V_{cb}|$. *Phys. Lett.*, B547:181–192, 2002.

[3] R. Akhoury and I. Z. Rothstein. The extraction of V_{ub} from inclusive B decays and the resummation of end point logs. *Phys. Rev.*, D54:2349–2362, 1996.

[4] M. S. Alam et al. First measurement of the rate for the inclusive radiative penguin decay $b \to s\gamma$. *Phys. Rev. Lett.*, 74:2885–2889, 1995.

[5] Ahmed Ali and G. Hiller. Perturbative QCD- and power-corrected hadron spectra and spectral moments in the decay $B \to X_s\ell^+\ell^-$. *Phys. Rev.*, D58:074001, 1998.

[6] Ahmed Ali and G. Hiller. Phenomenological profiles of the inclusive hadron spectra in the decay $B \to X_s\ell^+\ell^-$. *Phys. Rev.*, D60:034017, 1999.

[7] Ahmed Ali, G. Hiller, L. T. Handoko, and T. Morozumi. Power corrections in the decay rate and distributions in $B \to X_s\ell^+\ell^-$ in the standard model. *Phys. Rev.*, D55:4105–4128, 1997.

[8] H. M. Asatrian, H. H. Asatryan, A. Hovhannisyan, and V. Poghosyan. Complete bremsstrahlung corrections to the forward-backward asymmetries in $b \to X_s\ell^+\ell^-$. *Mod. Phys. Lett.*, A19:603–614, 2004.

[9] H. M. Asatrian, K. Bieri, C. Greub, and A. Hovhannisyan. NNLL corrections to the angular distribution and to the forward-backward asymmetries in $b \to X_s \ell^+ \ell^-$. *Phys. Rev.*, D66:094013, 2002.

[10] H. H. Asatryan, H. M. Asatrian, C. Greub, and M. Walker. Calculation of two-loop virtual corrections to $b \to s \ell^+ \ell^-$ in the standard model. *Phys. Rev.*, D65:074004, 2002.

[11] B. Aubert et al. $b \to s\gamma$ using a sum of exclusive modes. hep-ex/0207074.

[12] B. Aubert et al. Measurement of the $B \to X_s \ell^+ \ell^-$ branching fraction using a sum over exclusive modes. hep-ex/0308016.

[13] B. Aubert et al. Determination of the branching fraction for $B \to X_c l \nu$ decays and of $|V_{cb}|$ from hadronic-mass and lepton-energy moments. *Phys. Rev. Lett.*, 93:011803, 2004.

[14] B. Aubert et al. Measurement of the $B \to X_s \ell^+ \ell^-$ branching fraction with a sum over exclusive modes. *Phys. Rev. Lett.*, 93:081802, 2004.

[15] B. Aubert et al. Measurement of the inclusive charmless semileptonic branching ratio of B mesons and determination of $|V_{ub}|$. *Phys. Rev. Lett.*, 92:071802, 2004.

[16] B. Aubert et al. Measurements of moments of the hadronic mass distribution in semileptonic B decays. *Phys. Rev.*, D69:111103, 2004.

[17] Christopher Balzereit, Thomas Mannel, and Wolfgang Kilian. Evolution of the light-cone distribution function for a heavy quark. *Phys. Rev.*, D58:114029, 1998.

[18] R. Barate et al. A measurement of the inclusive $b \to s\gamma$ branching ratio. *Phys. Lett.*, B429:169–187, 1998.

[19] E. Barberio et al. Averages of b-hadron properties at the end of 2005. hep-ex/0603003.

[20] Christian W. Bauer and Craig N. Burrell. Nonperturbative corrections to $B \to X_s \ell^+ \ell^-$ with phase space restrictions. *Phys. Lett.*, B469:248–252, 1999.

[21] Christian W. Bauer and Craig N. Burrell. Nonperturbative corrections to moments of the decay $B \to X_s \ell^+ \ell^-$. *Phys. Rev.*, D62:114028, 2000.

[22] Christian W. Bauer, Sean Fleming, and Michael E. Luke. Summing Sudakov logarithms in $B \to X_s \gamma$ in effective field theory. *Phys. Rev.*, D63:014006, 2001.

[23] Christian W. Bauer, Sean Fleming, Dan Pirjol, and Iain W. Stewart. An effective field theory for collinear and soft gluons: heavy to light decays. *Phys. Rev.*, D63:114020, 2001.

[24] Christian W. Bauer, Zoltan Ligeti, Michael Luke, Aneesh V. Manohar, and Michael Trott. Global analysis of inclusive b decays. *Phys. Rev.*, D70:094017, 2004.

[25] Christian W. Bauer, Michael Luke, and Thomas Mannel. Subleading shape functions in $B \to X_u \ell \bar{\nu}$ and the determination of $|V_{ub}|$. *Phys. Lett.*, B543:261–268, 2002.

[26] Christian W. Bauer, Michael E. Luke, and Thomas Mannel. Light-cone distribution functions for B decays at subleading order in $1/m_b$. *Phys. Rev.*, D68:094001, 2003.

[27] Christian W. Bauer and Aneesh V. Manohar. Shape function effects in $B \to X_s \gamma$ and $B \to X_u \ell \bar{\nu}$ decays. *Phys. Rev.*, D70:034024, 2004.

[28] Christian W. Bauer, Dan Pirjol, Ira Z. Rothstein, and Iain W. Stewart. $B \to M_1 M_2$: Factorization, charming penguins, strong phases, and polarization. *Phys. Rev.*, D70:054015, 2004.

[29] Christian W. Bauer, Dan Pirjol, Ira Z. Rothstein, and Iain W. Stewart. On differences between SCET and QCDF for $B \to \pi\pi$ decays. *Phys. Rev.*, D72:098502, 2005.

[30] Christian W. Bauer, Dan Pirjol, and Iain W. Stewart. Soft-collinear factorization in effective field theory. *Phys. Rev.*, D65:054022, 2002.

[31] Christian W. Bauer, Dan Pirjol, and Iain W. Stewart. Factorization and endpoint singularities in heavy-to-light decays. *Phys. Rev.*, D67:071502, 2003.

[32] Christian W. Bauer, Dan Pirjol, and Iain W. Stewart. On power suppressed operators and gauge invariance in SCET. *Phys. Rev.*, D68:034021, 2003.

[33] Christian W. Bauer and Iain W. Stewart. Invariant operators in collinear effective theory. *Phys. Lett.*, B516:134–142, 2001.

[34] Thomas Becher and Richard J. Hill. Loop corrections to heavy-to-light form factors and evanescent operators in SCET. *JHEP*, 10:055, 2004.

[35] M. Beneke, G. Buchalla, M. Neubert, and C. T. Sachrajda. Comment on '$B \to M_1 M_2$: Factorization, charming penguins, strong phases, and polarization'. *Phys. Rev.*, D72:098501, 2005.

[36] M. Beneke, F. Campanario, T. Mannel, and B. D. Pecjak. Power corrections to $\bar{B} \to X_u \ell \bar{\nu}$ ($X_s \gamma$) decay spectra in the "shape-function" region. *JHEP*, 06:071, 2005.

[37] M. Beneke, A. P. Chapovsky, M. Diehl, and T. Feldmann. Soft-collinear effective theory and heavy-to-light currents beyond leading power. *Nucl. Phys.*, B643:431–476, 2002.

[38] M. Beneke and T. Feldmann. Multipole-expanded soft-collinear effective theory with non-abelian gauge symmetry. *Phys. Lett.*, B553:267–276, 2003.

[39] M. Beneke and T. Feldmann. Factorization of heavy-to-light form factors in soft-collinear effective theory. *Nucl. Phys.*, B685:249–296, 2004.

[40] M. Beneke, Y. Kiyo, and D. s. Yang. Loop corrections to sub-leading heavy quark currents in SCET. *Nucl. Phys.*, B692:232–248, 2004.

[41] Ikaros I. Y. Bigi, Mikhail A. Shifman, N. G. Uraltsev, and A. I. Vainshtein. On the motion of heavy quarks inside hadrons: Universal distributions and inclusive decays. *Int. J. Mod. Phys.*, A9:2467–2504, 1994.

[42] Ikaros I. Y. Bigi and N. G. Uraltsev. Gluonic enhancements in non-spectator beauty decays: An inclusive mirage though an exclusive possibility. *Phys. Lett.*, B280:271–280, 1992.

[43] Ikaros I. Y. Bigi, N. G. Uraltsev, and A. I. Vainshtein. Nonperturbative corrections to inclusive beauty and charm decays: QCD versus phenomenological models. *Phys. Lett.*, B293:430–436, 1992.

[44] Christoph Bobeth, Paolo Gambino, Martin Gorbahn, and Ulrich Haisch. Complete NNLO QCD analysis of $\bar{B} \to X_s \ell^+ \ell^-$ and higher order electroweak effects. *JHEP*, 04:071, 2004.

[45] Christoph Bobeth, Mikolaj Misiak, and Jorg Urban. Photonic penguins at two loops and m_t-dependence of BR($B \to X_s l^+ l^-$). *Nucl. Phys.*, B574:291–330, 2000.

[46] H. Boos, Th. Feldmann, T. Mannel, and B. D. Pecjak. Shape functions from $\bar{B} \to X_c \ell \bar{\nu}_\ell$. *Phys. Rev.*, D73:036003, 2006.

[47] S. W. Bosch, B. O. Lange, M. Neubert, and Gil Paz. Factorization and shape-function effects in inclusive B-meson decays. *Nucl. Phys.*, B699:335–386, 2004.

[48] Stefan W. Bosch, Bjorn O. Lange, Matthias Neubert, and Gil Paz. Proposal for a precision measurement of $|V_{ub}|$. *Phys. Rev. Lett.*, 93:221801, 2004.

[49] Stefan W. Bosch, Matthias Neubert, and Gil Paz. Subleading shape functions in inclusive B decays. *JHEP*, 11:073, 2004.

[50] G. Buchalla, G. Isidori, and S. J. Rey. Corrections of order $\Lambda^2_{\rm QCD}/m_c^2$ to inclusive rare B decays. *Nucl. Phys.*, B511:594–610, 1998.

[51] Andrzej J. Buras, Andrzej Czarnecki, Mikolaj Misiak, and Joerg Urban. Two-loop matrix element of the current-current operator in the decay $B \to X_s\gamma$. *Nucl. Phys.*, B611:488–502, 2001.

[52] Andrzej J. Buras, Andrzej Czarnecki, Mikolaj Misiak, and Jorg Urban. Completing the NLO QCD calculation of $\bar{B} \to X_s\gamma$. *Nucl. Phys.*, B631:219–238, 2002.

[53] Andrzej J. Buras and Mikolaj Misiak. $\bar{B} \to X_s\gamma$ after completion of the NLO QCD calculations. *Acta Phys. Polon.*, B33:2597–2612, 2002.

[54] Andrzej J. Buras and Manfred Munz. Effective Hamiltonian for $B \to X_s e^+ e^-$ beyond leading logarithms in the NDR and HV schemes. *Phys. Rev.*, D52:186–195, 1995.

[55] Craig N. Burrell, Michael E. Luke, and Alexander R. Williamson. Subleading shape function contributions to the hadronic invariant mass spectrum in $\bar{B} \to X_u \ell \bar{\nu}_l$ decay. *Phys. Rev.*, D69:074015, 2004.

[56] Francisco Campanario and Thomas Mannel. Reparametrization invariance in inclusive decays of heavy hadrons. *Phys. Rev.*, D65:094017, 2002.

[57] J. Charles et al. CP violation and the CKM matrix: Assessing the impact of the asymmetric B factories. *Eur. Phys. J.*, C41:1–131, 2005.

[58] Junegone Chay, Howard Georgi, and Benjamin Grinstein. Lepton energy distributions in heavy meson decays from QCD. *Phys. Lett.*, B247:399–405, 1990.

[59] Junegone Chay and Chul Kim. Collinear effective theory at subleading order and its application to heavy-light currents. *Phys. Rev.*, D65:114016, 2002.

[60] Junegone Chay, Chul Kim, and Adam K. Leibovich. Quark mass effects in the soft-collinear effective theory and $\bar{B} \to X_s\gamma$ in the endpoint region. *Phys. Rev.*, D72:014010, 2005.

[61] Jiunn-Wei Chen, Gautam Rupak, and Martin J. Savage. Non-$1/m_b^n$ power suppressed contributions to inclusive $B \to X_s l^+ l^-$ decays. *Phys. Lett.*, B410:285–289, 1997.

[62] S. Chen et al. Branching fraction and photon energy spectrum for $b \to s\gamma$. *Phys. Rev. Lett.*, 87:251807, 2001.

[63] Konstantin G. Chetyrkin, Mikolaj Misiak, and Manfred Munz. Weak radiative B-meson decay beyond leading logarithms. *Phys. Lett.*, B400:206–219, 1997.

[64] S. E. Csorna et al. Moments of the B meson inclusive semileptonic decay rate using neutrino reconstruction. *Phys. Rev.*, D70:032002, 2004.

[65] Fulvia De Fazio and Matthias Neubert. $B \to X_u l \bar{\nu}_l$ decay distributions to order α_s. *JHEP*, 06:017, 1999.

[66] Estia Eichten and Brian Hill. An effective field theory for the calculation of matrix elements involving heavy quarks. *Phys. Lett.*, B234:511, 1990.

[67] R. K. Ellis, W. Furmanski, and R. Petronzio. Power corrections to the parton model in QCD. *Nucl. Phys.*, B207:1, 1982.

[68] R. K. Ellis, W. Furmanski, and R. Petronzio. Unraveling higher twists. *Nucl. Phys.*, B212:29, 1983.

[69] Adam F. Falk, Elizabeth Jenkins, Aneesh V. Manohar, and Mark B. Wise. QCD corrections and the endpoint of the lepton spectrum in semileptonic B decays. *Phys. Rev.*, D49:4553–4559, 1994.

[70] Adam F. Falk, Michael E. Luke, and Martin J. Savage. Nonperturbative contributions to the inclusive rare decays $B \to X_s \gamma$ and $b \to X_s \ell^+ \ell^-$. *Phys. Rev.*, D49:3367–3378, 1994.

[71] Thorsten Feldmann and Tobias Hurth. Non-factorizable contributions to $B \to \pi\pi$ decays. *JHEP*, 11:037, 2004.

[72] Paolo Gambino and Mikolaj Misiak. Quark mass effects in $\bar{B} \to X_s\gamma$. *Nucl. Phys.*, B611:338–366, 2001.

[73] Einan Gardi. Radiative and semi-leptonic B-meson decay spectra: Sudakov resummation beyond logarithmic accuracy and the pole mass. *JHEP*, 04:049, 2004.

[74] Howard Georgi. An effective field theory for heavy quarks at low energies. *Phys. Lett.*, B240:447–450, 1990.

[75] A. Ghinculov, T. Hurth, G. Isidori, and Y. P. Yao. Forward-backward asymmetry in $B \to X_s\ell + \ell-$ at the NNLL level. *Nucl. Phys.*, B648:254–276, 2003.

[76] A. Ghinculov, T. Hurth, G. Isidori, and Y. P. Yao. NNLL QCD corrections to the decay $B \to X_s\ell^+\ell^-$. *Nucl. Phys. Proc. Suppl.*, 116:284–288, 2003.

[77] A. Ghinculov, T. Hurth, G. Isidori, and Y. P. Yao. The rare decay $B \to X_s\ell+\ell^-$ to NNLL precision for arbitrary dilepton invariant mass. *Nucl. Phys.*, B685:351–392, 2004.

[78] Lawrence Gibbons. The status of $|V_{ub}|$. *AIP Conf. Proc.*, 722:156–166, 2004.

[79] Martin Gremm and Anton Kapustin. Order $1/m_b^3$ corrections to $B \to X_c\ell\bar{\nu}$ decay and their implication for the measurement of $\bar{\Lambda}$ and λ_1. *Phys. Rev.*, D55:6924–6932, 1997.

[80] Martin Gremm, Anton Kapustin, Zoltan Ligeti, and Mark B. Wise. Implications of the $B \to X\ell\bar{\nu}_\ell$ lepton spectrum for heavy quark theory. *Phys. Rev. Lett.*, 77:20–23, 1996.

[81] Christoph Greub, Tobias Hurth, and Daniel Wyler. Virtual $o(\alpha_s)$ corrections to the inclusive decay $b \to s\gamma$. *Phys. Rev.*, D54:3350–3364, 1996.

[82] Benjamin Grinstein. The static quark effective theory. *Nucl. Phys.*, B339:253–268, 1990.

[83] Benjamin Grinstein and Dan Pirjol. Factorization in $B \to K\pi e^+e^-$ decays. hep-ph/0505155.

[84] Benjamin Grinstein, Martin J. Savage, and Mark B. Wise. $B \to X_s e^+e^-$ in the six-quark model. *Nucl. Phys.*, B319:271–290, 1989.

[85] Benjamin Grinstein, Roxanne P. Springer, and Mark B. Wise. Effective Hamiltonian for weak radiative B meson decay. *Phys. Lett.*, B202:138, 1988.

[86] Benjamin Grinstein, Roxanne P. Springer, and Mark B. Wise. Strong interaction effects in weak radiative $\bar{B}$ meson decay. *Nucl. Phys.*, B339:269–309, 1990.

[87] R. J. Hill, T. Becher, S. J. Lee, and M. Neubert. Sudakov resummation for subleading SCET currents and heavy-to-light form factors. *JHEP*, 07:081, 2004.

[88] Andre H. Hoang, Zoltan Ligeti, and Aneesh V. Manohar. B decay and the Υ mass. *Phys. Rev. Lett.*, 82:277–280, 1999.

[89] Andre H. Hoang, Zoltan Ligeti, and Aneesh V. Manohar. B decays in the upsilon expansion. *Phys. Rev.*, D59:074017, 1999.

[90] Tobias Hurth. Present status of inclusive rare B decays. *Rev. Mod. Phys.*, 75:1159–1199, 2003.

[91] M. Iwasaki et al. Improved measurement of the electroweak penguin process $B \to X_s \ell^+ \ell^-$. *Phys. Rev.*, D72:092005, 2005.

[92] R. L. Jaffe and M. Soldate. Twist four in the QCD analysis of leptoproduction. *Phys. Lett.*, B105:467–472, 1981.

[93] R. L. Jaffe and M. Soldate. Twist four in electroproduction: canonical operators and coefficient functions. *Phys. Rev.*, D26:49–68, 1982.

[94] H. Kakuno et al. Measurement of $|V_{ub}|$ using inclusive $B \to X_u \ell \nu$ decays with a novel X_u reconstruction method. *Phys. Rev. Lett.*, 92:101801, 2004.

[95] J. Kaneko et al. Measurement of the electroweak penguin process $B \to X_s \ell^+ \ell^-$. *Phys. Rev. Lett.*, 90:021801, 2003.

[96] I. A. Korchemskaya and G. P. Korchemsky. On lightlike Wilson loops. *Phys. Lett.*, B287:169–175, 1992.

[97] G. P. Korchemsky and G. Marchesini. Structure functions for large x and renormalization of Wilson loops. *Nucl. Phys.*, B406:225–258, 1993.

[98] G. P. Korchemsky and A. V. Radyushkin. Renormalization of the Wilson loops beyond the leading order. *Nucl. Phys.*, B283:342–364, 1987.

[99] Gregory P. Korchemsky and George Sterman. Infrared factorization in inclusive B meson decays. *Phys. Lett.*, B340:96–108, 1994.

[100] Michael Kraetz and Thomas Mannel. Subleading light cone distributions functions in the decays $\Lambda_b \to X_s \gamma$ and $\Lambda_b \to X_u \ell \bar{\nu}_l$. *Phys. Lett.*, B556:163–168, 2003.

[101] F. Kruger and L. M. Sehgal. Lepton polarization in the decays $B \to X_s \mu^+ \mu^-$ and $B \to X_s \tau^+ \tau^-$. *Phys. Lett.*, B380:199–204, 1996.

[102] Bjorn O. Lange. Shape-function independent relations of charmless inclusive B-decay spectra. *JHEP*, 01:104, 2006.

[103] Bjorn O. Lange, Matthias Neubert, and Gil Paz. Theory of charmless inclusive B decays and the extraction of V_{ub}. *Phys. Rev.*, D72:073006, 2005.

[104] Bjorn O. Lange, Matthias Neubert, and Gil Paz. A two-loop relation between inclusive radiative and semileptonic B decay spectra. *JHEP*, 10:084, 2005.

[105] Keith S. M. Lee, Zoltan Ligeti, Iain W. Stewart, and Frank J. Tackmann. Universality and m_X cut effects in $B \to X_s \ell^+ \ell^-$. hep-ph/0512191.

[106] Keith S. M. Lee and Iain W. Stewart. Factorization for power corrections to $B \to X_s \gamma$ and $B \to X_u \ell \bar{\nu}$. *Nucl. Phys.*, B721:325–406, 2005.

[107] Keith S. M. Lee and Iain W. Stewart. Shape-function effects and split matching in $B \to X_s \ell^+ \ell^-$. hep-ph/0511334.

[108] Adam K. Leibovich, Zoltan Ligeti, and Mark B. Wise. Enhanced subleading structure functions in semileptonic B decay. *Phys. Lett.*, B539:242–248, 2002.

[109] Adam K. Leibovich, Zoltan Ligeti, and Mark B. Wise. Comment on quark masses in SCET. *Phys. Lett.*, B564:231–234, 2003.

[110] Adam K. Leibovich, Ian Low, and I. Z. Rothstein. Extracting $|V_{ub}|$ from the hadronic mass spectrum of inclusive B decays. *Phys. Lett.*, B486:86–91, 2000.

[111] Adam K. Leibovich, Ian Low, and I. Z. Rothstein. Extracting V_{ub} without recourse to structure functions. *Phys. Rev.*, D61:053006, 2000.

[112] Adam K. Leibovich, Ian Low, and I. Z. Rothstein. On the resummed hadronic spectra of inclusive B decays. *Phys. Rev.*, D62:014010, 2000.

[113] Adam K. Leibovich and I. Z. Rothstein. The resummed rate for $B \to X_s \gamma$. *Phys. Rev.*, D61:074006, 2000.

[114] Michael E. Luke and Aneesh V. Manohar. Reparametrization invariance constraints on heavy particle effective field theories. *Phys. Lett.*, B286:348–354, 1992.

[115] Thomas Mannel and Matthias Neubert. Resummation of nonperturbative corrections to the lepton spectrum in inclusive $B \to X \ell \bar{\nu}$ decays. *Phys. Rev.*, D50:2037–2047, 1994.

[116] Thomas Mannel and Stefan Recksiegel. Radiatively corrected shape function for inclusive heavy hadron decays. *Phys. Rev.*, D63:094011, 2001.

[117] Thomas Mannel and Frank J. Tackmann. Shape function effects in $B \to X_c \ell \bar{\nu}_l$. *Phys. Rev.*, D71:034017, 2005.

[118] Aneesh V. Manohar, Thomas Mehen, Dan Pirjol, and Iain W. Stewart. Reparameterization invariance for collinear operators. *Phys. Lett.*, B539:59–66, 2002.

[119] Aneesh V. Manohar and Mark B. Wise. Inclusive semileptonic B and polarized Λ_b decays from QCD. *Phys. Rev.*, D49:1310–1329, 1994.

[120] Aneesh V. Manohar and Mark B. Wise. Heavy quark physics. *Camb. Monogr. Part. Phys. Nucl. Phys. Cosmol.*, 10:1–191, 2000.

[121] Mikolaj Misiak. The $b \to se^+e^-$ and $b \to s\gamma$ decays with next-to-leading logarithmic QCD corrections. *Nucl. Phys.*, B393:23–45, 1993.

[122] S. Moch, J. A. M. Vermaseren, and A. Vogt. The three-loop splitting functions in QCD: The non-singlet case. *Nucl. Phys.*, B688:101–134, 2004.

[123] Alfred H. Mueller. Perturbative QCD at high energies. *Phys. Rept.*, 73:237, 1981.

[124] Matthias Neubert. Analysis of the photon spectrum in inclusive $B \to X_s\gamma$ decays. *Phys. Rev.*, D49:4623–4633, 1994.

[125] Matthias Neubert. QCD based interpretation of the lepton spectrum in inclusive $\bar{B} \to X_u\ell\bar{\nu}$ decays. *Phys. Rev.*, D49:3392–3398, 1994.

[126] Matthias Neubert. Note on the extraction of $|V_{ub}|$ using radiative B decays. *Phys. Lett.*, B513:88–92, 2001.

[127] Matthias Neubert. Subleading shape functions and the determination of $|V_{ub}|$. *Phys. Lett.*, B543:269–275, 2002.

[128] Matthias Neubert. Impact of four-quark shape functions on inclusive B decay spectra. *Eur. Phys. J.*, C44:205–209, 2005.

[129] Matthias Neubert. Renormalization-group improved calculation of the $B \to X_s\gamma$ branching ratio. *Eur. Phys. J.*, C40:165–186, 2005.

[130] Dan Pirjol and Iain W. Stewart. A complete basis for power suppressed collinear-ultrasoft operators. *Phys. Rev.*, D67:094005, 2003.

[131] Mikhail A. Shifman and M. B. Voloshin. Preasymptotic effects in inclusive weak decays of charmed particles. *Sov. J. Nucl. Phys.*, 41:120, 1985.

[132] Edward V. Shuryak and A. I. Vainshtein. Theory of power corrections to deep inelastic scattering in quantum chromodynamics. I. q^{-2} effects. *Nucl. Phys.*, B199:451, 1982.

[133] Edward V. Shuryak and A. I. Vainshtein. Theory of power corrections to deep inelastic scattering in quantum chromodynamics. II. q^{-4} effects; polarized target. *Nucl. Phys.*, B201:141, 1982.

[134] George Sterman. Partons, factorization and resummation. hep-ph/960631.

[135] Frank J. Tackmann. Full-phase-space twist expansion in semileptonic and radiative B-meson decays. *Phys. Rev.*, D72:034036, 2005.

[136] M. B. Voloshin. Once again on electromagnetic properties of a domain wall interacting with charged fermions. *Phys. Rev.*, D63:125012, 2001.